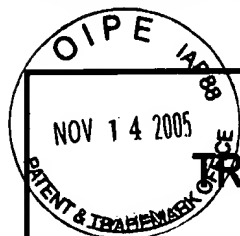


Please type a plus sign (+) inside this box ☐

+

PTO/SB/21 (6-99)

Approved for use through 09/30/2000. OMB 0651-0031  
Patent and Trademark Office: U.S. DEPARTMENT OF COMMERCE  
Under the Paperwork Reduction Act of 1995, no persons are required to respond to a collection of information unless it displays a valid OMB control number.



Under the Paperwork Reduction Act of 1995, no persons are required to respond to a collection of information unless it displays a valid OMB control number.

## TRANSMITTAL FORM

(to be used for all correspondence after initial filing)

<b>Application Number</b> 09/989,723			
		<b>Filing Date</b> NOVEMBER 19, 2001	
		<b>First Named Inventor</b> AVI ASHKENAZI	
		<b>Group/Art Unit</b> 1647	
		<b>Examiner Name</b> WEGERT, SANDRA L.	
<b>Total Number of Pages in This Submission</b>	123	<b>Attorney Docket Number</b>	39780-2730 P1C62

### ENCLOSURES (check all that apply)

<input type="checkbox"/> Fee Transmittal Form <input type="checkbox"/> Fee Attached <input type="checkbox"/> Amendment / Response <input type="checkbox"/> After Final <input type="checkbox"/> Version With Markings Showing Changes <input type="checkbox"/> Affidavits/declaration(s) <input type="checkbox"/> Extension of Time Request <input type="checkbox"/> Information Disclosure Statement <input type="checkbox"/> Certified Copy of Priority Document(s) <input type="checkbox"/> Response to Missing Parts/ Incomplete Application <input type="checkbox"/> Response to Missing Parts under 37 CFR 1.52 or 1.53 <input type="checkbox"/> Copy of Notice	<input type="checkbox"/> Copy of an Assignment <input type="checkbox"/> Drawing(s) <input type="checkbox"/> Licensing-related Papers <input type="checkbox"/> Petition Routing Slip (PTO/SB/69) and Accompanying Petition <input type="checkbox"/> Petition to Convert to a Provisional Application <input type="checkbox"/> Power of Attorney, by Assignee to Exclusion of Inventor Under 37 C.F.R. §3.71 With Revocation of Prior Powers <input type="checkbox"/> Terminal Disclaimer <input type="checkbox"/> Small Entity Statement <input type="checkbox"/> Request for Refund	<input type="checkbox"/> After Allowance Communication to Group <input type="checkbox"/> Appeal Communication to Board of Appeals and Interferences <input checked="" type="checkbox"/> <b>APPEAL COMMUNICATION TO GROUP (APPEAL NOTICE, BRIEF, REPLY BRIEF)</b> <input type="checkbox"/> Proprietary Information <input type="checkbox"/> Status Letter <input checked="" type="checkbox"/> <b>ADDITIONAL ENCLOSURE(S) (PLEASE IDENTIFY BELOW):</b> <input checked="" type="checkbox"/> <b>EVIDENCE APPENDIX ITEMS 1-7; and POSTCARD</b>
<b>Remarks</b> AUTHORIZATION TO CHARGE DEPOSIT ACCOUNT 08-1641 FOR ANY FEES DUE IN CONNECTION WITH THIS PAPER, REFERENCING ATTORNEY'S DOCKET NO. 39780-2730 P1C62.		

### SIGNATURE OF APPLICANT, ATTORNEY OR AGENT

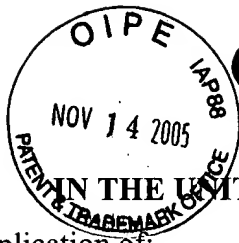
<b>Firm or Individual name</b>	<b>HELLER EHRMAN LLP</b>	<b>GINGER R. DREGER (Reg. No. 33,055)</b>
	<b>275 Middlefield Road, Menlo Park, California 94025</b>	<b>Telephone: (650) 324-7000 Facsimile: (650) 324-0638</b>
<b>Signature</b>		
<b>Date</b>	<b>NOVEMBER 14, 2005</b>	<b>Customer Number: 35489</b>

### CERTIFICATE OF EXPRESS MAILING

I hereby certify that this correspondence is being deposited with the United States Postal Service "Express Mail Post Office to Addressee" service under 37 C.F.R. §1.10 on the date indicated below and addressed to: <b>MAIL STOP APPEAL BRIEF - PATENTS</b> , Commissioner for Patents, PO Box 1450, Alexandria, Virginia 22313-1450, on this date: <b>NOVEMBER 14, 2005</b>			
Express Mail Label <b>EV 765 989 367 US</b>			
<b>Typed or printed name</b>	<b>C. FONG</b>		
<b>Signature</b>		<b>Date</b>	<b>NOVEMBER 14, 2005</b>

Burden Hour Statement: This form is estimated to take 0.2 hours to complete. Time will vary depending upon the needs of the individual case. Any comments on the amount of time you are required to complete this form should be sent to the Chief Information Officer, Patent and Trademark Office, Washington, DC 20231. DO NOT SEND FEES OR COMPLETED FORMS TO THIS ADDRESS. SEND TO: Mail Stop \_\_\_, Commissioner for Patents, P.O. Box 1450, Alexandria, VA 22313-1450.

BEST AVAILABLE COPY



IN THE UNITED STATES PATENT AND TRADEMARK OFFICE

In re application of:	)	Examiner: Wegert, Sandra
	)	
Avi ASHKENAZI, et al.	)	Art Unit: 1647
	)	
Application Serial No. 09/989,723	)	Confirmation No: 9893
	)	
Filed: November 19, 2001	)	Attorney's Docket No. 39780-2730 P1C62
	)	
For: <b>SECRETED AND TRANSMEMBRANE</b>	)	<b>Customer No. 35489</b>
<b>POLYPEPTIDES AND NUCLEIC</b>	)	
<b>ACIDS ENCODING THE SAME</b>	)	
	)	

---

EXPRESS MAIL LABEL NO. : EV 765 989 367 US  
DATE MAILED: NOVEMBER 14, 2005

**ON APPEAL TO THE BOARD OF PATENT APPEALS AND INTERFERENCES**

**APPELLANTS' BRIEF**

**MS: APPEAL BRIEF - PATENTS**

Commissioner for Patents  
P.O. Box 1450  
Alexandria, Virginia 22313-1450

Dear Sir:

This Appeal brief is filed in response to the Communication mailed on November 3, 2005 requiring the Appeal brief to be compliant with the format requirements of 37 C.F.R. 41.37(c). An Appeal Brief was timely filed with the required fees and a Request for a three month extension of time on August 30, 2005 in the above captioned patent application. A Final Office Action was mailed on October 20, 2004 and a Notice of Appeal was filed on April 1, 2005. Appellants hereby request consideration and appeal to the Board of Patent Appeals and Interferences from the final rejection in this case.

The Commissioner is authorized to charge any fees which may be required, including extension fees, or credit any overpayment to Deposit Account No. **08-1641** (referencing Attorney's Docket No. **39780-2730 P1C62**).

The following constitutes the Appellants' Brief on Appeal.

### **I. REAL PARTY IN INTEREST**

The real party in interest is Genentech, Inc., South San Francisco, California, by an assignment of the parent application, U.S. Serial No. 09/941,992 recorded November 16, 2001, at Reel 012176 and Frame 0450.

### **II. RELATED APPEALS AND INTERFERENCES**

The claims pending in the current application are directed to a polypeptide referred to herein as "PRO1097". There exist two related patent applications, (1) U.S. Serial No. 09/997,628, filed November 15, 2001 (containing claims directed to antibodies to the PRO1097 polypeptide), and (2) U.S. Serial No. 09/997,614, filed November 15, 2001 (containing claims directed to PRO1097 polypeptides). These two related applications are also under final rejection from the same Examiner and based upon the same outstanding rejection, therefore appeal of these final rejections are being pursued independently and concurrently herewith.

### **III. STATUS OF CLAIMS**

Claims 124, 129-131 and 135-145 are in this application.

Claims 1-123, 125-128 and 132-134 have been canceled.

Claims 124, 129-131 and 135-145 stand rejected and Appellants appeal the rejection of these claims.

A copy of the rejected claims in the present Appeal is provided in the Claims Appendix.

### **IV. STATUS OF AMENDMENTS**

In an Amendment filed on January 10, 2005 after the mailing of the Final Office of October 20, 2004, Claims 119-123 were canceled and Claims 124 and 139 were amended to more clearly claim what the Appellants always believed was the claimed subject matter in the present application. The claim amendments raised no new issues and placed the claims in better form for consideration on appeal. These cancellations and amendments to the claims were indicated as acceptable in a telephone conference with Examiner Wegert on August 24, 2005 for the purposes of this appeal. Hence, Claims 124, 129-131 and 135-145 are pending and are under

Appeal in this case. The rejection under 35 U.S.C. §112, first paragraph to Claims 119-123 (now canceled) for allegedly not satisfying the written description requirement is moot. The outstanding rejections are addressed with respect to the pending claims.

Further, in an Amendment filed on August 25, 2005 after the mailing of the Final Office action of October 20, 2004, a declaration by Audrey Goddard, Ph.D. was filed. Entry of this declaration was indicated as acceptable in a telephone conference with Examiner Wegert on August 24, 2005 for the purposes of this appeal.

#### **V. SUMMARY OF CLAIMED SUBJECT MATTER**

Independent Claim 124 is directed to an isolated nucleic acid of SEQ ID NO: 348; the full-length coding sequence of the nucleic acid sequence of SEQ ID NO: 348; or the full-length coding sequence of the cDNA deposited under ATCC accession number 203044, and encodes for the PRO1097 polypeptide. The PRO1097 gene was shown for the first time to be significantly amplified in human lung or colon cancers as compared to normal, non-cancerous human tissue controls (2.313 to 2.346 fold in two different lung primary tumors and 2.114 to 2.532 fold in three different colon primary tumors). This is set forth in the specification, at least in the 'Gene Amplification assay,' Example 170, page 539, line 19, to page 555, line 5 (specifically, see Table 9B, page 551). The profiles of various primary lung or colon tumors used for screening the PRO polypeptide compounds of the invention in the gene amplification assay are summarized on Table 8, page 546 of the specification. This feature is carried by all claims dependent directly or indirectly from Claim 124, namely, Claims 129-138. Methods for selecting a host are generally set forth in the specification at, for example, in Examples 140-143 and page 376, line 12 onwards (Claims 137-138), and describes the expression of PRO nucleic acids in various host cells, including *E. coli*, yeast and Baculovirus-infected insect cells. Methods for selecting a vector are generally set forth in the specification at, for example, on page 378, line 8 (Claims 135 and 136).

Independent Claim 139 is directed to an isolated nucleic acid consisting of at least 30 nucleotide fragment of the nucleic acid sequence of SEQ ID NO: 348, or a complement thereof, that specifically hybridizes under highly stringent conditions to (a) the nucleic acid sequence of SEQ ID NO: 348 or a complement thereof; or (b) the full-length coding sequence of the cDNA deposited under ATCC accession number 203044 or a complement thereof and wherein the



isolated nucleic acid molecule is suitable for use as a PCR primer or probe. Methods for using high stringent hybridization conditions recited in Claim 139 are provided, for example, on page 312, line 33 onwards. Pending Claims 140-145 depend from Claim 139. Methods for using polynucleotides encoding PRO as hybridization probes consisting of nucleotide fragments of varying lengths is described at, for example, on page 285, line 11 onwards, and describes probes of at least 50 nucleotides (Claim 140), 60 nucleotides (Claim 141), 70 nucleotides (Claim 142), 80 nucleotides (Claim 143), 90 nucleotides (Claim 144) and 100 nucleotides (Claim 145).

Finally, the amino acid sequence of the native "PRO1097" polypeptide and the nucleic acid sequence encoding this polypeptide (referred to in the present application as "DNA59841-1460") are shown in the present specification as SEQ ID NOs: 349 and 348, respectively, and in Figures 244 and 243, respectively. Page 299, lines 30-33 of the specification provides the description for Figures 244 and 243. The isolation of cDNA clones encoding PRO1097 of SEQ ID NO:348 is described in Example 107, page 489 of the specification. The specification discloses that various portions of the encoded PRO1097 polypeptide possess significant sequence similarity to the glycoprotease family of proteins and the acyltransferase ChoActase/COT/CPT family (see, for example, pages 218-220, lines 31-34).

## **VI. GROUNDS OF REJECTION TO BE REVIEWED ON APPEAL**

1. Whether Claims 124, 129-131 and 135-145 should be accorded priority of provisional Application 60/141,037, filed 19 November, 2001.
2. Whether Claims 124, 129-131 and 135-145 satisfy the utility/ enablement requirement under 35 U.S.C. §101/112, first paragraph.

## **VII. ARGUMENTS**

### **Summary of the Arguments**

#### **Issue 1: Priority**

The instant application has not been granted the earlier priority date on the grounds that "although disclosing the same experimental assays as the instant specification, do not enable the instant invention and therefore do not impart Utility..."

Appellants submit that data derived from the Gene Amplification assay was first disclosed in U. S. Application Serial No. 60/141,037, filed 19 November, 2001 for the claimed

PRO1097 encoding gene. Appellants further submit that, the same detailed reasons discussed below under the section on Issue II: Utility/ Enablement, are sufficient to also establish patentable utility for U. S. Application Serial No. 60/141,037. Hence, Appellants should be able to rely upon this provisional application to provide an effective filing date of 19 November, 2001 for the instant application.

#### Issue 2: Utility/ Enablement

Claims 124, 129-131 and 135-145 stand rejected under 35 U.S.C. §101/ 112, first paragraph as allegedly lacking either a specific and substantial asserted utility or a well established utility.

Patentable utility for the PRO1097 polypeptides is based upon the gene amplification data for the gene encoding the PRO1097 polypeptide. The specification discloses that the gene encoding PRO1097 showed amplification, ranging from 2.313 to 2.346 fold in two different lung primary tumors and 2.114 to 2.532 fold in three different colon primary tumors. The Declaration of Dr. Audrey Goddard, submitted with Appellants' Response filed August 25, 2005, explains that a gene identified as being amplified at least 2-fold by the disclosed gene amplification assay in a tumor sample relative to a normal sample is useful as a marker for the diagnosis of cancer, and for monitoring cancer development and/or for measuring the efficacy of cancer therapy. Therefore, the gene amplification levels of 2.313 to 2.346 fold for lung primary tumors and 2.114 to 2.532 fold for colon tumors is not a "small increase" as the Examiner contends (page 4 of Final Office action dated October 20, 2004). Appellants also submit that, as any skilled artisan in the field of oncology would easily appreciate, not all tumor markers are generally associated with every tumor, or even with most tumors. Therefore, whether the PRO1097 gene is amplified in few tumor samples or in the vast majority of tumor samples studied is not relevant to its identification as a tumor marker, or its patentable utility. Rather, the fact that the amplification data for PRO1097 is considered significant is what lends support to its usefulness as a tumor marker. Thus, a positive result does indicate the presence of cancer, while a negative result requires further follow up testing, testing which is considered routine by one skilled in the art of oncology and is not considered undue.

The Examiner further asserted on page 4 of the Final Office Action mailed October 20, 2004 that amplification of the PRO1097 polynucleotide does not impart a specific, substantial,

and credible utility to the PRO1097 polypeptide since, “there is no evidence regarding whether or not PRO1097 mRNA or polypeptide levels are also increased in this cancer.” In support of this assertion, the Examiner cited references by Pennica *et al.*, Haynes *et al.* and Hu *et al.*

First of all, the claims are directed to nucleic acids, not polypeptides, therefore, the issue of whether there is a correlation between gene amplification and polypeptide expression levels is irrelevant. One of skill in the art would understand how to use the claimed nucleic acids to detect amplification of the gene encoding PRO1097, and how to use the gene amplification results to diagnose cancer. Thus the question of whether or not PRO1097 mRNA or polypeptide levels are also increased in these cancers has no relevance to the utility of the claimed nucleic acid molecules. Moreover, the teachings of Pennica *et al.*, Haynes *et al.* or Hu *et al.*, do not conclusively establish a *prima facie* case for lack of utility.

Instead, Appellants submit that based on the gene amplification data and the substantial, credible, asserted utility of the PRO1097 gene in the diagnosis of lung or colon cancer, one of ordinary skill would know exactly how to make and use these claimed nucleic acids for the diagnosis of cancers, without any undue experimentation.

### **Response to Rejections**

#### **ISSUE 1. U.S. Provisional Application No. 60/141,037 Satisfies the Utility Requirement of 35 U.S.C. § 101/ § 112, First Paragraph based on the results of the Gene Amplification assay**

Appellants have asserted that U.S. Provisional Application No. 60/141,037, filed November 19, 2001, discloses the gene amplification assay (shown in Example 170 of the instant specification) and establishes patentable utility for the claimed PRO1097 nucleic acids.

Appellants submit, for the reasons set forth below under Issue 2 for Utility/ Enablement, that the results of the gene amplification assay disclosed in the specification of U.S. Application No. 60/141,037, provides at least one credible, substantial and specific asserted utility for the claimed PRO1097 nucleic acids under 35 U.S.C. §101/§112, first paragraph. Accordingly, Appellants respectfully request that the subject matter of the instant claims be granted the November 19, 2001, priority date of U.S. Provisional Application No. 60/141,037.

**ISSUE 2. Claims 124, 129-131 and 135-145 are supported by a credible, specific and substantial asserted utility, and thus meet the utility requirement of 35 U.S.C. § 101/ 112, first paragraph**

The sole basis for the Examiner's rejection of Claims 124, 129-131 and 135-145 under this section is that the data presented in Example 170 of the present specification is allegedly insufficient under the present legal standards to establish a patentable utility under 35 U.S.C. § 101 for the presently claimed subject matter.

Claims 124, 129-131 and 135-145 stand further rejected under 35 U.S.C. §112, first paragraph, allegedly "since the claimed invention is not supported by either a specific and substantial asserted utility or a well established utility for the reasons set forth above, one skilled in the art clearly would not know how to use the claimed invention."

Appellants strongly disagree and, therefore, respectfully traverse the rejection.

**A. The Legal Standard For Utility Under 35 U.S.C. § 101**

According to 35 U.S.C. § 101:

Whoever invents or discovers any new and *useful* process, machine, manufacture, or composition of matter, or any new and *useful* improvement thereof, may obtain a patent therefor, subject to the conditions and requirements of this title. (Emphasis added.)

In interpreting the utility requirement, in *Brenner v. Manson*<sup>1</sup> the Supreme Court held that the *quid pro quo* contemplated by the U.S. Constitution between the public interest and the interest of the inventors required that a patent applicant disclose a "substantial utility" for his or her invention, i.e. a utility "where specific benefit exists in currently available form."<sup>2</sup> The Court concluded that "a patent is not a hunting license. It is not a reward for the search, but compensation for its successful conclusion. A patent system must be related to the world of commerce rather than the realm of philosophy."<sup>3</sup>

---

<sup>1</sup> *Brenner v. Manson*, 383 U.S. 519, 148 U.S.P.Q. (BNA) 689 (1966).

<sup>2</sup> *Id.* at 534, 148 U.S.P.Q. (BNA) at 695.

<sup>3</sup> *Id.* at 536, 148 U.S.P.Q. (BNA) at 696.

Later, in *Nelson v. Bowler*<sup>4</sup> the C.C.P.A. acknowledged that tests evidencing pharmacological activity of a compound may establish practical utility, even though they may not establish a specific therapeutic use. The court held that “since it is crucial to provide researchers with an incentive to disclose pharmaceutical activities in as many compounds as possible, we conclude adequate proof of any such activity constitutes a showing of practical utility.”<sup>5</sup>

In *Cross v. Iizuka*<sup>6</sup> the C.A.F.C. reaffirmed *Nelson*, and added that *in vitro* results might be sufficient to support practical utility, explaining that “*in vitro* testing, in general, is relatively less complex, less time consuming, and less expensive than *in vivo* testing. Moreover, *in vitro* results with the particular pharmacological activity are generally predictive of *in vivo* test results, i.e. there is a reasonable correlation there between.”<sup>7</sup> The court perceived “No insurmountable difficulty” in finding that, under appropriate circumstances, “*in vitro* testing, may establish a practical utility.”<sup>8</sup>

The case law has also clearly established that Appellants’ statements of utility are usually sufficient, unless such statement of utility is unbelievable on its face.<sup>9</sup> The PTO has the initial burden to prove that Appellants’ claims of usefulness are not believable on their face.<sup>10</sup> In general, an Applicant’s assertion of utility creates a presumption of utility that will be sufficient

---

<sup>4</sup> *Nelson v. Bowler*, 626 F.2d 853, 206 U.S.P.Q. (BNA) 881 (C.C.P.A. 1980).

<sup>5</sup> *Id.* at 856, 206 U.S.P.Q. (BNA) at 883.

<sup>6</sup> *Cross v. Iizuka*, 753 F.2d 1047, 224 U.S.P.Q. (BNA) 739 (Fed. Cir. 1985).

<sup>7</sup> *Id.* at 1050, 224 U.S.P.Q. (BNA) at 747.

<sup>8</sup> *Id.*

<sup>9</sup> *In re Gazave*, 379 F.2d 973, 154 U.S.P.Q. (BNA) 92 (C.C.P.A. 1967).

<sup>10</sup> *Ibid.*

to satisfy the utility requirement of 35 U.S.C. §101, “unless there is a reason for one skilled in the art to question the objective truth of the statement of utility or its scope.”<sup>11, 12</sup>

Compliance with 35 U.S.C. §101 is a question of fact.<sup>13</sup> The evidentiary standard to be used throughout *ex parte* examination in setting forth a rejection is a preponderance of the totality of the evidence under consideration.<sup>14</sup> Thus, to overcome the presumption of truth that an assertion of utility by the applicant enjoys, the Examiner must establish that it is more likely than not that one of ordinary skill in the art would doubt the truth of the statement of utility. Only after the Examiner made a proper *prima facie* showing of lack of utility, does the burden of rebuttal shift to the applicant. The issue will then be decided on the totality of evidence.

The well established case law is clearly reflected in the Utility Examination Guidelines (“Utility Guidelines”)<sup>15</sup>, which acknowledge that an invention complies with the utility requirement of 35 U.S.C. §101, if it has at least one asserted “specific, substantial, and credible utility” or a “well-established utility.” Under the Utility Guidelines, a utility is “specific” when it is particular to the subject matter claimed. For example, it is generally not enough to state that a nucleic acid is useful as a diagnostic without also identifying the conditions that are to be diagnosed.

In explaining the “substantial utility” standard, M.P.E.P. §2107.01 cautions, however, that Office personnel must be careful not to interpret the phrase “immediate benefit to the public” or similar formulations used in certain court decisions to mean that products or services based on the claimed invention must be “currently available” to the public in order to satisfy the

---

<sup>11</sup> *In re Langer*, 503 F.2d 1380,1391, 183 U.S.P.Q. (BNA) 288, 297 (C.C.P.A. 1974).

<sup>12</sup> *See also In re Jolles*, 628 F.2d 1322, 206 USPQ 885 (C.C.P.A. 1980); *In re Irons*, 340 F.2d 974, 144 USPQ 351 (1965); *In re Sichert*, 566 F.2d 1154, 1159, 196 USPQ 209, 212-13 (C.C.P.A. 1977).

<sup>13</sup> *Raytheon v. Roper*, 724 F.2d 951, 956, 220 U.S.P.Q. (BNA) 592, 596 (Fed. Cir. 1983) cert. denied, 469 US 835 (1984).

<sup>14</sup> *In re Oetiker*, 977 F.2d 1443, 1445, 24 U.S.P.Q.2d (BNA) 1443, 1444 (Fed. Cir. 1992).

<sup>15</sup> 66 Fed. Reg. 1092 (2001).

utility requirement. “Rather, any reasonable use that an applicant has identified for the invention that can be viewed as providing a public benefit should be accepted as sufficient, at least with regard to defining a ‘substantial’ utility.”<sup>16</sup> Indeed, the Guidelines for Examination of Applications for Compliance With the Utility Requirement,<sup>17</sup> gives the following instruction to patent examiners: “If the applicant has asserted that the claimed invention is useful for any particular practical purpose . . . and the assertion would be considered credible by a person of ordinary skill in the art, do not impose a rejection based on lack of utility.”

**B. Proper Application of the Legal Standard**

Appellants respectfully submit that the data presented in Example 170 starting on page 539 of the specification of the specification and the cumulative evidence of record, which underlies the current dispute, indeed support a “specific, substantial and credible” asserted utility for the presently claimed invention.

Example 170 describes the results obtained using a very well-known and routinely employed polymerase chain reaction (PCR)-based assay, the TaqMan<sup>TM</sup> PCR assay, also referred to herein as the gene amplification assay. This assay allows one to quantitatively measure the level of gene amplification in a given sample, say, a tumor extract, or a cell line. It was well known in the art at the time the invention was made that gene amplification is an essential mechanism for oncogene activation. Appellants isolated genomic DNA from a variety of primary cancers and cancer cell lines that are listed in Table 9 (pages 539 onwards of the specification), including primary lung and colon cancers of the type and stage indicated in Table 8 (page 546). The tumor samples were tested in triplicates with Taqman<sup>TM</sup> primers and with internal controls, beta-actin and GADPH in order to quantitatively compare DNA levels between samples (page 548, lines 33-34). As a negative control, DNA was isolated from the cells of ten normal healthy individuals, which was pooled and used as a control (page 539, lines 27-29) and also, no-template controls (page 548, lines 33-34). The results of TaqMan<sup>TM</sup> PCR are reported in  $\Delta C_t$  units, as explained in the passage on page 539, lines 37-39. One unit corresponds to one PCR

---

<sup>16</sup> M.P.E.P. §2107.01.

<sup>17</sup> M.P.E.P. §2107 II (B)(1).

cycle or approximately a 2-fold amplification, relative to control, two units correspond to 4-fold, 3 units to 8-fold amplification and so on . Using this PCR-based assay, Appellants showed that the gene encoding for PRO1097 was amplified, that is, it showed approximately 1.21- 1.23  $\Delta C_t$  units for lung tumors and 1.08-1.34  $\Delta C_t$  units for colon tumors which corresponds to  $2^{1.21}$ - $2^{1.23}$ - fold amplification in lung and  $2^{1.08}$ - $2^{1.34}$ - fold amplification in colon tumors respectively, or **2.313 to 2.346 fold** in two different lung primary tumors and **2.114 to 2.532 fold** in three different colon primary tumors.

Previously, in the Office Action mailed April 30, 2004, the Examiner stated based on Hittelman *et al.* that such a “slight increase in clone numbers in cancerous tissue is no doubt due to an increased number of chromosomes, a very common characteristic of cancerous and non-cancerous epithelial cells.” Appellants disagree.

Hittelman studied premalignant lesions and suggests that epithelial tumors develop through a multistep process driven by genetic instability (see abstract). Hittelman showed that a subset of the same molecular changes found in associated tumor were also found in premalignant lesions, suggesting that these premalignant lesions might represent precursor lesions for associated tumors, i.e., a manifestation of a multistep tumorigenesis process. (See Hittelman, page 4, last three lines). Appellants therefore submit that, contrary to the Examiner’s rejection, the Hittelman reference strongly supports the Appellants position that there is utility in identifying genetic biomarkers in epithelial tissues at cancer risk (also see Hittelman, abstract, line 4-7). Hittelman adds on page 2, fourth paragraph, line 3 that “it is important to identify individuals at significantly increased cancer risk who might best benefit from different types of intervention”. Taken together, even if Appellants were to show that the observed PRO1097 gene amplification were due to chromosomal aneuploidy (which Appellants do not contend to), identifying genetic biomarkers like the PRO1097 gene with this aneuploidy is a very important and useful step, according to Hittelman, in identifying individuals at significantly increased cancer risk. Therefore, Hittelman supports at least one utility for the PRO1097 gene, that is, as a genetic biomarker for cancer or precancerous cells. As one skilled in the art would clearly know, early detection of lung cancer provides information in advance about risk assessment, prognosis and therapy for lung cancer.

Further, the Examiner acknowledges that there was a “increase” in DNA, but stated that the increase was “very small” (Office action mailed April 30, 2004). Regarding this rejection



Appellants submit that the Examiner seems to be applying a heightened utility standard in this instance, which is legally incorrect. Instead, whether this “increase” is “significant” needs to be addressed. As evidence that the “increase in DNA” in the gene amplification assay is significant, Appellants submitted a Declaration by Dr. Audrey Goddard in the Supplemental response filed August 25, 2005. The Declaration by Dr. Audrey Goddard provides a statement by an expert in the relevant art stating that “fold amplification” values of at least 2-fold are considered significant in the TaqMan™ PCR gene amplification assay. Appellants particularly draw the Board’s attention to page 3 of the Goddard Declaration which clearly states that:

It is further my considered scientific opinion that an at least **2-fold increase** in gene copy number in a tumor tissue sample relative to a normal (*i.e.*, non-tumor) sample is significant and useful in that the detected increase in gene copy number in the tumor sample relative to the normal sample serves as a basis for using relative gene copy number as quantitated by the TaqMan PCR technique as a diagnostic marker for the presence or absence of tumor in a tissue sample of unknown pathology. Accordingly, a gene identified as being amplified at least 2-fold by the quantitative TaqMan PCR assay in a tumor sample relative to a normal sample is **useful as a marker for the diagnosis of cancer**, for monitoring cancer development and/or for measuring the efficacy of cancer therapy. (Emphasis added).

Accordingly, the 2.313 to 2.346 fold in two different lung primary tumors and 2.114 to 2.532 fold in three different colon primary tumors would be considered significant and credible by one skilled in the art, based upon the facts disclosed in the Goddard Declaration.

Further, Appellants submit that the fact that two lung tumor samples and three colon tumor samples tested positive in this study does not make the gene amplification data, by any means, less significant or spurious. As any skilled artisan in the field of oncology would easily appreciate, not all tumor markers are generally associated with every tumor, or even, with most tumors. In fact, some tumor markers are useful for identifying rare malignancies. That is, the association of the tumor marker with a particular type of tumor lesion may be rare, or, the occurrence of that particular kind of tumor lesion itself may be rare. In either event, even these rare tumor markers, which may not give a positive hit with most common tumors, have great value in tumor diagnosis, and consequently, in tumor prognosis. The skilled artisan would know that such tumor markers are very useful for better classification of tumors. Therefore, whether the PRO1097 gene is amplified in two lung/ three colon tumors or in most tumors is not relevant to its identification as a tumor marker, or its patentable utility. Rather, whether the

amplification data for PRO1097 is significant is what lends support to its usefulness as a tumor marker. It was well known in the art at the time of filing of the application that gene amplification, which occurs in most solid tumors like lung and colon cancers, is generally associated with poor prognosis. Therefore, the PRO1097 gene becomes an important diagnostic marker to identify such malignant lung or colon cancers, even if the malignancy associated with PRO1097 molecule is a rare occurrence. Accordingly, the present specification clearly discloses enough evidence that the gene encoding the PRO1097 polypeptide is significantly amplified in certain types of lung or colon tumors and is therefore, a valuable diagnostic marker for identifying certain types of lung or colon cancers.

**C. The Utility of the Claimed Nucleic Acids Does Not Depend Upon the Properties of the Encoded Polypeptide**

On page 4 of the final Office Action mailed October 20, 2005, the Examiner points out that “there is no evidence regarding whether or not PRO1097 mRNA or polypeptide levels are also increased in this cancer”. The Examiner points out, especially on page 4-5 of the Final Office Action, that:

“what is often seen is a lack of correlation between DNA amplification and increased peptide levels (Pennica *et al.*) As discussed by Haynes *et al.*, polypeptide levels cannot be accurately predicted from mRNA levels...the literature cautions researchers against drawing conclusions based on small changes in transcript expression levels between normal and cancerous tissue.”

Appellants strongly disagree. First of all, Appellants submit that the instant claims are directed to nucleic acids, not polypeptides, therefore, the issue of whether there is a correlation between gene amplification and polypeptide expression levels is irrelevant. One of skill in the art would understand how to use the claimed nucleic acids to detect amplification of the gene encoding PRO1097, and how to use the gene amplification results to diagnose cancer. Thus the question of whether or not PRO1097 mRNA or polypeptide levels are also increased in these cancers has no relevance to the utility of the claimed nucleic acid molecules.

The claimed nucleic acids can be used in cancer diagnosis without any knowledge regarding the function or cellular role of the encoded protein. Appellants submit that the law clearly states that “it is not a requirement of patentability that an inventor correctly set forth, or even know, how or why the invention works.” *Newman v. Quigg*, 11 USPQ2d 1340 (Fed. Cir.

1989). Accordingly, the disclosure or identification of the mechanism by which PRO1097 is associated with cancer is not required in order to establish the patentable utility of the claimed PRO1097 nucleic acids.

**D. A prima facie case of lack of utility has not been established**

The Examiner further cited Hu *et al.*, to show that “the literature cautions researchers against drawing conclusions based on small changes in transcript expression levels between normal and cancerous tissues” (Page 5 of the Final Office action mailed October 20, 2004).

First of all, as discussed above, the increase in DNA copy number for the PRO1097 gene is significant and would not be considered “small” according to the Goddard declaration. Further, contrary to the Examiner’s assertion, the cited Hu *et al.* reference does not conclusively establish a *prima facie* case for lack of utility for the PRO1097 molecule. The Hu *et al.* reference is entitled “Analysis of Genomic and Proteomic Data using Advanced Literature Mining” (emphasis added). Therefore, as the title itself suggests, the conclusions in this reference are based upon statistical analysis of information obtained from published literature, and not from experimental data. Hu *et al.* performed statistical analysis to provide evidence for a relationship between mRNA expression and biological function of a given molecule (as in disease). The conclusions of Hu *et al.* however, only apply to a specific type of breast tumor (estrogen receptor (ER)-positive breast tumor) and cannot be generalized to breast cancer genes in general, let alone to cancer genes in general. Interestingly, the observed correlation was only found among ER-positive (breast) tumors not ER-negative tumors.” (See page 412, left column).

Moreover, the analytical methods utilized by Hu *et al.* have certain statistical drawbacks, as the authors themselves admit. For instance, according to Hu *et al.*, “different statistical methods” were applied to “estimate the strength of gene-disease relationships and evaluated the results.” (See page 406, left column, emphasis added). Using these different statistical methods, Hu *et al.* “[a]ssessed the relative strengths of gene-disease relationships based on the frequency of both co-citation and single citation.” (See page 411, left column). As is well known in the art, different statistical methods allow different variables to be manipulated to affect the resulting outcome. In this regard, the authors disclose that, “Initial attempts to search the literature” using the list of genes, gene names, gene symbols, and frequently used synonyms generated by the authors “revealed several sources of false positives and false negatives.” (See page 406, right

column). The authors add that the false positives caused by “duplicative and unrelated meanings for the term” were “difficult to manage.” Therefore, in order to minimize such false positives, Hu *et al.* disclose that these terms “had to be eliminated entirely, thereby reducing the false positive rate but unavoidably under-representing some genes.” *Id.* (emphasis added). Hence, Hu *et al.* had to manipulate certain aspects of the input data, in order to generate, in their opinion, meaningful results. Further, because the frequency of citation for a given molecule and its relationship to disease only reflects the current research interest of a molecule, and not the true biological function of the molecule, as the authors themselves acknowledge, the “[r]elationship established by frequency of co-citation do not necessarily represent a true biological link.” (See page 411, right column). Therefore, based on these findings, the authors add, “[t]his may reflect a bias in the literature to study the more prevalent type of tumor in the population. Furthermore, this emphasizes that caution must be taken when interpreting experiments that may contain subpopulations that behave very differently.” *Id.* (Emphasis added). In other words, some molecules may have been underrepresented merely because they were less frequently cited or studied in literature compared to other more well-cited or studied genes. Therefore, Hu *et al.*’s conclusions are not based on genes/mRNA *in general*.

Appellants submit that, based on the nature of the statistical analysis performed herein, and in particular, based on Hu’s analysis of only *one* class of genes, namely, the estrogen receptor (ER)-positive breast tumor genes, the conclusions drawn by the Examiner, namely that, “genes displaying a 5-fold change or less (mRNA expression) in tumors compared to normal showed no evidence of a correlation between altered gene expression and a known role in the disease (in general)” is not reliably supported.

In conclusion, when the proper legal standard is used, a *prima facie* case of lack of utility has not been met based on the cited references Pennica *et al.*, Haynes *et al.* or Hu *et al.* by the Examiner.

On the contrary, Appellants submit that Example 170 in the specification discloses evidence to show that the PRO1097 gene is amplified in lung or colon cancers, and is therefore useful in the diagnosis of these cancers.

Thus, based on the asserted utility for the PRO1097 gene in the diagnosis of selected lung or colon tumors, the reduction to practice of the instantly claimed nucleic acid sequence of SEQ ID NO: 348 in the present application (also see page 305), the disclosure of the step-by-step

protocols for making and isolating cDNA clones encoding PRO1097 of SEQ ID NO:348 at least in Example 107, page 489 of the specification, the disclosure of a step-by-step protocol for expressing PRO1097 cDNA in appropriate host cells (in Examples 140-143 and page 376, line 12), the step-by-step protocol of the gene amplification assay in Example 170, the skilled artisan would know exactly how to make and use the claimed nucleic acids for the diagnosis of lung or colon cancers. Appellants submit that based on the detailed information presented in the specification and the advanced state of the art in oncology, the skilled artisan would not have found any experimentation associated with testing lung or colon tumors, given the present disclosure, 'undue'.

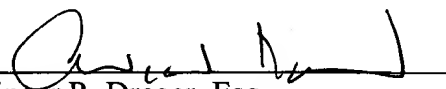
Therefore, since the instantly claimed invention is supported by either a credible, specific and substantial asserted utility or a well-established utility, and since the present specification clearly teaches one skilled in the art "how to make and use" the claimed invention without undue experimentation, Appellants respectfully request reconsideration and reversal of this outstanding rejection under 35 U.S.C. §101 and §112, First Paragraph to Claims 124, 129-131 and 135-145.

### **CONCLUSION**

For the reasons given above, Appellants submit that present specification clearly describes, details and provides a patentable utility for the claimed invention. Moreover, it is respectfully submitted that based upon this disclosed patentable utility, the present specification clearly teaches "how to use" the presently claimed nucleic acid. As such, Appellants respectfully request reconsideration and reversal of the outstanding rejection of claims 124, 129-131 and 135-145.

Respectfully submitted,

Date: November 14, 2005

  
Ginger R. Dreger, Esq.  
Reg. No. 33,055

**HELLER EHRMAN LLP**  
275 Middlefield Road  
Menlo Park, California 94025-3506  
Telephone: (650) 324-7000  
Facsimile: (650) 324-0638

## VIII. CLAIMS APPENDIX

### Claims on Appeal

124. An isolated nucleic acid comprising:

- (a) the nucleic acid sequence of SEQ ID NO: 348;
- (b) the full-length coding sequence of the nucleic acid sequence of SEQ ID NO: 348;

or

(c) the full-length coding sequence of the cDNA deposited under ATCC accession number 203044.

129. The isolated nucleic acid of Claim 124 comprising the nucleic acid sequence of SEQ ID NO: 348.

130. The isolated nucleic acid of Claim 124 comprising the full-length coding sequence of the nucleic acid sequence of SEQ ID NO: 348.

131. The isolated nucleic acid of Claim 124 comprising the full-length coding sequence of the cDNA deposited under ATCC accession number 203044.

135. A vector comprising the nucleic acid of Claim 124.

136. The vector of Claim 135, wherein said nucleic acid is operably linked to control sequences recognized by a host cell transformed with the vector.

137. A host cell comprising the vector of Claim 135.

138. The host cell of Claim 137, wherein said cell is a CHO cell, an *E. coli* or a yeast cell.

139. An isolated nucleic acid molecule consisting of a fragment of the nucleic acid sequence of SEQ ID NO: 348, or a complement thereof, of at least 20 nucleotides in length that hybridizes under stringent conditions to:

- (a) the nucleic acid sequence of SEQ ID NO: 348 or a complement thereof;
- (b) the full-length coding sequence of the cDNA deposited under ATCC accession number 203044 or a complement thereof;

wherein, said stringent conditions use 50% formamide, 5X SSC, 50 mM sodium phosphate (pH 6.8), 0.1% sodium pyrophosphate, 5X Denhardt's solution, sonicated salmon sperm DNA (50 µg/ml), 0.1% SDS, and 10% dextran sulfate at 42°C, and washes at 42°C in 0.2X SSC, at 55°C in 50% formamide followed by a high-stringency wash at 55°C in 0.1X SSC, EDTA; wherein said isolated nucleic acid molecule is suitable for use as a PCR primer or probe.

140. The isolated nucleic acid molecule of Claim 139 that is at least 50 nucleotides or above in length.

141. The isolated nucleic acid molecule of Claim 139 that is at least 60 nucleotides or above in length.

142. The isolated nucleic acid molecule of Claim 139 that is at least 70 nucleotides or above in length.

143. The isolated nucleic acid molecule of Claim 139 that is at least 80 nucleotides or above in length.

144. The isolated nucleic acid molecule of Claim 139 that is at least 90 nucleotides or above in length.

145. The isolated nucleic acid molecule of Claim 139 that is at least 100 nucleotides or above in length.

## IX. EVIDENCE APPENDIX

1. Hittelman *et al.* "Genetic instability in epithelial tissues at risk for cancer," *Ann. NY Acad Sci.* **952**:1-12 (2001).
2. Crowell *et al.* "Detection of trisomy 7 in nonmalignant bronchial epithelium from lung cancer patients and individuals at risk for lung cancer," *Cancer Epidemiol.* **5**:631-637 (1996).
3. Pennica *et al.*, "WISP genes are members of the connective tissue growth factor family that are up-regulated in Wnt-1-transformed cells and aberrantly expressed in human colon tumors," *Proc. Natl. Acad. Sci. USA* **95**:14717-14722 (1998).
4. Haynes *et al.*, "Proteome analysis: Biological assay or data archive?" *Electrophoresis* **19**:1862-1871 (1996).
5. Kobayashi *et al.*, 2000, Accession No. D00102.
6. Hu *et al.*, "Analysis of genomic and proteomic data using advanced literature mining," *Journal of Proteome Research* **2**:405-412 (2003).
7. Declaration of Audrey Goddard, Ph.D. under 35 C.F.R. 1.132, with attached Exhibits A-G:
  - A. Curriculum Vitae of Audrey D. Goddard, Ph.D.
  - B. Higuchi, R. *et al.*, "Simultaneous amplification and detection of specific DNA sequences," *Biotechnology* **10**:413-417 (1992).
  - C. Livak, K.J., *et al.*, "Oligonucleotides with fluorescent dyes at opposite ends provide a quenched probe system useful for detecting PCR product and nucleic acid hybridization," *PCR Methods Appl.* **4**:357-362 (1995).
  - D. Heid, C.A. *et al.*, "Real time quantitative PCR," *Genome Res.* **6**:986-994 (1996).
  - E. Pennica, D. *et al.*, "WISP genes are members of the connective tissue growth factor family that are up-regulated in Wnt-1-transformed cells and aberrantly expressed in human colon tumors," *Proc. Natl. Acad. Sci. USA* **95**:14717-14722 (1998).
  - F. Pitti, R.M. *et al.*, "Genomic amplification of a decoy receptor for Fas ligand in lung and colon cancer," *Nature* **396**:699-703 (1998).
  - G. Bieche, I. *et al.*, "Novel approach to quantitative polymerase chain reaction using real-time detection: Application to the detection of gene amplification in breast cancer," *Int. J. Cancer* **78**:661-666 (1998).



Items 1-5 were made of record by the Examiner in the Office Action mailed April 30, 2004.

Items 3-4 and 6 were made of record by the Examiner in the Final Office Action mailed October 20, 2004.

Item 7 was submitted with the Appellants' Response filed on August 25, 2005 and whose entry was indicated as acceptable in a telephone conference with Examiner Wegert on August 24, 2005.

**X. RELATED PROCEEDINGS APPENDIX**

None

## Genetic Instability in Epithelial Tissues at Risk for Cancer

WALTER N. HITTELMAN

Department of Experimental Therapeutics, The University of Texas  
M. D. Anderson Cancer Center, Houston, Texas 77030, USA

**ABSTRACT:** Epithelial tumors develop through a multistep process driven by genomic instability frequently associated with etiologic agents such as prolonged tobacco smoke exposure or human papilloma virus (HPV) infection. The purpose of the studies reported here was to examine the nature of genomic instability in epithelial tissues at cancer risk in order to identify tissue genetic biomarkers that might be used to assess an individual's cancer risk and response to chemopreventive intervention. As part of several chemoprevention trials, biopsies were obtained from risk tissues (i.e., bronchial biopsies from chronic smokers, oral or laryngeal biopsies from individuals with premalignancy) and examined for chromosome instability using *in situ* hybridization. Nearly all biopsy specimens show evidence for chromosome instability throughout the exposed tissue. Increased chromosome instability was observed with histologic progression in the normal to tumor transition of head and neck squamous cell carcinomas. Chromosome instability was also seen in premalignant head and neck lesions, and high levels were associated with subsequent tumor development. In bronchial biopsies of current smokers, the level of ongoing chromosome instability correlated with smoking intensity (e.g., packs/day), whereas the chromosome index (average number of chromosome copies per cell) correlated with cumulative tobacco exposure (i.e., pack-years). Spatial chromosome analyses of the epithelium demonstrated multifocal clonal outgrowths. In former smokers, random chromosome instability was reduced; however, clonal populations appeared to persist for many years, perhaps accounting for continued lung cancer risk following smoking cessation.

**KEYWORDS:** chromosome instability; epithelial cells; aerodigestive tract; chemoprevention; cancer risk

### THE NEED FOR BIOMARKERS OF CANCER RISK AND RESPONSE TO INTERVENTION

Epithelial cancers remain a major health challenge in the world. Despite improvements in staging and the application and integration of surgery, radiotherapy, and chemotherapy, the 5-year survival rate for individuals with lung cancer is only about 15%.<sup>1</sup> Even if strategies for early detection are successful and lung cancers are detected at a stage where local tumor resection and treatment is curative, these patients will still be at significant risk for developing second primary tumors

Address for correspondence: Dr. Walter N. Hittelman, Department of Experimental Therapeutics, The University of Texas M. D. Anderson Cancer Center, 1515 Holcombe Blvd. (Box 19), Houston, Texas 77030. Voice: 713-792-2961; fax: 713-792-3754.  
whittelm@mdanderson.org

associated with the problem of field cancerization.<sup>2</sup> Similarly, for individuals with a first head and neck primary tumor, even if the first malignancy is successfully treated, the risk of developing a second primary in the tobacco smoke-exposed field is approximately 40%.<sup>3</sup> Similar cancer risk estimates exist for individuals who exhibit severe dysplasia in premalignant epithelial lesions.<sup>4</sup> For these reasons, it is important to focus on chemopreventive strategies to prevent the development of epithelial malignancies.

Several problems confront chemoprevention trials designed to identify efficacious agents.<sup>5</sup> First, chemoprevention trials with cancer incidence as a primary endpoint require tens of thousands of subjects and tens of years of intervention and follow-up for statistical evaluation. For example, a recently reported trial involved 30,000 subjects and required 10 years in order to examine the impact of prevention strategies on lung cancer development, only to find a possible increased lung cancer incidence in current smokers who received  $\beta$ -carotene.<sup>6</sup>

The problem of large, long-term trials results from the difficulty in identifying individuals at highest cancer risk who might best benefit from chemopreventive intervention. For example, 20 pack-year smokers, while known to be at relatively increased risk for developing lung cancer, have approximately a 10% lifetime risk for developing lung cancer.<sup>7</sup> This seriously limits the number of potentially useful strategies that can be clinically explored. A second problem facing chemoprevention trials is that little is known about what agents are likely to have efficacy, and even less is known regarding proper doses, schedules, and durations of treatment. Part of the reason for this problem is that too little is known about the physiologic processes that drive epithelial cancer development.

In order to reduce the number of subjects and the time required to carry out chemoprevention trials and thus allow the exploration of multiple prevention strategies, two types of advances are necessary. First, it is important to identify individuals at significantly increased cancer risk who might best benefit from different types of intervention. Second, in order to allow the rapid identification of agents, doses, and schedules of potentially efficacious agents, it is necessary to identify and validate surrogate endpoints of response that indicate whether the agents are having a positive impact on the target tissue during the chemopreventive intervention.

One approach to identifying individuals at increased aerodigestive tract cancer risk is to explore epidemiologic features of potential subjects. Molecular epidemiologic studies are beginning to identify intrinsic host factors that place some individuals at increased cancer risk, especially those with a chronic smoking history.<sup>8</sup> Most intrinsic factors identified thus far reflect levels of carcinogen metabolism, repair capabilities of the host following DNA damage, and other measures of intrinsic cellular sensitivity to mutagens. While these factors can provide statistically significant risk ratios in case-control studies that are controlled for tobacco exposure, the detected risk ratios usually fall in the range of 1.5 to 10. Unfortunately, this is not sufficient for the individualization of treatment and is not sufficiently high to significantly reduce the numbers of subjects required for chemoprevention trials with cancer incidence as the primary endpoint.

Another approach to identifying individuals at increased cancer risk is to directly examine the target tissue of individuals with known carcinogen exposure (e.g., chronic tobacco smoke exposure), who have evidence of target organ dysfunction

(e.g., chronic obstructive pulmonary disease, changes in voice quality), or who have clinical evidence of premalignancy (e.g., bronchial metaplasia/dysplasia, oral leukoplakia/erythroplakia, cervical intraepithelial neoplasia). The conventional standard for assessing cancer risk in these situations is the degree of histological change. However, while individuals who show moderate to severe dysplasia are known to be at increased cancer risk when compared to individuals with lesser histologic changes, it is often difficult to distinguish reactive changes to carcinogenic insult from initiated and progressing lesions. Similarly, upon cessation of carcinogenic insult, histologic changes may reverse yet cancer risk may continue for many years. For example, while smoking cessation is associated with decreased bronchial metaplasia,<sup>9</sup> increased lung cancer risk continues for many years beyond smoking cessation.<sup>10</sup> In fact, nearly half the newly diagnosed lung cancer cases in the USA occur in former smokers.<sup>11</sup>

The development of assays to identify individuals at high epithelial cancer risk and to directly assess response to intervention in the target tissue is therefore an important research goal. Such assays should be objective and easily quantifiable and, if possible, minimally invasive. Moreover, they should reflect both the disease process and the targeted pathway and thereby be useful in assessing risk and monitoring response to intervention as well as directly testing the hypothesized mechanism of action of the chemopreventive strategy.

In the chemoprevention setting it is important to recognize that one does not know the location of the future cancer. Thus, assays must necessarily be carried out on random biopsies of the field at risk. Even if there are clinically evident premalignant lesions, this does not mean that this is the likely site for a future malignancy. For example, nearly half of the cancers that develop in individuals with oral leukoplakia arise away from the original index lesion. Similarly, since many newly diagnosed lung cancers arise in the peripheral parts of the lung (e.g., adenocarcinomas), especially in former smokers, and since endobronchoscopy predominantly accesses central components of the lung, it is important to identify biomarkers that can reflect global processes ongoing in the target epithelial field associated with increased cancer risk. Their discovery requires a better understanding of the tumorigenesis process in epithelial fields at cancer risk.

#### THE RATIONALE FOR STUDYING GENOMIC INSTABILITY AS A MARKER OF RISK

Tumors of the aerodigestive tract have been proposed to reflect a "field cancerization" process whereby the whole tissue is exposed to carcinogenic insult (e.g., tobacco smoke) and is at increased risk for multistep tumor development.<sup>12,13</sup> Several types of clinical and laboratory data support this notion, including the frequent occurrence of synchronous primary and subsequent second primary tumors in the aerodigestive tract (frequently exhibiting dissimilar histologies as well as distinct genetic signatures<sup>14-16</sup>) and the presence of premalignant lesions that precede and/or accompany the tumor in the exposed tissue field.<sup>17</sup> The notion of a multistep tumorigenesis process is further supported by serial clinical and histologic evaluations of

target tissue or exfoliated cells where increasing degrees of histological abnormalities are observed over time.<sup>18</sup>

A working model for aerodigestive tract tumorigenesis is illustrated in FIGURE 1. Tumorigenesis in the face of carcinogenic exposure likely involves a chronic process of tissue injury and wound healing. DNA damage induced by the carcinogen is likely fixed into permanent genetic changes (e.g., chromosome damage, chromosome non-disjunction, gene mutation, gene deletion, etc.) during the process of proliferation. This damage would be expected to be distributed throughout the exposed tissue field leading to a background of generalized genomic damage (depicted in FIGURE 1 as a background mat of increasing density). Chronic injury and repair likely leads to the accumulation of cells with increasing amounts of genetic changes as well as the outgrowth of abnormal clones (triangles in FIGURE 1) carrying an accumulation of genetic changes important for selective survival, dysregulated growth, and preferential epithelial take-over by initiated clones (see FIGURE 2).

Cellular and molecular evidence for the field carcinogenesis and multistep tumorigenesis model comes from many laboratories.<sup>19,20</sup> With the advent of a wide array of molecular technologies, a large number of specific molecular genetic and epigenetic changes involving specific oncogenes, tumor suppressor genes, cell regulatory genes, and repair genes have now been described for aerodigestive tract cancers. The identification of these specific molecular changes have now provided probes to explore specific events occurring in premalignant lesions adjacent to aerodigestive tract tumors.<sup>21-24</sup> Frequently, these premalignant lesions showed a subset of the same molecular changes found in the associated tumor, suggesting that these lesions might represent precursor lesions for the associated tumors (i.e., a manifestation of

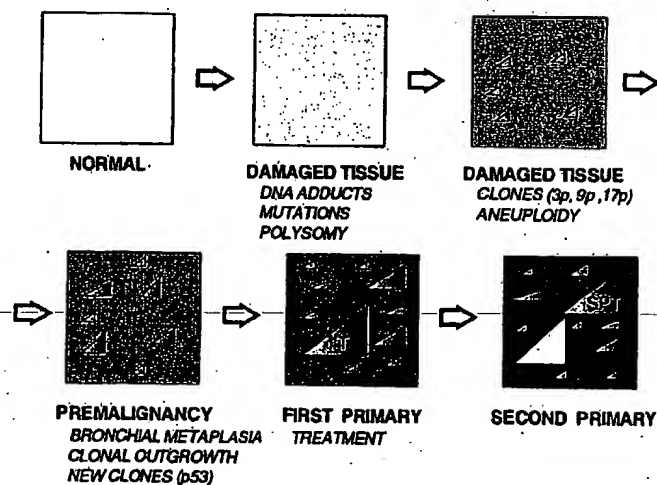


FIGURE 1. Field cancerization and multistep tumorigenesis.

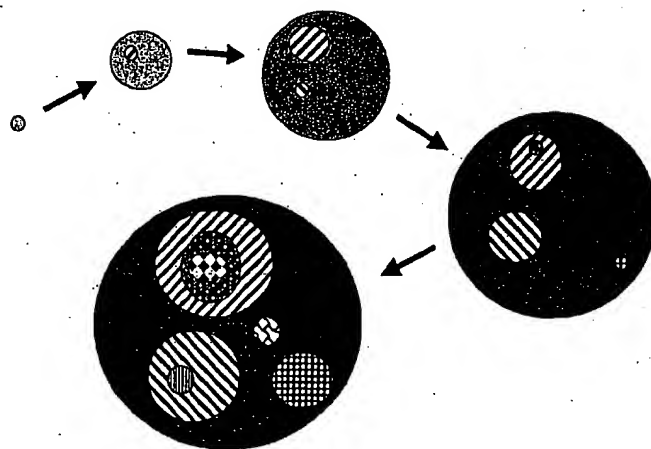


FIGURE 2. Multiple focal clonal evolution during multistep tumorigenesis.

a multistep tumorigenesis process). For example, studies of the premalignant lesions adjacent to head and neck tumors have provided evidence for a gradual accumulation of genetic alterations accompanied by evidence for dysregulation of cellular control mechanisms (e.g., alterations in expression of PCNA, EGFR, TGF- $\beta$ , p53, and cyclin D1).<sup>25-28</sup>

These types of studies have now also been applied to the target epithelium of individuals at increased risk for aerodigestive tract cancer (i.e., individuals with a chronic smoking/alcohol history and/or prior aerodigestive tract cancer). Several groups (using polymerase chain reaction, PCR, analysis of microdissected epithelium) have now demonstrated the presence of clonal outgrowths in the target premalignant epithelium of individuals at increased risk for cancer.<sup>29-31</sup> For example, examination of bronchial biopsies derived from individuals with a 20 pack-year smoking history demonstrated that 76% of the cases showed evidence for LOH (3p14, 9p21, or 17p13) in at least one of six lung biopsy sites. On a per site basis, some form of LOH was observed in 25% of the sites examined.<sup>29</sup>

If aerodigestive tract cancer development reflects a field cancerization process involving multistep events, then risk and response information should be able to be derived from random biopsies or exfoliated cells from the field at risk or from assessments of tissue undergoing similar processes. Hypothetically, lesions exhibiting the greatest degree of genomic instability, clonal outgrowth, and abnormal epithelial regulation would be at the highest relative aerodigestive tract cancer risk. Similarly, an active chemopreventive intervention might be expected to decrease these manifestations of risk. Reduced risk manifestations include decreased levels of ongoing genetic instability, decreased frequency of clonal outgrowths, and increased epithelial growth regulation.

### THE MEASUREMENT OF CHROMOSOME INSTABILITY USING CHROMOSOME *IN SITU* HYBRIDIZATION

Molecular genetic techniques, while extremely useful for detecting clonal changes in target tissues, are somewhat limited in their ability to detect random genetic instability. Conventional cytogenetic assays are useful for detecting chromosome instability and clonal chromosome changes. However, they require numbers of dividing cells for karyotypic analysis that are difficult to attain in the setting of biopsies acquired during the course of a chemoprevention trial. A technique was therefore needed that would allow chromosome instability measurements in situations where few cells are available (e.g. small biopsies, brushings, or sputum samples) and where the target material might be fixed. It was also desirable to have a technique that would be adaptable to tissue sections, whereby spatial information could be retained and genotype/phenotype associations could be determined on the same or adjacent tissue sections. The technique of *in situ* hybridization (ISH) involves the use of DNA probes that recognize either chromosome-specific repetitive target sequences, chromosome single gene copy sequences, or sequences along the whole chromosome length or chromosome segments.<sup>32</sup> We have adapted the ISH technique for formalin-fixed, paraffin-embedded tissue sections and have applied it to a variety of tissues, including the aerodigestive tract.<sup>33,34</sup>

Using probes that label the centromere regions of specific chromosomes, this assay permits determination of the average chromosome number per cell for each specimen. This assay is also useful for detecting generalized chromosome instability during the tumorigenesis process. Normal diploid populations should have two copies of each autosomal chromosome and should rarely show three or more chromosome copies per cell (chromosome polysomy), especially in tissue sections where nuclear truncation results in an under-representation of chromosome copy number. Thus, the detection of cells with three or more chromosome copies would indicate the presence of chromosome instability.

To examine this technique's potential for characterizing the multistep tumorigenesis process in the aerodigestive tract, we measured the fraction of cells exhibiting three or more chromosome copies in apparently contiguous epithelial transitions from normal to hyperplastic to dysplastic to carcinomas, all on a single tissue slice of head and neck squamous cell carcinomas.<sup>34</sup> In these specimens, greater than 35% of the cases of adjacent "normal" epithelium, greater than 65% of the cases of hyperplastic epithelium, and greater than 95% of the dysplastic and tumor regions showed evidence of chromosome polysomy. Of interest, similar transitions of chromosome instability were observed with at least four different chromosome probes. Similar trends have also been observed in amenable tissue from other epithelial malignancies, including cervix, bladder, and breast.<sup>35</sup> These results thus suggested that the notions of field cancerization and multistep tumorigenesis might apply to several epithelial tissues and that measures of chromosome instability might be useful for monitoring this process.

In the situations described above, the premalignant lesions examined might be considered to represent epithelium at 100% risk of being in a cancer field, since they were located in the adjacent epithelium to the cancer. This then raises the question of the nature of genetic instability in the epithelium of individuals at increased risk



for developing cancer. To explore this issue, we obtained biopsies during the course of leukoplakia chemoprevention trials exploring the use of 13-*cis*-retinoic acid in reversing leukoplakia and probed them for genetic instability using *in situ* hybridization. In one retrospective study and in one prospective study of subjects with oral leukoplakia, the results indicate that those subjects whose pretreatment biopsies harbor relatively high levels of genomic instability (i.e., more than 3% of the cells examined showing at least 3 chromosome 9 copies per cell) have a significantly higher likelihood of suffering early onset of head and neck cancer.<sup>36,37</sup> Interestingly, half of the tumors that did develop occurred away from the biopsy site used to measure genetic instability. This result suggests that genomic instability measurements in carcinogen-exposed tissue can provide useful cancer risk estimates.

#### THE RELATIONSHIP BETWEEN TOBACCO EXPOSURE AND CHROMOSOME INSTABILITY

In recent years, the aerodigestive tract chemoprevention group at M.D. Anderson Cancer Center has initiated three sequential biomarker-associated chemoprevention trials involving chronic smokers with a greater than 20 pack-year smoking history. In each of these studies, endobronchial biopsies were obtained from six defined sites within the lung, including the carina and at bifurcation points at the upper, middle, and lower right lung and at the upper and lower left lung. Biopsies were obtained prior to and following chemopreventive intervention and were subjected to *in situ* hybridization analysis in addition to analyses for other biomarkers. The first important finding was that some degree of chromosome polysomy was evident in all lung sites examined, and this was observed independently of the particular chromosome probe utilized.<sup>38</sup> This finding supports the notion that random chromosome changes may be occurring throughout the exposed lung field.

In a second study, bronchial biopsies were obtained from individuals with a 20 pack-year smoking history. In this study, most of the subjects involved were current smokers.<sup>39</sup> Interestingly, all cases who showed metaplasia at one of six biopsy sites also showed chromosome polysomy in at least one biopsy site; overall, 88% of the sites showed some evidence of chromosome 9 polysomy.<sup>40</sup> Evidence for genetic instability was also detected in patients who did not show evidence of bronchial metaplasia in any of six biopsy sites despite a strong smoking history. In fact, more than 90% of the cases and more than 60% of the sites showed significant chromosome polysomy (i.e., at least three copies in at least 2 % of the cells examined). These results suggest that the lungs of long-term smokers show significant evidence of genetic instability, and this instability can be detected throughout the accessible bronchial tree, even when bronchial metaplasia is not evident.

These studies in current smokers has allowed us to examine the relationship between the levels of genetic instability detected and subject characteristics such as smoking status (current or former), smoking history, and lung tissue pathologic changes. Evaluable biopsy material has now been obtained from more than 108 current smokers, including more than 480 evaluable biopsy sites. The mean metaplasia index in these current smokers was 30.4%. For the total population studied, the median chromosome index for the bronchial biopsies was 1.41 (range, 1.04-1.61)

and the median chromosome polysomy index was 2.0% (range 0–8.7%). This can be compared to a mean chromosome index between 1.2–1.4 for lymphocytes and very rare chromosome polysomy. Interestingly, the intrasubject variability in chromosome instability was relatively low in most subjects and was less than the intersubject variability. These results suggested that chronic smokers harbor detectable chromosome instability throughout the accessible bronchial tree (supporting the field carcinogenesis notion) and that information from one biopsy site might yield representative information for the rest of the lung field.

Since most of the current smokers exhibited bronchial metaplasia in at least one of the biopsied sites, this allowed us to examine the relationship between chromosome instability and histologic changes, both on a site-by-site basis and on a per case basis. On a site-by-site basis, the chromosome indices of lesions showing squamous metaplasia were similar to those not showing metaplasia (i.e., median 1.43 vs. 1.43), and the degree of chromosome polysomy in metaplastic lesions were only slightly higher than in non-metaplastic sites (medians: 2.2% vs. 1.8%, respectively). Thus, the presence or absence of squamous metaplasia at a biopsy site does not necessarily correlate with the degree of underlying genomic instability. On the other hand, those subjects with metaplasia indices of at least 15% also showed higher levels of chromosome polysomy than did subjects with metaplasia index below 15% (medians: 2.4% vs. 1.8%,  $p = 0.005$ ). Thus, these chromosome instability assessments in current smokers appeared to reflect a more global process in the lung field.

Tobacco exposure has been shown to significantly increase the risk of developing lung cancer, and the degree of risk is related to the extent of tobacco exposure. We were interested in determining the relationship between individuals' smoking history parameters and the levels of chromosome change found in their lungs following years of tobacco exposure. While there was significant intersubject variation for similar tobacco exposure histories, overall there was a significant correlation between the degree of chromosome polysomy and the intensity of ongoing tobacco exposure (packs/day,  $p = 0.02$  on a per site basis) and with the extent of tobacco exposure (pack-years,  $p = 0.003$ ). Thus the amount of chromosome polysomy reflects the intensity and extent of tobacco exposure. At the same time, individuals with similar smoking histories showed widely divergent amounts of chromosome polysomy, possibly reflecting differences in intrinsic sensitivity between subjects. There was also strong correlation between the chromosome index and the duration of the smoking history (smoking years) and total accumulated exposure (pack-years,  $p = 0.0001$ ). These results suggest that tobacco exposure is associated with the initiation and accumulation of chromosome instability in the exposed lung; however individuals are differentially sensitive to carcinogenic insult. The working hypothesis is that those individuals who accumulate the highest degree of chromosome changes will be at the highest lung cancer risk.

Many of the bronchial biopsies from chronic smokers examined by *in situ* hybridization showed a rise in the chromosome index above that expected for a diploid cell population, especially in subjects with an extensive smoking history. The rise in chromosome index was also accompanied by an increase in the fraction of cells exhibiting at least 3 chromosome copies per cell. To determine if a rise in the tissue chromosome index was due to clonal expansion of populations with chromosome trisomy, the chromosome copy number and relative coordinates of each cell scored in

the bronchial epithelium was recorded and a spatial genetic map was created.<sup>41</sup> We then developed algorithms for calculating localized chromosome indices within the tissue. Since trisomic clones would have, on average, three chromosomes instead of two, those cells involved in neighborhoods with chromosome indices three-halves that of diploid populations could be marked as being part of a trisomic clone. Similarly, groups of cells with chromosome indices half that of diploid populations could be marked as being part of a monosomic clone. This allowed the generation of a second-order, two-dimensional genetic map representation of the bronchial epithelium showing the relative locations of cells involved in monosomic and trisomic clonal outgrowths. When adjacent tissue sections from the same bronchial biopsy were probed separately for different chromosomes, the detected clones appeared to occupy separate subregions of the epithelium. This result suggests that not only are the lungs of chronic smokers undergoing a process of genetic instability, they are experiencing the outgrowth of multiple clones throughout the exposed lung field, as postulated by the models shown in FIGURES 1 and 2. One advantage of this clonal approach is that the contribution of both monosomic and multisomic clones can be detected.

Since smoking cessation has been suggested to reduce the lung cancer risk, it was of interest to determine whether the levels of chromosome instability would decrease following smoking cessation. This question was possible to examine because our third sequential chemoprevention trial involved subjects who had discontinued smoking. So far, more than 220 subjects (more than 650 biopsies) who have quit smoking (mean 9.9 quit-years) have been evaluated for chromosome instability in their lungs. Despite the fact that the mean metaplasia index in this group is 5.8% (considerably less than that in current smokers), chromosome instability is still observed in the majority of subjects.<sup>42</sup> While the mean chromosome polysomy level is reduced to 1.0%, some individuals continue to show polysomy levels above 5%. Interestingly, while the overall chromosome polysomy levels were reduced in these individuals who stopped smoking, the mean chromosome index remained at about 1.4 with some individuals exhibiting chromosome indices as high as 1.8. Initial chromosome mapping studies suggest that while random chromosome instability seems to decrease following smoking cessation, the clonal outgrowths may remain for many years in the lung. The working hypothesis is that those individuals who show the greatest degree of remaining chromosome instability are at the highest lung cancer risk despite smoking cessation. Long-term follow-up on these subjects will be necessary to test this hypothesis.

---

#### SUMMARY AND CONCLUSIONS

Aerodigestive tract tumorigenesis appears to be a multistep process taking place throughout the tissue fields of exposure. When viewed in the context of chromosome changes, carcinogen exposure appears to be associated with the random acquisition of chromosome polysomy throughout the exposed field, the degree of which is related to the degree and extent of carcinogen exposure as well as to the intrinsic susceptibility of the exposed individual. Continued exposure leads to continued acquisition of new changes and, in association with chronic wound-healing processes, to the

accumulation of clonal outgrowths throughout the target tissue. Although the ultimate malignancy may occur in only one or few tissue sites, manifestations of the instability process that drives tumorigenesis is globally present in the tissue. Thus random biopsies may provide useful risk information for the exposed field as a whole. Even when carcinogen exposure is reduced or chemopreventive strategies are initiated and histologic manifestations of the tumorigenesis process subside, the genetic scars of prior exposure remain in the form of clonal outgrowths and may explain continued lung cancer risk in ex-smokers. Future chemoprevention strategies need to focus on reducing the degree of chromosome instability and on trying to eliminate residual abnormal clonal outgrowths in the aerodigestive tract. In this setting, the measurement of chromosome instability in the target tissue will be useful in assessing cancer risk as well as response to intervention.

#### ACKNOWLEDGMENTS

The studies reviewed here represent one component of the collaborative efforts of the Aerodigestive Tract Chemoprevention team at The University of Texas M.D. Anderson Cancer Center, Houston, Texas. The studies were supported in part by National Institutes of Health-National Cancer Institute Grants CA-52051, CA-68437, CA 79437, CA 16672, CA 68089, CN 25433, CA 86390, CA 70907, NIH DE 13157, and the State of Texas Tobacco Research Fund.

#### REFERENCES

1. LANDIS, S.H., T. MURRAY, S. BOLDEN & P.A. WINGO. 1998. Cancer statistics, 1998. *CA Cancer J. Clin.* 48: 6-29.
2. JOHNSON, B.E. 1998. Second lung cancers in patients after treatment for an initial lung cancer. *J. Natl. Cancer Inst.* 90: 1335-1345.
3. LIPPMAN, S.M. & W.K. HONG. 1989. Second malignant tumors in head and neck squamous cell carcinoma: The overshadowing threat for patients with early stage of disease. *Int. J. Radiat. Oncol. Biol. Phys.* 17: 691-694.
4. SILVERMAN, S.J., JR., M. GORSKY & F. LOZADA. 1984. Oral leukoplakia and malignant transformation: a follow-up study of 257 patients. *Cancer* 53: 563-568.
5. LIPPMAN, S.M., J.S. LEE, R. LOTAN, *et al.* 1990. Biomarkers as intermediate endpoints in chemoprevention trials. *J. Natl. Cancer Inst.* 82: 555-560.
6. HEINONEN, O.P., D. ALBANES & THE ALPHA-TOCOPHEROL, BETA CAROTENE CANCER PREVENTION STUDY GROUP. 1994. The effect of vitamin E and beta carotene on the incidence of lung cancer and other cancers in male smokers. *N. Engl. J. Med.* 330: 1029-1035.
7. PETO, R., S. DARBY, H. DEO, *et al.* 2000. Smoking, smoking cessation, and lung cancer in the UK since 1950: combination of national statistics with two case-control studies. *Brit. Med. J.* 321: 323-329.
8. PERERA, F.P. 1996 Molecular epidemiology: insights into cancer susceptibility, risk assessment, and prevention. *J. Natl. Cancer Inst.* 88: 496-509.
9. LEE, J.S., S.M. LIPPMAN, S.E. BENNER, *et al.* 1994. Randomized placebo-controlled trial of isotretinoin in chemoprevention of bronchial squamous metaplasia. *J. Clin. Oncol.* 12: 937-941.

10. U.S. DEPARTMENT OF HEALTH AND HUMAN SERVICES. 1990. The health benefits of smoking cessation: a report of the Surgeon General. U.S. Department of Health and Human Services, Public Health Service, Centers for Disease Control, Center for Chronic Disease Prevention and Health Promotion, Office on Smoking and Health. DHHS Pub. No. (CDC) 90-8416.
11. TONG, L., M.R. SPITZ, J.J. FAEGER, *et al.* 1996. Lung cancer in former smokers. *Cancer* 78: 1004-1010.
12. SLAUGHTER, D.P., H.W. SOUTHWICK & W. SMEJKAL. 1953. Field cancerization in oral stratified squamous epithelium: clinical implications of multicentric origin. *Cancer* 6: 963-968.
13. FARBER, E. 1984. The multistep nature of cancer development. *Cancer Res.* 44: 4217-4223.
14. CHUNG, K.Y., T. MUKHOPADHYAY, J. KIM, *et al.* 1993. Discordant p53 gene mutations in primary head and neck cancers and corresponding second primary cancers of the upper aerodigestive tract. *Cancer Res.* 53: 1676-1683.
15. SCHOLLES, A.G.M., J.A. WOOLGAR, M.A. BOYLE, *et al.* 1998. Synchronous oral carcinomas: independent or common clonal origin? *Cancer Res.* 58: 2003-2006.
16. GLUCKMAN, J.O., J.D. CRISSMAN & J.O. DONEGAN. 1980. Multicentric squamous cell carcinoma of the upper aerodigestive tract. *Head Neck Surg.* 3: 90-96.
17. AUERBACH, O., A.P. STOUT, E.C. HAMMOND, *et al.* 1961. Changes in bronchial epithelium in relation to cigarette smoking and in relation to lung cancer. *N. Engl. J. Med.* 265: 253-267.
18. SACCOMANNO, G., V.E. ARCHER, O. AUERBACH, *et al.* 1974. Development of carcinoma of the lung as reflected in exfoliated cells. *Cancer* 33: 256-270.
19. IZZO, J.G. & W.N. HITTELMAN. 1999. Characterization of multistep tumorigenesis by in situ hybridization. *In* Introduction to Fluorescence In Situ Hybridization: Principles and Clinical Applications. M. Andreeff & D. Pinkel, Eds.: 173-208. John Wiley & Sons, Inc. New York.
20. HITTELMAN, W.N. 1999. Molecular cytogenetic evidence for multistep tumorigenesis: implications for risk assessment and early detection. *In* Molecular Pathology of Cancer. S. Srivastava, D.E. Hensen & A. Gazdar, Eds.: 385-404. IOS Press. Amsterdam, The Netherlands.
21. SUNDARESAN, V., P. GANLY, R. HASLETON, *et al.* 1992. p53 and chromosome 3 abnormalities, characteristic of malignant lung tumours, are detectable in preinvasive lesions of the bronchus. *Oncogene* 7: 1989-1997.
22. KISHIMOTO, Y., K. SUGIO, J.Y. HUNG, *et al.* 1995. Allele-specific loss in chromosome 9p loci in preneoplastic lesions accompanying non-small-cell lung cancers. *J. Natl. Cancer Inst.* 87: 1224-1229.
23. CALIFANO, J., P. VAN DER RIET, W. WESTRA, *et al.* 1996. Genetic progression model for head and neck cancer: implications for field cancerization. *Cancer Res.* 56: 2488-2492.
24. PARK I.W., I.I. WISTUBA, A. MAITRA, *et al.* 1999. Multiple clonal abnormalities in the bronchial epithelium of patients with lung cancer. *J. Natl. Cancer Inst.* 91: 1863-1868.
25. SHIN, D.M., N. VORAVUD, J.Y. RO, *et al.* 1994. Sequential increases in proliferating cell nuclear antigen expression in head and neck tumorigenesis: a potential biomarker. *J. Natl. Cancer Inst.* 85: 971-978.
26. SHIN, D.M., J.Y. RO, W.K. HONG, *et al.* 1994. Dysregulation of epidermal growth factor receptor expression in premalignant lesions during head and neck tumorigenesis. *Cancer Res.* 54: 3153-3159.
27. SHIN, D.M., J. KIM, J.Y. RO, *et al.* 1994. Activation of p53 gene expression in premalignant lesions during head and neck tumorigenesis. *Cancer Res.* 54: 321-326.
28. IZZO, J.G., V.A. PAPADIMITRAKOPOULOU, X.Q. LI, *et al.* 1998. Dysregulated cyclin D1 expression early in head and neck tumorigenesis: in vivo evidence for an association with subsequent gene amplification. *Oncogene* 17: 2313-2322.
29. MAO, L., J.S. LEE, J.M. KURIE, *et al.* 1997. Clonal genetic alterations in the lungs of current and former smokers. *J. Natl. Cancer Inst.* 89: 857-862.

30. WISTUBA, I.I., S. LAM, C. BEHRENS, *et al.* 1997. Molecular damage in the bronchial epithelium of current and former smokers. *J. Natl. Cancer Inst.* 89: 1366-1373.
31. MAO, L., J.S. LEE, Y.H. FAN, *et al.* 1996. Frequent microsatellite alterations at chromosomes 9p21 and 3p14 in oral premalignant lesions and their value in cancer risk assessment. *Nature Med.* 2: 682-685.
32. PODDIGHE, P.J., F.C. RAMAKERS & A.H. HOPMAN. 1992. Interphase cytogenetics of tumours. *J. Pathol.* 166: 215-224.
33. KIM, S.Y., J.S. LEE, J.Y. RO, *et al.* 1993. Interphase cytogenetics in paraffin sections of lung tumors by non-isotopic *in situ* hybridization. Mapping genotype/phenotype heterogeneity. *Am. J. Pathol.* 142: 307-317.
34. VORAVUD, N., D.M. SHIN, J.Y. RO, *et al.* 1993. Increased polysomies of chromosomes 7 and 17 during head and neck multistage tumorigenesis. *Cancer Res.* 53: 2874-2883.
35. HITTELMAN, W.N. 1999. Genetic instability assessments in the lung cancerization field. *In Lung Tumors: Fundamental Biology and Clinical Management.* C. Brambilla & E. Brambilla, Eds.: 255-267. Marcel Dekker, New York.
36. LEE, J.S., S.Y. KIM, W.K. HONG, *et al.* 1993. Detection of chromosomal polysomy in oral leukoplakia, a premalignant lesion. *J. Natl. Cancer Inst.* 85: 1951-1954.
37. LEE, J.J., W.K. HONG, W.N. HITTELMAN, *et al.* 2000. Predicting cancer development in oral leukoplakia: ten years of translational research. *Clin. Cancer Res.* 6: 1702-1710.
38. HITTELMAN W.N., R. YU, J. KURIE, *et al.* 1997. Evidence for genomic instability and clonal outgrowth in the bronchial epithelium of smokers [abstract]. *Proc. Am. Assoc. Cancer Res.* 38: 3097.
39. KURIE, J.M., J.S. LEE, P.R. KHURI, *et al.* N-(4-hydroxyphenyl)retinamide in the chemoprevention of squamous metaplasia and dysplasia of the bronchial epithelium. 2000. *Clin. Cancer Res.* 6: 2973-2979.
40. HITTELMAN, W.N., J.S. LEE, R.C. MORICE, *et al.* 1999. Lack of biomarker modulation in bronchial biopsies of chronic smokers following treatment with N-(4-hydroxyphenyl)retinamide (4-HPR). *Proc. Am. Assoc. Cancer Res.* 40: 2837.
41. HITTELMAN, W.N., J.S. LEE, N. CHEONG, *et al.* 1991. The chromosome view of "field cancerization" and multistep carcinogenesis. Implications for chemopreventive approaches. *In Chemoprevention of Cancer.* V. Pastorino & W.K. Hong, Eds.: 41-47. Georg Thieme Verlag, Stuttgart, Germany.
42. HITTELMAN, W.N., J.J. LEE, J.S. LEE, *et al.* 1998. Persistent genetic instability despite decreased proliferation in human lung tissue following smoking cessation. *Proc. AACR* 39: 336.

## Detection of Trisomy 7 in Nonmalignant Bronchial Epithelium from Lung Cancer Patients and Individuals at Risk for Lung Cancer<sup>1</sup>

Richard E. Crowell, Frank D. Gilliland, R. Thomas Temes, Heidi J. Harms, Robin E. Neft, Evelyn Heaphy, Dennis H. Auckley, Lida A. Crooks, Scott W. Jordan, Jonathan M. Samet, John F. Lechner, and Steven A. Belinsky<sup>2</sup>

Departments of Medicine [R. E. C., E. H., D. H. A.], Surgery [R. T. T.], and Pathology [L. A. C., S. W. J.], Albuquerque Veterans Administration Medical Center and the University of New Mexico Health Sciences Center, Albuquerque, New Mexico 87131; Inhalation Toxicology Research Institute, Albuquerque, New Mexico 87115 [H. J. H., R. E. N., J. F. L., S. A. B.]; Department of Epidemiology and Cancer Control Program, University of New Mexico Cancer Research and Treatment Center, Albuquerque, New Mexico 87131 [F. D. G.]; and Department of Epidemiology, Johns Hopkins University, Baltimore, Maryland 21231 [J. M. S.]

### Abstract

Early identification and subsequent intervention are needed to decrease the high mortality rate associated with lung cancer. The examination of bronchial epithelium for genetic changes could be a valuable approach to identify individuals at greatest risk. The purpose of this investigation was to assay cells recovered from nonmalignant bronchial epithelium by fluorescence *in situ* hybridization for trisomy of chromosome 7, an alteration common in non-small cell lung cancer. Bronchial epithelium was collected during bronchoscopy from 16 cigarette smokers undergoing clinical evaluation for possible lung cancer and from seven individuals with a prior history of underground uranium mining. Normal bronchial epithelium was obtained from individuals without a prior history of smoking (never smokers). Bronchial cells were collected from a segmental bronchus in up to four different lung lobes for cytology and tissue culture. Twelve of 16 smokers were diagnosed with lung cancer. Cytological changes found in bronchial epithelium included squamous metaplasia, hyperplasia, and atypical glandular cells. These changes were present in 33, 12, and 47% of sites from lung cancer patients, smokers, and former uranium miners, respectively. Less than 10% of cells recovered from the diagnostic brush had cytological changes, and in several cases, these changes were present within different lobes from the same patient. Background

frequencies for trisomy 7 were  $1.4 \pm 0.3\%$  in bronchial epithelial cells from never smokers. Eighteen of 42 bronchial sites from lung cancer patients showed significantly elevated frequencies of trisomy 7 compared to never smoker controls. Six of the sites positive for trisomy 7 also contained cytological abnormalities. Trisomy 7 was found in six of seven patients diagnosed with squamous cell carcinoma, one of one patient with adenosquamous cell carcinoma, but in only one of four patients with adenocarcinoma. A significant increase in trisomy 7 frequency was detected in cytologically normal bronchial epithelium collected from four sites in one cancer-free smoker, whereas epithelium from the other smokers did not contain this chromosome abnormality. Finally, trisomy 7 was observed in almost half of the former uranium miners; three of seven sites positive for trisomy 7 also exhibited hyperplasia. Two of the former uranium miners who were positive for trisomy 7 developed squamous cell carcinoma 2 years after collection of bronchial cells. To determine whether the increased frequency of trisomy 7 reflects generalized aneuploidy or specific chromosomal duplication, a subgroup of samples was evaluated for trisomy of chromosome 2; the frequency was not elevated in any of the cases as compared with controls. The studies described in this report are the first to detect and quantify the presence of trisomy 7 in subjects at risk for lung cancer. These results also demonstrate the ability to detect genetic changes in cytologically normal cells, suggesting that molecular analyses may enhance the power for detecting premalignant changes in bronchial epithelium in high-risk individuals.

### Introduction

Although lung cancer is the leading cause of cancer death in the United States (1), early detection and intervention could decrease the high mortality rate associated with this disease if sensitive screening approaches could be developed (2-4). Early detection may be feasible because the entire respiratory tract is exposed to inhaled carcinogens; therefore, the whole lung is at risk for developing multiple, independently initiated sites. This "field cancerization" condition (5) is supported clinically by a high frequency of second primary tumors in lung cancer patients (6-9) and by the occurrence of progressive histological premalignant changes throughout the lower respiratory tract of cigarette smokers (10, 11). Moreover, recent studies using pathological tissues obtained after lung resection or autopsy have identified genetic aberrations associated with lung cancer in nonmalignant bronchial epithelium adjacent to tumors (12-16).

Although examination of pathological samples is useful for identifying genetic changes associated with carcinogenesis, this invasive approach for collection of clinical samples nec-

Received 1/23/96; revised 4/16/96; accepted 4/17/96.

The costs of publication of this article were defrayed in part by the payment of page charges. This article must therefore be hereby marked advertisement in accordance with 18 U.S.C. Section 1734 solely to indicate this fact.

<sup>1</sup>This work was supported in whole or in part by the Office of Health and Environmental Research, United States Department of Energy, under Contracts DE-AC04-76V01013 and DE-FG03-92ER61520; by NIH Grant 5P50CA58184; and by the Dedicated Health Research Funds of the University of New Mexico School of Medicine.

<sup>2</sup>To whom requests for reprints should be addressed, at Inhalation Toxicology Research Institute, P. O. Box 5890, Albuquerque, NM 87185. Phone: (505) 845-1165; Fax: (505) 845-1198.

essary for early detection would not be appropriate for screening. However, bronchial epithelial cells harvested using routine clinical procedures could be examined for genetic changes as an initial approach for detecting individuals at high risk for lung cancer. This approach could also provide genetic markers for evaluating the effectiveness of chemoprevention regimens. Bronchoscopy provides direct access to viable cells within the airways and is a commonly used tool for obtaining samples from the lower respiratory tract, including bronchial epithelium (17). This procedure can be used to repeatedly sample the bronchial epithelium over time and to collect viable cells that can be expanded through tissue culture for functional assays.

Because of field cancerization, genetic abnormalities should be dispersed throughout the bronchial epithelium of persons at risk for lung cancer. The purpose of this investigation was to test this hypothesis by sampling nonmalignant bronchial epithelium from distinct locations within four different lobes of the lung from persons at risk for lung cancer and then assaying the bronchial cells for the presence of specific genetic abnormalities. Trisomy of chromosome 7 was examined in these cells, because this alteration is common in solid tumors, including lung cancer, of several different organ systems (18, 19). In addition, trisomy 7 has been detected in premalignant lesions such as villous adenoma of the colon (20), in the colonic mucosa of individuals with familial polyposis (21), and in the far margins of some resected lung tumors (22). Our results demonstrate that trisomy 7 can be detected in nonmalignant bronchial epithelium from patients with lung cancer distant to the site of the tumor and in individuals without tumors who are at high risk for lung cancer development. Together, these studies suggest that an extra copy of chromosome 7 may be an intermediate biomarker of ongoing field carcinogenesis.

## Materials and Methods

**Subject Recruitment.** Bronchial epithelium was collected from 16 cigarette smokers undergoing a diagnostic workup for possible lung cancer and from 7 individuals with a prior history of underground uranium mining, 5 of whom were also smokers. Three individuals who had never smoked were also recruited to obtain bronchial epithelium not exposed directly to either tobacco smoke or radon progeny.

**Pathology and Exposure History.** Twelve of the 16 cigarette smokers who underwent diagnostic bronchoscopy were diagnosed with NSCLC.<sup>3</sup> Seven tumors were characterized histologically as SCCs, four tumors were ACs, and one tumor was an adenosquamous cell carcinoma. Lung cancer was not evident in the other four subjects. Smoking histories ranged from 15 to 120 pack-years (defined as the number of cigarettes smoked per day times the number of years smoked). All of the former uranium miners worked underground between 2 and 20 years, with a range of 27–527 working level months. Five of the seven miners had smoking histories that ranged from 20–60 pack-years.

**Bronchoscopic Collection and Processing of Bronchial Epithelium.** A protocol was developed for harvesting viable bronchial epithelium from the lower respiratory tract using a standard cytology brush during bronchoscopy. After introduc-

tion into the lower respiratory tract, the bronchoscope was directed into each upper and lower lobe, and the carinal margin of a segmental orifice, usually the second and third bifurcation within the upper and lower lobes, respectively, was brushed. These sites were chosen because (a) they are high-deposition areas for particles; (b) they are associated frequently with histological changes in smokers; and (c) they represent sites where tumors commonly occur (11, 23). The area was first washed with saline to remove any nonadherent cells. Sites were not brushed if a tumor was visualized within 5 cm of the site. After brushing, the brush was withdrawn, placed in serum-free medium, and kept on ice until processed. Each site was brushed twice. The procedure was well tolerated by all subjects, and no complications were noted related to the brushing procedure.

Bronchial cells were collected from only two of the sites in two of the subjects, from three sites in two subjects, and from all four sites in the remaining subjects. Although only two sites were brushed initially in case 1, cells were obtained from all four sites in this subject during a repeat bronchoscopy performed after the initial procedure did not yield a diagnosis. Samples were obtained from all four sites in the cancer-free current smokers and in the never smokers. In addition, bronchial epithelial cells derived at autopsy by Clonetics, Inc. (San Diego, CA) from four never smokers were also obtained to serve as additional controls. Only two sites sampled from most of the former uranium miners were available for analysis because cells recovered from the other sites had been used exclusively for cytology in another investigation.<sup>4</sup>

**Bronchial Epithelial Cell Culture.** Replicative cultures of the bronchial epithelial cells obtained by the procedure described above were established in our laboratory (24) using a serum-free medium (BEGM; Clonetics, Inc.) that is optimal for growth of these cells. Cells were removed from brushes by vigorous shaking in BEGM; cells from one brush were prepared for cytological analyses, and cells from the other brush were washed, resuspended in BEGM, seeded onto 60-mm fibronectin-coated plates, and grown at 37°C in 3% CO<sub>2</sub> and 21% O<sub>2</sub> until 80% confluence. Prior to passage, aliquots of cells were cryopreserved and stored at -145°C; other samples of cells were fixed in methanol-acetic acid (3:1). Next, the cells were washed four to six times in methanol:acetic acid and then dropped onto slides (about 2 × 10<sup>5</sup> cells/slide). The effects of cell culture on the frequency of trisomy 7 in nonmalignant bronchial epithelium were examined by placing cells dispersed from brushes directly onto microscope slides followed by fixation.

**Cytology.** Cells from one brush from each bronchial collection site were prepared for cytological analysis by smearing the cells across a microscope slide. The cells were then fixed with 96% ethanol and stained according to the Papanicolaou procedure (25) to facilitate morphological evaluation by a cytopathologist.

**Detection of Trisomy 2 and Trisomy 7.** Trisomy 2 and trisomy 7 were determined by hybridization of cells with a biotinylated chromosome 2 or 7 centromere probe (Oncor; Gaithersburg, MD). The probes were denatured in hybridization buffer at 70°C for 5 min, and the slides were immersed in 70% formamide-2× SSPE at 70°C for 2 min. The probe was then applied to the slides, which were incubated in a humidified chamber at 37°C for 16 h. After incubation, the slides were washed in 0.25× SSPE (10 mM sodium phosphate monobasic monohydrate; 1 mM ethylenediamine tetraacetic acid disodium

salt, dihydrate 72°C. and 10 mM avidin. Cell counts were made in each field. Data Analysis: The number of trisomy 7 cells in each field was divided by the total number of cells in the field to give the frequency of trisomy 7. This was compared with the frequency of trisomy 7 in the control slides.

## Results

**Cytology.** Cells from the only cytology patients, were cytologically normal. Cells collected from with cytological abnormalities, although collected from the

Two of the cytologically normal cells, whereas no cells were collected from three never smokers. Hyperplasia was observed at four sites from people (Table 1). Culturing of cells from these brushes, establishing replicative cultures, and does not indicate that the cells have the potential for becoming malignant. Some of the cells from the uranium miners, after several passages (a number of cells underwent 30 passages), inhibited an increase in cell number.

**Detection of Trisomy 7.** Background level of trisomy 7 was determined from autopsy specimens collected from bronchial cell lines. Epithelial cell lines recruited from normal cells contained trisomy 7 with values ranging from 0 to 100%. Those reported to have trisomy 7 from controls) were

Passage 1 cells were examined (43%) samples of trisomy 7 at field 1). Three subjects (7 and 12), trisomy 7 was detected. Six of the 18 cytologically abnormal

<sup>3</sup> The abbreviations used are: NSCLC, non-small cell lung cancer; SCC, squamous cell cancer; AC, adenocarcinoma; EGFR, epidermal growth factor receptor; FISH, fluorescence *in situ* hybridization; LOH, loss of heterozygosity; BEGM, Bronchial Epithelial Growth Medium.

<sup>4</sup> Unpublished data.



salt, dihydrate; 150 mM sodium chloride, pH 7.4) for 5 min at 72°C, and the probe was detected with fluorescein-labeled avidin. Cell nuclei were visualized with propidium iodide.

**Data Analysis.** The number of centromeric hybridization signals in each cell were evaluated in 400 cells/slide, and the frequency of trisomy 7 on each slide was calculated by dividing the total number of cells expressing three hybridization signals by the total number of cells counted on each slide. Twenty % of the slides were scored by a second person, and frequencies for trisomy 7 differed by <0.4%. The total number of sites positive for trisomy 7 in subjects with SCC and AC were compared using Fisher's exact test.

## Results

**Cytology.** Squamous metaplasia and atypical glandular cells, the only cytological abnormalities observed in lung cancer patients, were present in 32% of the samples (Table 1). These cytological changes were observed in <10% of the cells recovered from the diagnostic brush. Two subjects had three sites with cytological abnormalities, and five subjects had no cytological abnormalities. No samples contained tumor cells by cytology, although one of four sites in five subjects was collected from the same lobe where a tumor was later diagnosed.

Two of the 16 sites in smokers without lung cancer were cytologically abnormal (both in the same person; Table 2), whereas no atypical cells were present in the 12 sites from the three never smokers (Table 3). In former uranium miners, hyperplasia was present in bronchial cells collected from all four sites from one person, and in one site in two additional people (Table 2).

**Culturing of Bronchial Epithelial Cells.** The efficiency of establishing replicative cultures of the cells obtained by bronchial brushing was 100%. The serum-free medium used for these cultures is optimal for growing bronchial epithelial cells and does not support fibroblastic cell replication (25). Therefore, the cells were uniformly epitheloid in appearance. Growth potential was evaluated by passaging cells from all seven of the uranium miner cases and cases 1-6 from the lung cancer patients. Some of these cultures were maintained for up to nine passages (a minimum of 16 population doublings), and many underwent 30 divisions before senescence. However, none exhibited an indefinite population-doubling potential.

**Detection of Trisomy 7 in Nonmalignant Bronchial Epithelium.** Background rates of trisomy 7 were determined by examining normal human bronchial epithelial cell lines derived from autopsy cases of never smokers and bronchial epithelium collected from never smokers during bronchoscopy. In bronchial cell lines (passage 2) from four donors and bronchial epithelial cell samples obtained by bronchial brushing from the recruited never smokers (Table 3), only  $1.4 \pm 0.3\%$  (SD) of the cells contained three hybridization signals for chromosome 7 with values ranging from 1 to 1.8%. These values agree with those reported by the manufacturer of the probe. Therefore, trisomy 7 frequencies of >2.0% (>2 SD above the mean for controls) were considered significantly different from controls.

Passage 1 or 2 bronchial cells from lung cancer patients were examined for trisomy 7. Eighteen of the 42 bronchial sites (43%) sampled from the 12 lung cancer patients contained trisomy 7 at frequencies ranging from 2.3 to 6.0% (Table 1; Fig. 1). Three subjects (cases 1, 2, and 11) displayed trisomy 7 in all sites collected during bronchoscopy, and in two subjects (cases 7 and 12), trisomy 7 was found in three of four sites (Table 1). Six of the 18 sites positive for trisomy 7 also contained cytologically abnormal cells. Trisomy 7 was found in six of seven

Table 1 Frequency of trisomy 7 in bronchial epithelial cells from lung cancer patients

Case	Age	Smoking (pack-yr)	Tumor diagnosis	Brush location	Cytological diagnosis	Trisomy 7 (frequency, %)
1	64	104	SCC	RLL <sup>a</sup>	N	2.8 <sup>b</sup>
				RUL	AGC	4.0 <sup>b</sup>
				RLL <sup>c</sup>	N	3.0 <sup>b</sup>
				RUL <sup>c</sup>	N	4.0 <sup>b</sup>
				LLL <sup>c</sup>	N	6.0 <sup>b</sup>
2	69	26	SCC	LUL <sup>c</sup>	SM	4.3 <sup>b</sup>
				RUL	SM	2.8 <sup>b</sup>
				LLL	SM	3.3 <sup>b</sup>
3	65	120	SCC	LUL	N	3.8 <sup>b</sup>
				RLL	AGC	2.0
				RUL	AGC	2.3 <sup>b</sup>
4	52	90	AC	LLL	AGC	2.0
				RLL	SM	1.5
				RUL	N	1.8
5	70	50	SCC	LLL	SM	1.5
				LUL	SM	1.8
				RLL	N	1.5
6	61	93	AC	RUL	N	1.5
				RUL	N	1.3
				LLL	N	2.0
7	58	40	SCC	LUL	N	1.5
				RLL	N	1.8
				RUL	N	2.3 <sup>b</sup>
8	59	120	AdSCC	LLL	N	2.5 <sup>b</sup>
				LUL	N	2.8 <sup>b</sup>
				RLL	N	1.5
9	65	71	SCC	RUL	N	2.0
				LLL	N	2.5 <sup>b</sup>
				LUL	AGC	2.0
10	63	45	AC	RLL	SM	2.0
				RUL	N	2.5 <sup>b</sup>
				RUL	N	1.0
11	61	95	AC	LLL	N	1.8
				LUL	N	1.8
				RLL	N	1.3
12	76	17	SCC	LLL	N	2.5 <sup>b</sup>
				LUL	N	2.8 <sup>b</sup>
				RLL	N	2.0
				RUL	N	2.3 <sup>b</sup>
				LLL	N	2.3 <sup>b</sup>
				LUL	N	2.3 <sup>b</sup>

<sup>a</sup> RLL, right lower lobe; RUL, right upper lobe; LLL, left lower lobe; LUL, left upper lobe; AGC, atypical glandular cells; SM, squamous metaplasia; N, normal cells; AdSCC, adenosquamous carcinoma.

<sup>b</sup>  $P < 0.05$  as compared to never-smoker controls.

<sup>c</sup> Resampled 4 months later.

patients diagnosed with SCC, whereas only one of four patients with AC displayed trisomy 7 in any site collected at bronchoscopy. Case 7, which had histological features of both SCC and AC, had one site positive for trisomy 7. The frequency of positive trisomy 7 sites in all patients with SCC within this small sample population was significantly greater than in AC patients ( $P < 0.005$ ).

The reproducibility of detecting trisomy 7 at sites found to be positive for this abnormality was investigated in one patient (case 1) who required repeat bronchoscopy for clinical reasons. Trisomy 7 was increased similarly in the two sites brushed during both procedures, although cytological examination showed atypical cells in one site from the first bronchoscopy and cytologically normal cells from the same site collected

Table 2 Frequency of trisomy 7 in bronchial epithelial cells from cancer-free smokers and former uranium miners

Case	Age	Smoking (pack-yrs)	Radon exposure (WLMs) <sup>a</sup>	Brush location	Cytological diagnosis	Trisomy 7 (frequency, %)
13	81	15	0	RLL	N	1.8
				RUL	AGC	1.5
				LLL	N	1.8
				LUL	SM	2.0
14	34	24	0	RLL	N	1.3
				RUL	N	1.3
				LLL	N	1.0
				LUL	N	1.3
15	68	51	0	RLL	N	4.0 <sup>b</sup>
				RUL	N	3.0 <sup>b</sup>
				LLL	N	4.3 <sup>b</sup>
				LUL	N	3.5 <sup>b</sup>
16	45	30	0	RLL	N	1.3
				RUL	N	1.5
				LLL	N	2.0
				LUL	N	1.8
17	59	8	27	LLL	N	3.0 <sup>b</sup>
				LUL	N	3.0 <sup>b</sup>
18	65	9	516	LUL	N	1.3
				RUL	N	3.3 <sup>b</sup>
19	64	30	235	LUL	N	1.5
				RLL	N	1.0
20	56	0	186	LUL	N	2.0
				RLL	N	2.3 <sup>b</sup>
21	64	0	214	RLL	H	1.8
				LUL	N	1.8
22	64	9	577	RLL	H	0.8
				LLL	H	1.3
23	67	31	124	LUL	H	2.8 <sup>b</sup>
				RLL	H	2.5 <sup>b</sup>
				RUL	H	3.3 <sup>b</sup>

<sup>a</sup> Abbreviations are as indicated in Table 1 footnote. WLM, working level month; H, hyperplasia.

<sup>b</sup>  $P < 0.05$  as compared to never-smoker controls.

during the second procedure (Table 1). The other two sites collected during the second bronchoscopy also showed elevated frequencies of trisomy 7 in this patient.

Trisomy 7 was detected in cytologically normal bronchial epithelium collected from four sites in one (case 15) of the cancer-free smokers (Table 2). Bronchial cells from the other smokers did not contain this chromosome abnormality. In the former uranium miners (cases 17–23), seven of 15 sites collected during bronchoscopy were positive for trisomy 7. Three of the positive sites were found in one subject (case 23) and also contained basal cell hyperplasia. However, the other four samples positive for trisomy 7 showed no cytological abnormality.

Two of the former uranium miners (cases 18 and 23) developed lung cancer within 2 years of bronchial cell collection. SCC was diagnosed in the right upper lobe of both subjects. As noted in Table 2, both cases were positive for trisomy 7 in the right upper lobe brushing site obtained at the initial bronchoscopy.

**Tissue Culture Effects on Trisomy 7 Expression in Bronchial Epithelium.** The effect of tissue culture on trisomy 7 frequency was assessed by comparing the frequency of this chromosome abnormality in freshly isolated bronchial epithelium obtained directly from bronchial brushes ("preculture") to passage 1 cells. This comparison was conducted on cells collected from two different bronchial sites in three different subjects [(cases 11 and 16 and donor 7 (never smoker)]. Cultured samples positive for trisomy 7 in case 11 were also

Table 3 Interphase analysis of chromosome 7 in normal human bronchial epithelial cells

Bronchial epithelial cell lines were established from never smokers (Clonetics) after autopsy and from volunteers. The normal distribution of chromosome 7 copy number as detected by FISH is shown by the percentage of cells exhibiting 1, 2, 3, or 4 hybridization signals. Four hundred cells containing hybridization signal were counted per donor.

Donor	Age	Brush location	Number of hybridization signals/cell (%)			
			1	2	3	4
1	6	NA <sup>a</sup>	3.5	92.0	1.5	3.0
		NA	2.3	95.5	1.3	1.0
		NA	1.5	94.7	1.8	2.0
		NA	2.0	94.8	1.0	2.3
		RLL	1.0	95.5	1.8	1.7
2	17	RUL	0.5	98.3	1.0	0.2
		LLL	1.3	96.5	1.0	1.2
		LUL	1.0	96.3	1.2	1.5
		RLL	1.0	96.8	1.0	1.2
		RUL	2.5	93.3	1.7	2.5
3	41	LLL	2.0	94.8	1.5	1.7
		LUL	1.8	94.2	1.8	2.2
		RLL	0.5	98.2	0.8	0.5
		RUL	0.5	97.2	1.3	1.0
		LLL	1.2	96.8	1.3	0.7
4	45	LUL	1.0	96.0	1.5	1.5
5	35					
6	33					
7						

<sup>a</sup> Abbreviations are as indicated in the legend to Table 1. NA, not applicable.

positive in preculture cells from the same bronchial collection site, whereas sites negative for trisomy 7 in cultured cells from case 16 and the never smoker were also negative in preculture cells (data not shown). Values for trisomy 7 differed by  $<0.3\%$  between preculture and cultured cells. The effect of passaging cells on the frequency of trisomy 7 was also examined in bronchial cells from case 1. Trisomy 7 frequency was similar in cells from passages 1, 4, and 7.

**Frequency of Trisomy 2 in Nonmalignant Bronchial Epithelium.** Aneuploidy has been detected in bronchial squamous metaplasia, a likely precursor to SCC (26). To determine whether the increased frequency of trisomy 7 detected in the current study reflects generalized aneuploidy or a specific chromosomal duplication, a subgroup of samples was evaluated for trisomy of chromosome 2. The frequency of trisomy 2 in never smokers was  $1.5 \pm 0.4\%$  (data not shown). Bronchial cells from eight subjects, six of whom had elevated frequencies for trisomy 7, were evaluated. The frequency for trisomy of chromosome 2 did not differ from never smokers (Table 4).

## Discussion

The studies described in this report are the first to detect and quantify an increase in trisomy 7 in the airway cells of subjects at risk for lung cancer. The presence of trisomy 7 appeared to be a specific chromosome gain and not due to generalized aneuploidy in these cells. In addition, trisomy 7 in nonmalignant epithelium from lung cancer patients was associated with SCC tumor histology, suggesting that patients with this genetic change may be at greater risk for developing SCC than other histological forms of lung cancer. This supposition was supported by the fact that two cancer-free former uranium miners with bronchial cells positive for trisomy 7 ultimately developed SCC. Finally, these results demonstrate the ability to detect genetic changes in cytologically normal cells, suggesting that molecular analyses may enhance the power for detecting

Fig. 1. FISH bronchial ep is apparent field. Magni

Table 4 Trisomy 2 in nonmalignant bronchial epithelial cells

Case	Trisomy 2 (%)
1	1.5
2	1.5
7	1.5
8	1.5
13	1.5
15	1.5
19	1.5
23	1.5

<sup>a</sup> Abbreviat

premalig individual  
Cig:  
ers to rac  
cinogens  
gens and  
inhaled

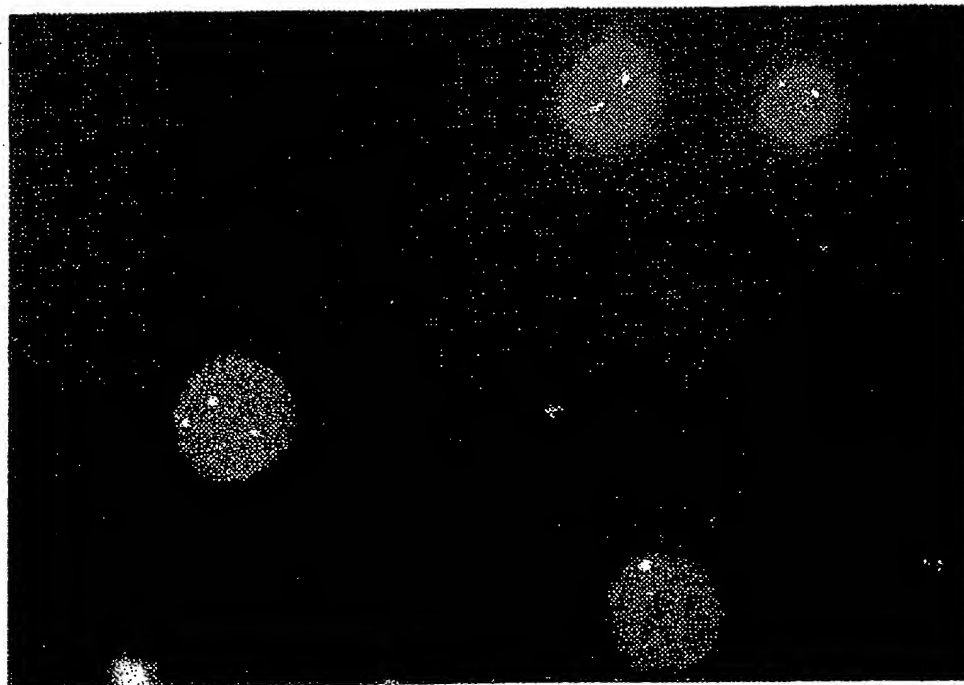


Fig. 1. FISH for chromosome 7 in bronchial epithelial cells. Trisomy 7 is apparent in one cell from this field. Magnification,  $\times 530$ .

Table 4 Frequency of trisomy 2 in bronchial epithelial cells from lung cancer patients, cancer-free smokers, and former uranium miners

Case	Tumor diagnosis	Brush location	Trisomy 2 (frequency, %)
1	SCC	RLL <sup>a</sup>	1.5
		RUL	1.8
		LLL	1.8
		LUL	1.0
2	SCC	LLI	1.0
		LUL	1.0
		RLI	1.5
7	SCC	RUL	2.1
		LLI	1.8
		LUL	1.5
		RLL	0.3
8	AC	RUL	1.5
		LLI	0.8
		RLL	1.0
13	None	RUL	0.8
		LLL	1.0
		LUL	1.3
		RLL	1.8
15	None	RUL	2.0
		LLL	1.0
		LUL	1.3
		LUL	1.9
19	None	RLL	0.8
		RLI	1.5
23	None	RLI	1.5

<sup>a</sup> Abbreviations are as indicated in legend to Table 1.

pre-malignant changes in bronchial epithelium in high-risk individuals.

Cigarette smoking and the exposure of underground miners to radon progeny are both well-established respiratory carcinogens (27, 28). Tobacco smoke contains numerous mutagens and carcinogens, and radon progeny that have been inhaled and deposited on the respiratory epithelium release  $\alpha$

particles capable of damaging DNA (28). Although comparison between findings in the cigarette smokers and the former uranium miners is constrained by the number of participants in the two groups, trisomy 7 was found in both groups. These results are consistent with the synergism between smoking and radon progeny, which suggests commonality in the pathways by which the two carcinogens cause lung cancer (29).

The bronchial brushing method used for collecting cells from the lower respiratory tract is rapid (10–12 min total for two brushes at four different sites), well tolerated by the patient, and permits collection of viable bronchial cells that can be expanded through tissue culture at 100% efficiency. The stability of these cells in culture was evident by the fact that the frequency of trisomy 7 did not differ between primary brush cells and cells propagated for up to seven passages. Furthermore, this procedure is amenable to the production of sufficient cell numbers ( $1 \times 10^8$ ) at low passage (one or two) to accommodate multiple molecular analyses. Although the media used in culturing of bronchial epithelial cells did not appear to provide a selective growth advantage to cells harboring an additional chromosome 7, the modulation of medium supplements might lead to the establishment of clonal populations of pre-malignant cells. Such cell populations would greatly facilitate the identification of additional early gene changes in respiratory carcinogenesis.

The detection of trisomy 7 in multiple nonmalignant sites within the bronchial tree supports the theory of field cancerization (5), which states that diffuse exposure of the entire respiratory tract to inhaled carcinogens causes the development of multiple, independently initiated sites that can lead to tumor development. Although the frequency of this chromosome abnormality was relatively low (2.3–6.0%), these values were consistent with the low percentage of cells within each brush sample (10%) that exhibited abnormal cytology. These results are also similar to studies of chromosome gain in patients with head and neck cancer where trisomy 7 was detected at frequen-

cies of 2, 3, and 21% in histologically normal, hyperplastic, and dysplastic cells, respectively (30).

The detection of trisomy 7 in normal, hyperplastic, and metaplastic bronchial epithelium from cancer-free patients extends a recent report describing LOH at chromosomes 3p, 5q, and 9p in dysplastic premalignant bronchial lesions harvested from current and former smokers by bronchoscopy (31). The inability to detect LOH at these chromosome loci in normal or early premalignant epithelium may stem from a difference in sensitivity between the methodologies used. The low frequency of trisomy 7 and cytologically abnormal cells collected from bronchoscopy is consistent with a lack of clonality within the brush cells. FISH assays on interphase cells permit screening of individual cells, and sensitivity for detection is limited only by the number of cells examined. In contrast, microsatellite analyses for LOH cannot detect nonclonal changes but require that the chromosome alteration be present in approximately 40–50% of the sample (32, 33).

The role of trisomy 7 in lung cancer development has not been elucidated. Increased expression of EGFR, which is located on chromosome 7 (34), is observed in 50–80% of NSCLCs (16, 35, 36). EGFR expression appears greater in SCC than AC (35, 36) and is amplified in some cell lines derived from SCC (37). These findings corroborate our hypothesis that acquisition of trisomy 7 in bronchial epithelium could be prognostic for development of SCC. Moreover, expression of this gene is also increased in nonmalignant bronchial epithelium from NSCLC patients (16, 35) and in normal or premalignant epithelium adjacent to head and neck tumors (38). Thus, altered expression of EGFR could enable cells that have acquired additional genetic changes to proliferate continually and escape from terminal differentiation (39). In addition, the *c-met* oncogene is also located on chromosome 7 and is overexpressed in NSCLCs (40, 41). This oncogene encodes a transmembrane tyrosine kinase (42) that functions as a receptor for the hepatocyte growth factor (43) and is involved in sustaining the growth of NSCLC cells in culture (44).

Previous studies have detected mutations in p53 (12, 14, 35), chromosome losses at 9p21 (45) and 3p (46) in preinvasive bronchial lesions, and simple chromosome rearrangements in normal bronchial epithelium from proximal airways (47) of lung cancer patients. The prevalence of these genetic changes in normal epithelium from persons at risk for lung cancer should be quantified by FISH to define the temporal sequences of somatic genetic changes that precede the development of clonal lesions in the lung. This information will be invaluable in providing biological markers that can qualitatively estimate the extent of field-cancerization in persons at risk for lung cancer and can be used to assess the efficacy of chemoprevention trials. Ultimately, the efficiency for detecting these biological markers in bronchial epithelium versus exfoliated epithelial cells within sputum must be established to support the use of a "genetic-based" screening approach for individuals at high risk for lung cancer. The results of the current investigation have identified one potential biomarker, trisomy 7, that may be useful in early detection and intervention for lung carcinogenesis.

## References

- Boring, C. C., Squires, T. S., and Tong, T. Cancer statistics, 1993. *J. Clin. Oncol.* 11: 1–26, 1993.
- Lippman, S. M., Benner, S. E., and Hong, W. K. Cancer chemoprevention. *J. Clin. Oncol.* 12: 851–873, 1994.
- Lippman, S. M., and Spitz, M. R. Intervention in the premalignant process. *Cancer Bull.* 43: 473–474, 1991.
- Berlin, N. I., Buncher, C. R., Fontana, R. S., Frost, J. K., and Melamed, M. R. The National Cancer Institute cooperative early lung cancer detection program. Early lung cancer detection. *Am. Rev. Respir. Dis.* 130: 545–570, 1984.
- Slaughter, D. P., Southwick, H. W., and Smejkal, W. Field cancerization in oral stratified squamous epithelium. Clinical implications of multicentric origin. *Cancer (Phila.)* 5: 963–968, 1953.
- van Hordégum, P. C., Wagenaar, S. S., Corrin, B., Baak, J. P., Berkel, J., and Vanderschueren, R. G. Second primary lung cancer: importance of long term follow-up. *Thorax*, 44: 788–793, 1989.
- Boice, J. D., and Fraumeni, J. F. Second cancer following cancer of the respiratory system in Connecticut, 1935–1982. *J. Natl. Cancer Inst. Monogr.* 68: 83–98, 1985.
- Pairolero, P. C., Williams, D. E., Bergsrahl, E. J., Fichler, J. M., Bernatz, P. E., and Payne, N. J. Postsurgical stage I bronchogenic carcinoma. Morbid implications of recurrent disease. *Ann. Thorac. Surg.* 38: 331–338, 1984.
- Shields, T. W., Humphrey, E. W., Higgins, G. A., and Keohn, R. J. Long term survivors after resection of lung carcinoma. *J. Thorac. Cardiovasc. Surg.* 76: 439–442, 1978.
- Auerbach, O., Stout, A. P., Hammond, E. C., and Garfinkel, L. Changes in bronchial epithelium in relation to cigarette smoking and in relation to lung cancer. *N. Engl. J. Med.* 276: 111–118, 1962.
- Auerbach, O., Hammond, E. C., and Garfinkel, L. Changes in bronchial epithelium in relation to cigarette smoking, 1955–1960 vs. 1970–1977. *N. Engl. J. Med.* 300: 381–386, 1979.
- Sundaresan, V., Ganly, P., Hasleton, P., Rudd, R., Sinha, G., Bleehen, N. M., and Rabbitts, P. p53 and chromosome 3 abnormalities, characteristic of malignant lung tumors, are detectable in preinvasive lesions of the bronchus. *Oncogene*, 7: 1989–1997, 1992.
- Sozzi, G., Miozzo, M., Donghi, R., Pilotti, S., Cariani, C. T., Pastorino, U., Pianta, G. P., and Pierotti, M. A. Deletions of 17p and p53 mutations in preneoplastic lesions of the lung. *Cancer Res.* 52: 6079–6082, 1992.
- Bennett, W. P., Colby, T. V., Travis, W. D., Borkowski, A., Jones, R. T., Lane, D. P., Metcalf, R. A., Samet, J. M., Takeshima, Y., Gu, J. R., Vähäkangas, K. H., Soini, N., Pääkkö, P., Welsh, J. A., Trump, B. F., and Harris, C. C. p53 protein accumulates frequently in early bronchial neoplasia. *Cancer Res.* 53: 4817–4822, 1993.
- Sozzi, G., Miozzo, M., Pastorino, U., Pilotti, S., Donghi, R., Giarola, M., Gregorio, L. D., Manenti, G., Radice, P., Minoletti, F., Porta, G. D., and Pierotti, M. A. Genetic evidence for an independent origin of multiple preneoplastic and neoplastic lung lesions. *Cancer Res.* 55: 135–149, 1995.
- Sozzi, G., Miozzo, M., Tagliabue, E., Calderone, C., Lombardi, L., Pilotti, S., Pastorino, U., Pierotti, M. A., and Porta, G. D. Cytogenetic abnormalities and overexpression of receptors for growth factors in normal bronchial epithelium and tumor samples of lung cancer patients. *Cancer Res.* 51: 400–404, 1991.
- Campbell, A. M., Chavez, P., Vignola, A. M., Bousquet, J., Couret, L., Michel, F. B., and Godard, P. H. Functional characteristics of bronchial epithelium obtained by brushing from asthmatic and normal subjects. *Am. Rev. Respir. Dis.* 147: 529–534, 1993.
- Testa, J., and Siegfried, J. M. Chromosome abnormalities in human non-small cell lung cancer. *Cancer Res.* 52 (Suppl.): 2702–2706, 1992.
- Matturri, L., and Lavezzi, A. M. Recurrent chromosome alterations in non-small cell lung cancer. *Eur. J. Histochem.* 38: 53–58, 1994.
- Reichmann, A., Martin, P., and Levin, B. Karyotypic findings in a colonic villous adenoma. *Cancer Genet. Cytogenet.* 7: 51–57, 1982.
- Moertel, C. A., DeWald, G. W., Coffey, R. J., and Gordon, H. Cytogenetic examination of colonic mucosa in familial polyposis. In: *Proceedings of the Second International Conference on Chromosomes in Solid Tumors*. Tucson, Arizona Cancer Center, pp. 41–48. University of Arizona, 1987.
- Lee, J. S., Pathak, S., Hopwood, V., Tomasovic, B., Mullins, T. D., Baker, F. L., Spitzer, G., and Neidhart, J. A. Involvement of chromosome 7 in primary lung tumor and nonmalignant normal lung tissue. *Cancer Res.* 47: 6349–6352, 1987.
- Isikawa, Y., Nakagawa, K., Satoh, Y., Kitagawa, T., Sugano, H., Hirano, T., and Tsuchiya, E. Hot spots of chromatin accumulation at bifurcations of chromatin workers' bronchi. *Cancer Res.* 54: 2342–2346, 1994.
- Lechner, J. F., and LaVeck, M. A. A serum-free method for culturing normal human bronchial epithelial cells at clonal density. *J. Tissue Culture Methods*, 2: 43–48, 1985.
- Saccomanno, G. *Pulmonary Cytology*. Ed. 2. Chicago: American Society of Clinical Pathologists Press, 1986.
- Lee, J. S., Lippman, S. M., Hong, W. K., Ro, J. Y., Kim, S. Y., Lotan, R., and Hittelman, W. N. Determination of biomarkers for intermediate end points in chemoprevention. *Cancer Res.* 52 (Suppl.): 2702s–2710s, 1992.
- United States Department of Health and Human Services. Reducing the Health Consequences of Smoking: 25 Years of Progress. A Report of the Surgeon General. Department of Health and Human Services Publication No. (CDC) 89–8411. W. Services, Pub. Disease Prev.
- National Effects of 10 Deposited at 1988.
- Lubin, J. E., Kusiak, J. Woodward, miners and 1817–827, 19
- Voravud W. N. In: multistage 10
- Thibervi G. and Pal premalignant 5133–5139.
- Shiseki, Yokota, J. F non-small cell
- Merlo, Sidransky, E. Cancer Res.
- Spurr, I. Brodmer, W. homologues
- Rusch, of p53 or 11 neoplasia, a Cancer Res.
- Veale, I. growth factor 1987.
- Tadashi K., Rikimur

89-8411. Washington, DC: United States Department of Health and Human Services, Public Health Service, Centers for Disease Control, Center for Chronic Disease Prevention and Health Promotion, Office on Smoking and Health, 1989.

28. National Research Council. Report of the Committee on the Biological Effects of Ionizing Radiation: Health Effects of Radon and Other Internally Deposited  $\alpha$  Emitters (BEIR IV). Washington DC: National Academy Press, 1988.

29. Lubin, J. H., Boice, J. D., Jr., Edling, C., Hornung, R. W., Howe, G. R., Kunz, E., Kusiak, R. A., Morrison, H. L., Radford, E. P., Samet, J. M., Tirmarche, M., Woodward, A., Yan, S. X., and Pierce, D. A. Lung cancer in radon-exposed miners and estimation of risk from indoor exposure. *J. Natl. Cancer Inst.* 87: 817-827, 1995.

30. Voravud, N., Shin, D. M., Ro, J. Y., Lee, J. S., Hong, W. K., and Hittelman, W. N. Increased polysomies of chromosomes 7 and 17 during head and neck multistage tumorigenesis. *Cancer Res.* 53: 2874-2883, 1993.

31. Thiberville, L., Payne, P., Vielkind, J., LeRiche, J., Horsman, D., Nouvet, G., and Palcic, B. Evidence of cumulative gene losses with progression of premalignant epithelial lesions to carcinoma of the bronchus. *Cancer Res.* 55: 5133-5139, 1995.

32. Shiseki, M., Kohno, T., Nishikawa, R., Sameshima, Y., Mizoguchi, H., and Yokota, J. Frequent allelic loss on chromosomes 2q, 18q, and 22q in advanced non-small cell lung carcinoma. *Cancer Res.* 54: 5643-5648, 1994.

33. Merlo, A., Mabry, M., Gabrielson, E., Vollmer, R., Baylin, S. B., and Sidransky, D. Frequent microsatellite instability in primary small cell lung cancer. *Cancer Res.* 54: 2098-2101, 1994.

34. Spurr, N. K., Solomon, B., Jansson, M., Sheen, D., Goodfellow, P. N., Bodmer, W. F., and Venter, B. Chromosomal localization of the human homologues to the oncogenes *erb-A* and *B*. *EMBO J.* 3: 159-164, 1984.

35. Rusch, V., Klimstra, D., Linkov, L., and Dmitrovsky, E. Aberrant expression of p53 or the epidermal growth factor receptor is frequent in early bronchial neoplasia, and coexpression precedes squamous cell carcinoma development. *Cancer Res.* 55: 1365-1372, 1995.

36. Veale, D., Ashcroft, T., March, C., Gibson, G. J., and Harris, A. L. Epidermal growth factor receptors in non-small cell lung cancer. *Br. J. Cancer* 55: 513-516, 1987.

37. Tadashi, Y., Kamata, N., Kawano, H., Shimizu, S., Kuroki, T., Toyoshima, K., Rikimura, K., Nomura, N., Ishizaki, R., Pastan, I., Gambou, J., and Shimizu, N.

High incidence of amplification of the epidermal growth factor receptor gene in human squamous carcinoma cell lines. *Cancer Res.* 46: 414-416, 1986.

38. Shin, D. M., Ro, J. Y., Hong, W. K., and Hittelman, W. N. Dysregulation of epidermal growth factor receptor expression in premalignant lesions during head and neck tumorigenesis. *Cancer Res.* 54: 3153-3159, 1994.

39. Soschek, C. M., and King, L. B. Functional and structural characteristics of EGF and its receptor and their relationship to transforming proteins. *J. Cell. Biochem.* 31: 135-152, 1986.

40. Prat, M., Narsimhan, R. P., Crepaldi, T., Nicotra, M. R., Natali, P. G., and Comoglio, P. M. The receptor encoded by the human *c-met* oncogene is expressed in hepatocytes, epithelial cells, and solid tumors. *Int. J. Cancer* 49: 323-328, 1991.

41. Liu, C., and Tsao, M-S. *In vitro* and *in vivo* expression of transforming growth factor  $\alpha$  and tyrosine kinase receptors in human non-small cell lung carcinoma cell lines. *Am. J. Pathol.* 142: 1155-1162, 1993.

42. Giordano, S., Ponzetto, C., Di Renzo, M. F., Cooper, S., and Comoglio, P. M. Tyrosine kinase receptor indistinguishable from the *c-met* protein. *Nature (Lond.)* 339: 155-156, 1989.

43. Naldini, L., Vigna, E., Narsimhan, R. P., Gandino, G., Zarnegar, R., Michalopoulos, G. K., and Comoglio, P. M. Hepatocyte growth factor (HGF) stimulates the tyrosine kinase activity of the receptor encoded by the proto-oncogene *c-MET*. *Oncogene* 6: 501-504, 1991.

44. Liu, C., and Tsao, M-S. Proto-oncogene and growth factor/receptor expression in the establishment of primary human non-small cell lung carcinoma cell lines. *Am. J. Pathol.* 142: 413-423, 1991.

45. Kishimoto, Y., Sugio, K., Hung, J. Y., Virmani, A. K., McIntire, D. D., Minna, J. D., and Gazdar, A. F. Allele-specific loss in chromosome 9p loci in preneoplastic lesions accompanying non-small-cell lung cancers. *J. Natl. Cancer Inst.* 87: 1224-1229, 1995.

46. Hung, J., Kishimoto, Y., Sugio, K., Virmani, A., McIntire, D. D., Minna, J. D., and Gazdar, A. F. Allele-specific chromosome 3p deletions occur at an early stage in the pathogenesis of lung carcinoma. *JAMA* 273: 558-563, 1995.

47. Pastorino, U., Sozzi, G., Miozzo, M., Tagliabue, E., Pilotti, S., and Pierotti, M. A. Genetic changes in lung cancer. *J. Cell. Biochem.* 17F (Suppl.): 237-248, 1993.

## **WISP genes are members of the connective tissue growth factor family that are up-regulated in Wnt-1-transformed cells and aberrantly expressed in human colon tumors**

DIANE PENNICA\*<sup>†</sup>, TODD A. SWANSON\*, JAMES W. WELSH\*, MARGARET A. ROY<sup>‡</sup>, DAVID A. LAWRENCE\*, JAMES LEE<sup>‡</sup>, JENNIFER BRUSH<sup>‡</sup>, LISA A. TANEYHILL<sup>§</sup>, BETHANNE DEUEL<sup>‡</sup>, MICHAEL LEW<sup>¶</sup>, COLIN WATANABE<sup>¶</sup>, ROBERT L. COHEN\*, MONA F. MELHEM\*\*, GENE G. FINLEY\*\*, PHIL QUIRKE<sup>††</sup>, AUDREY D. GODDARD<sup>‡</sup>, KENNETH J. HILLAN<sup>¶</sup>, AUSTIN L. GURNEY<sup>‡</sup>, DAVID BOTSTEIN<sup>‡,‡‡</sup>, AND ARNOLD J. LEVINE<sup>§</sup>

Departments of \*Molecular Oncology, <sup>‡</sup>Molecular Biology, <sup>§</sup>Scientific Computing, and <sup>¶</sup>Pathology, Genentech Inc., 1 DNA Way, South San Francisco, CA 94080; \*\*University of Pittsburgh School of Medicine, Veterans Administration Medical Center, Pittsburgh, PA 15240; <sup>††</sup>University of Leeds, Leeds, LS29JT United Kingdom; <sup>‡‡</sup>Department of Genetics, Stanford University, Palo Alto, CA 94305; and <sup>§</sup>Department of Molecular Biology, Princeton University, Princeton, NJ 08544

Contributed by David Botstein and Arnold J. Levine, October 21, 1998

**ABSTRACT** Wnt family members are critical to many developmental processes, and components of the Wnt signaling pathway have been linked to tumorigenesis in familial and sporadic colon carcinomas. Here we report the identification of two genes, *WISP-1* and *WISP-2*, that are up-regulated in the mouse mammary epithelial cell line C57MG transformed by Wnt-1, but not by Wnt-4. Together with a third related gene, *WISP-3*, these proteins define a subfamily of the connective tissue growth factor family. Two distinct systems demonstrated *WISP* induction to be associated with the expression of Wnt-1. These included (i) C57MG cells infected with a Wnt-1 retroviral vector or expressing Wnt-1 under the control of a tetracycline repressible promoter, and (ii) Wnt-1 transgenic mice. The *WISP-1* gene was localized to human chromosome 8q24.1-8q24.3. *WISP-1* genomic DNA was amplified in colon cancer cell lines and in human colon tumors and its RNA overexpressed (2- to >30-fold) in 84% of the tumors examined compared with patient-matched normal mucosa. *WISP-3* mapped to chromosome 6q22-6q23 and also was overexpressed (4- to >40-fold) in 63% of the colon tumors analyzed. In contrast, *WISP-2* mapped to human chromosome 20q12-20q13 and its DNA was amplified, but RNA expression was reduced (2- to >30-fold) in 79% of the tumors. These results suggest that the *WISP* genes may be downstream of Wnt-1 signaling and that aberrant levels of *WISP* expression in colon cancer may play a role in colon tumorigenesis.

Wnt-1 is a member of an expanding family of cysteine-rich, glycosylated signaling proteins that mediate diverse developmental processes such as the control of cell proliferation, adhesion, cell polarity, and the establishment of cell fates (1, 2). Wnt-1 originally was identified as an oncogene activated by the insertion of mouse mammary tumor virus in virus-induced mammary adenocarcinomas (3, 4). Although Wnt-1 is not expressed in the normal mammary gland, expression of Wnt-1 in transgenic mice causes mammary tumors (5).

In mammalian cells, Wnt family members initiate signaling by binding to the seven-transmembrane spanning Frizzled receptors and recruiting the cytoplasmic protein Dishevelled (Dsh) to the cell membrane (1, 2, 6). Dsh then inhibits the kinase activity of the normally constitutively active glycogen synthase kinase-3 $\beta$  (GSK-3 $\beta$ ) resulting in an increase in  $\beta$ -catenin levels. Stabilized  $\beta$ -catenin interacts with the transcription factor TCF/Lef1, forming a complex that appears in

the nucleus and binds TCF/Lef1 target DNA elements to activate transcription (7, 8). Other experiments suggest that the adenomatous polyposis coli (APC) tumor suppressor gene also plays an important role in Wnt signaling by regulating  $\beta$ -catenin levels (9). APC is phosphorylated by GSK-3 $\beta$ , binds to  $\beta$ -catenin, and facilitates its degradation. Mutations in either APC or  $\beta$ -catenin have been associated with colon carcinomas and melanomas, suggesting these mutations contribute to the development of these types of cancer, implicating the Wnt pathway in tumorigenesis (1).

Although much has been learned about the Wnt signaling pathway over the past several years, only a few of the transcriptionally activated downstream components activated by Wnt have been characterized. Those that have been described cannot account for all of the diverse functions attributed to Wnt signaling. Among the candidate Wnt target genes are those encoding the nodal-related 3 gene, *Xnr3*, a member of the transforming growth factor (TGF)- $\beta$  superfamily, and the homeobox genes, *engrailed*, *gooseoid*, *twin* (*Xtwn*), and *siamois* (2). A recent report also identifies *c-myc* as a target gene of the Wnt signaling pathway (10).

To identify additional downstream genes in the Wnt signaling pathway that are relevant to the transformed cell phenotype, we used a PCR-based cDNA subtraction strategy, suppression subtractive hybridization (SSH) (11), using RNA isolated from C57MG mouse mammary epithelial cells and C57MG cells stably transformed by a Wnt-1 retrovirus. Overexpression of Wnt-1 in this cell line is sufficient to induce a partially transformed phenotype, characterized by elongated and refractile cells that lose contact inhibition and form a multilayered array (12, 13). We reasoned that genes differentially expressed between these two cell lines might contribute to the transformed phenotype.

In this paper, we describe the cloning and characterization of two genes up-regulated in Wnt-1 transformed cells, *WISP-1* and *WISP-2*, and a third related gene, *WISP-3*. The *WISP* genes are members of the CCN family of growth factors, which includes connective tissue growth factor (CTGF), Cyr61, and *nov*, a family not previously linked to Wnt signaling.

### **MATERIALS AND METHODS**

**SSH.** SSH was performed by using the PCR-Select cDNA Subtraction Kit (CLONTECH). Tester double-stranded

Abbreviations: TGF, transforming growth factor; CTGF, connective tissue growth factor; SSH, suppression subtractive hybridization; VWC, von Willebrand factor type C module.

Data deposition: The sequences reported in this paper have been deposited in the Genbank database (accession nos. AF100777, AF100778, AF100779, AF100780, and AF100781).

<sup>†</sup>To whom reprint requests should be addressed. e-mail: diane@gene.com.

The publication costs of this article were defrayed in part by page charge payment. This article must therefore be hereby marked "advertisement" in accordance with 18 U.S.C. §1734 solely to indicate this fact.

© 1998 by The National Academy of Sciences 0027-8424/98/9514717-6\$2.00/0 PNAS is available online at www.pnas.org.



cDNA was synthesized from 2  $\mu$ g of poly(A)<sup>+</sup> RNA isolated from the C57MG/Wnt-1 cell line and driver cDNA from 2  $\mu$ g of poly(A)<sup>+</sup> RNA from the parent C57MG cells. The subtracted cDNA library was subcloned into a pGEM-T vector for further analysis.

**cDNA Library Screening.** Clones encoding full-length mouse *WISP-1* were isolated by screening a  $\lambda$ gt10 mouse embryo cDNA library (CLONTECH) with a 70-bp probe from the original partial clone 568 sequence corresponding to amino acids 128–169. Clones encoding full-length human *WISP-1* were isolated by screening  $\lambda$ gt10 lung and fetal kidney cDNA libraries with the same probe at low stringency. Clones encoding full-length mouse and human *WISP-2* were isolated by screening a C57MG/Wnt-1 or human fetal lung cDNA library with a probe corresponding to nucleotides 1463–1512. Full-length cDNAs encoding *WISP-3* were cloned from human bone marrow and fetal kidney libraries.

**Expression of Human *WISP* RNA.** PCR amplification of first-strand cDNA was performed with human Multiple Tissue cDNA panels (CLONTECH) and 300  $\mu$ M of each dNTP at 94°C for 1 sec, 62°C for 30 sec, 72°C for 1 min, for 22–32 cycles. *WISP* and glyceraldehyde-3-phosphate dehydrogenase primer sequences are available on request.

**In Situ Hybridization.** <sup>33</sup>P-labeled sense and antisense riboprobes were transcribed from an 897-bp PCR product corresponding to nucleotides 601–1440 of mouse *WISP-1* or a 294-bp PCR product corresponding to nucleotides 82–375 of mouse *WISP-2*. All tissues were processed as described (40).

**Radiation Hybrid Mapping.** Genomic DNA from each hybrid in the Stanford G3 and Genebridge4 Radiation Hybrid Panels (Research Genetics, Huntsville, AL) and human and hamster control DNAs were PCR-amplified, and the results were submitted to the Stanford or Massachusetts Institute of Technology web servers.

**Cell Lines, Tumors, and Mucosa Specimens.** Tissue specimens were obtained from the Department of Pathology (University of Pittsburgh) for patients undergoing colon resection and from the University of Leeds, United Kingdom. Genomic DNA was isolated (Qiagen) from the pooled blood of 10 normal human donors, surgical specimens, and the following ATCC human cell lines: SW480, COLO 320DM, HT-29, WiDr, and SW403 (colon adenocarcinomas), SW620 (lymph node metastasis, colon adenocarcinoma), HCT 116 (colon carcinoma), SK-CO-1 (colon adenocarcinoma, ascites), and HM7 (a variant of ATCC colon adenocarcinoma cell line LS 174T). DNA concentration was determined by using Hoechst dye 33258 intercalation fluorimetry. Total RNA was prepared by homogenization in 7 M GuSCN followed by centrifugation over CsCl cushions or prepared by using RNeasy.

**Gene Amplification and RNA Expression Analysis.** Relative gene amplification and RNA expression of *WISPs* and *c-myc* in the cell lines, colorectal tumors, and normal mucosa were determined by quantitative PCR. Gene-specific primers and fluorogenic probes (sequences available on request) were designed and used to amplify and quantitate the genes. The relative gene copy number was derived by using the formula  $2^{\Delta Ct}$  where  $\Delta Ct$  represents the difference in amplification cycles required to detect the *WISP* genes in peripheral blood lymphocyte DNA compared with colon tumor DNA or colon tumor RNA compared with normal mucosal RNA. The  $\Delta$ -method was used for calculation of the SE of the gene copy number or RNA expression level. The *WISP*-specific signal was normalized to that of the glyceraldehyde-3-phosphate dehydrogenase housekeeping gene. All TaqMan assay reagents were obtained from Perkin-Elmer Applied Biosystems.

## RESULTS

**Isolation of *WISP-1* and *WISP-2* by SSH.** To identify Wnt-1-inducible genes, we used the technique of SSH using the

mouse mammary epithelial cell line C57MG and C57MG cells that stably express Wnt-1 (11). Candidate differentially expressed cDNAs (1,384 total) were sequenced. Thirty-nine percent of the sequences matched known genes or homologues, 32% matched expressed sequence tags, and 29% had no match. To confirm that the transcript was differentially expressed, semiquantitative reverse transcription-PCR and Northern analysis were performed by using mRNA from the C57MG and C57MG/Wnt-1 cells.

Two of the cDNAs, *WISP-1* and *WISP-2*, were differentially expressed, being induced in the C57MG/Wnt-1 cell line, but not in the parent C57MG cells or C57MG cells overexpressing Wnt-4 (Fig. 1A and B). Wnt-4, unlike Wnt-1, does not induce the morphological transformation of C57MG cells and has no effect on  $\beta$ -catenin levels (13, 14). Expression of *WISP-1* was up-regulated approximately 3-fold in the C57MG/Wnt-1 cell line and *WISP-2* by approximately 5-fold by both Northern analysis and reverse transcription-PCR.

An independent, but similar, system was used to examine *WISP* expression after Wnt-1 induction. C57MG cells expressing the *Wnt-1* gene under the control of a tetracycline-repressible promoter produce low amounts of Wnt-1 in the repressed state but show a strong induction of *Wnt-1* mRNA and protein within 24 hr after tetracycline removal (8). The levels of Wnt-1 and *WISP* RNA isolated from these cells at various times after tetracycline removal were assessed by quantitative PCR. Strong induction of Wnt-1 mRNA was seen as early as 10 hr after tetracycline removal. Induction of *WISP* mRNA (2- to 6-fold) was seen at 48 and 72 hr (data not shown). These data support our previous observations that show that *WISP* induction is correlated with Wnt-1 expression. Because the induction is slow, occurring after approximately 48 hr, the induction of *WISPs* may be an indirect response to Wnt-1 signaling.

cDNA clones of human *WISP-1* were isolated and the sequence compared with mouse *WISP-1*. The cDNA sequences of mouse and human *WISP-1* were 1,766 and 2,830 bp in length, respectively, and encode proteins of 367 aa, with predicted relative molecular masses of  $\approx$ 40,000 ( $M_r$  40 K). Both have hydrophobic N-terminal signal sequences, 38 conserved cysteine residues, and four potential N-linked glycosylation sites and are 84% identical (Fig. 2A).

Full-length cDNA clones of mouse and human *WISP-2* were 1,734 and 1,293 bp in length, respectively, and encode proteins of 251 and 250 aa, respectively, with predicted relative molecular masses of  $\approx$ 27,000 ( $M_r$  27 K) (Fig. 2B). Mouse and human *WISP-2* are 73% identical. Human *WISP-2* has no potential N-linked glycosylation sites, and mouse *WISP-2* has one at

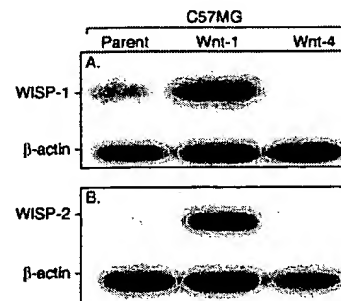


FIG. 1. *WISP-1* and *WISP-2* are induced by Wnt-1, but not Wnt-4, expression in C57MG cells. Northern analysis of *WISP-1* (A) and *WISP-2* (B) expression in C57MG, C57MG/Wnt-1, and C57MG/Wnt-4 cells. Poly(A)<sup>+</sup> RNA (2  $\mu$ g) was subjected to Northern blot analysis and hybridized with a 70-bp mouse *WISP-1*-specific probe (amino acids 278–300) or a 190-bp *WISP-2*-specific probe (nucleotides 1438–1627) in the 3' untranslated region. Blots were rehybridized with human  $\beta$ -actin probe.

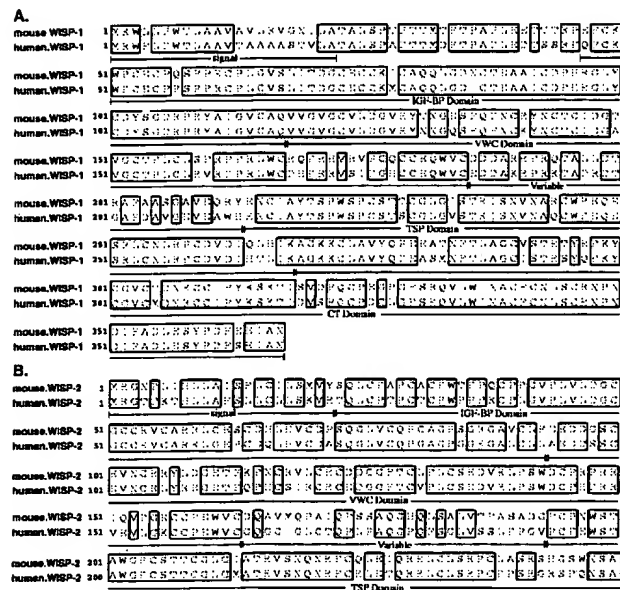


FIG. 2. Encoded amino acid sequence alignment of mouse and human *WISP-1* (A) and mouse and human *WISP-2* (B). The potential signal sequence, insulin-like growth factor-binding protein (IGF-BP), VWC, thrombospondin (TSP), and C-terminal (CT) domains are underlined.

position 197. *WISP-2* has 28 cysteine residues that are conserved among the 38 cysteines found in *WISP-1*.

**Identification of *WISP-3*.** To search for related proteins, we screened expressed sequence tag (EST) databases with the *WISP-1* protein sequence and identified several ESTs as potentially related sequences. We identified a homologous protein that we have called *WISP-3*. A full-length human *WISP-3* cDNA of 1,371 bp was isolated corresponding to those ESTs that encode a 354-aa protein with a predicted molecular mass of 39,293. *WISP-3* has two potential N-linked glycosylation sites and 36 cysteine residues. An alignment of the three human *WISP* proteins shows that *WISP-1* and *WISP-3* are the most similar (42% identity), whereas *WISP-2* has 37% identity with *WISP-1* and 32% identity with *WISP-3* (Fig. 3A).

***WISPs* Are Homologous to the CTGF Family of Proteins.** Human *WISP-1*, *WISP-2*, and *WISP-3* are novel sequences; however, mouse *WISP-1* is the same as the recently identified *Elm1* gene. *Elm1* is expressed in low, but not high, metastatic mouse melanoma cells, and suppresses the *in vivo* growth and metastatic potential of K-1735 mouse melanoma cells (15). Human and mouse *WISP-2* are homologous to the recently described rat gene, *rCop-1* (16). Significant homology (36–44%) was seen to the CCN family of growth factors. This family includes three members, CTGF, Cyr61, and the protooncogene *nov*. CTGF is a chemotactic and mitogenic factor for fibroblasts that is implicated in wound healing and fibrotic disorders and is induced by TGF- $\beta$  (17). Cyr61 is an extracellular matrix signaling molecule that promotes cell adhesion, proliferation, migration, angiogenesis, and tumor growth (18, 19). *nov* (nephroblastoma overexpressed) is an immediate early gene associated with quiescence and found altered in Wilms tumors (20). The proteins of the CCN family share functional, but not sequence, similarity to Wnt-1. All are secreted, cysteine-rich heparin binding glycoproteins that associate with the cell surface and extracellular matrix.

*WISP* proteins exhibit the modular architecture of the CCN family, characterized by four conserved cysteine-rich domains (Fig. 3B) (21). The N-terminal domain, which includes the first 12 cysteine residues, contains a consensus sequence (GCGC-CXXC) conserved in most insulin-like growth factor (IGF)-

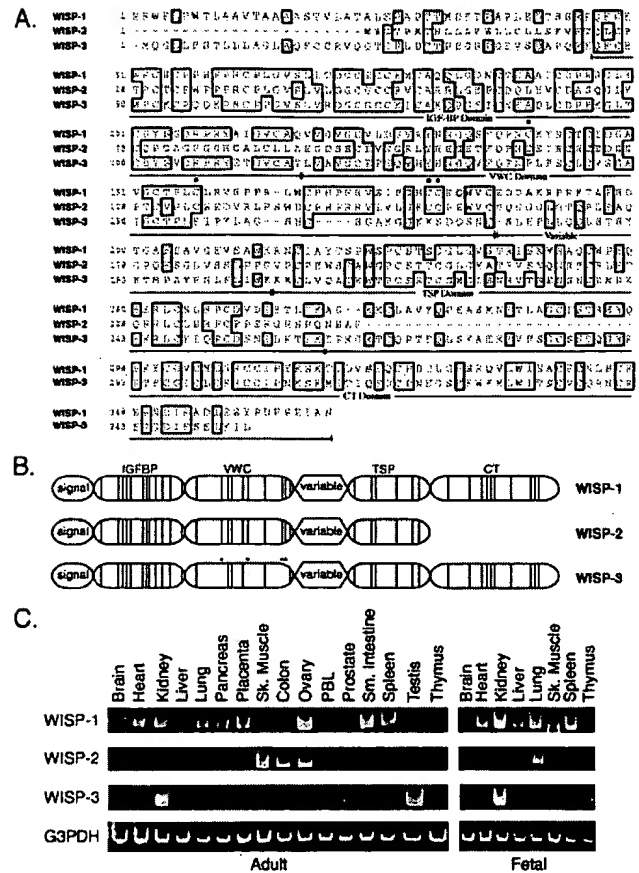


FIG. 3. (A) Encoded amino acid sequence alignment of human *WISPs*. The cysteine residues of *WISP-1* and *WISP-2* that are not present in *WISP-3* are indicated with a dot. (B) Schematic representation of the *WISP* proteins showing the domain structure and cysteine residues (vertical lines). The four cysteine residues in the VWC domain that are absent in *WISP-3* are indicated with a dot. (C) Expression of *WISP* mRNA in human tissues. PCR was performed on human multiple-tissue cDNA panels (CLONTECH) from the indicated adult and fetal tissues.

binding proteins (BP). This sequence is conserved in *WISP-2* and *WISP-3*, whereas *WISP-1* has a glutamine in the third position instead of a glycine. CTGF recently has been shown to specifically bind IGF (22) and a truncated *nov* protein lacking the IGF-BP domain is oncogenic (23). The von Willebrand factor type C module (VWC), also found in certain collagens and mucins, covers the next 10 cysteine residues, and is thought to participate in protein complex formation and oligomerization (24). The VWC domain of *WISP-3* differs from all CCN family members described previously, in that it contains only six of the 10 cysteine residues (Fig. 3A and B). A short variable region follows the VWC domain. The third module, the thrombospondin (TSP) domain is involved in binding to sulfated glycoconjugates and contains six cysteine residues and a conserved WSXCSXCG motif first identified in thrombospondin (25). The C-terminal (CT) module containing the remaining 10 cysteines is thought to be involved in dimerization and receptor binding (26). The CT domain is present in all CCN family members described to date but is absent in *WISP-2* (Fig. 3A and B). The existence of a putative signal sequence and the absence of a transmembrane domain suggest that *WISPs* are secreted proteins, an observation supported by an analysis of their expression and secretion from mammalian cell and baculovirus cultures (data not shown).

**Expression of *WISP* mRNA in Human Tissues.** Tissue-specific expression of human *WISPs* was characterized by PCR



analysis on adult and fetal multiple tissue cDNA panels. *WISP-1* expression was seen in the adult heart, kidney, lung, pancreas, placenta, ovary, small intestine, and spleen (Fig. 3C). Little or no expression was detected in the brain, liver, skeletal muscle, colon, peripheral blood leukocytes, prostate, testis, or thymus. *WISP-2* had a more restricted tissue expression and was detected in adult skeletal muscle, colon, ovary, and fetal lung. Predominant expression of *WISP-3* was seen in adult kidney and testis and fetal kidney. Lower levels of *WISP-3* expression were detected in placenta, ovary, prostate, and small intestine.

**In Situ Localization of *WISP-1* and *WISP-2*.** Expression of *WISP-1* and *WISP-2* was assessed by *in situ* hybridization in mammary tumors from Wnt-1 transgenic mice. Strong expression of *WISP-1* was observed in stromal fibroblasts lying within the fibrovascular tumor stroma (Fig. 4 A–D). However, low-level *WISP-1* expression also was observed focally within tumor cells (data not shown). No expression was observed in normal breast. Like *WISP-1*, *WISP-2* expression also was seen in the tumor stroma in breast tumors from Wnt-1 transgenic animals (Fig. 4 E–H). However, *WISP-2* expression in the stroma was in spindle-shaped cells adjacent to capillary vessels, whereas

the predominant cell type expressing *WISP-1* was the stromal fibroblasts.

**Chromosome Localization of the *WISP* Genes.** The chromosomal location of the human *WISP* genes was determined by radiation hybrid mapping panels. *WISP-1* is approximately 3.48 cR from the meiotic marker AFM259xc5 [logarithm of odds (lod) score 16.31] on chromosome 8q24.1 to 8q24.3, in the same region as the human locus of the *novH* family member (27) and roughly 4 Mbs distal to *c-myc* (28). Preliminary fine mapping indicates that *WISP-1* is located near D8S1712 STS. *WISP-2* is linked to the marker SHGC-33922 (lod = 1,000) on chromosome 20q12–20q13.1. Human *WISP-3* mapped to chromosome 6q22–6q23 and is linked to the marker AFM211ze5 (lod = 1,000). *WISP-3* is approximately 18 Mbs proximal to CTGF and 23 Mbs proximal to the human cellular oncogene *MYB* (27, 29).

**Amplification and Aberrant Expression of *WISPs* in Human Colon Tumors.** Amplification of protooncogenes is seen in many human tumors and has etiological and prognostic significance. For example, in a variety of tumor types, *c-myc* amplification has been associated with malignant progression and poor prognosis (30). Because *WISP-1* resides in the same general chromosomal location (8q24) as *c-myc*, we asked whether it was a target of gene amplification, and, if so, whether this amplification was independent of the *c-myc* locus. Genomic DNA from human colon cancer cell lines was assessed by quantitative PCR and Southern blot analysis. (Fig. 5 A and B). Both methods detected similar degrees of *WISP-1* amplification. Most cell lines showed significant (2- to 4-fold) amplification, with the HT-29 and WiDr cell lines demonstrating an 8-fold increase. Significantly, the pattern of amplification observed did not correlate with that observed for *c-myc*, indicating that the *c-myc* gene is not part of the amplicon that involves the *WISP-1* locus.

We next examined whether the *WISP* genes were amplified in a panel of 25 primary human colon adenocarcinomas. The relative *WISP* gene copy number in each colon tumor DNA was compared with pooled normal DNA from 10 donors by quantitative PCR (Fig. 6). The copy number of *WISP-1* and *WISP-2* was significantly greater than one, approximately 2-fold for *WISP-1* in about 60% of the tumors and 2- to 4-fold for *WISP-2* in 92% of the tumors ( $P < 0.001$  for each). The copy number for *WISP-3* was indistinguishable from one ( $P = 0.166$ ). In addition, the copy number of *WISP-2* was significantly higher than that of *WISP-1* ( $P < 0.001$ ).

The levels of *WISP* transcripts in RNA isolated from 19 adenocarcinomas and their matched normal mucosa were

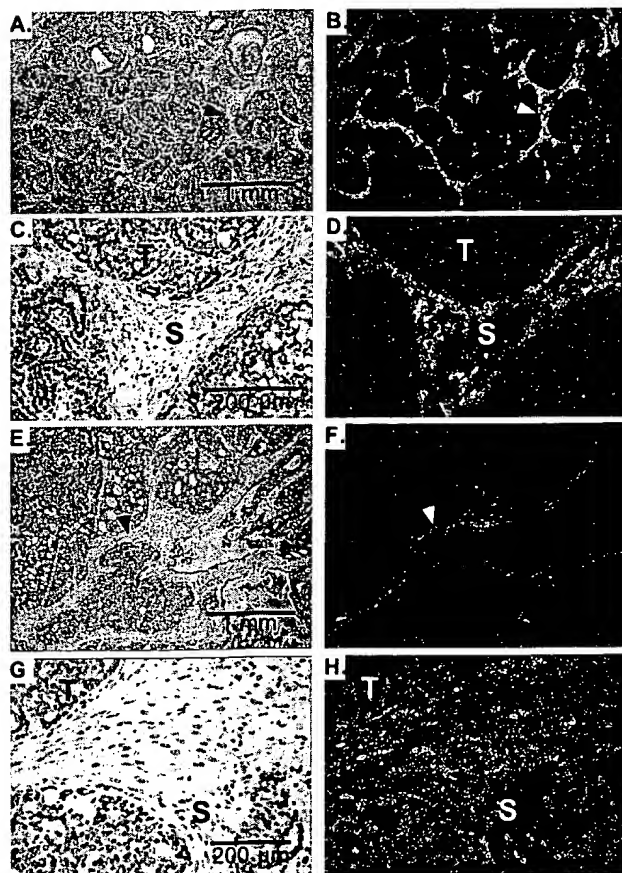


FIG. 4. (A, C, E, and G) Representative hematoxylin/eosin-stained images from breast tumors in Wnt-1 transgenic mice. The corresponding dark-field images showing *WISP-1* expression are shown in B and D. The tumor is a moderately well-differentiated adenocarcinoma showing evidence of adenoid cystic change. At low power (A and B), expression of *WISP-1* is seen in the delicate branching fibrovascular tumor stroma (arrowhead). At higher magnification, expression is seen in the stromal(s) fibroblasts (C and D), and tumor cells are negative. Focal expression of *WISP-1*, however, was observed in tumor cells in some areas. Images of *WISP-2* expression are shown in E–H. At low power (E and F), expression of *WISP-2* is seen in cells lying within the fibrovascular tumor stroma. At higher magnification, these cells appeared to be adjacent to capillary vessels whereas tumor cells are negative (G and H).

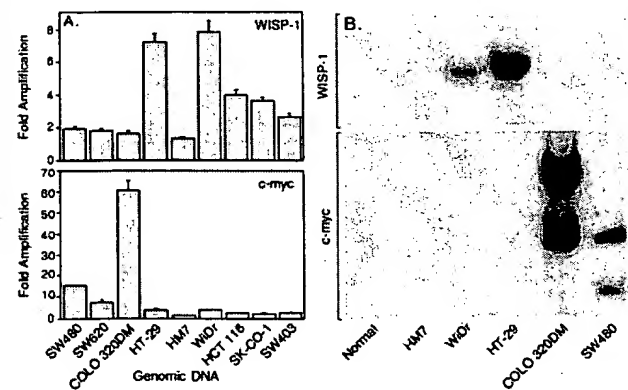


FIG. 5. Amplification of *WISP-1* genomic DNA in colon cancer cell lines. (A) Amplification in cell line DNA was determined by quantitative PCR. (B) Southern blots containing genomic DNA (10  $\mu$ g) digested with *EcoRI* (*WISP-1*) or *XbaI* (*c-myc*) were hybridized with a 100-bp human *WISP-1* probe (amino acids 186–219) or a human *c-myc* probe (located at bp 1901–2000). The *WISP* and *myc* genes are detected in normal human genomic DNA after a longer film exposure.

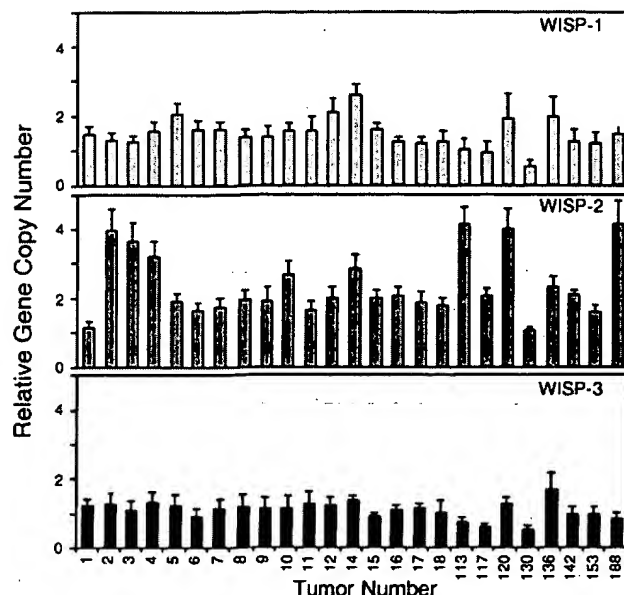


FIG. 6. Genomic amplification of *WISP* genes in human colon tumors. The relative gene copy number of the *WISP* genes in 25 adenocarcinomas was assayed by quantitative PCR, by comparing DNA from primary human tumors with pooled DNA from 10 healthy donors. The data are means  $\pm$  SEM from one experiment done in triplicate. The experiment was repeated at least three times.

assessed by quantitative PCR (Fig. 7). The level of *WISP-1* RNA present in tumor tissue varied but was significantly increased (2- to >25-fold) in 84% (16/19) of the human colon tumors examined compared with normal adjacent mucosa. Four of 19 tumors showed greater than 10-fold overexpression. In contrast, in 79% (15/19) of the tumors examined, *WISP-2* RNA expression was significantly lower in the tumor than the mucosa. Similar to *WISP-1*, *WISP-3* RNA was overexpressed in 63% (12/19) of the colon tumors compared with the normal

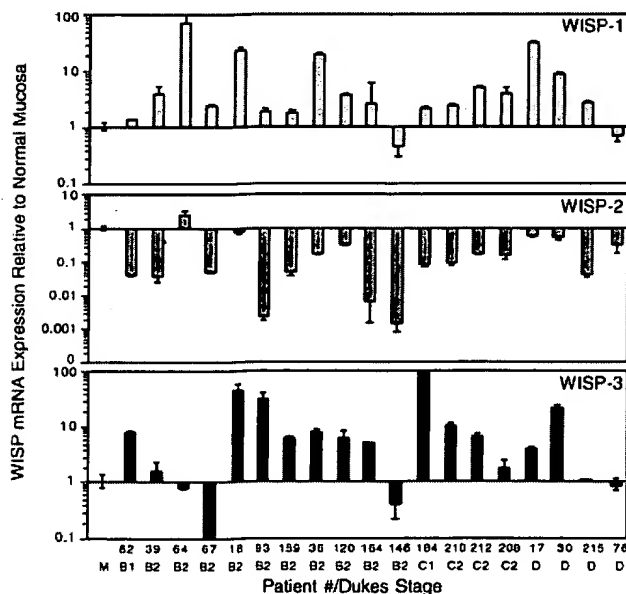


FIG. 7. *WISP* RNA expression in primary human colon tumors relative to expression in normal mucosa from the same patient. Expression of *WISP* mRNA in 19 adenocarcinomas was assayed by quantitative PCR. The Dukes stage of the tumor is listed under the sample number. The data are means  $\pm$  SEM from one experiment done in triplicate. The experiment was repeated at least twice.

mucosa. The amount of overexpression of *WISP-3* ranged from 4- to >40-fold.

## DISCUSSION

One approach to understanding the molecular basis of cancer is to identify differences in gene expression between cancer cells and normal cells. Strategies based on assumptions that steady-state mRNA levels will differ between normal and malignant cells have been used to clone differentially expressed genes (31). We have used a PCR-based selection strategy, SSH, to identify genes selectively expressed in C57MG mouse mammary epithelial cells transformed by Wnt-1.

Three of the genes isolated, *WISP-1*, *WISP-2*, and *WISP-3*, are members of the CCN family of growth factors, which includes CTGF, Cyr61, and *nov*, a family not previously linked to Wnt signaling.

Two independent experimental systems demonstrated that *WISP* induction was associated with the expression of Wnt-1. The first was C57MG cells infected with a Wnt-1 retroviral vector or C57MG cells expressing Wnt-1 under the control of a tetracycline-repressible promoter, and the second was in Wnt-1 transgenic mice, where breast tissue expresses Wnt-1, whereas normal breast tissue does not. No *WISP* RNA expression was detected in mammary tumors induced by polyoma virus middle T antigen (data not shown). These data suggest a link between Wnt-1 and *WISPs* in that in these two situations, *WISP* induction was correlated with Wnt-1 expression.

It is not clear whether the *WISPs* are directly or indirectly induced by the downstream components of the Wnt-1 signaling pathway (i.e.,  $\beta$ -catenin-TCF-1/Lef1). The increased levels of *WISP* RNA were measured in Wnt-1-transformed cells, hours or days after Wnt-1 transformation. Thus, *WISP* expression could result from Wnt-1 signaling directly through  $\beta$ -catenin transcription factor regulation or alternatively through Wnt-1 signaling turning on a transcription factor, which in turn regulates *WISPs*.

The *WISPs* define an additional subfamily of the CCN family of growth factors. One striking difference observed in the protein sequence of *WISP-2* is the absence of a CT domain, which is present in CTGF, Cyr61, *nov*, *WISP-1*, and *WISP-3*. This domain is thought to be involved in receptor binding and dimerization. Growth factors, such as TGF- $\beta$ , platelet-derived growth factor, and nerve growth factor, which contain a cysteine knot motif exist as dimers (32). It is tempting to speculate that *WISP-1* and *WISP-3* may exist as dimers, whereas *WISP-2* exists as a monomer. If the CT domain is also important for receptor binding, *WISP-2* may bind its receptor through a different region of the molecule than the other CCN family members. No specific receptors have been identified for CTGF or *nov*. A recent report has shown that integrin  $\alpha_v\beta_3$  serves as an adhesion receptor for Cyr61 (33).

The strong expression of *WISP-1* and *WISP-2* in cells lying within the fibrovascular tumor stroma in breast tumors from Wnt-1 transgenic animals is consistent with previous observations that transcripts for the related CTGF gene are primarily expressed in the fibrous stroma of mammary tumors (34). Epithelial cells are thought to control the proliferation of connective tissue stroma in mammary tumors by a cascade of growth factor signals similar to that controlling connective tissue formation during wound repair. It has been proposed that mammary tumor cells or inflammatory cells at the tumor interstitial interface secrete TGF- $\beta$ 1, which is the stimulus for stromal proliferation (34). TGF- $\beta$ 1 is secreted by a large percentage of malignant breast tumors and may be one of the growth factors that stimulates the production of CTGF and *WISPs* in the stroma.

It was of interest that *WISP-1* and *WISP-2* expression was observed in the stromal cells that surrounded the tumor cells

(epithelial cells) in the Wnt-1 transgenic mouse sections of breast tissue. This finding suggests that paracrine signaling could occur in which the stromal cells could supply WISP-1 and WISP-2 to regulate tumor cell growth on the WISP extracellular matrix. Stromal cell-derived factors in the extracellular matrix have been postulated to play a role in tumor cell migration and proliferation (35). The localization of WISP-1 and WISP-2 in the stromal cells of breast tumors supports this paracrine model.

An analysis of WISP-1 gene amplification and expression in human colon tumors showed a correlation between DNA amplification and overexpression, whereas overexpression of WISP-3 RNA was seen in the absence of DNA amplification. In contrast, WISP-2 DNA was amplified in the colon tumors, but its mRNA expression was significantly reduced in the majority of tumors compared with the expression in normal colonic mucosa from the same patient. The gene for human WISP-2 was localized to chromosome 20q12-20q13, at a region frequently amplified and associated with poor prognosis in node negative breast cancer and many colon cancers, suggesting the existence of one or more oncogenes at this locus (36-38). Because the center of the 20q13 amplicon has not yet been identified, it is possible that the apparent amplification observed for WISP-2 may be caused by another gene in this amplicon.

A recent manuscript on *rCop-1*, the rat orthologue of WISP-2, describes the loss of expression of this gene after cell transformation, suggesting it may be a negative regulator of growth in cell lines (16). Although the mechanism by which WISP-2 RNA expression is down-regulated during malignant transformation is unknown, the reduced expression of WISP-2 in colon tumors and cell lines suggests that it may function as a tumor suppressor. These results show that the WISP genes are aberrantly expressed in colon cancer and suggest that their altered expression may confer selective growth advantage to the tumor.

Members of the Wnt signaling pathway have been implicated in the pathogenesis of colon cancer, breast cancer, and melanoma, including the tumor suppressor gene adenomatous polyposis coli and  $\beta$ -catenin (39). Mutations in specific regions of either gene can cause the stabilization and accumulation of cytoplasmic  $\beta$ -catenin, which presumably contributes to human carcinogenesis through the activation of target genes such as the WISPs. Although the mechanism by which Wnt-1 transforms cells and induces tumorigenesis is unknown, the identification of WISPs as genes that may be regulated downstream of Wnt-1 in C57MG cells suggests they could be important mediators of Wnt-1 transformation. The amplification and altered expression patterns of the WISPs in human colon tumors may indicate an important role for these genes in tumor development.

We thank the DNA synthesis group for oligonucleotide synthesis, T. Baker for technical assistance, P. Dowd for radiation hybrid mapping, K. Willert and R. Nusse for the tet-repressible C57MG/Wnt-1 cells, V. Dixit for discussions, and D. Wood and A. Bruce for artwork.

- Cadigan, K. M. & Nusse, R. (1997) *Genes Dev.* **11**, 3286-3305.
- Dale, T. C. (1998) *Biochem. J.* **329**, 209-223.
- Nusse, R. & Varmus, H. E. (1982) *Cell* **31**, 99-109.
- van Ooyen, A. & Nusse, R. (1984) *Cell* **39**, 233-240.
- Tsukamoto, A. S., Grosschedl, R., Guzman, R. C., Parslow, T. & Varmus, H. E. (1988) *Cell* **55**, 619-625.
- Brown, J. D. & Moon, R. T. (1998) *Curr. Opin. Cell Biol.* **10**, 182-187.
- Molenaar, M., van de Wetering, M., Oosterwegel, M., Peterson-Maduro, J., Godsave, S., Korinek, V., Roose, J., Destree, O. & Clevers, H. (1996) *Cell* **86**, 391-399.
- Korinek, V., Barker, N., Willert, K., Molenaar, M., Roose, J., Wagenaar, G., Markman, M., Lamers, W., Destree, O. & Clevers, H. (1998) *Mol. Cell Biol.* **18**, 1248-1256.
- Munemitsu, S., Albert, I., Souza, B., Rubinfeld, B. & Polakis, P. (1995) *Proc. Natl. Acad. Sci. USA* **92**, 3046-3050.
- He, T. C., Sparks, A. B., Rago, C., Hermeking, H., Zawel, L., da Costa, L. T., Morin, P. J., Vogelstein, B. & Kinzler, K. W. (1998) *Science* **281**, 1509-1512.
- Diatchenko, L., Lau, Y. F., Campbell, A. P., Chenchik, A., Moqadam, F., Huang, B., Lukyanov, S., Lukyanov, K., Gurskaya, N., Sverdlov, E. D. & Siebert, P. D. (1996) *Proc. Natl. Acad. Sci. USA* **93**, 6025-6030.
- Brown, A. M., Wildin, R. S., Prendergast, T. J. & Varmus, H. E. (1986) *Cell* **46**, 1001-1009.
- Wong, G. T., Gavin, B. J. & McMahon, A. P. (1994) *Mol. Cell Biol.* **14**, 6278-6286.
- Shimizu, H., Julius, M. A., Giarre, M., Zheng, Z., Brown, A. M. & Kitajewski, J. (1997) *Cell Growth Differ.* **8**, 1349-1358.
- Hashimoto, Y., Shindo-Okada, N., Tani, M., Nagamachi, Y., Takeuchi, K., Shiroishi, T., Toma, H. & Yokota, J. (1998) *J. Exp. Med.* **187**, 289-296.
- Zhang, R., Averboukh, L., Zhu, W., Zhang, H., Jo, H., Dempsey, P. J., Coffey, R. J., Pardee, A. B. & Liang, P. (1998) *Mol. Cell Biol.* **18**, 6131-6141.
- Grotendorst, G. R. (1997) *Cytokine Growth Factor Rev.* **8**, 171-179.
- Kireeva, M. L., Mo, F. E., Yang, G. P. & Lau, L. F. (1996) *Mol. Cell Biol.* **16**, 1326-1334.
- Babic, A. M., Kireeva, M. L., Kolesnikova, T. V. & Lau, L. F. (1998) *Proc. Natl. Acad. Sci. USA* **95**, 6355-6360.
- Martinerie, C., Huff, V., Joubert, I., Badzioch, M., Saunders, G., Strong, L. & Perbal, B. (1994) *Oncogene* **9**, 2729-2732.
- Bork, P. (1993) *FEBS Lett.* **327**, 125-130.
- Kim, H. S., Nagalla, S. R., Oh, Y., Wilson, E., Roberts, C. T., Jr. & Rosenfeld, R. G. (1997) *Proc. Natl. Acad. Sci. USA* **94**, 12981-12986.
- Joliet, V., Martinerie, C., Dambrine, G., Plassiart, G., Brisac, M., Crochet, J. & Perbal, B. (1992) *Mol. Cell Biol.* **12**, 10-21.
- Mancuso, D. J., Tuley, E. A., Westfield, L. A., Worrall, N. K., Shelton-Inloes, B. B., Sorace, J. M., Alevy, Y. G. & Sadler, J. E. (1989) *J. Biol. Chem.* **264**, 19514-19527.
- Holt, G. D., Pangburn, M. K. & Ginsburg, V. (1990) *J. Biol. Chem.* **265**, 2852-2855.
- Voorberg, J., Fontijn, R., Calafat, J., Janssen, H., van Mourik, J. A. & Pannekoek, H. (1991) *J. Cell Biol.* **113**, 195-205.
- Martinerie, C., Viegas-Pequignot, E., Guenard, I., Dutrillaux, B., Nguyen, V. C., Bernheim, A. & Perbal, B. (1992) *Oncogene* **7**, 2529-2534.
- Takahashi, E., Hori, T., O'Connell, P., Leppert, M. & White, R. (1991) *Cytogenet. Cell. Genet.* **57**, 109-111.
- Meese, E., Meltzer, P. S., Witkowski, C. M. & Trent, J. M. (1989) *Genes Chromosomes Cancer* **1**, 88-94.
- Garte, S. J. (1993) *Crit. Rev. Oncol.* **4**, 435-449.
- Zhang, L., Zhou, W., Velculescu, V. E., Kern, S. E., Hruban, R. H., Hamilton, S. R., Vogelstein, B. & Kinzler, K. W. (1997) *Science* **276**, 1268-1272.
- Sun, P. D. & Davies, D. R. (1995) *Annu. Rev. Biophys. Biomol. Struct.* **24**, 269-291.
- Kireeva, M. L., Lam, S. C. T. & Lau, L. F. (1998) *J. Biol. Chem.* **273**, 3090-3096.
- Frazier, K. S. & Grotendorst, G. R. (1997) *Int. J. Biochem. Cell Biol.* **29**, 153-161.
- Wernert, N. (1997) *Virchows Arch.* **430**, 433-443.
- Tanner, M. M., Tirkkonen, M., Kallioniemi, A., Collins, C., Stokke, T., Karhu, R., Kowbel, D., Shadravan, F., Hintz, M., Kuo, W. L., *et al.* (1994) *Cancer Res.* **54**, 4257-4260.
- Brinkmann, U., Gallo, M., Polymeropoulos, M. H. & Pastan, I. (1996) *Genome Res.* **6**, 187-194.
- Bischoff, J. R., Anderson, L., Zhu, Y., Mossie, K., Ng, L., Souza, B., Schryver, B., Flanagan, P., Clairvoyant, F., Ginther, C., *et al.* (1998) *EMBO J.* **17**, 3052-3065.
- Morin, P. J., Sparks, A. B., Korinek, V., Barker, N., Clevers, H., Vogelstein, B. & Kinzler, K. W. (1997) *Science* **275**, 1787-1790.
- Lu, L. H. & Gillett, N. (1994) *Cell Vision* **1**, 169-176.

## Review

Paul A. Haynes  
Steven P. Gygi  
Daniel Figgeys  
Ruedi Aebersold

Department of Molecular  
Biotechnology, University of  
Washington, Seattle, WA, USA

## Proteome analysis: Biological assay or data archive?

In this review we examine the current state of proteome analysis. There are three main issues discussed: why it is necessary to study proteomes; how proteomes can be analyzed with current technology; and how proteome analysis can be used to enhance biological research. We conclude that proteome analysis is an essential tool in the understanding of regulated biological systems. Current technology, while still mostly limited to the more abundant proteins, enables the use of proteome analysis both to establish databases of proteins present, and to perform biological assays involving measurement of multiple variables. We believe that the utility of proteome analysis in future biological research will continue to be enhanced by further improvements in analytical technology.

### Contents

1	Introduction .....	1862
2	Rationale for proteome analysis .....	1862
2.1	Correlation between mRNA and protein expression levels .....	1863
2.2	Proteins are dynamically modified and processed .....	1863
2.3	Proteomes are dynamic and reflect the state of a biological system .....	1863
3	Description and assessment of current proteome analysis technology .....	1863
3.1	Technical requirements of proteome technology .....	1863
3.2	2D electrophoresis – mass spectrometry: a common implementation of proteome analysis .....	1864
3.3	Protein identification by LC-MS/MS, capillary LC-MS/MS and CE-MS/MS .....	1865
3.3.1	LC-MS/MS .....	1865
3.3.2	Capillary LC-MS .....	1865
3.3.3	CE-MS/MS .....	1865
3.4	Assessment of 2-DE-MS proteome technology .....	1866
4	Utility of proteome analysis for biological research .....	1868
4.1	The proteome as a database .....	1868
4.2	The proteome as a biological assay .....	1868
5	Concluding remarks .....	1870
6	References .....	1870

### 1 Introduction

A proteome has been defined as the protein complement expressed by the genome of an organism, or, in multicellular organisms, as the protein complement expressed by a tissue or differentiated cell [1]. In the most common implementation of proteome analysis the proteins extracted from the cell or tissue analyzed are separated by high

resolution two-dimensional gel electrophoresis (2-DE), detected in the gel and identified by their amino acid sequence. The ease, sensitivity and speed with which gel-separated proteins can be identified by the use of recently developed mass spectrometric techniques have dramatically increased the interest in proteome technology. One of the most attractive features of such analyses is that complex biological systems can potentially be studied in their entirety, rather than as a multitude of individual components. This makes it far easier to uncover the many complex, and often obscure, relationships between mature gene products in cells. Large-scale proteome characterization projects have been undertaken for a number of different organisms and cell types. Microbial proteome projects currently in progress include, for example: *Saccharomyces cerevisiae* [2], *Salmonella enterica* [3], *Spiroplasma melliferum* [4], *Mycobacterium tuberculosis* [5], *Ochrobactrum anthropi* [6], *Haemophilus influenzae* [7], *Synechocystis* spp. [8], *Escherichia coli* [9], *Rhizobium leguminosarum* [10], and *Dictyostelium discoideum* [11]. Proteome projects underway for tissues of more complex organisms include those for: human bladder squamous cell carcinomas [12], human liver [13], human plasma [13], human keratinocytes [12], human fibroblasts [12], mouse kidney [12], and rat serum [14]. In this manuscript we critically assess the concept of proteome analysis and the technical feasibility of establishing complete proteome maps, and discuss ways in which proteome analysis and biological research intersect.

### 2 Rationale for proteome analysis

The dramatic growth in both the number of genome projects and the speed with which genome sequences are being determined has generated huge amounts of sequence information, for some species even complete genomic sequences ([15–17]). The description of the state of a biological system by the quantitative measurement of system components has long been a primary objective in molecular biology. With recent technical advances including the development of differential display-PCR [18], cDNA microarray and DNA chip technology [19, 20] and serial analysis of gene expression (SAGE) [21, 22], it is now feasible to establish global and quantitative mRNA expression maps of cells and tissues, in which the sequence of all the genes is known, at a speed and sensitivity which is not matched by current

Correspondence: Professor Ruedi Aebersold, Department of Molecular Biotechnology, University of Washington, Box 357730, Seattle, WA, 98195, USA (Tel: +206-685-4235; Fax: +206-685-6392; E-mail: ruedi@u.washington.edu)

Abbreviations: CID, collision-induced dissociation; MS/MS, tandem mass spectrometry; SAGE, serial analysis of gene expression

Keywords: Proteome / Two-dimensional polyacrylamide gel electrophoresis / Tandem mass spectrometry

protein analysis technology. Given the long-standing paradigm in biology that DNA synthesizes RNA which synthesizes protein, and the ability to rapidly establish global, quantitative mRNA expression maps, the questions which arise are why technically complex proteome projects should be undertaken and what specific types of information could be expected from proteome projects which cannot be obtained from genomic and transcript profiling projects. We see three main reasons for proteome analysis to become an essential component in the comprehensive analysis of biological systems. (i) Protein expression levels are not predictable from the mRNA expression levels, (ii) proteins are dynamically modified and processed in ways which are not necessarily apparent from the gene sequence, and (iii) proteomes are dynamic and reflect the state of a biological system.

## 2.1 Correlation between mRNA and protein expression levels

Interpretations of quantitative mRNA expression profiles frequently implicitly or explicitly assume that for specific genes the transcript levels are indicative of the levels of protein expression. As part of an ongoing study in our laboratory, we have determined the correlation of expression at the mRNA and protein levels for a population of selected genes in the yeast *Saccharomyces cerevisiae* growing at mid-log phase (S. P. Gygi *et al.*, submitted for publication). mRNA expression levels were calculated from published SAGE frequency tables [22]. Protein expression levels were quantified by metabolic radiolabeling of the yeast proteins, liquid scintillation counting of the protein spots separated by high resolution 2-DE and mass spectrometric identification of the protein(s) migrating to each spot. The selected 80 samples constitute a relatively homogeneous group with respect to predicted half-life and expression level of the protein products. Thus far, we have found a general trend but no strong correlation between protein and transcript levels (Fig. 1). For some genes studied equivalent mRNA transcript levels translated into protein abundances which varied by more than 50-fold. Similarly, equivalent steady-state protein expression levels were maintained by transcript levels varying by as much as 40-fold (S. P. Gygi *et al.*, submitted). These results suggest that even for a population of genes predicted to be relatively homogeneous with respect to protein half-life and gene expression, the protein levels cannot be accurately predicted from the level of the corresponding mRNA transcript.

## 2.2 Proteins are dynamically modified and processed

In the mature, biologically active form many proteins are post-translationally modified by glycosylation, phosphorylation, prenylation, acylation, ubiquitination or one or more of many other modifications [23] and many proteins are only functional if specifically associated or complexed with other molecules, including DNA, RNA, proteins and organic and inorganic cofactors. Frequently, modifications are dynamic and reversible and may alter the precise three-dimensional structure and the state of activity of a protein. Collectively, the state of modification of the proteins which constitute a biological system

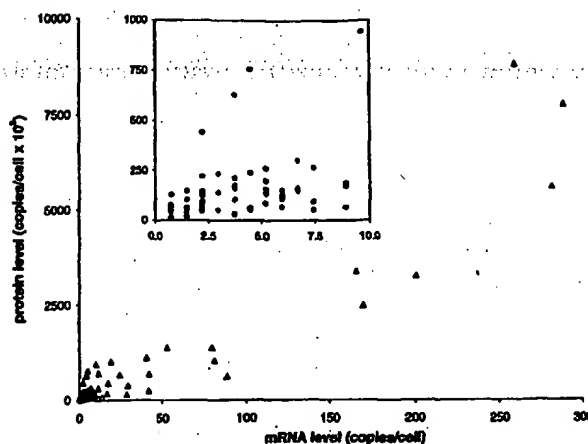


Figure 1. Correlation between mRNA and protein levels in yeast cells. For a selected population of 80 genes, protein levels were measured by  $^{35}$ S-radiolabeling and mRNA levels were calculated from published SAGE tables. Inset: expanded view of the low abundance region. For more experimental details, also see Figs. 5 and 6, (S. P. Gygi *et al.*, submitted).

are important indicators for the state of the system. The type of protein modification and the sites modified at a specific cellular state can usually not be determined from the gene sequence alone.

## 2.3 Proteomes are dynamic and reflect the state of a biological system

A single genome can give rise to many qualitatively and quantitatively different proteomes. Specific stages of the cell cycle and states of differentiation, responses to growth and nutrient conditions, temperature and stress, and pathological conditions represent cellular states which are characterized by significantly different proteomes. The proteome, in principle, also reflects events that are under translational and post-translational control. It is therefore expected that proteomics will be able to provide the most precise and detailed molecular description of the state of a cell or tissue, provided that the external conditions defining the state are carefully determined. In answer to the question of whether the study of proteomes is necessary for the analysis of biomolecular systems, it is evident that the analysis of mature protein products in cells is essential as there are numerous levels of control of protein synthesis, degradation, processing and modification, which are only apparent by direct protein analysis.

## 3 Description and assessment of current proteome analysis technology

### 3.1 Technical requirements of proteome technology

In biological systems the level of expression as well as the states of modification, processing and macro-molecular association of proteins are controlled and modulated depending on the state of the system. Comprehensive analysis of the identity, quantity and state of modification of proteins therefore requires the detection and



quantitation of the proteins which constitute the system, and analysis of differentially processed forms. There are a number of inherent difficulties in protein analysis which complicate these tasks. First, proteins cannot be amplified. It is possible to produce large amounts of a particular protein by over-expression in specific cell systems. However, since many proteins are dynamically post-translationally modified, they cannot be easily amplified in the form in which they finally function in the biological system. It is frequently difficult to purify from the native source sufficient amounts of a protein for analysis. From a technological point of view this translates into the need for high sensitivity analytical techniques. Second, many proteins are modified and processed post-translationally. Therefore, in addition to the protein identity, the structural basis for differentially modified isoforms also needs to be determined. The distribution of a constant amount of protein over several differentially modified isoforms further reduces the amount of each species available for analysis. The complexity and dynamics of post-translational protein editing thus significantly complicates proteome studies. Third, proteins vary dramatically with respect to their solubility in commonly used solvents. There are few, if any, solvent conditions in which all proteins are soluble and which are also compatible with protein analysis. This makes the development of protein purification methods particularly difficult since both protein purification and solubility have to be achieved under the same conditions. Detergents, in particular sodium dodecyl sulfate (SDS), are frequently added to aqueous solvents to maintain protein solubility. The compatibility with SDS is a big advantage of SDS polyacrylamide gel electrophoresis (SDS-PAGE) over other protein separation techniques. Thus, SDS-PAGE and two-dimensional gel electrophoresis, which also uses SDS and other detergents, are the most general and preferred methods for the purification of small amounts of proteins, provided that activity does not necessarily need to be maintained. Lastly, the number of proteins in a given cell system is typically in the thousands. Any attempt to identify and categorize all of these must use methods which are as rapid as possible to allow completion of the project within a reasonable time frame. Therefore, a successful, general proteomics technology requires high sensitivity, high throughput, the ability to differentiate differentially modified proteins, and the ability to quantitatively display and analyze all the proteins present in a sample.

### 3.2 2-D electrophoresis – mass spectrometry: a common implementation of proteome analysis

The most common currently used implementation of proteome analysis technology is based on the separation of proteins by two-dimensional (IEF/SDS-PAGE) gel electrophoresis and their subsequent identification and analysis by mass spectrometry (MS) or tandem mass spectrometry (MS/MS). In 2-DE, proteins are first separated by isoelectric focusing (IEF) and then by SDS-PAGE, in the second, perpendicular dimension. Separated proteins are visualized at high sensitivity by staining or autoradiography, producing two-dimensional arrays of proteins. 2-DE gels are, at present, the most commonly used means of global display of proteins in complex

samples. The separation of thousands of proteins has been achieved in a single gel [24, 25] and differentially modified proteins are frequently separated. Due to the compatibility of 2-DE with high concentrations of detergents, protein denaturants and other additives promoting protein solubility, the technique is widely used.

The second step of this type of proteome analysis is the identification and analysis of separated proteins. Individual proteins from polyacrylamide gels have traditionally been identified using *N*-terminal sequencing [26, 27], internal peptide sequencing [28, 29], immunoblotting or comigration with known proteins [30]. The recent dramatic growth of large-scale genomic and expressed sequence tag (EST) sequence databases has resulted in a fundamental change in the way proteins are identified by their amino acid sequence. Rather than by the traditional methods described above, protein sequences are now frequently determined by correlating mass spectral or tandem mass spectral data of peptides derived from proteins, with the information contained in sequence databases [31–33].

There are a number of alternative approaches to proteome analysis currently under development. There is considerable interest in developing a proteome analysis strategy which bypasses 2-DE altogether, because it is considered a relatively slow and tedious process, and because of perceived difficulties in extracting proteins from the gel matrix for analysis. However, 2-DE as a starting point for proteome analysis has many advantages compared to other techniques available today. The most significant strengths of the 2-DE-MS approach include the relatively uniform behavior of proteins in gels, the ability to quantify spots and the high resolution and simultaneous display of hundreds to thousands of proteins within a reasonable time frame.

A schematic diagram of a typical procedure of the identification of gel-separated proteins is shown in Fig. 2. Protein spots detected in the gel are enzymatically or chemically fragmented and the peptide fragments are isolated for analysis, as already indicated, most frequently by MS or MS/MS. There are numerous protocols for the generation of peptide fragments from gel-separated proteins. They can be grouped into two categories, digestion in the gel slice [28, 34] or digestion after electrotransfer out of the gel onto a suitable membrane ([29, 35–37] and reviewed in [38]). In most instances either technique is applicable and yields good results. The analysis of MS or MS/MS data is an important step in the whole process because MS instruments can generate an enormous amount of information which cannot easily be managed manually. Recently, a number of groups have developed software systems dedicated to the use of peptide MS and MS/MS spectra for the identification of proteins. Proteins are identified by correlating the information contained in the MS spectra of protein digests or MS/MS spectra of individual peptides with data contained in DNA or protein sequence databases.

The systems we are currently using in our laboratory are based on the separation of the peptides contained in protein digests by narrow bore or capillary liquid chromatog-

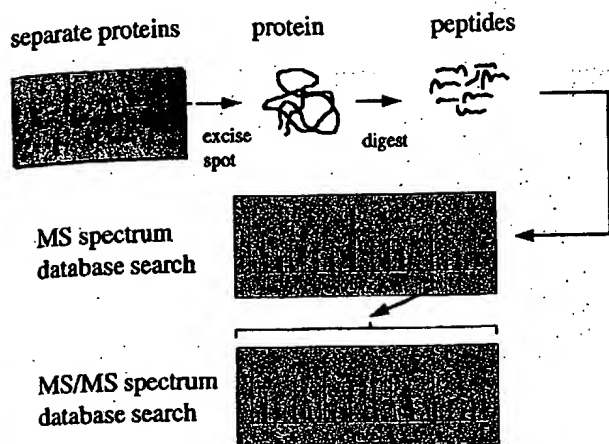


Figure 2. Schematic diagram of a procedure for identification of gel-separated proteins. Peptides can either be separated by a technique such as LC or CE, or infused as a mixture and sorted in the MS. Database searching can either be performed on peptide masses from an MS spectrum, peptide fragment masses from CID spectra of peptides, or a combination of both.

raphy [39, 40] or capillary electrophoresis [41], the analysis of the separated peptides by electrospray ionization (ESI) MS/MS, and the correlation of the generated peptide spectra with sequence databases using the SEQUEST program developed at the University of Washington [32, 33]. The system automatically performs the following operations: a particular peptide ion characterized by its mass-to-charge ratio is selected in the MS out of all the peptide ions present in the system at a particular time; the selected peptide ion is collided in a collision cell with argon (collision-induced dissociation, CID) and the masses of the resulting fragment ions are determined in the second sector of the tandem MS; this experimentally determined CID spectrum is then correlated with the CID spectra predicted from all the peptides in a sequence database which have essentially the same mass as the peptide selected for CID; this correlation matches the isolated peptide with a sequence segment in a database and thus identifies the protein from which the peptide was derived. There are a number of alternative programs which use peptide CID spectra for protein identification, but we use the SEQUEST system because it is currently the most highly automated program and has proven to be successful, versatile and robust.

### 3.3 Protein identification by LC-MS/MS, capillary LC-MS/MS and CE-MS/MS

It has been demonstrated repeatedly that MS has a very high intrinsic sensitivity. For the routine analysis of gel-separated proteins at high sensitivity, the most significant challenge is the handling of small amounts of sample. The crux of the problem is the extraction and transfer of peptide mixtures generated by the digestion of low nanogram amounts of protein, from gels into the MS/MS system without significant loss of sample or introduction of unwanted contaminants. We employ three different systems for introducing gel-purified samples into an MS, depending on the level of sensitivity

required. As an approximate guideline, for samples containing tens of picomoles of peptides, LC-MS/MS is most appropriate; for samples containing low picomole amounts to high femtomole amounts we use capillary LC-MS/MS; and for samples containing femtomoles or less, CE-MS/MS is the method of choice.

#### 3.3.1 LC-MS/MS

The coupling of an MS to an HPLC system using a 0.5 mm diameter or bigger reverse phase (RP) column has been described in detail [42]. This system has several advantages if a large number of samples are to be analyzed and all are available in sufficient quantity. The LC-MS and database searching program can be run in a fully automated mode using an autosampler, thus maximizing sample throughput and minimizing the need for operator interference. The relatively large column is tolerant of high levels of impurities from either gel preparation or sample matrix. Lastly, if configured with a flow-splitter and micro-sprayer [40], analyses can be performed on a small fraction of the sample (less than 5%) while the remainder of the sample is recovered in very pure solvents. This latter feature is particularly useful when an orthogonal technique is also used to analyze peptide fractions, such as scintillation of an introduced radiolabel, and this data can be correlated with peptides identified by CID spectra.

#### 3.3.2 Capillary LC-MS

An increase of sensitivity of approximately tenfold can be achieved by using a capillary LC system with a 100  $\mu$ m ID column rather than a 0.5 mm ID column as referred to above. Since very low flow rates are required for such columns, most reports have used a precolumn flow splitting system for producing solvent gradients. We have recently described the design and construction of a novel gradient mixing system which enables the formation of reproducible gradients at very low flow rates (low nL/min) without the need for flow splitting (A. Ducret *et al.*, submitted for publication). Using this capillary LC-MS/MS system we were able to identify gel-separated proteins if low picomole to high femtomole amounts were loaded onto the gel [40]. This system is as yet not automated and, like all capillary LC systems, is prone to blockage of the columns by microparticulates when analyzing gel-separated proteins.

#### 3.3.3 CE-MS/MS

The highest level of sensitivity for analyzing gel-separated proteins can be achieved by using capillary electrophoresis – mass spectrometry (CE-MS). We have described in the past a solid-phase extraction capillary electrophoresis (SPE-CE) system which was used with triple quadrupole and ion trap ESI-MS/MS systems for the identification of proteins at the low femtomole to sub-femtomole sensitivity level [43, 44]. While this system is highly sensitive, its operation is labor-intensive and its operation has not been automated. In order to devise an analytical system with both the sensitivity of a CE and the level of automation of LC, we have constructed

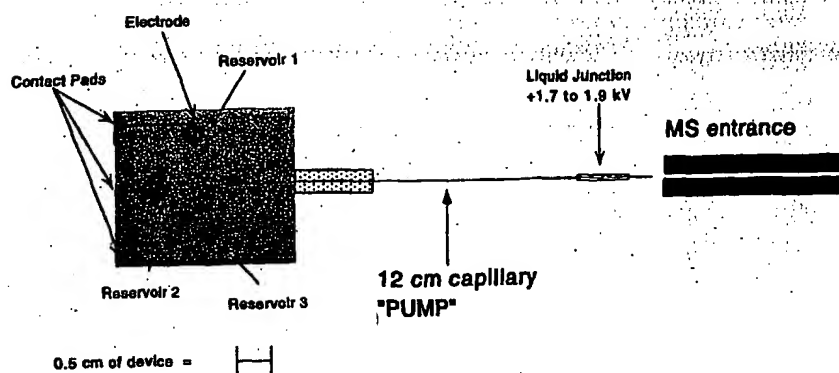


Figure 3. Schematic illustration of a microfabricated analytical system for CE, consisting of a micromachined device, coated capillary electroosmotic pump, and microelectrospray interface. The dimensions of the channels and reservoir are as indicated in the text. The channels on the device were graphically enhanced to make them more visible. Reproduced from [45], with permission.

microfabricated devices for the introduction of samples into ESI-MS for high-sensitivity peptide analysis.

The basic device is a piece of glass into which channels of 10–30  $\mu\text{m}$  in depth and 50–70  $\mu\text{m}$  in diameter are etched by using photolithography/etching techniques similar to the ones used in the semiconductor industry. (A simple device is shown in Fig. 3). The channels are connected to an external high voltage power supply [45]. Samples are manipulated on the device and off the device to the MS by applying different potentials to the reservoirs. This creates a solvent flow by electroosmotic pumping which can be redirected by changing the position of the electrode. Therefore, without the need for valves or gates and without any external pumping, the flow can be redirected by simply switching the position of the electrodes on the device. The direction and rate of the flow can be modulated by the size and the polarity of the electric field applied and also by the charge state of the surface.

The type of data generated by the system is illustrated in Fig. 4, which shows the mass spectrum of a peptide sample representing the tryptic digest of carbonic anhydrase at 290 fmol/ $\mu\text{L}$ . Each numbered peak indicates a peptide successfully identified as being derived from carbonic an-

hydrase. Some of the unassigned signals may be chemical or peptide contaminants. The MS is programmed to automatically select each peak and subject the peptide to CID. The resulting CID spectra are then used to identify the protein by correlation with sequence databases. Therefore, this system allows us to concurrently apply a number of protein digests onto the device, to sequentially mobilize the samples, to automatically generate CID spectra of selected peptide ions and to search sequence databases for protein identification. These steps are performed automatically without the need for user input and proteins can be identified at very low femtomole level sensitivity at a rate of approximately one protein per 15 min.

#### 3.4 Assessment of 2-DE-MS proteome technology

Using a combination of the analytical techniques described above we have identified the 80 protein spots indicated in Fig. 5. The protein pattern was generated by separating a total of 40 microgram of protein contained in a total cell lysate of the yeast strain YPH499 by high resolution 2-DE and silver staining of the separated proteins. To estimate how far this type of proteome analysis can penetrate towards the identification of low abundance proteins, we have calculated the codon bias of the genes encoding the respective proteins. Codon bias is a

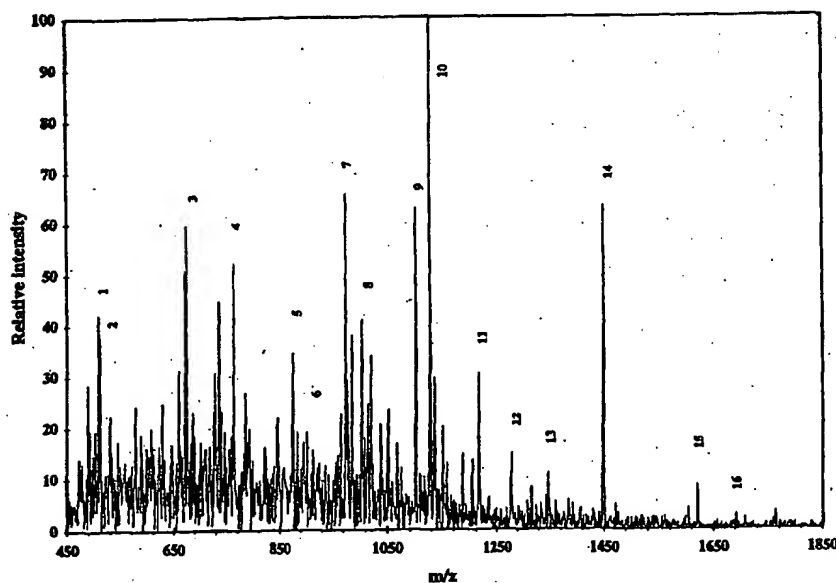


Figure 4. MS spectrum of a tryptic digest of carbonic anhydrase using the microfabricated system shown in Fig. 3. 290 fmol/ $\mu\text{L}$  of carbonic anhydrase tryptic digest was infused into a Finnigan LCQ ion trap MS. Each peak was selected for CID, and those which were identified as containing peptides derived from carbonic anhydrase are numbered. Reproduced from [45], with permission.



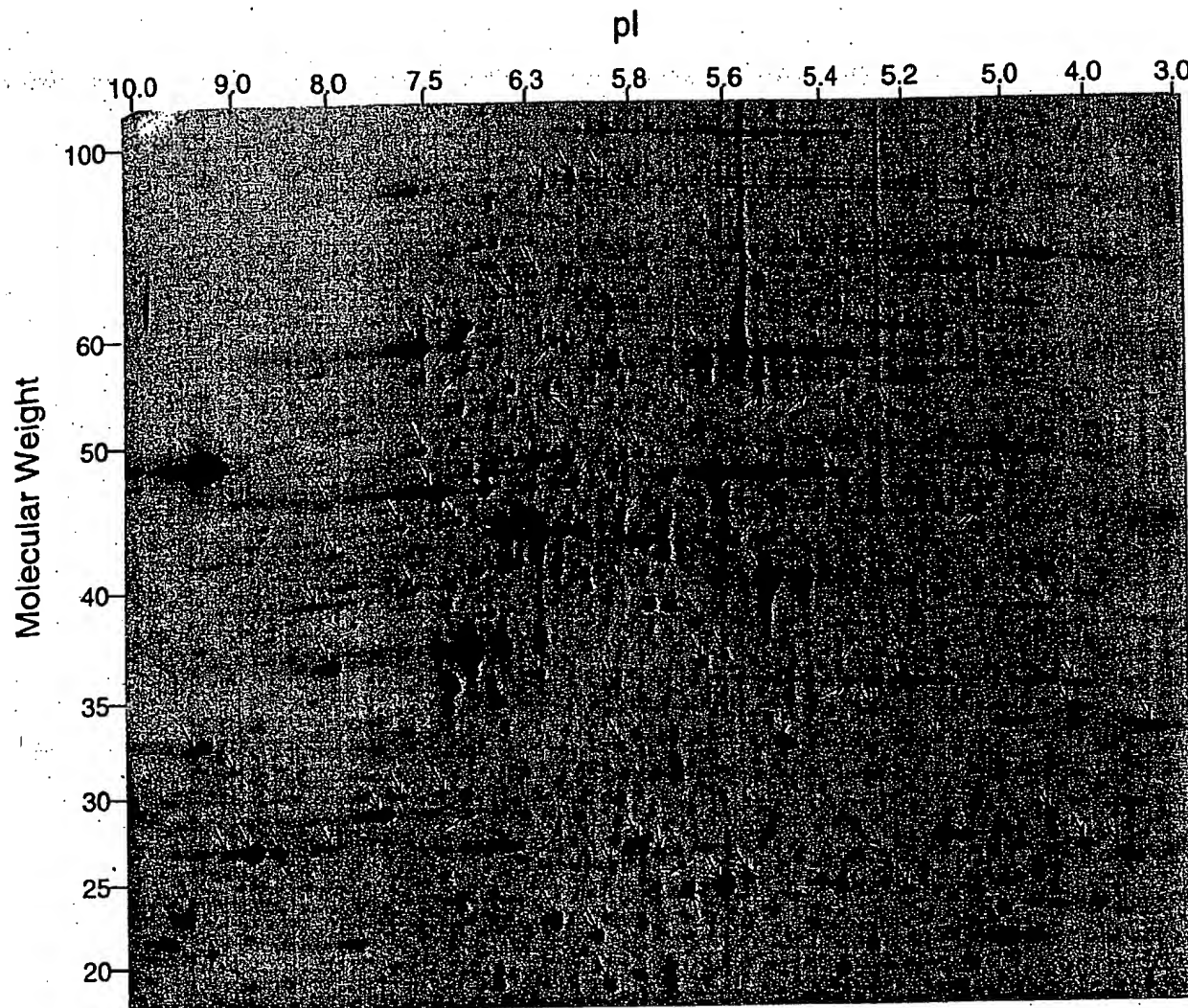


Figure 5. 2-DE separation of a lysate of yeast cells, with identified proteins highlighted. The first dimension of separation was an IPG from pH 3–10, and the second dimension was a 10%T SDS-PAGE gel. Proteins were visualized by silver staining. Further details of experimental procedures are included in S. P. Gygi *et al.* (submitted).

calculated measure of the degree of redundancy of triplet DNA codons used to produce each amino acid in a particular gene sequence. It has been shown to be a useful indicator of the level of the protein product of a particular gene sequence present in a cell [46]. The general rule which applies is that the higher the value of the codon bias calculated for a gene, the more abundant the protein product of that gene becomes. The calculated codon bias values corresponding to the proteins identified in Fig. 5 are shown in Fig. 6b. Nearly all of the proteins identified (> 95%) have codon bias values of > 0.2, indicating they are highly abundant in cells. In contrast, codon bias values calculated for the entire yeast genome (Fig. 6a) show that the majority of proteins present in the proteome have a codon bias of < 0.2 and are thus of low abundance.

This finding is of considerable importance in our assessment of the current status of proteome analysis technology. It is clear that even using highly sensitive analytical techniques, we are only able to visualize and identify the

more abundant proteins. Since many important regulatory proteins are present only at low abundance, these would not be amenable to analysis using such techniques. This situation would be exacerbated in the analysis of proteomes containing many more proteins than the approximately 6000 gene products present in yeast cells [16]. In the analysis of, for example, the proteome of any human cells, there are potentially 50 000–100 000 gene products [47]. Inherent limitations on the amount of protein that can be loaded on 2-DE, and the number of components that can be resolved, indicate that only the most highly abundant fraction of the many gene products could be successfully analyzed. One approach that has been employed to circumvent these limitations is the use of very narrow range immobilized pH gradient strips for the first-dimension separation of 2-DE [48]. Since only those proteins which focus within the narrow range will enter the second dimension of separation, a much higher sample loading within the desired range is possible. This, in turn, can lead to the visualization and identification of less abundant proteins.

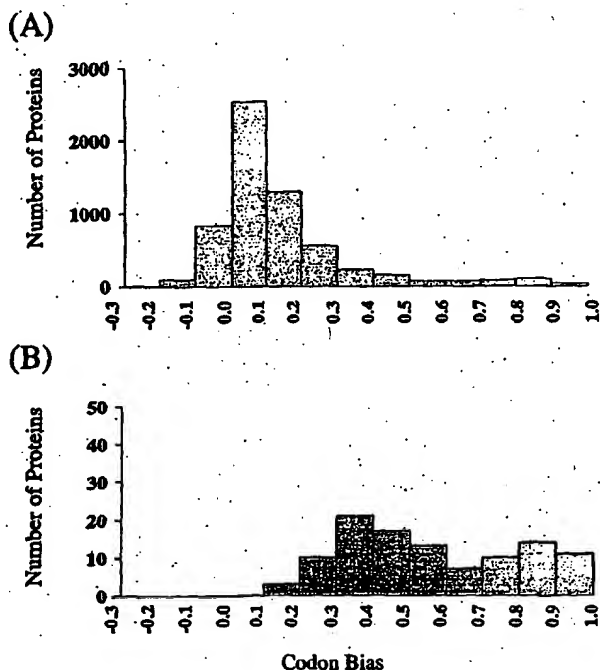


Figure 6. Calculated codon bias values for yeast proteins. (A) Distribution of calculated values for the entire yeast proteome. (B) Distribution of calculated values for the subset of 80 identified proteins also shown in Figs. 1 and 5. Further details of experimental procedures are included in S. P. Gygi *et al.* (submitted).

#### 4 Utility of proteome analysis for biological research

For the success of proteomics as a mainstream approach to the analysis of biological systems it is essential to define how proteome analysis and biological research projects intersect. Without a clear plan for the implementation of proteome-type approaches into biological research projects the full impact of the technology can not be realized. The literature indicates that proteome analysis is used both as a database/data archive, and as a biological assay or biological research tool.

##### 4.1 The proteome as a database

The use of proteomics as a database or data archive essentially entails an attempt to identify all the proteins in a cell or species and to annotate each protein with the known biological information that is relevant for each protein. The level of annotation can, of course, be extensive. The most common implementation of this idea is the separation of proteins by high resolution 2-DE, the identification of each detected protein spot and the annotation of the protein spots in a 2-DE gel database format. This approach is complicated by the fact that it is difficult to precisely define a proteome and to decide which proteome should be represented in the database. In contrast to the genome of a species, which is essentially static, the proteome is highly dynamic. Processes such as differentiation, cell activation and disease can all significantly change the proteome of a species. This is illustrated in Fig. 7. The figure shows two high-resolu-

tion 2-DE maps of proteins isolated from rat serum. Fig. 7A is from the serum of normal rats, while Fig. 7B is from the serum of rats in acute-phase serum after prior treatment with an inflammation-causing agent [49]. It is obvious that the protein patterns are significantly different in several areas, raising the question of exactly which proteome is being described.

Therefore, a comprehensive proteome database of a species or cell type needs to contain all of the parameters which describe the state and the type of the cells from which the proteins were extracted as well as the software tools to search the database with queries which reflect the dynamics of biological systems. A comprehensive proteome database should be capable of quantitatively describing the fate of each protein if specific systems and pathways are activated in the cell. Specifically, the quantity, the degree of modification, the subcellular location and the nature of molecules specifically interacting with a protein as well as the rate of change of these variables should be described. Using these admittedly stringent criteria, there is currently no complete proteome database. A number of such databases are, however, in the process of being constructed. The most advanced among them, in our opinion, are the yeast protein database YPD [50] (accessible at <http://www.ypd.com>) and the human 2D-PAGE databases of the Danish Centre for Human Genome Research [12] (accessible at <http://biobase.dk/cgi-bin/celis>). While neither can be considered complete as not all of the potential gene products are identified, both contain extensive annotation of supplemental information for many of the spots which are positively identified in reference samples.

##### 4.2 The proteome as a biological assay

The use of proteome analysis as a biological assay or research tool represents an alternative approach to integrating biology with proteomics. To investigate the state of a system, samples are subjected to a specific process that allows the quantitative or qualitative measurement of some of the variables which describe the system. In typical biochemical assays one variable (e.g., enzyme activity) of a single component (e.g., a particular enzyme) is measured. Using proteomics as an assay, multiple variables (e.g., expression level, rate of synthesis, phosphorylation state, etc.) are measured concurrently on many (ideally all) of the proteins in a sample. The use of proteomics as an assay is a less far-reaching proposition than the construction of a comprehensive proteome database. It does, however, represent a pragmatic approach which can be adapted to investigate specific systems and pathways, as long as the interpretation of the results takes into account that with current technology not all of the variables which describe the system can be observed (see Section 3.4).

A common implementation of proteome analysis as a biological assay is when a 2-DE protein pattern generated from the analysis of an experimental sample is compared to an array of reference patterns representing different states of the system under investigation. The state of the experimental system at the time the sample was generated is therefore determined by the quantita-

tive comparative analysis of hundreds to a few thousand proteins. Comparative analysis of the 2-DE patterns furthermore highlights quantitative and qualitative differences in the protein profiles which correlate with the state of the system. For this type of analysis it is not essential that all the proteins are identified or even visu-

alized, although the results become more informative as more proteins are compared. It is obvious, however, that the possibility to identify any protein deemed characteristic for a particular state dramatically enhances this approach by opening up new avenues for experimentation.

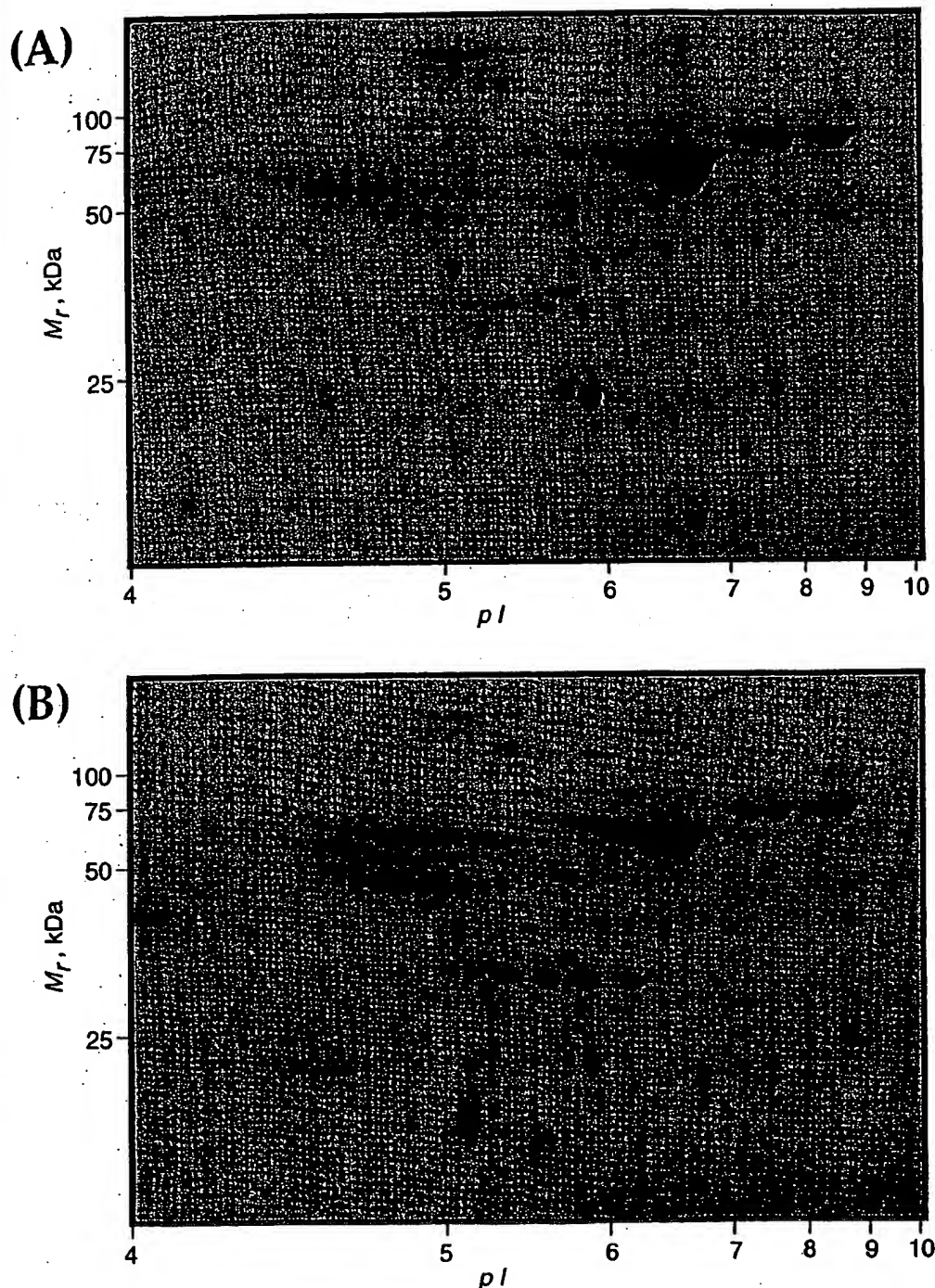


**Figure 7.** High resolution 2-DE map of proteins isolated from rat serum with or without prior exposure to an inflammation-causing agent. (A) normal rat serum, (B) acute-phase serum from rats which had previously been exposed to an inflammation-causing agent. The first dimension of separation is an IPG from pH 4–10, and the second dimension is a 7.5–17.5%T gradient SDS-PAGE gel. Proteins were visualized by staining with amido black. Further details of experimental procedures are included in [14, 49].

Proteome analysis as a biological assay has been successfully used in the field of toxicology, to characterize disease states or to study differential activation of cells. The approach is limited, of course, by the fact that only the visible protein spots are included in the assay, and it is well known that a substantial but far from complete fraction of cellular proteins are detected if a total cell lysate is separated by 2-DE. Proteins may not be detected in 2-DE gels because they are not abundant enough to be visualized by the detection method used, because they do not migrate within the boundaries (size, pI) resolved by the gel, because they are not soluble under the conditions used, or for other reasons.

A different way to use proteome analysis as a biological assay to define the state of a biological system is to take advantage of the wealth of information contained in 2-DE protein patterns. 2-DE is referred to as two-dimensional because of the electrophoretic mobility and the isoelectric points which define the position of each protein in a 2-DE pattern. In addition to the two dimensions used to generate the protein patterns, a number of additional data dimensions are contained in the protein patterns. Some of these dimensions such as protein expression level, phosphorylation state, subcellular location, association with other proteins, rate of synthesis or degradation indicate the activity state of a protein or a biological system. Comparative analysis of 2-DE protein patterns representing different states is therefore ideally suited for the detection, identification and analysis of suitable markers. Once again it must be emphasized that in this type of experiment only a fraction of the cellular proteins is analyzed. Since many regulatory proteins are of low abundance, this limitation is a concern, particularly in cases in which regulatory pathways are being investigated.

### 5 Concluding remarks

In this report we have addressed three main issues related to proteome analysis. First, we have discussed the rationale for studying proteomes. Second, we have assessed the technical feasibility of analyzing proteomes and described current proteome technology, and third, we have analyzed the utility of proteome analysis for biological research. It is apparent that proteome analysis is an essential tool in the analysis of biological systems. The multi-level control of protein synthesis and degradation in cells means that only the direct analysis of mature protein products can reveal their correct identities, their relevant state of modification and/or association and their amounts. Recently developed methods have enabled the identification of proteins at ever-increasing sensitivity levels and at a high level of automation of the analytical processes. A number of technical challenges, however, remain. While it is currently possible to identify essentially any protein spots that can be visualized by common staining methods, it is apparent that without prior enrichment only a relatively small and highly selected population of long-lived, highly expressed proteins is observed. There are many more proteins in a given cell which are not visualized by such methods. Frequently it is the low abundance proteins that execute key regulatory functions.

We have outlined the two principal ways proteome analysis is currently being used to intersect with biological research projects: the proteome as a database or data archive and proteome analysis as a biological assay. Both approaches have in common that at present they are conceptually and technically limited. Current proteome databases typically are limited to one cell type and one state of a cell and therefore do not account for the dynamics of biological systems. The use of proteome analysis as a biological assay can provide a wealth of information, but it is limited to the proteins detected and is therefore not truly proteome-wide. These limitations in proteomics are to a large extent a reflection of the fact that proteins in their fully processed form cannot easily be amplified and are therefore difficult to isolate in amounts sufficient for analysis or experimentation. The fact that to date no complete proteome has been described further attests to these difficulties. With continued rapid progress in protein analysis technology, however, we anticipate that the goal of complete proteome analysis will eventually become attainable.

*We would like to acknowledge the funding for our work from the National Science Foundation Science and Technology Center for Molecular Biotechnology and from the NIH. We thank Yvan Rochon and Bob Franza for providing the yeast gel shown and Elisabetta Gianazza for providing the rat serum gels shown.*

Received April 21, 1998

### 6 References

- [1] Wilkins, M. R., Pasquali, C., Appel, R. D., Ou, K., Golaz, O., Sanchez, J.-C., Yan, J. X., Gooley, A. A., Hughes, G., Humphery-Smith, I., Williams, K. L., Hochstrasser, D. F., *Bio/Technology* 1996, 14, 61–65.
- [2] Hodges, P. E., Payne, W. E., Garrels, J. I., *Nucleic Acids Res.* 1998, 26, 68–72.
- [3] O'Connor, C. D., Farris, M., Fowler, R., Qi, S. Y., *Electrophoresis* 1997, 18, 1483–1490.
- [4] Cordwell, S. J., Basseal, D. J., Humphery-Smith, I., *Electrophoresis* 1997, 18, 1335–1346.
- [5] Urquhart, B. L., Atsalos, T. E., Roach, D., Basseal, D. J., Bjellqvist, B., Britton, W. L., Humphery-Smith, I., *Electrophoresis* 1997, 18, 1384–1392.
- [6] Wasinger, V. C., Bjellqvist, B., Humphery-Smith, I., *Electrophoresis* 1997, 18, 1373–1383.
- [7] Link, A. J., Hays, L. G., Carmack, E. B., Yates III, J. R., *Electrophoresis* 1997, 18, 1314–1334.
- [8] Sazuka, T., Ohara, O., *Electrophoresis* 1997, 18, 1252–1258.
- [9] VanBogelen, R. A., Abshire, K. Z., Moldover, B., Olson, E. R., Neidhardt, F. C., *Electrophoresis* 1997, 18, 1243–1251.
- [10] Guerreiro, N., Redmond, J. W., Rolfe, B. G., Djordjevic, M. A., *Mol. Plant Microbe Interact.* 1997, 10, 506–516.
- [11] Yan, J. X., Tonella, L., Sanchez, J.-C., Wilkins, M. R., Packer, N. H., Gooley, A. A., Hochstrasser, D. F., Williams, K. L., *Electrophoresis* 1997, 18, 491–497.
- [12] Celis, J., Gromov, P., Ostergaard M., Madsen, P., Honoré, B., Deigaard, K., Olsen, E., Vorum, H., Kristensen, D. B., Gromova, I., Haunso, A., Van Damme, J., Puype, M., Vandekerckhove, J., Rasmussen, H. H., *FEBS Lett.* 1996, 398, 129–134.
- [13] Appel, R. D., Sanchez, J.-C., Bairoch, A., Golaz, O., Miu, M., Vargas, J. R., Hochstrasser, D. F., *Electrophoresis* 1993, 14, 1232–1238.
- [14] Haynes, P., Miller, I., Aebersold, R., Gemeiner, M., Eberini, I., Lovati, R. M., Manzoni, C., Vignati, M., Gianazza, E., *Electrophoresis* 1998, 19, 1484–1492.

- [15] Fleischmann, R. D., Adams, M. D., White, O., Clayton, R. A., Kirkness, E. F., Kerlavage, A. R., Bult, C. J., Tomb, J.-F., Dougherty, B. A., Merrick, J. M., McKenney, K., Sutton, G., FitzHugh, W., Fields, C., Gocayne, J. D., Scott, J., Shirley, R., Liu, L.-I., Glodek, A., Kelley, J. M., Weidman, J. F., Phillips, C. A., Spriggs, T., Hedblom, E., Cotton, M. D., Utterback, T. R., Hanna, N. C., Nguyen, D. T., Saudek, D. M., Brandon, R. C., Fine, L. D., Fritchman, J. L., Fuhrmann, J. L., Geoghegan, N. S. M., Gnehm, C. L., McDonald, L. A., Small, K. V., Fraser, C. M., Smith, C. O., Venter, J. C., *Science* 1995, 269, 496-512.
- [16] Goffeau, A., Barrell, B. G., Bussey, H., Davis, R. W., Dujon, B., Feldmann, H., Galibert, F., Hoheisel, J. D., Jacq, C., Johnston, M., Louis, E. J., Mewes, H. W., Murakami, Y., Philippsen, P., Tettelin, H., Oliver, S. G., *Science* 1996, 274, 546.
- [17] Fraser, C. M., Casjens, S., Huang, W. M., Sutton, G. G., Clayton, R., Lathigra, R., White, O., Ketchum, K. A., Dodson, R., Hickey, E. K., Gwinn, M., Dougherty, B., Tomb, J. F., Fleischmann, R. D., Richardson, D., Peterson, J., Kerlavage, A. R., Quackenbush, J., Salzberg, S., Hanson, M., van Vugt, R., Palmer, N., Adams, M. D., Gocayne, J., Weidman, J., Utterback, T., Watthey, T., McDonald, L., Artiach, P., Bowman, C., Garland, S., Fujii, C., Cotton, M. D., Horst, K., Roberts, K., Hatch, B., Smith, H. O., Venter, J. C., *Nature* 1997, 390, 580-586.
- [18] Liang, P., Pardee, A. B., *Science* 1992, 257, 967-971.
- [19] Lashkari, D. A., DeRisi, J. L., McCusker, J. H., Namath, A. F., Gentile, C., Hwang, S. Y., Brown, P. O., Davis, R. W., *Proc. Natl. Acad. Sci. USA* 1997, 94, 13057-13062.
- [20] Shalon, D., Smith, S. J., Brown, P. O., *Genome Res.* 1996, 6, 639-645.
- [21] Velculescu, V. E., Zhang, L., Vogelstein, B., Kinzler, K. W., *Science* 1995, 270, 484-487.
- [22] Velculescu, V. E., Zhang, L., Zhou, W., Vogelstein, J., Basrai, M. A., Bassett, D. E., Hieter, P., Vogelstein, B., Kinzler, K. W., *Cell* 1997, 88, 243-251.
- [23] Krishna, R. G., Wold, P., *Adv. Enzymol.* 1993, 67, 265-298.
- [24] G6rg, A., Postel, W., Gunther, S., *Electrophoresis* 1988, 9, 531-546.
- [25] Klose, J., Kobalz, U., *Electrophoresis* 1995, 16, 1034-1059.
- [26] Matsudaira, P., *J. Biol. Chem.* 1987, 262, 10035-10038.
- [27] Aebersold, R. H., Teplow, D. B., Hood, L. E., Kent, S. B., *J. Biol. Chem.* 1986, 261, 4229-4238.
- [28] Rosenfeld, J., Capdevielle, J., Guillemot, J. C., Ferrara, P., *Anal. Biochem.* 1992, 203, 173-179.
- [29] Aebersold, R. H., Leavitt, J., Saavedra, R. A., Hood, L. E., Kent, S. B., *Proc. Natl. Acad. Sci. USA* 1987, 84, 6970-6974.
- [30] Honoré, B., Leffers, H., Madsen, P., Celis, J. E., *Eur. J. Biochem.* 1993, 218, 421-430.
- [31] Mann, M., Wilm, M., *Anal. Chem.* 1994, 66, 4390-4399.
- [32] Eng, J., McCormack, A. L., Yates III, J. R., *J. Amer. Mass Spectrom.* 1994, 5, 976-989.
- [33] Yates III, J. R., Eng, J. K., McCormack, A. L., Schieltz, D., *Anal. Chem.* 1995, 67, 1426-1436.
- [34] Shevchenko, A., Wilm, M., Vorm, O., Mann, M., *Anal. Chem.* 1996, 68, 850-858.
- [35] Hess, D., Covey, T. C., Winz, R., Brownsey, R. W., Aebersold, R., *Protein Sci.* 1993, 2, 1342-1351.
- [36] van Oostveen, I., Ducret, A., Aebersold, R., *Anal. Biochem.* 1997, 247, 310-318.
- [37] Lui, M., Tempst, P., Erdjument-Bromage, H., *Anal. Biochem.* 1996, 241, 156-166.
- [38] Patterson, S. D., Aebersold, R. A., *Electrophoresis* 1995, 16, 1791-1814.
- [39] Ducret, A., Foyn, Brunn, C., Bures, E. J., Marhaug, G., Husby, G. R. A., *Electrophoresis* 1996, 17, 866-876.
- [40] Haynes, P. A., Fripp, N., Aebersold, R., *Electrophoresis* 1998, 19, 939-945.
- [41] Figeys, D., Van Oostveen, I., Ducret, A., Aebersold, R., *Anal. Chem.* 1996, 68, 1822-1828.
- [42] Ducret, A., Van Oostveen, I., Eng, J. K., Yates III, J. R., Aebersold, R., *Protein Sci.* 1997, 7, 706-719.
- [43] Figeys, D., Ducret, A., Yates III, J. R., Aebersold, R., *Nature Biotech.* 1996, 14, 1579-1583.
- [44] Figeys, D., Aebersold, R., *Electrophoresis* 1997, 18, 360-368.
- [45] Figeys, D., Ning, Y., Aebersold, R., *Anal. Chem.* 1997, 69, 3153-3160.
- [46] Garrels, J. I., McLaughlin, C. S., Warner, J. R., Fletcher, B., Latter, G. I., Kobayashi, R., Schwender, B., Volpe, T., Anderson, D. S., Mesquita-Fuentes, R., Payne, W. E., *Electrophoresis* 1997, 18, 1347-1360.
- [47] Schuler, G. D., Boguski, M. S., Stewart, E. A., Stein, L. D., Gyapay, G., Rice, K., White, R. E., Rodriguez-Tome, P., Aggarwal, A., Bajorek, E., Bentolila, S., Birren, B. B., Butler, A., Castle, A. B., Chiannilkulchai, N., Chu, A., Clee, C., Cowles, S., Day, P. J., Dibling, T., Drouot, N., Dunham, I., Duprat, S., Edwards, C., Fan, J.-B., Fang, N., Fizames, C., Garrett, C., Green, L., Hadley, D., Harris, M., Harrison, P., Brady, S., Hicks, A., Holloway, E., Hul, L., Hussain, S., Louis-Dit-Sully, C., Ma, J., MacGilvery, A., Mader, C., Maratukulam, A., Matise, T. C., McKusick, K. B., Morissette, J., Mungall, A., Musclet, D., Nusbaum, H. C., Page, D. C., Peck, A., Perkins, S., Piercy, M., Qin, F., Quackenbush, J., Ranby, S., Reif, T., Rozen, S., Sanders, X., She, X., Silva, J., Slonim, D. K., Soderlund, C., Sun, W.-L., Tabar, P., Thangarajah, T., Vega-Czarny, N., Vollrath, D., Voyticky, S., Wilmer, T., Wu, X., Adams, M. D., Auffray, C., Walter, N. A. R., Brandon, R., Dehejia, A., Goodfellow, P. N., Houlgatte, R., Hudson, J. R., Jr., Ide, S. E., Iorio, K. R., Lee, W. Y., Seki, N., Nagase, T., Ishikawa, K., Nomura, N., Phillips, C., Polymeropoulos, M. H., Sandusky, M., Schmitt, K., Berry, R., Swanson, K., Torres, R., Venter, J. C., Sikela, J. M., Beckmann, J. S., Weissenbach, J., Myers, R. M., Cox, D. R., James, M. R., Bentley, D., et al. *Science* 1996, 274, 540-546.
- [48] Sanchez, J.-C., Rouge, V., Pisteur, M., Ravier, F., Tonella, L., Moosmayer, M., Wilkins, M. R., Hochstrasser, D. F., *Electrophoresis* 1997, 18, 324-327.
- [49] Miller, I., Haynes, P., Gemeiner, M., Aebersold, R., Manzoni, C., Lovati, M. R., Vignati, M., Eberlin, I., Gianazza, E., *Electrophoresis* 1998, 19, 1493-1500.
- [50] Garrels, J. I., *Nucleic Acids Res.* 1996, 24, 46-49.





481 cccagtaccc cttccatgtg cctctcctca gctcccagaa gatggtgtat ccagggctgc  
541 aggaaccctg gctgcactcg atgtaccacg gggctgcgtt ccagctcacc caggagagacc  
601 agctatccac ccacacagat ggcattcccc acctagtcct cagccctagt actgtcttct  
661 ttggagcctt cgctctgtag aacttgga aaatccagaaa gaaaaaataa ttgatttcaa  
721 gaccttctcc ccattctgcc tccattctga ccatttcagg ggtcgtcacc acctctcctt  
781 tggccattcc aacagctcaa gtcttccctg atcaagtcac cggagctttc aaagaaggaa  
841 ttctaggcat cccaggggac cacacctccc tgaaccatcc ctgatgtctg tctggctgag  
901 gatttcaagc ctgcctagga attcccagcc caaagctgtt ggtcttgtcc accagctagg  
961 tggggcctag atccacacac agaggaagag caggcacatg gaggagcttg ggggatgact  
1021 agaggcaggg aggggactat ttatgaaggc aaaaaaatta aattatttat ttatggagga  
1081 tggagagagg gaataataga agaactcca aggagaaaca gagacaggcc caagagatga  
1141 agagtgagag ggcattgcga caaggctgac caagagagaa agaagtaggc atgagggatc  
1201 acagggcccc agaaggcagg gaaaggctct gaaagccagc tgccgaccag agccccaac  
1261 ggaggcatct gcattctcga tgaagcccaa taaacctctt ttctccccct

//

[Disclaimer](#) | [Write to the Help Desk](#)  
[NCBI](#) | [NLM](#) | [NIH](#)

Apr 19 2004 07:23:43

## Analysis of Genomic and Proteomic Data Using Advanced Literature Mining

Yanhui Hu, Lisa M. Hines, Haifeng Weng, Dongmei Zuo, Miguel Rivera, Andrea Richardson, and Joshua LaBaer\*

*Institute of Proteomics, Harvard Medical School—BCMP, 240 Longwood Avenue, Boston, Massachusetts 02115*

Received March 13, 2003

High-throughput technologies, such as proteomic screening and DNA micro-arrays, produce vast amounts of data requiring comprehensive analytical methods to decipher the biologically relevant results. One approach would be to manually search the biomedical literature; however, this would be an arduous task. We developed an automated literature-mining tool, termed MedGene, which comprehensively summarizes and estimates the relative strengths of all human gene–disease relationships in Medline. Using MedGene, we analyzed a novel micro-array expression dataset comparing breast cancer and normal breast tissue in the context of existing knowledge. We found no correlation between the strength of the literature association and the magnitude of the difference in expression level when considering changes as high as 5-fold; however, a significant correlation was observed ( $r = 0.41$ ;  $p = 0.05$ ) among genes showing an expression difference of 10-fold or more. Interestingly, this only held true for estrogen receptor (ER) positive tumors, not ER negative. MedGene identified a set of relatively understudied, yet highly expressed genes in ER negative tumors worthy of further examination.

**Keywords:** bioinformatics • micro-array • text mining • gene-disease association • breast cancer

### Introduction

At its current pace, the accumulation of biomedical literature outpaces the ability of most researchers and clinicians to stay abreast of their own immediate fields, let alone cover a broader range of topics. For example, to follow a single disease, e.g., breast cancer, a researcher would have had to scan 130 different journals and read 27 papers per day in 1999.<sup>1</sup> This problem is accentuated with high-throughput technologies such as DNA micro-arrays and proteomics, which require the analysis of large datasets involving thousands of genes, many of which are unfamiliar to a particular researcher. In any microarray experiment, thousands of genes may demonstrate statistically significant expression changes, but only a fraction of these may be relevant to the study. The ability to interpret these datasets would be enhanced if they could be compared to a comprehensive summary of what is known about all genes. Thus, there is a need to summarize existing knowledge in a format that allows for the rapid analysis of associations between genes and diseases or other specific biological concepts.

One solution to this problem is to compile structured digital resources, such as the Breast Cancer Gene Database<sup>1</sup> and the Tumor Gene Database.<sup>2</sup> However, as these resources are hand-curated, the labor-intensive review process becomes a rate-limiting step in the growth of the database. As a result, these

databases have a limited scale and the genes are not selected in a systematic fashion.

An alternative approach is automated text mining: a method which involves automated information extraction by searching documents for text strings and analyzing their frequency and context. This approach has been used successfully in several instances for biological applications. In most cases, it has been applied to extract information about the relationships or interactions that proteins or genes have with one another, in the literature or by functional annotation.<sup>3–7</sup> Thus far, few publications have applied text-mining to examine the global relationships between genes and diseases. Perez-Iratxeta et al. automatically examined the GO (Gene Ontology) annotation of genes and their predicted chromosomal locations in order to identify genes linked to inherited disorders.<sup>8</sup>

To obtain a more global understanding of disease development, it would be valuable to incorporate information regarding all possible gene-disease relationships, including biochemical, physiological, pharmacological, epidemiological, as well as genetic. This information would enable comprehensive comparisons between large experimental datasets and existing knowledge in the literature. This would accomplish two things. First, it would serve to validate experiments by demonstrating that known responses occur as predicted. Second, it would rapidly highlight which genes are corroborated by the literature and which genes are novel in a given context. We have utilized a computational approach to literature mining to produce a

\* To whom correspondence should be addressed: jlaBaer@hms.harvard.edu.



comprehensive set of gene-disease relationships. In addition, we have developed a novel approach to assess the strength of each association based on the frequency of citation and co-citation. We applied this tool to help interpret the data from a large micro-array gene expression experiment comparing normal and cancerous breast tissue.

## Methods

**MedGene Database.** MedGene is a relational database, storing disease and gene information from NCBI, text mining results, statistical scores, and hyperlinks to the primary literature. MedGene has a web-based user interface for users to query the database (<http://hipseq.med.harvard.edu/MedGene/>).

**Text Mining Algorithms.** MeSH files were downloaded from the MeSH web site at NLM (National Library of Medicine) (<http://www.nlm.nih.gov/mesh/meshhome.html>) and human disease categories were selected. LocusLink files were downloaded from the LocusLink web site at NCBI (<http://www.ncbi.nih.gov/LocusLink/>). Official/preferred gene symbol, official/preferred gene name, and gene alternative symbols and names, all relevant annotations and URLs for each LocusLink record, were collected. Gene search terms were used for literature searching and included all qualified gene names, gene symbols, and gene family terms. Primary gene keys, predominantly qualified gene family terms and gene official/preferred symbols, were used to index Medline records. If the official/preferred gene symbols did not meet the standards to be an index, then qualified gene official/preferred names were used. A local copy of Medline records (up to July, 2002) was pre-selected.

A JAVA module examined the MeSH terms and then indexed each Medline record with the appropriate disease terms. A separate JAVA module was used to examine the titles and abstracts for gene search terms and then to index the gene-related Medline records with the relevant primary gene key(s).

**Statistical Methods.** For every gene and disease pair, we counted records that were indexed for both gene and disease (double positive hits), for disease only (disease single hits), for gene-only (gene single hits), and for neither gene nor disease (double negative hits) to generate a  $2 \times 2$  contingency table. On the basis of the contingency table-framework, we applied different statistical methods to estimate the strength of gene-disease relationships and evaluated the results. These methods included chi-square analysis, Fisher's exact probabilities, relative risk of gene, and relative risk of disease<sup>16</sup> (<http://hipseq.med.harvard.edu/MedGene/>). In addition, we computed the "product of frequency", which is the product of the proportion of disease/gene double hits to disease single hits and the proportion of disease/gene double hits to gene single hits. To obtain a normal distribution, we transformed all the statistical scores using the natural logarithm. We selected the log of the product of frequency (LPF) to validate MedGene and to use for the analysis with the micro-array data. Spearman rank-correlation coefficients were used to assess the linear relationship between LPF and micro-array fold change in expression level.

**Global Analysis.** Diseases with at least 50 related genes were selected for clustering analysis, and the LPF scores were normalized with total score for each disease. Hierarchical clustering was done with the "Cluster" software and the clustering result was visualized using "TreeView" (<http://rana.lbl.gov/EisenSoftware.htm>).

**Breast Tissue Micro-Arrays.** Eighty-nine breast cancer samples (79% ER-positive) and 7 normal breast tissue samples were selected from the Harvard Breast SPORE frozen tissue repository and were representative of the spectrum of histological types, grades, and hormone receptor immuno-phenotypes of breast cancer. Biotinylated cRNA, generated from the total RNA extracted from the bulk tumor, was hybridized to Affymetrix U95A oligo-nucleotide micro-arrays. These micro-arrays consist of 12 400 probes, which represent approximately 9000 genes. Raw expression values were obtained using GENE-CHIP software from Affymetrix, and then further analyzed using the DNA-Chip Analyzer (dChip) custom software.

## Results

**Automated Indexing of Medline Records by Disease and Gene.** To study the gene-disease associations in the literature, we first compiled complete lists for human diseases and human genes. To index all Medline records that were relevant to human diseases, the Medical Subject Heading (MeSH) index of Medline records was utilized. MeSH is a controlled medical vocabulary from the National Library of Medicine and consists of a set of terms or subject headings that are arranged in both an alphabetic and an hierarchical structure. Medline records are reviewed manually and MeSH terms are added to each with software assistance.<sup>9,10</sup> Twenty-three human disease category headings along with all of their child terms (see the Supporting Information, Supplemental Table 1, or visit [http://hipseq.med.harvard.edu/MedGene/publication/s\\_Table1.html](http://hipseq.med.harvard.edu/MedGene/publication/s_Table1.html)) were selected from the 2002 MeSH index creating a list of 4033 human diseases.

No index comparable to the MeSH index exists for genes, and thus, it was necessary to apply a string search algorithm for gene names or symbols found in Medline text. A complete list of genes, gene names, gene symbols, and frequently used synonyms were collected from the LocusLink database at NCBI,<sup>11,12</sup> which contains 53 259 independent records keyed by an official gene symbol or name (June 18<sup>th</sup>, 2002). For the purposes of this study, no distinction was made between genes and their gene products. Authors often use the same name for both, differentiating the two only by the use of italics, if at all. For the intended use of this study, this lack of distinction is unlikely to have a large effect and may in fact be beneficial.

Initial attempts to search the literature using these lists revealed several sources of false positives and false negatives (Table 1). False positives primarily arose when the searched term had other meanings, whereas false negatives arose from syntax discrepancies necessitating the development of filters to reduce these errors. The syntax issues were readily handled by including alternate syntax forms in the search terms. The false positive cases, caused by duplicative and unrelated meanings for the terms, were more difficult to manage. Where possible, case sensitive string mapping reduced inappropriate citations. In many cases, however, this was not sufficient and the terms had to be eliminated entirely, thereby reducing the false positive rate but unavoidably under-representing some genes.

For the purposes of data tracking, a primary gene key was selected to represent all synonyms that correspond to each gene. Medline records were indexed with a primary gene key when any synonym for that key was found in the title or abstract. Case-insensitive string mapping was used for all searches except as noted above. No additional weight was

**Table 1.** Systematic Sources of False Positives and False Negatives in Unfiltered Data<sup>a</sup>

source of error	error type	example	filter solution
gene symbol/name is not unique	false positive	MAG—myelin associated glycoprotein MAG—malignancy-associated protein	eliminate this term
gene symbol is unrelated abbreviation	false positive	PA—pallid homologue (mouse), pallidin (also abbrev. for Pennsylvania)	eliminate this term
gene symbol/name has language meaning	false positive	WAS—Wiskott–Aldrich Syndrome (also the word “was”)	case-sensitive string search
nonstandard syntax	false negative	BAG-1 instead of BAC1	add dash term
unofficial gene name/symbol	false negative	P53 instead of TP53	add all gene nicknames
nonspecified gene name	false negative	estrogen receptor instead of Estrogen receptor 1	add family stem term

<sup>a</sup> In preliminary studies, Medline was searched for co-occurrence of genes and diseases and the resulting output was evaluated to identify error sources that were amenable to global filters. Each error source is categorized by the type of error it causes: false positives are suggested relationships that are not real and false negatives are real relationships that are underrepresented. The filter solutions used are indicated. Note that in some cases, the filter solution itself introduces error. In general, error rates maximized sensitivity, even at the expense of specificity if needed.

added for multiple occurrences of a term or the co-occurrence of multiple synonyms for the same gene key.

Medline records were searched with all qualified gene identifiers, such as the official/preferred gene symbol, the official/preferred gene name, all gene nicknames and all syntax variants. In situations where there are several members of a gene family or splice variants, some authors prefer to use a shortened gene family name, e.g., estrogen receptor instead of estrogen receptor 1 (*ESR1*), creating a source of false negatives. For this reason, gene family stem terms were created for all genes that have an alpha or numerical suffix (e.g., *IL2RA*, *TGFβ*, *ESR1*, etc.) and then used to search the literature. The family stem terms were handled separately from the specific gene names so that it would be clear when linkages were made to the gene family versus a specific member in that family.

To improve performance and accuracy, some pre-selection was applied to the records that were scanned. First, review articles were eliminated to avoid redundant treatment of citations. Second, non-English journals were removed because the natural language filters were only relevant to English publications. Finally, journals unlikely to contain primary data about gene-disease relationships were also removed (e.g., *Int. J. Health Educ.*, *Bedside Nurse*, and *J. Health Econ.*). Together, these filters reduced the 12 198 221 Medline publications (July 2002) by 37%.

**Ranking the Relative Strengths of Gene-Disease Associations.** In total, there were 618 708 gene-disease co-citations, in which 16% (8297) of all studied genes had been associated to a disease and 96% (3875) of all diseases had been associated to at least one gene. To rank the relative strengths of gene-disease relationships, we tested several different statistical methods and examined the results. With the exception of the relative risk estimates, the methods provided similar results with respect to the rank order of the gene-disease association strengths. However, after comparing the results to other databases and after consulting disease experts, the log of the product of frequency (LPF) was selected for further analysis because it gave the best results overall.

**Validation of MedGene.** In developing this tool, it was important to minimize the number of missed genes (false negatives) and miscalled genes (false positives). However, in situations when these goals were in conflict, inclusiveness was prioritized. To determine the false negative rate in MedGene, breast cancer was used as a test case because it was associated with more genes than any other human disease and because

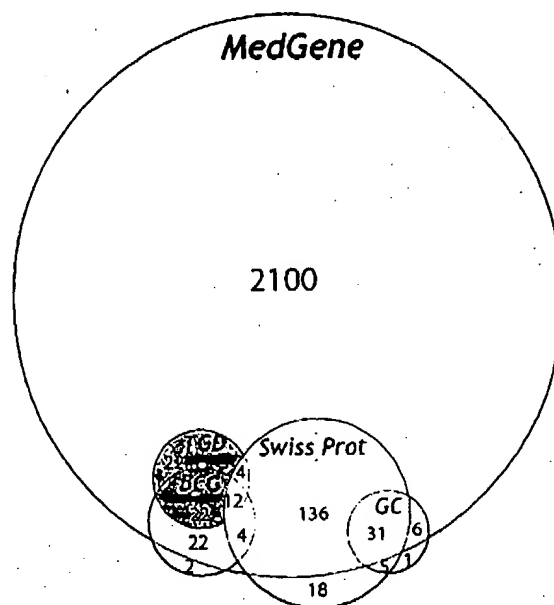


**Figure 1.** Estimation of the false negative rate by comparison with hand-curated databases. The breast cancer-related genes identified by MedGene were compared with those listed in several other databases including the Tumor Gene Database (TGD),<sup>2</sup> the Breast Cancer Gene Database (BCG),<sup>1</sup> GeneCards (GC)<sup>17</sup> and Swissprot.<sup>18</sup> Genes were considered false negatives if they were represented in at least one of these other databases and not in MedGene and their link to breast cancer was supported by at least one literature reference. All literature references were verified by manual review to confirm their validity. The number of genes in each database or shared by more than one database is indicated. The false negative rate was calculated by genes missed at MedGene (26)/total number of nonoverlapping genes in other databases (285).

there were several public databases that link genes to breast cancer. We compared the list of breast cancer-related genes from MedGene to these databases, illustrated in Figure 1. Among the 285 distinct breast cancer-related genes that were supported by at least one literature citation in these hand-curated databases, 26 were absent from MedGene, suggesting a false negative rate of approximately 9%. To determine why these were missed, all literature references for these genes (80

papers) were reviewed manually (see the Supporting Information, Supplemental Table 2, or visit [http://hipseq.med.harvard.edu/MedGene/publication/s\\_Table\\_2.html](http://hipseq.med.harvard.edu/MedGene/publication/s_Table_2.html)). Among these papers, most false negatives were caused by nonstandard gene terms or gene terms eliminated by our specificity filters. Few genes were missed because they were only mentioned in review papers (0.4%) or they appeared only in the body of the manuscript but not the abstract or title (1.1%). Of note, MedGene identified approximately 2000 additional breast cancer-related genes not listed in any other database.

To assess the false positive error rate, two complementary approaches were used: a detailed analysis of one disease and a global examination of 1000 diseases. The detailed approach examined the false positive error rate and its sources, whereas the global approach tested whether the overall results made biomedical sense.

Using the LPF, 1467 genes related to prostate cancer were assembled in rank order. We then retrieved approximately 300 Medline records each for the highest ranked 100 and the lowest ranked 200 genes and manually reviewed the titles and abstracts to determine the verity of the association. Nearly 80% of the highest ranked 100 genes fell into one of the five categories that reflect meaningful gene-disease relationships (see the Supporting Information, Supplemental Table 3, or visit [http://hipseq.med.harvard.edu/MedGene/publication/s\\_Table\\_3.html](http://hipseq.med.harvard.edu/MedGene/publication/s_Table_3.html)). Among the lowest ranked 200 genes, approximately 70% reflected true relationships. Of the 600 records reviewed, there were only two in which the association between the gene and the disease was described as negative. Both were genes with very low scores. In both cases, the authors did not argue the absence of any relationship, but rather that a particular feature of the gene or protein was not shown to be related to human prostate cancer.<sup>13,14</sup>

The coincidence of some gene symbols with medical abbreviations, chemical abbreviations and biological abbreviations resulted in most of the false positives (see the Supporting Information, Supplemental Table 4, or visit [http://hipseq.med.harvard.edu/MedGene/publication/s\\_Table\\_4.html](http://hipseq.med.harvard.edu/MedGene/publication/s_Table_4.html)), emphasizing the importance of the filters that were added in the search algorithm (Table 1). Without the filters, the false positive rate more than doubled, and the false negative rate rose dramatically (data not shown). For example, among the papers about breast cancer, there were only 12 Medline records that referred to *ESR1* and 10 to *ESR2*, whereas almost 2000 papers mentioned estrogen receptor without specifying *ESR1* or *ESR2*; this latter group was detected by the family stem term filter.

To further validate these results, a global analysis of the gene-disease relationships described by MedGene was performed. For this experiment, it was reasoned that the more closely related the diseases are to one another, the more they will be related to the same gene sets. Thus, if the relationships defined by MedGene accurately reflected the literature, then an unsupervised hierarchical clustering of the gene data should group diseases in a manner consistent with common medical thinking. Conversely, if the clustered diseases do not make sense biologically or medically, it may reflect excessive false positives, false negatives, or inappropriate scoring of the data.

To execute this experiment, the gene sets and the corresponding LPF values for 1000 randomly selected diseases (each with at least 50 gene relationships) were used as a dataset for clustering the diseases. A review of the results showed that the resulting disease clusters were indeed logical based upon common medical knowledge (see the Supporting Information,

Supplemental Figure 1, or visit [http://hipseq.med.harvard.edu/MedGene/publication/s\\_Figure\\_1.html](http://hipseq.med.harvard.edu/MedGene/publication/s_Figure_1.html)). For example, in one such cluster shown in Figure 2, diabetes and its complications grouped together and were also closely linked to diseases associated with starvation states.

The number of genes associated with a given disease can be estimated by adjusting the MedGene number up by the false negative rate (~9%) and down by the false positive rate (~26% on average). Using this, the average disease has  $103.7 \pm 45.3$  (mean  $\pm$  s.d.) genes associated with it, although the range is quite broad with 2359 genes related to breast cancer, 2122 genes related to lung cancer and no genes related to a number of diseases.

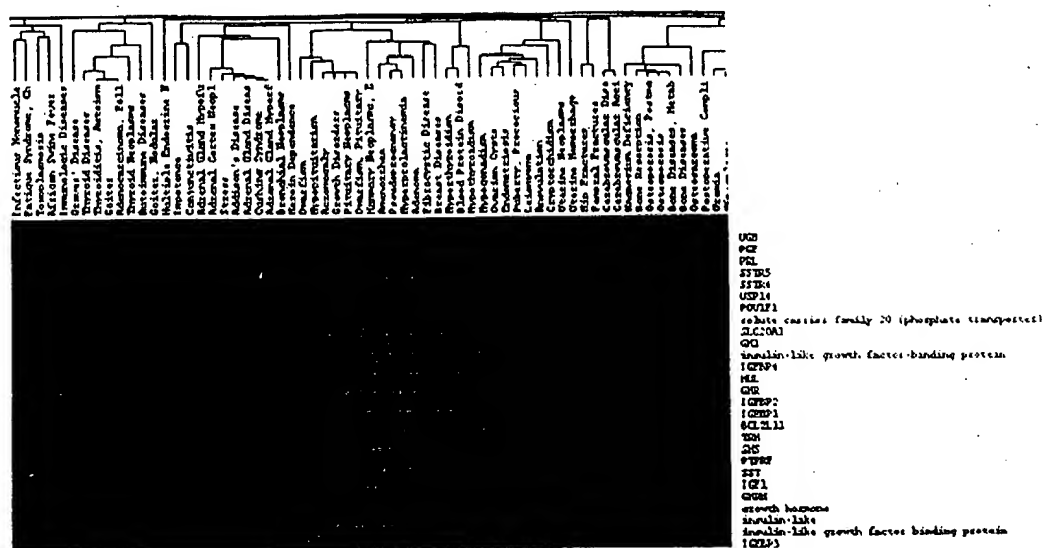
**Applying MedGene to the Analysis of Large Datasets.** Access to a comprehensive summary of the genes linked to human diseases provided an opportunity to analyze data obtained from a high-throughput experiment. We compared the MedGene breast cancer gene list to a gene expression data set generated from a micro-array analysis comparing breast cancer and normal breast tissue samples. Micro-array analysis identified 2286 genes that had greater than a 1-fold difference in mean expression level between breast cancer samples and normal breast samples. Using MedGene, we sorted the 2286 genes into four classes: 555 genes directly linked to breast cancer in the literature by gene term search (first-degree association by gene name); 328 genes directly linked by family term search (first-degree association by family term); 1021 genes linked to breast cancer only through other breast cancer genes (second-degree association); and 505 genes not previously associated with breast cancer. (See the Supporting Information, Supplemental Figure 2, or visit [http://hipseq.med.harvard.edu/MedGene/publication/s\\_Figure\\_2.html](http://hipseq.med.harvard.edu/MedGene/publication/s_Figure_2.html).) Among the 505 previously unrelated genes, 467 were either newly identified genes or genes that had not previously been associated with any disease. Among the remaining 38 genes, 9 had been related to other cancers, specifically esophageal, colon, uterine, skin, and cervix.

To determine whether the genes highlighted by the micro-array analysis were more likely to have been previously linked to breast cancer in the literature, we created a two-dimensional plot of the fold change of expression level between breast cancer and normal tissue versus the literature score (LPF) (Figure 3A). There was a broad spread of expression changes among the genes directly linked to breast cancer ranging from less than 1-fold change (68%) to over 40-fold (0.3%). Notably, the majority of genes with greater than 10-fold expression changes were linked to breast cancer by first-degree association.

Among all 754 genes directly linked to breast cancer in the literature, there was no correlation between LPF and micro-array fold change ( $r = 0.018$ ,  $p$ -value = 0.62). However, when we stratified the analysis based on the magnitude of the fold change, we observed an increasing trend in correlation (Figure 3B) suggesting that genes with a more substantial change in expression level were more likely to have a stronger association in the literature. For genes that had 10-fold change or more in expression level, the correlation increased to 0.41 ( $p$ -value = 0.05).

When we evaluated the micro-array data separately for ER positive and ER negative tumors, the trend in correlation between fold change and literature score was highly dependent on estrogen receptor status. Interestingly, there was a similar trend in correlation for ER positive tumors, but no trend in correlation for ER negative tumors.

A



B

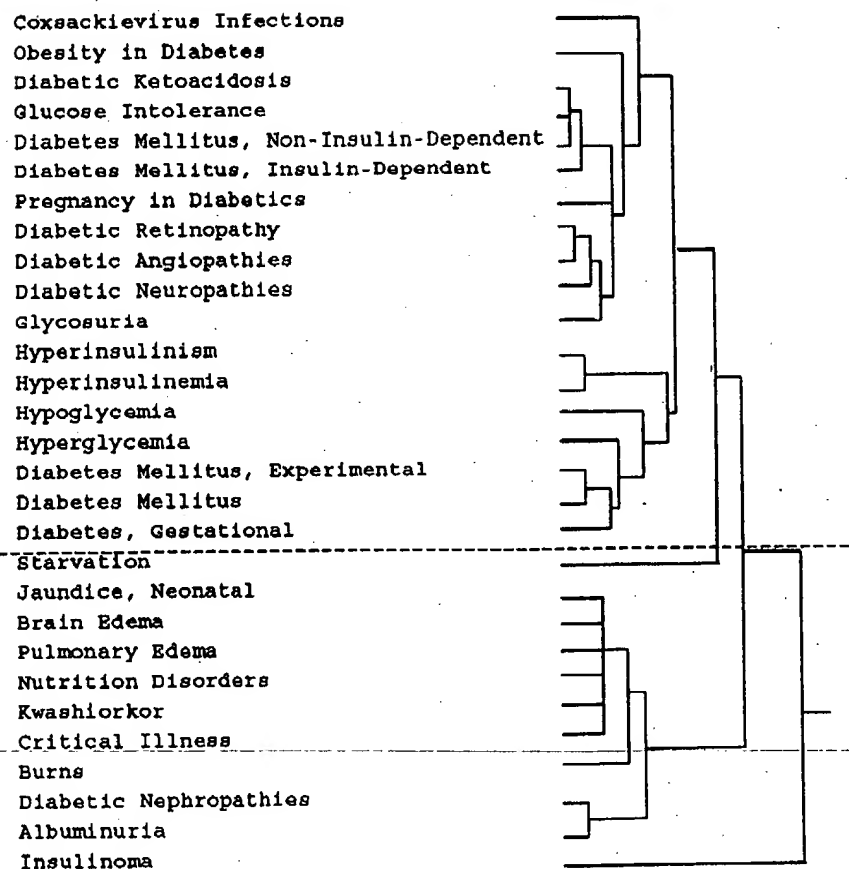


**Figure 2.** Global validation by clustering analysis. 2(A). The gene sets and the corresponding LPF values for 1000 diseases, each with at least 50 gene relationships, were used in an unsupervised clustering of the diseases based on the gene patterns associated with them. A sample of the data is shown here. 2(B). One of the resulting clusters is shown that corresponds to blood sugar states. Diabetes terms (above the line) and starvation states terms (under the line) clustered together. Within these groups, there is also clustering of diabetic small vessel complications, altered serum chemistries, nutritional disorders, etc. (Supplemental Figure 1: [http://hipseq.med.harvard.edu/MedGene/publication/s\\_Figure\\_1.html](http://hipseq.med.harvard.edu/MedGene/publication/s_Figure_1.html)).

Finally, to validate our findings, we computed similar correlations between the breast cancer expression data and LPF scores generated by MedGene for hypertension, a

disease unrelated to breast cancer. As expected, we did not observe an increasing trend in correlation for hypertension.

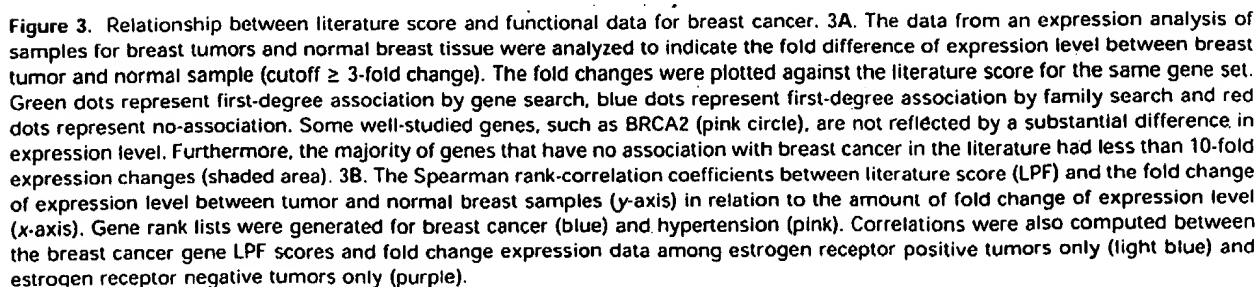


Table 2. Top 25 Genes Related to Selected Human Diseases\*

breast neoplasms	hypertension	rheumatoid arthritis	bipolar disorder	atherosclerosis
estrogen receptor	<i>REN</i>	<i>RA</i>	<i>ERDA1</i>	apolipoprotein
<i>PCR</i>	<i>DBP</i>	<i>TNFRSF10A</i>	<i>SNAP29</i>	<i>APOE</i>
<i>ERBB2</i>	<i>LEP</i>	<i>CRP</i>	<i>PFKL</i>	<i>LDLR</i>
<i>BRCA1</i>	<i>AGT</i>	<i>AS</i>	<i>DRD2</i>	<i>ELN</i>
<i>BRCA2</i>	<i>INS</i>	<i>ESR1</i>	<i>TRH</i>	<i>ARG1</i>
<i>EGFR</i>	kallikrein	<i>HLA-DRB1</i>	<i>IMPA2</i>	<i>APOB</i>
<i>CYP19</i>	<i>ACE</i>	<i>DR1</i>	<i>HTR3A</i>	<i>APOA1</i>
<i>TFF1</i>	endothelin	interleukin	<i>DRD3</i>	<i>MSR1</i>
<i>PSEN2</i>	<i>S100A6</i>	<i>TNF</i>	<i>REM</i>	<i>LPL</i>
<i>TP53</i>	<i>BDK</i>	<i>IL6</i>	<i>KCNN3</i>	<i>PONI</i>
				plasminogen
<i>CES3</i>	<i>DIANPH</i>	collagen	<i>DRD4</i>	activator inhibitor
<i>CEACAM5</i>	<i>SAR1</i>	<i>IL1A</i>	<i>HTR2C</i>	<i>PLG</i>
				vascular cell
<i>ERBB3</i>	<i>PIH</i>	<i>ACR</i>	<i>KELN</i>	adhesion molecule
cyclin	<i>CD59</i>	<i>TNFRSF12</i>	<i>DBH</i>	<i>ATOH1</i>
<i>COX5A</i>	<i>ALB</i>	<i>IL2</i>	<i>MAOA</i>	<i>VWF</i>
cathepsin	<i>CYP11B2</i>	<i>CHI3L1</i>	<i>COMT</i>	<i>INS</i>
<i>ERBB4</i>	<i>MAT2B</i>	<i>IL8</i>	<i>HTR2A</i>	<i>ARG2</i>
	angiotensin			
<i>TRAM</i>	receptor	interleukin 1	<i>SYNJ1</i>	<i>ABCA1</i>
		matrix		
<i>CCND1</i>	<i>ACTR2</i>	metalloproteinase	<i>INPP1</i>	<i>OLR1</i>
<i>EGF</i>	<i>NPPA</i>	interferon	<i>NEDD4L</i>	collagen
<i>MUC1</i>	<i>LVM</i>	<i>CD68</i>	<i>FRA13C</i>	<i>MCP</i>
			transducer of	
insulin-like	<i>DBH</i>	<i>IL4</i>	<i>ERBB2</i>	lipoprotein
<i>BCL2</i>	<i>NPY</i>	<i>IL17</i>	<i>BAIAP3</i>	<i>APOA2</i>
				intercellular
mucin	<i>POMC</i>	<i>MMP3</i>	<i>ATP1B3</i>	adhesion molecule
<i>FGF3</i>	neuropeptide	<i>SIL</i>	<i>DRD5</i>	<i>RAB27A</i>

\* MedGene results for the top 25 genes associated with breast neoplasms, hypertension, rheumatoid arthritis, bipolar disorder, and atherosclerosis, respectively, ranked by LPF scores. The hyperlink to all the papers co-citing the gene and the disease is available at MedGene website (<http://hipseq.med.harvard.edu/MedGene/>).

## Discussion

The Human Genome Project heralded a new era in biological research where the emphasis on understanding specific pathways has expanded to global studies of genomic organization and biological systems. High-throughput technologies can provide novel insight into comprehensive biological function but also introduces new challenges. The utility of these technologies is limited to the ability to generate, analyze, and interpret large gene lists. MedGene, a relational database derived by mining the information in Medline, was created to address this need. MedGene users can query for a rank-ordered list of human gene-disease relationships (Table 2) for one or more diseases. Each entry is hyperlinked to the original papers supporting each association and to other relevant databases.

MedGene is an innovative extension of previous text mining approaches. Perez-Iratxeta et al. used the GO annotation and their chromosomal locations to predict genes that may contribute to inherited disorders.<sup>8</sup> MedGene takes a broader view and includes all diseases and all possible gene-disease relationships. Furthermore, MedGene utilizes co-citation to indicate a relationship rather than GO annotation, which is limited to the subset of genes that have GO annotation. Our approach is complementary to that taken by Chaussabel and Sher, who used the frequency of co-cited terms to cluster genes into a hierarchy of gene-gene relationships.<sup>6</sup>

A unique aspect of this tool is the ability to assess the relative strengths of gene-disease relationships based on the frequency of both co-citation and single citation. This presupposes that most co-citations describe a positive association, often referred to as publication bias<sup>15</sup> and is supported by our observations

that negative associations are rare (Supplemental Table 3: [http://hipseq.med.harvard.edu/MedGene/publication/s\\_Table3.html](http://hipseq.med.harvard.edu/MedGene/publication/s_Table3.html)). Of course, relationships established by frequency of co-citation do not necessarily represent a true biological link; however, it is strong evidence to support a true relationship.

Another important feature of MedGene is the implementation of software filters that substantially reduced the error rate. We estimate that less than 10% of all associations were missed and at least 70% of even the weakest associations were real. For this study, all of the filters that we applied were general ones, e.g., expanding the list of all gene names to address the different syntax forms used by different journals, eliminating gene names that correspond to common English words, etc. The majority of the remaining search term ambiguities were idiosyncratic and difficult to identify systematically without causing a significant rise in false negatives. Alternative approaches, such as the examination of the nearest neighbor terms, need to be considered to further reduce the false positive rate.

It is not uncommon to see expression changes in microarray experiments as small as 2-fold reported in the literature. Even when these expression changes are statistically significant, it is not always clear if they are biologically meaningful. When comparing expression levels of disease to normal tissue, one expects an enrichment of known disease-related genes to appear in the altered expression group. MedGene provided a unique opportunity to test this notion in the context of existing knowledge on a novel breast cancer micro-array dataset. For genes displaying a 5-fold change or less in tumors compared to normal, there was no evidence of a correlation between altered gene expression and a known role in the disease. This

**Table 3.** Genes with Large Expression Changes in ER- but Not in ER+ Breast Tumors

gene symbol	fold change (ER+)	fold change (ER-)
KRTHB1	1.0	610.8
BRS3	1.2	89.4
DKK1	1.2	69.8
ZIC1	1.9	59.6
TLR1	1.0	38.5
KIAA0680	2.6	33.2
CDKN3	1.0	30.6
EBI2	4.0	27.9
CZMB	3.8	21.9
STK18	4.7	18.6
GPR49	1.0	14.6
MYO10	1.6	14.4
LAD1	-1.0	13.5
POLE2	4.2	13.0
HMG4	4.4	12.9
BCL2L11	-1.2	12.3
LRP8	2.9	12.2
CCNB2	1.0	11.8
CCNE2	4.0	11.6
FCB	-4.3	11.1
KNSL6	2.9	10.9
HIF5	3.0	10.2
SERPINH2	4.6	10.2
YAP1	1.0	10.0
LPHB	-1.3	-10.4
TCEA2	-1.1	-10.8
TFF1	1.3	-11.4
COL17A1	-4.1	-15.7
POP5	1.1	-16.2
BPAG1	-4.6	-22.3
PDZK1	-1.1	-36.8
VEGFC	-2.8	-51.5
MUC6	-1.4	-64.9
SERPINA5	-1.0	-83.1
MEIS1	-1.6	-85.9
CA12	2.4	-150.3

Table 3. MedGene identified a set of relatively understudied, yet highly expressed genes in ER negative, but not ER positive breast tumors. All of these genes have either never been co-cited with breast cancer or have a weak association except those marked with an \*.

reflects the many genes whose role in breast cancer may not involve large changes in expression in sporadic tumors (e.g., *BRCA1* and *BRCA2*) and genes whose modest changes in expression may be unrelated to the disease. Strikingly, among genes with a 10-fold change or more in expression level, there was a strong and significant correlation between expression level and a published role in the disease, providing the first global validation of the micro-array approach to identifying disease-specific genes.

The results derived from MedGene have two implications. First, a careful hunt for corroborating evidence of a role in breast cancer should precede any further study of genes with less than 5-fold expression level changes. Second, any genes with 10-fold changes or more are likely to be related to breast cancer and warrant attention. It is likely that this threshold will change depending on the disease as well as the experiment.

Interestingly, the observed correlation was only found among ER-positive tumors, not ER-negative. This may reflect a bias in the literature to study the more prevalent type of tumor in the population. Furthermore, this emphasizes that caution must be taken when interpreting experiments that may contain subpopulations that behave very differently. The MedGene approach identified a set of relatively understudied, yet highly expressed genes in ER-negative tumors that are worthy of further examination (Table 3).

In conclusion, we have developed an automated method of summarizing and organizing the vast biomedical literature. To our knowledge, the resulting database is the most comprehensive and accurate of its kind. By generating a score that reflects the strength of the association, it provides an important tool for the rapid and flexible analysis of large datasets from various high-throughput screening experiments. Furthermore, it can be used for selecting subsets of genes for functional studies, for building disease-specific arrays, for looking at genes common to multiple diseases and various other high-throughput applications. In the future, it will be possible to enhance the utility of the MedGene database by building links between genes and other MeSH terms as well as other biological processes and concepts, such as cell division and responses to small molecules.

**Acknowledgment.** We would like to thank P. Braun, L. Garraway, J. Pearlberg, and other members of our institute for helpful discussion. Many thanks to the NLM (National Library of Medicine) for licensing of MEDLINE and the annotation effort of adding MeSH indexes for MEDLINE abstracts. This work was funded by grants from the Breast Cancer Research Foundation and an NHLBI PGA Grant (Vol HL66582-02).

**Supporting Information Available:** Twenty-three human disease category headings along with all of their child terms selected from the 2002 MeSH Index (Supplemental Table 1); analysis of the causes of false negatives in MedGene (Supplemental Table 2); meaningful gene-disease relationships found in MedGene (Supplemental Table 3); causes for incorrect assignment of gene indexes (Supplemental Table 4); a review of the results, showing that the resulting disease clusters were indeed logical (Supplemental Figure 1); and a review of the results showing that among the 505 previously unrelated genes, 467 were either newly identified genes or genes that had not previously been associated with any disease (Supplemental Figure 2). This material is available free of charge via the Internet at <http://pubs.acs.org> and at the web sites mentioned in the text.

## References

- (1) Baasiri, R. A.; Glasser, S. R.; Steffen, D. L.; Wheeler, D. A. *Oncogene* 1999, 18, 7958-7965.
- (2) Steffen, D. L.; Levine, A. E.; Yarus, S.; Baasiri, R. A.; Wheeler, D. A. *Bioinformatics* 2000, 16, 639-649.
- (3) Marcotte, E. M.; Xenarios, I.; Eisenberg, D. *Bioinformatics* 2001, 17, 359-363.
- (4) Ono, T.; Hishigaki, H.; Tanigami, A.; Takagi, T. *Bioinformatics* 2001, 17, 155-161.
- (5) Jenssen, T. K.; Laegreid, A.; Komorowski, J.; Hovig, E. *Nat. Genet.* 2001, 28, 21-28.
- (6) Chaussabel, D.; Sher, A. *Genome Biol.* 2002, 3, RESEARCH0055.
- (7) Gibbons, F. D.; Roth, F. P. *Genome Res.* 2002, 12, 1574-1581.
- (8) Perez-Iratxeta, C.; Bork, P.; Andrade, M. A. *Nat. Genet.* 2002, 31, 316-319.
- (9) Funk, M. E.; Reid, C. A. *Bull. Med. Libr. Assoc.* 1983, 71, 176-183.
- (10) Humphrey, S. M.; Miller, N. E. *J. Am. Soc. Inf. Sci.* 1987, 38, 184-196.
- (11) Maglott, D. R.; Katz, K. S.; Sicotte, H.; Pruitt, K. D. *Nucleic Acids Res.* 2000, 28, 126-128.
- (12) Pruitt, K. D.; Maglott, D. R. *Nucleic Acids Res.* 2001, 29, 137-140.
- (13) Wadelius, M.; Andersson, A. O.; Johansson, J. E.; Wadelius, C.; Rane, E. *Pharmacogenetics* 1999, 9, 333-340.
- (14) Adam, R. M.; Borer, J. C.; Williams, J.; Eastham, J. A.; Loughlin, K. R.; Freeman, M. R. *Endocrinology* 1999, 140, 5866-5875.
- (15) Montori, V. M.; Smieja, M.; Guyatt, C. H. *Mayo Clin. Proc.* 2000, 75, 1284-1288.
- (16) Denenberg, V. H. *Statistics Experimental Design for Behavioral and Biological Researchers*; Wiley-Liss: New York, 1976.
- (17) Rebhan, M.; Chalifa-Caspi, V.; Prilusky, J.; Lancet, D. *Trends Genet.* 1997, 13, 163.
- (18) Bairoch, A.; Apweiler, R. *Nucleic Acids Res.* 2000, 28, 45-48. PR0340227

PATENT

IN THE UNITED STATES PATENT AND TRADEMARK OFFICE

In re Application of: Ashkenazi et al.	Group Art Unit: 1647
Serial No.: 09/903,925	Examiner: Fozia Hamid
Filed: July 11, 2001	<b>CERTIFICATE OF MAILING</b> I hereby certify that this correspondence is being deposited with the United States Postal Service with sufficient postage as first class mail in an envelope addressed to: Assistant Commissioner of Patents, Washington, D.C. 20231 on  Date
For: SECRETED AND TRANSMEMBRANE POLYPEPTIDES AND NUCLEIC ACIDS	

**DECLARATION OF AUDREY D. GODDARD, Ph.D UNDER 37 C.F.R. § 1.132**

Assistant Commissioner of Patents  
Washington, D.C. 20231

Sir:

I, Audrey D. Goddard, Ph.D. do hereby declare and say as follows:

1. I am a Senior Clinical Scientist at the Experimental Medicine/BioOncology, Medical Affairs Department of Genentech, Inc., South San Francisco, California 94080.
2. Between 1993 and 2001, I headed the DNA Sequencing Laboratory at the Molecular Biology Department of Genentech, Inc. During this time, my responsibilities included the identification and characterization of genes contributing to the oncogenic process, and determination of the chromosomal localization of novel genes.
3. My scientific Curriculum Vitae, including my list of publications, is attached to and forms part of this Declaration (Exhibit A).



Serial No.: \*

Filed: \*

4. I am familiar with a variety of techniques known in the art for detecting and quantifying the amplification of oncogenes in cancer, including the quantitative TaqMan PCR (i.e., "gene amplification") assay described in the above captioned patent application.

5. The TaqMan PCR assay is described, for example, in the following scientific publications: Higuchi *et al.*, Biotechnology 10:413-417 (1992) (Exhibit B); Livak *et al.*, PCR Methods Appl. 4:357-362 (1995) (Exhibit C) and Heid *et al.*, Genome Res. 6:986-994 (1996) (Exhibit D). Briefly, the assay is based on the principle that successful PCR yields a fluorescent signal due to Taq DNA polymerase-mediated exonuclease digestion of a fluorescently labeled oligonucleotide that is homologous to a sequence between two PCR primers. The extent of digestion depends directly on the amount of PCR, and can be quantified accurately by measuring the increment in fluorescence that results from decreased energy transfer. This is an extremely sensitive technique, which allows detection in the exponential phase of the PCR reaction and, as a result, leads to accurate determination of gene copy number.

6. The quantitative fluorescent TaqMan PCR assay has been extensively and successfully used to characterize genes involved in cancer development and progression. Amplification of protooncogenes has been studied in a variety of human tumors, and is widely considered as having etiological, diagnostic and prognostic significance. This use of the quantitative TaqMan PCR assay is exemplified by the following scientific publications: Pennica *et al.*, Proc. Natl. Acad. Sci. USA 95(25):14717-14722 (1998) (Exhibit E); Pitti *et al.*, Nature 396(6712):699-703 (1998) (Exhibit F) and Bieche *et al.*, Int. J. Cancer 78:661-666 (1998) (Exhibit G), the first two of which I am co-author. In particular, Pennica *et al.* have used the quantitative TaqMan PCR assay to study relative gene amplification of WISP and c-myc in various cell lines, colorectal tumors and normal mucosa. Pitti *et al.* studied the genomic amplification of a decoy receptor for Fas ligand in lung and colon cancer, using the quantitative TaqMan PCR assay. Bieche *et al.* used the assay to study gene amplification in breast cancer.

Serial No.: \*

Filed: \*

7. It is my personal experience that the quantitative TaqMan PCR technique is technically sensitive enough to detect at least a 2-fold increase in gene copy number relative to control. It is further my considered scientific opinion that an at least 2-fold increase in gene copy number in a tumor tissue sample relative to a normal (i.e., non-tumor) sample is significant and useful in that the detected increase in gene copy number in the tumor sample relative to the normal sample serves as a basis for using relative gene copy number as quantitated by the TaqMan PCR technique as a diagnostic marker for the presence or absence of tumor in a tissue sample of unknown pathology. Accordingly, a gene identified as being amplified at least 2-fold by the quantitative TaqMan PCR assay in a tumor sample relative to a normal sample is useful as a marker for the diagnosis of cancer, for monitoring cancer development and/or for measuring the efficacy of cancer therapy.

8. I declare further that all statements made herein of my own knowledge are true and that all statements made on information and belief are believed to be true. I declare that these statements were made with the knowledge that willful false statements and the like so made are punishable by fine or imprisonment, or both, under Section 1001 of Title 18 of the United States Code, and that such willful false statements may jeopardize the validity of the application or any patent issuing thereon.

Jan. 16, 2003

Date

Audrey D. Goddard

Audrey D. Goddard, Ph.D.

**AUDREY D. GODDARD, Ph.D.**

Genentech, Inc.  
1 DNA Way  
South San Francisco, CA, 94080  
650.225.6429  
goddarda@gene.com

110 Congo St.  
San Francisco, CA, 94131  
415.841.9154  
415.819.2247 (mobile)  
agoddard@pacbell.net

**PROFESSIONAL EXPERIENCE**

**Genentech, Inc.**  
**South San Francisco, CA**

**1993-present**

**2001 - present      Senior Clinical Scientist**  
Experimental Medicine / BioOncology, Medical Affairs

**Responsibilities:**

- *Companion diagnostic oncology products*
- *Acquisition of clinical samples from Genentech's clinical trials for translational research*
- *Translational research using clinical specimen and data for drug development and diagnostics*
- *Member of Development Science Review Committee, Diagnostic Oversight Team, 21 CFR Part 11 Subteam*

**Interests:**

- *Ethical and legal implications of experiments with clinical specimens and data*
- *Application of pharmacogenomics in clinical trials*

**1998 - 2001      Senior Scientist**

Head of the DNA Sequencing Laboratory, Molecular Biology Department, Research

**Responsibilities:**

- *Management of a laboratory of up to nineteen –including postdoctoral fellow, associate scientist, senior research associate and research assistants/associate levels*
- *Management of a \$750K budget*
- *DNA sequencing core facility supporting a 350+ person research facility.*
- *DNA sequencing for high throughput gene discovery, - ESTs, cDNAs, and constructs*
- *Genomic sequence analysis and gene identification*
- *DNA sequence and primary protein analysis*

**Research:**

- *Chromosomal localization of novel genes*
- *Identification and characterization of genes contributing to the oncogenic process*
- *Identification and characterization of genes contributing to inflammatory diseases*
- *Design and development of schemes for high throughput genomic DNA sequence analysis*
- *Candidate gene prediction and evaluation*

**1993 - 1998            Scientist**

Head of the DNA Sequencing Laboratory, Molecular Biology Department, Research

**Responsibilities**

- *DNA sequencing core facility supporting a 350+ person research facility*
- *Assumed responsibility for a pre-existing team of five technicians and expanded the group into fifteen, introducing a level of middle management and additional areas of research*
- *Participated in the development of the basic plan for high throughput secreted protein discovery program – sequencing strategies, data analysis and tracking, database design*
- *High throughput EST and cDNA sequencing for new gene identification.*
- *Design and implementation of analysis tools required for high throughput gene identification.*
- *Chromosomal localization of genes encoding novel secreted proteins.*

**Research:**

- *Genomic sequence scanning for new gene discovery.*
- *Development of signal peptide selection methods.*
- *Evaluation of candidate disease genes.*
- *Growth hormone receptor gene SNPs in children with Idiopathic short stature*

**Imperial Cancer Research Fund  
London, UK with Dr. Ellen Solomon**

**1989-1992**

**6/89 –12/92 Postdoctoral Fellow**

- Cloning and characterization of the genes fused at the acute promyelocytic leukemia translocation breakpoints on chromosomes 17 and 15.
- Prepared a successfully funded European Union multi-center grant application

**McMaster University  
Hamilton, Ontario, Canada with Dr. G. D. Sweeney**

**1983**

**5/83 – 8/83: NSERC Summer Student**

- *In vitro* metabolism of  $\beta$ -naphthoflavone in C57Bl/6J and DBA mice

**EDUCATION**

**Ph.D.**

"Phenotypic and genotypic effects of mutations in the human retinoblastoma gene."

**Supervisor:** Dr. R. A. Phillips

University of Toronto  
Toronto, Ontario, Canada.  
Department of Medical  
Biophysics.

1989

**Honours B.Sc**

"The *in vitro* metabolism of the cytochrome P-448 inducer  $\beta$ -naphthoflavone in C57BL/6J mice."

**Supervisor:** Dr. G. D. Sweeney

McMaster University,  
Hamilton, Ontario, Canada.  
Department of Biochemistry

1983

## ACADEMIC AWARDS

Imperial Cancer Research Fund Postdoctoral Fellowship	1989-1992
Medical Research Council Studentship	1983-1988
NSERC Undergraduate Summer Research Award	1983
Society of Chemical Industry Merit Award (Hons. Biochem.)	1983
Dr. Harry Lyman Hooker Scholarship	1981-1983
J.L.W. Gill Scholarship	1981-1982
Business and Professional Women's Club Scholarship	1980-1981
Wyerhauser Foundation Scholarship	1979-1980

## INVITED PRESENTATIONS

Genentech's gene discovery pipeline: High throughput identification, cloning and characterization of novel genes. Functional Genomics: From Genome to Function, Litchfield Park, AZ, USA. October 2000

High throughput identification, cloning and characterization of novel genes. G2K: Back to Science, Advances in Genome Biology and Technology I. Marco Island, FL, USA. February 2000

Quality control in DNA Sequencing: The use of Phred and Phrap. Bay Area Sequencing Users Meeting, Berkeley, CA, USA. April 1999

High throughput secreted protein identification and cloning. Tenth International Genome Sequencing and Analysis Conference, Miami, FL, USA. September 1998

The evolution of DNA sequencing: The Genentech perspective. Bay Area Sequencing Users Meeting, Berkeley, CA, USA. May 1998

Partial Growth Hormone Insensitivity: The role of GH-receptor mutations in Idiopathic Short Stature. Tenth Annual National Cooperative Growth Study Investigators Meeting, San Francisco, CA, USA. October, 1996

Growth hormone (GH) receptor defects are present in selected children with non-GH-deficient short stature: A molecular basis for partial GH-insensitivity. 76<sup>th</sup> Annual Meeting of The Endocrine Society, Anaheim, CA, USA. June 1994

A previously uncharacterized gene, myl, is fused to the retinoic acid receptor alpha gene in acute promyelocytic leukemia. XV International Association for Comparative Research on Leukemia and Related Disease, Padua, Italy. October 1991

## PATENTS

Goddard A, Godowski PJ, Gurney AL. NL2 Tie ligand homologue polypeptide. Patent Number: 6,455,496. Date of Patent: Sept. 24, 2002.

**Goddard A**, Godowski PJ and Gurney AL. NL3 Tie ligand homologue nucleic acids. Patent Number: 6,426,218. Date of Patent: July 30, 2002.

Godowski P, Gurney A, Hillan KJ, Botstein D, **Goddard A**, Roy M, Ferrara N, Tumas D, Schwall R. NL4 Tie ligand homologue nucleic acid. Patent Number: 6,4137,770. Date of Patent: July 2, 2002.

Ashkenazi A, Fong S, **Goddard A**, Gurney AL, Napier MA, Tumas D, Wood WI. Nucleic acid encoding A-33 related antigen poly peptides. Patent Number: 6,410,708. Date of Patent: Jun. 25, 2002.

Botstein DA, Cohen RL, **Goddard AD**, Gurney AL, Hillan KJ, Lawrence DA, Levine AJ, Pennica D, Roy MA and Wood WI. WISP polypeptides and nucleic acids encoding same. Patent Number: 6,387,657. Date of Patent: May 14, 2002.

**Goddard A**, Godowski PJ and Gurney AL. Tie ligands. Patent Number: 6,372,491. Date of Patent: April 16, 2002.

Godowski PJ, Gurney AL, **Goddard A** and Hillan K. TIE ligand homologue antibody. Patent Number: 6,350,450. Date of Patent: Feb. 26, 2002.

Fong S, Ferrara N, **Goddard A**, Godowski PJ, Gurney AL, Hillan K and Williams PM. Tie receptor tyrosine kinase ligand homologues. Patent Number: 6,348,351. Date of Patent: Feb. 19, 2002.

**Goddard A**, Godowski PJ and Gurney AL. Ligand homologues. Patent Number: 6,348,350. Date of Patent: Feb. 19, 2002.

Attie KM, Carlsson LMS, Gesundheit N and **Goddard A**. Treatment of partial growth hormone insensitivity syndrome. Patent Number: 6,207,640. Date of Patent: March 27, 2001.

Fong S, Ferrara N, **Goddard A**, Godowski PJ, Gurney AL, Hillan K and Williams PM. Nucleic acids encoding NL-3. Patent Number: 6,074,873. Date of Patent: June 13, 2000

Attie K, Carlsson LMS, Gesundheit N and **Goddard A**. Treatment of partial growth hormone insensitivity syndrome. Patent Number: 5,824,642. Date of Patent: October 20, 1998

Attie K, Carlsson LMS, Gesundheit N and **Goddard A**. Treatment of partial growth hormone insensitivity syndrome. Patent Number: 5,646,113. Date of Patent: July 8, 1997

Multiple additional provisional applications filed

## PUBLICATIONS

Seshasayee D, Dowd P, Gu Q, Erickson S, **Goddard AD** Comparative sequence analysis of the *HER2* locus in mouse and man. Manuscript in preparation.

Abuzzahab MJ, **Goddard A**, Grigorescu F, Lautier C, Smith RJ and Chernausek SD. Human IGF-1 receptor mutations resulting in pre- and post-natal growth retardation. Manuscript in preparation.

Aggarwal S, Xie, M-H, Foster J, Frantz G, Stinson J, Corpuz RT, Simmons L, Hillan K, Yansura DG, Vandlen RL, **Goddard AD** and Gurney AL. FHFR, a novel receptor for the fibroblast growth factors. Manuscript submitted.

Adams SH, Chui C, Schilbach SL, Yu XX, **Goddard AD**, Grimaldi JC, Lee J, Dowd P, Colman S., Lewin DA. (2001) BFIT, a unique acyl-CoA thioesterase induced in thermogenic brown adipose tissue: Cloning, organization of the human gene, and assessment of a potential link to obesity. *Biochemical Journal* **360**: 135-142.

Lee J, Ho WH, Maruoka M, Corpuz RT, Baldwin DT, Foster JS, **Goddard AD**, Yansura DG, Vandlen RL, Wood WI, Gurney AL. (2001) IL-17E, a novel proinflammatory ligand for the IL-17 receptor homolog IL-17Rh1. *Journal of Biological Chemistry* **276**(2): 1660-1664.

Xie M-H, Aggarwal S, Ho W-H, Foster J, Zhang Z, Stinson J, Wood WI, **Goddard AD** and Gurney AL. (2000) Interleukin (IL)-22, a novel human cytokine that signals through the interferon-receptor related proteins CRF2-4 and IL-22R. *Journal of Biological Chemistry* **275**: 31335-31339.

Weiss GA, Watanabe CK, Zhong A, **Goddard A** and Sidhu SS. (2000) Rapid mapping of protein functional epitopes by combinatorial alanine scanning. *Proc. Natl. Acad. Sci. USA* **97**: 8950-8954.

Guo S, Yamaguchi Y, Schilbach S, Wada T., Lee J, **Goddard A**, French D, Handa H, Rosenthal A. (2000) A regulator of transcriptional elongation controls vertebrate neuronal development. *Nature* **408**: 366-369.

Yan M, Wang L-C, Hymowitz SG, Schilbach S, Lee J, **Goddard A**, de Vos AM, Gao WQ, Dixit VM. (2000) Two-amino acid molecular switch in an epithelial morphogen that regulates binding to two distinct receptors. *Science* **290**: 523-527.

Sehl PD, Tai JTN, Hillan KJ, Brown LA, **Goddard A**, Yang R, Jin H and Lowe DG. (2000) Application of cDNA microarrays in determining molecular phenotype in cardiac growth, development, and response to injury. *Circulation* **101**: 1990-1999.

Guo S, Brush J, Teraoka H, **Goddard A**, Wilson SW, Mullins MC and Rosenthal A. (1999) Development of noradrenergic neurons in the zebrafish hindbrain requires BMP, FGF8, and the homeodomain protein soulless/Phox2A. *Neuron* **24**: 555-566.

Stone D, Murone, M, Luoh, S, Ye W, Armanini P, Gurney A, Phillips HS, Brush, J, **Goddard A**, de Sauvage FJ and Rosenthal A. (1999) Characterization of the human suppressor of fused; a negative regulator of the zinc-finger transcription factor Gli. *J. Cell Sci.* **112**: 4437-4448.

Xie M-H, Holcomb I, Deuel B, Dowd P, Huang A, Vagts A, Foster J, Liang J, Brush J, Gu Q, Hillan K, **Goddard A** and Gurney, A.L. (1999) FGF-19, a novel fibroblast growth factor with unique specificity for FGFR4. *Cytokine* **11**: 729-735.

- Yan M, Lee J, Schilbach S, **Goddard A** and Dixit V. (1999) mE10, a novel caspase recruitment domain-containing proapoptotic molecule. *J. Biol. Chem.* **274**(15): 10287-10292.
- Gurney AL, Marsters SA, Huang RM, Pitti RM, Mark DT, Baldwin DT, Gray AM, Dowd P, Brush J, Heldens S, Schow P, **Goddard AD**, Wood WI, Baker KP, Godowski PJ and Ashkenazi A. (1999) Identification of a new member of the tumor necrosis factor family and its receptor, a human ortholog of mouse GITR. *Current Biology* **9**(4): 215-218.
- Ridgway JBB, Ng E, Kern JA, Lee J, Brush J, **Goddard A** and Carter P. (1999) Identification of a human anti-CD55 single-chain Fv by subtractive panning of a phage library using tumor and nontumor cell lines. *Cancer Research* **59**: 2718-2723.
- Pitti RM, Marsters SA, Lawrence DA, Roy M, Kischkel FC, Dowd P, Huang A, Donahue CJ, Sherwood SW, Baldwin DT, Godowski PJ, Wood WI, Gurney AL, Hillan KJ, Cohen RL, **Goddard AD**, Botstein D and Ashkenazi A. (1998) Genomic amplification of a decoy receptor for Fas ligand in lung and colon cancer. *Nature* **396**(6712): 699-703.
- Pennica D, Swanson TA, Welsh JW, Roy MA, Lawrence DA, Lee J, Brush J, Taneyhill LA, Deuel B, Lew M, Watanabe C, Cohen RL, Melhem MF, Finley GG, Quirke P, **Goddard AD**, Hillan KJ, Gurney AL, Botstein D and Levine AJ. (1998) WISP genes are members of the connective tissue growth factor family that are up-regulated in wnt-1-transformed cells and aberrantly expressed in human colon tumors. *Proc. Natl. Acad. Sci. USA.* **95**(25): 14717-14722.
- Yang RB, Mark MR, Gray A, Huang A, Xie MH, Zhang M, **Goddard A**, Wood WI, Gurney AL and Godowski PJ. (1998) Toll-like receptor-2 mediates lipopolysaccharide-induced cellular signalling. *Nature* **395**(6699): 284-288.
- Merchant AM, Zhu Z, Yuan JQ, **Goddard A**, Adams CW, Presta LG and Carter P. (1998) An efficient route to human bispecific IgG. *Nature Biotechnology* **16**(7): 677-681.
- Marsters SA, Sheridan JP, Pitti RM, Brush J, **Goddard A** and Ashkenazi A. (1998) Identification of a ligand for the death-domain-containing receptor Apo3. *Current Biology* **8**(9): 525-528.
- Xie J, Murone M, Luoh SM, Ryan A, Gu Q, Zhang C, Bonifas JM, Lam CW, Hynes M, **Goddard A**, Rosenthal A, Epstein EH Jr. and de Sauvage FJ. (1998) Activating Smoothed mutations in sporadic basal-cell carcinoma. *Nature.* **391**(6662): 90-92.
- Marsters SA, Sheridan JP, Pitti RM, Huang A, Skubatch M, Baldwin D, Yuan J, Gurney A, **Goddard AD**, Godowski P and Ashkenazi A. (1997) A novel receptor for Apo2L/TRAIL contains a truncated death domain. *Current Biology.* **7**(12): 1003-1006.
- Hynes M, Stone DM, Dowd M, Pitts-Meek S, **Goddard A**, Gurney A and Rosenthal A. (1997) Control of cell pattern in the neural tube by the zinc finger transcription factor *Gli-1*. *Neuron* **19**: 15-26.
- Sheridan JP, Marsters SA, Pitti RM, Gurney A., Skubatch M, Baldwin D, Ramakrishnan L, Gray CL, Baker K, Wood WI, **Goddard AD**, Godowski P, and Ashkenazi A. (1997) Control of TRAIL-Induced Apoptosis by a Family of Signaling and Decoy Receptors. *Science* **277** (5327): 818-821.



**Goddard AD**, Dowd P, Chernauek S, Geffner M, Gertner J, Hintz R, Hopwood N, Kaplan S, Plotnick L, Rogol A, Rosenfield R, Saenger P, Mauras N, Hershkopf R, Angulo M and Attie, K. (1997) Partial growth hormone insensitivity: The role of growth hormone receptor mutations in idiopathic short stature. *J. Pediatr.* **131**: S51-55.

Klein RD, Sherman D, Ho WH, Stone D, Bennett GL, Moffat B, Vandlen R, Simmons L, Gu Q, Hongo JA, Devaux B, Poulsen K, Armanini M, Nozaki C, Asai N, **Goddard A**, Phillips H, Henderson CE, Takahashi M and Rosenthal A. (1997) A GPI-linked protein that interacts with Ret to form a candidate neurturin receptor. *Nature*. **387**(6634): 717-21.

Stone DM, Hynes M, Armanini M, Swanson TA, Gu Q, Johnson RL, Scott MP, Pennica D, **Goddard A**, Phillips H, Noll M, Hooper JE, de Sauvage F and Rosenthal A. (1996) The tumour-suppressor gene patched encodes a candidate receptor for Sonic hedgehog. *Nature* **384**(6605): 129-34.

Marsters SA, Sheridan JP, Donahue CJ, Pitti RM, Gray CL, **Goddard AD**, Bauer KD and Ashkenazi A. (1996) Apo-3, a new member of the tumor necrosis factor receptor family, contains a death domain and activates apoptosis and NF-kappa  $\beta$ . *Current Biology* **6**(12): 1669-76.

Rothe M, Xiong J, Shu HB, Williamson K, **Goddard A** and Goeddel DV. (1996) I-TRAF is a novel TRAF-interacting protein that regulates TRAF-mediated signal transduction. *Proc. Natl. Acad. Sci. USA* **93**: 8241-8246.

Yang M, Luoh SM, **Goddard A**, Reilly D, Henzel W and Bass S. (1996) The bglX gene located at 47.8 min on the Escherichia coli chromosome encodes a periplasmic beta-glucosidase. *Microbiology* **142**: 1659-65.

**Goddard AD** and Black DM. (1996) Familial Cancer in Molecular Endocrinology of Cancer. Waxman, J. Ed. Cambridge University Press, Cambridge UK, pp.187-215.

Treanor JJS, Goodman L, de Sauvage F, Stone DM, Poulson KT, Beck CD, Gray C, Armanini MP, Pollocks RA, Hefti F, Phillips HS, **Goddard A**, Moore MW, Buj-Bello A, Davis AM, Asai N, Takahashi M, Vandlen R, Henderson CE and Rosenthal A. (1996) Characterization of a receptor for GDNF. *Nature* **382**: 80-83.

Klein RD, Gu Q, **Goddard A** and Rosenthal A. (1996) Selection for genes encoding secreted proteins and receptors. *Proc. Natl. Acad. Sci. USA* **93**: 7108-7113.

Winslow JW, Moran P, Valverde J, Shih A, Yuan JQ, Wong SC, Tsai SP, **Goddard A**, Henzel WJ, Hefti F and Caras I. (1995) Cloning of AL-1, a ligand for an Eph-related tyrosine kinase receptor involved in axon bundle formation. *Neuron* **14**: 973-981.

Bennett BD, Zeigler FC, Gu Q, Fendly B, **Goddard AD**, Gillett N and Matthews W. (1995) Molecular cloning of a ligand for the EPH-related receptor protein-tyrosine kinase Htk. *Proc. Natl. Acad. Sci. USA* **92**: 1866-1870.

Huang X, Yuang J, **Goddard A**, Foulis A, James RF, Lernmark A, Pujol-Borrell R, Rabinovitch A, Somoza N and Stewart TA. (1995) Interferon expression in the pancreases of patients with type I diabetes. *Diabetes* **44**: 658-664.

**Goddard AD**, Yuan JQ, Fairbairn L, Dexter M, Borrow J, Kozak C and Solomon E. (1995) Cloning of the murine homolog of the leukemia-associated PML gene. *Mammalian Genome* **6**: 732-737.

- Goddard AD, Covello R, Luoh SM, Clackson T, Attie KM, Gesundheit N, Rundle AC, Wells JA, Carlsson LMTI and The Growth Hormone Insensitivity Study Group. (1995) Mutations of the growth hormone receptor in children with idiopathic short stature. *N. Engl. J. Med.* **333**: 1093-1098.
- Kuo SS, Moran P, Gripp J, Armanini M, Phillips HS, Goddard A and Caras IW. (1994) Identification and characterization of Batk, a predominantly brain-specific non-receptor protein tyrosine kinase related to Csk. *J. Neurosci. Res.* **38**: 705-715.
- Mark MR, Scadden DT, Wang Z, Gu Q, Goddard A and Godowski PJ. (1994) Rse, a novel receptor-type tyrosine kinase with homology to Axl/Ufo, is expressed at high levels in the brain. *Journal of Biological Chemistry* **269**: 10720-10728.
- Borrow J, Shipley J, Howe K, Kiely F, Goddard A, Sheer D, Srivastava A, Antony AC, Fioretos T, Mitelman F and Solomon E. (1994) Molecular analysis of simple variant translocations in acute promyelocytic leukemia. *Genes Chromosomes Cancer* **9**: 234-243.
- Goddard AD and Solomon E. (1993) Genetics of Cancer. *Adv. Hum. Genet.* **21**: 321-376.
- Borrow J, Goddard AD, Gibbons B, Katz F, Swirsky D, Fioretos T, Dube I, Winfield DA, Kingston J, Hagemeijer A, Rees JKH, Lister AT and Solomon E. (1992) Diagnosis of acute promyelocytic leukemia by RT-PCR: Detection of *PML-RARA* and *RARA-PML* fusion transcripts. *Br. J. Haematol.* **82**: 529-540.
- Goddard AD, Borrow J and Solomon E. (1992) A previously uncharacterized gene, PML, is fused to the retinoic acid receptor alpha gene in acute promyelocytic leukemia. *Leukemia* **6 Suppl 3**: 117S-119S.
- Zhu X, Dunn JM, Goddard AD, Squire JA, Becker A, Phillips RA and Gallie BL. (1992) Mechanisms of loss of heterozygosity in retinoblastoma. *Cytogenet. Cell. Genet.* **59**: 248-252.
- Foulkes W, Goddard A. and Patel K. (1991) Retinoblastoma linked with Seascale [letter]. *British Med. J.* **302**: 409.
- Goddard AD, Borrow J, Freemont PS and Solomon E. (1991) Characterization of a novel zinc finger gene disrupted by the t(15;17) in acute promyelocytic leukemia. *Science* **254**: 1371-1374.
- Solomon E, Borrow J and Goddard AD. (1991) Chromosomal aberrations in cancer. *Science* **254**: 1153-1160.
- Pajunen L, Jones TA, Goddard A, Sheer D, Solomon E, Pihlajaniemi T and Kivirikko KI. (1991) Regional assignment of the human gene coding for a multifunctional peptide (P4HB) acting as the  $\beta$ -subunit of prolyl-4-hydroxylase and the enzyme protein disulfide isomerase to 17q25. *Cytogenet. Cell. Genet.* **56**: 165-168.
- Borrow J, Black DM, Goddard AD, Yagle MK, Frischauf A.-M and Solomon E. (1991) Construction and regional localization of a *NotI* linking library from human chromosome 17q. *Genomics* **10**: 477-480.
- Borrow J, Goddard AD, Sheer D and Solomon E. (1990) Molecular analysis of acute promyelocytic leukemia breakpoint cluster region on chromosome 17. *Science* **249**: 1577-1580.

Myers JC, Jones TA, Pohjolainen E-R, Kadri AS, **Goddard AD**, Sheer D, Solomon E and Pihlajaniemi T. (1990) Molecular cloning of 5(IV) collagen and assignment of the gene to the region of the X-chromosome containing the Alport Syndrome locus. *Am. J. Hum. Genet.* **46**: 1024-1033.

Gallie BL, Squire JA, **Goddard A**, Dunn JM, Canton M, Hinton D, Zhu X and Phillips RA. (1990) Mechanisms of oncogenesis in retinoblastoma. *Lab. Invest.* **62**: 394-408.

**Goddard AD**, Phillips RA, Greger V, Passarge E, Hopping W, Gallie BL and Horsthemke B. (1990) Use of the RB1 cDNA as a diagnostic probe in retinoblastoma families. *Clinical Genetics* **37**: 117-126.

Zhu XP, Dunn JM, Phillips RA, **Goddard AD**, Paton KE, Becker A and Gallie BL. (1989) Germline, but not somatic, mutations of the RB1 gene preferentially involve the paternal allele. *Nature* **340**: 312-314.

Gallie BL, Dunn JM, **Goddard A**, Becker A and Phillips RA. (1988) Identification of mutations in the putative retinoblastoma gene. In Molecular Biology of The Eye: Genes, Vision and Ocular Disease. UCLA Symposia on Molecular and Cellular Biology, New Series, Volume 88. J. Piatigorsky, T. Shinohara and P.S. Zelenka, Eds. Alan R. Liss, Inc., New York, 1988, pp. 427-436.

**Goddard AD**, Balakier H, Canton M, Dunn J, Squire J, Reyes E, Becker A, Phillips RA and Gallie BL. (1988) Infrequent genomic rearrangement and normal expression of the putative RB1 gene in retinoblastoma tumors. *Mol. Cell. Biol.* **8**: 2082-2088.

Squire J, Dunn J, **Goddard A**, Hoffman T, Musarella M, Willard HF, Becker AJ, Gallie BL and Phillips RA. (1986) Cloning of the esterase D gene: A polymorphic gene probe closely linked to the retinoblastoma locus on chromosome 13. *Proc. Natl. Acad. Sci. USA* **83**: 6573-6577.

Squire J, **Goddard AD**, Canton M, Becker A, Phillips RA and Gallie BL (1986) Tumour induction by the retinoblastoma mutation is independent of N-myc expression. *Nature* **322**: 555-557.

**Goddard AD**, Heddle JA, Gallie BL and Phillips RA. (1985) Radiation sensitivity of fibroblasts of bilateral retinoblastoma patients as determined by micronucleus induction *in vitro*. *Mutation Research* **152**: 31-38.

## RESEARCH

## SIMULTANEOUS AMPLIFICATION AND DETECTION OF SPECIFIC DNA SEQUENCES

Russell Higuchi\*, Gavin Dollinger<sup>1</sup>, P. Sean Walsh and Robert GriffithRoche Molecular Systems, Inc., 1400 53rd St., Emeryville, CA 94608. <sup>1</sup>Chiron Corporation, 1400 53rd St., Emeryville, CA 94608. \*Corresponding author.

We have enhanced the polymerase chain reaction (PCR) such that specific DNA sequences can be detected without opening the reaction tube. This enhancement requires the addition of ethidium bromide (EtBr) to a PCR. Since the fluorescence of EtBr increases in the presence of double-stranded (ds) DNA an increase in fluorescence in such a PCR indicates a positive amplification, which can be easily monitored externally. In fact, amplification can be continuously monitored in order to follow its progress. The ability to simultaneously amplify specific DNA sequences and detect the product of the amplification both simplifies and improves PCR and may facilitate its automation and more widespread use in the clinic or in other situations requiring high sample throughput.

Although the potential benefits of PCR<sup>1</sup> to clinical diagnostics are well known<sup>2,3</sup>, it is still not widely used in this setting, even though it is four years since thermostable DNA polymerases<sup>4</sup> made PCR practical. Some of the reasons for its slow acceptance are high cost, lack of automation of pre- and post-PCR processing steps, and false positive results from carryover-contamination. The first two points are related in that labor is the largest contributor to cost at the present stage of PCR development. Most current assays require some form of "downstream" processing once thermocycling is done in order to determine whether the target DNA sequence was present and has amplified. These include DNA hybridization<sup>5,6</sup>, gel electrophoresis with or without use of restriction digestion<sup>7,8</sup>, HPLC<sup>9</sup>, or capillary electrophoresis<sup>10</sup>. These methods are labor-intensive, have low throughput, and are difficult to automate. The third point is also closely related to downstream processing. The handling of the PCR product in these downstream processes increases the chances that amplified DNA will spread through the typing lab, resulting in a risk of

"carryover" false positives in subsequent testing<sup>11</sup>.

These downstream processing steps would be eliminated if specific amplification and detection of amplified DNA took place simultaneously within an unopened reaction vessel. Assays in which such different processes take place without the need to separate reaction components have been termed "homogeneous". No truly homogeneous PCR assay has been demonstrated to date, although progress towards this end has been reported. Chehab, et al.<sup>12</sup>, developed a PCR product detection scheme using fluorescent primers that resulted in a fluorescent PCR product. Allele-specific primers, each with different fluorescent tags, were used to indicate the genotype of the DNA. However, the unincorporated primers must still be removed in a downstream process in order to visualize the result. Recently, Holland, et al.<sup>13</sup>, developed an assay in which the endogenous 5' exonuclease assay of *Taq* DNA polymerase was exploited to cleave a labeled oligonucleotide probe. The probe would only cleave if PCR amplification had produced its complementary sequence. In order to detect the cleavage products, however, a subsequent process is again needed.

We have developed a truly homogeneous assay for PCR and PCR product detection based upon the greatly increased fluorescence that ethidium bromide and other DNA binding dyes exhibit when they are bound to ds-DNA<sup>14-16</sup>. As outlined in Figure 1, a prototypic PCR

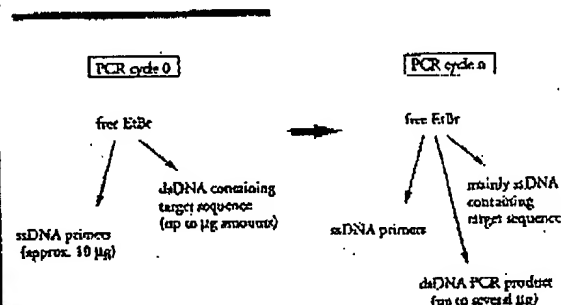


**FIGURE 1** Principle of simultaneous amplification and detection of PCR product. The components of a PCR containing EtBr that are fluorescent are listed—EtBr itself, EtBr bound to either ssDNA or dsDNA. There is a large fluorescence enhancement when EtBr is bound to DNA and binding is greatly enhanced when DNA is double-stranded. After sufficient (n) cycles of PCR, the net increase in dsDNA results in additional EtBr binding, and a net increase in total fluorescence.

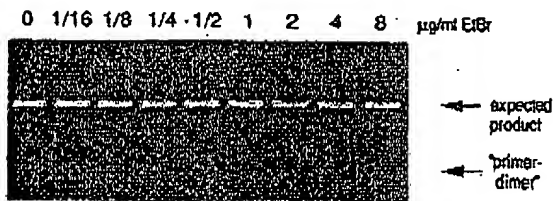


**FIGURE 2** Gel electrophoresis of PCR amplification products of the human, nuclear gene, HLA DQ $\alpha$ , made in the presence of increasing amounts of EtBr (up to 8  $\mu$ g/ml). The presence of EtBr has no obvious effect on the yield or specificity of amplification.

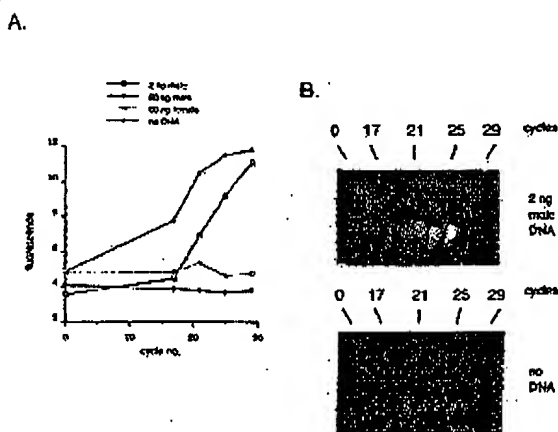


**FIGURE 3** (A) Fluorescence measurements from PCRs that contain 0.5  $\mu$ g/ml EtBr and that are specific for Y-chromosome repeat sequences. Five replicate PCRs were begun containing each of the DNAs specified. At each indicated cycle, one of the five replicate PCRs for each DNA was removed from thermocycling and its fluorescence measured. Units of fluorescence are arbitrary. (B) UV photograph of PCR tubes (0.5 ml Eppendorf-style, polypropylene micro-centrifuge tubes) containing reactions, those starting from 2 ng male DNA and control reactions without any DNA, from (A).

begins with primers that are single-stranded DNA (ssDNA), dNTPs, and DNA polymerase. An amount of dsDNA containing the target sequence (target DNA) is also typically present. This amount can vary, depending on the application, from single-cell amounts of DNA<sup>17</sup> to micrograms per PCR<sup>18</sup>. If EtBr is present, the reagents that will fluoresce, in order of increasing fluorescence, are free EtBr itself, and EtBr bound to the single-stranded DNA primers and to the double-stranded target DNA (by its intercalation between the stacked bases of the DNA double-helix). After the first denaturation cycle, target DNA will be largely single-stranded. After a PCR is completed, the most significant change is the increase in the amount of dsDNA (the PCR product itself) of up to several micrograms. Formerly free EtBr is bound to the additional dsDNA, resulting in an increase in fluorescence. There is also some decrease in the amount of ssDNA primer, but because the binding of EtBr to ssDNA is much less than to dsDNA, the effect of this change on the total fluorescence of the sample is small. The fluorescence increase can be measured by directing excitation illumination through the walls of the amplification vessel

before and after, or even continuously during, thermocycling.

## RESULTS

**PCR in the presence of EtBr.** In order to assess the affect of EtBr in PCR, amplifications of the human HLA DQ $\alpha$  gene<sup>19</sup> were performed with the dye present at concentrations from 0.06 to 8.0  $\mu$ g/ml (a typical concentration of EtBr used in staining of nucleic acids following gel electrophoresis is 0.5  $\mu$ g/ml). As shown in Figure 2, gel electrophoresis revealed little or no difference in the yield or quality of the amplification product whether EtBr was absent or present at any of these concentrations, indicating that EtBr does not inhibit PCR.

**Detection of human Y-chromosome specific sequences.** Sequence-specific, fluorescence enhancement of EtBr as a result of PCR was demonstrated in a series of amplifications containing 0.5  $\mu$ g/ml EtBr and primers specific to repeat DNA sequences found on the human Y-chromosome<sup>20</sup>. These PCRs initially contained either 60 ng male, 60 ng female, 2 ng male human or no DNA. Five replicate PCRs were begun for each DNA. After 0, 17, 21, 24 and 29 cycles of thermocycling, a PCR for each DNA was removed from the thermocycler, and its fluorescence measured in a spectrofluorometer and plotted vs. amplification cycle number (Fig. 3A). The shape of this curve reflects the fact that by the time an increase in fluorescence can be detected, the increase in DNA is becoming linear and not exponential with cycle number. As shown, the fluorescence increased about three-fold over the background fluorescence for the PCRs containing human male DNA, but did not significantly increase for negative control PCRs, which contained either no DNA or human female DNA. The more male DNA present to begin with—60 ng versus 2 ng—the fewer cycles were needed to give a detectable increase in fluorescence. Gel electrophoresis on the products of these amplifications showed that DNA fragments of the expected size were made in the male DNA containing reactions and that little DNA synthesis took place in the control samples.

In addition, the increase in fluorescence was visualized by simply laying the completed, unopened PCRs on a UV transilluminator and photographing them through a red filter. This is shown in figure 3B for the reactions that began with 2 ng male DNA and those with no DNA.

**Detection of specific alleles of the human  $\beta$ -globin gene.** In order to demonstrate that this approach has adequate specificity to allow genetic screening, a detection of the sickle-cell anemia mutation was performed. Figure 4 shows the fluorescence from completed amplifications containing EtBr (0.5  $\mu$ g/ml) as detected by photography of the reaction tubes on a UV transilluminator. These reactions were performed using primers specific for either the wild-type or sickle-cell mutation of the human  $\beta$ -globin gene<sup>21</sup>. The specificity for each allele is imparted by placing the sickle-mutation site at the terminal 3' nucleotide of one primer. By using an appropriate primer annealing temperature, primer extension—and thus amplification—can take place only if the 3' nucleotide of the primer is complementary to the  $\beta$ -globin allele present<sup>21,22</sup>.

Each pair of amplifications shown in Figure 4 consists of a reaction with either the wild-type allele specific (left tube) or sickle-allele specific (right tube) primers. Three different DNAs were typed: DNA from a homozygous, wild-type  $\beta$ -globin individual (AA); from a heterozygous sickle  $\beta$ -globin individual (AS); and from a homozygous sickle  $\beta$ -globin individual (SS). Each DNA (50 ng genomic DNA to start each PCR) was analyzed in triplicate (3 pairs

monoclonal

ess the  
HLA  
sent at  
oncen-  
taining  
2, gel  
yield  
Br was  
indicat-

fic se-  
ment of  
ries of  
rimers  
human  
either  
DNA.  
After 0,  
each  
is fluo-  
plotted  
of this  
case in  
DNA is  
umber.  
cc-fold  
ontain-  
ncrease  
her no  
DNA  
fewer  
in fluo-  
f these  
the ex-  
taining  
in the

ualized  
n a UV  
h a red  
ms that  
JA.  
-globin  
ich has  
etection  
Figure  
ications  
ography  
These  
for ci-  
human  
nparted  
ual 3'  
primer  
has am-  
c of the  
ent 21,22  
nsists of  
the (left  
Three  
zygous,  
ozygous  
ozygous  
genomic  
(3 pairs

of reactions each). The DNA type was reflected in the relative fluorescence intensities in each pair of completed amplifications. There was a significant increase in fluorescence only where a  $\beta$ -globin allele DNA matched the primer set. When measured on a spectrofluorometer (data not shown), this fluorescence was about three times that present in a PCR where both  $\beta$ -globin alleles were mismatched to the primer set. Gel electrophoresis (not shown) established that this increase in fluorescence was due to the synthesis of nearly a microgram of a DNA fragment of the expected size for  $\beta$ -globin. There was little synthesis of dsDNA in reactions in which the allele-specific primer was mismatched to both alleles.

**Continuous monitoring of a PCR.** Using a fiber optic device, it is possible to direct excitation illumination from a spectrofluorometer to a PCR undergoing thermocycling and to return its fluorescence to the spectrofluorometer. The fluorescence readout of such an arrangement, directed at an EtBr-containing amplification of Y-chromosome specific sequences from 25 ng of human male DNA, is shown in Figure 5. The readout from a control PCR with no target DNA is also shown. Thirty cycles of PCR were monitored for each.

The fluorescence trace as a function of time clearly shows the effect of the thermocycling. Fluorescence intensity rises and falls inversely with temperature. The fluorescence intensity is minimum at the denaturation temperature (94°C) and maximum at the annealing/extension temperature (50°C). In the negative-control PCR, these fluorescence maxima and minima do not change significantly over the thirty thermocycles, indicating that there is little dsDNA synthesis without the appropriate target DNA, and there is little if any bleaching of EtBr during the continuous illumination of the sample.

In the PCR containing male DNA, the fluorescence maxima at the annealing/extension temperature begin to increase at about 4000 seconds of thermocycling, and continue to increase with time, indicating that dsDNA is being produced at a detectable level. Note that the fluorescence minima at the denaturation temperature do not significantly increase, presumably because at this temperature there is no dsDNA for EtBr to bind. Thus the course of the amplification is followed by tracking the fluorescence increase at the annealing temperature. Analysis of the products of these two amplifications by gel electrophoresis showed a DNA fragment of the expected size for the male DNA containing sample and no detectable DNA synthesis for the control sample.

#### DISCUSSION

Downstream processes such as hybridization to a sequence-specific probe can enhance the specificity of DNA detection by PCR. The elimination of these processes means that the specificity of this homogeneous assay depends solely on that of PCR. In the case of sickle-cell disease, we have shown that PCR alone has sufficient DNA sequence specificity to permit genetic screening. Using appropriate amplification conditions, there is little non-specific production of dsDNA in the absence of the appropriate target allele.

The specificity required to detect pathogens can be more or less than that required to do genetic screening, depending on the number of pathogens in the sample and the amount of other DNA that must be taken with the sample. A difficult target is HIV, which requires detection of a viral genome that can be at the level of a few copies per thousands of host cells<sup>6</sup>. Compared with genetic screening, which is performed on cells containing at least one copy of the target sequence, HIV detection requires both more specificity and the input of more total

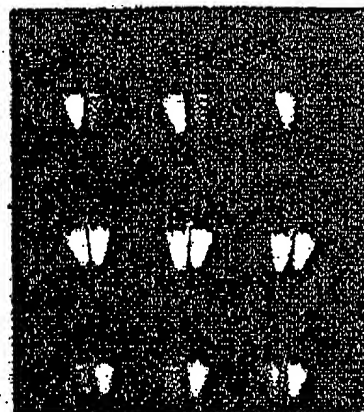


**FIGURE 4** UV photograph of PCR tubes containing amplifications using EtBr that are specific to wild-type (A) or sickle (S) alleles of the human  $\beta$ -globin gene. The left of each pair of tubes contains allele-specific primers to the wild-type alleles, the right tube primers to the sickle allele. The photograph was taken after 30 cycles of PCR, and the input DNAs and the alleles they contain are indicated. Fifty ng of DNA was used to begin PCR. Typing was done in triplicate (3 pairs of PCR's) for each input DNA.

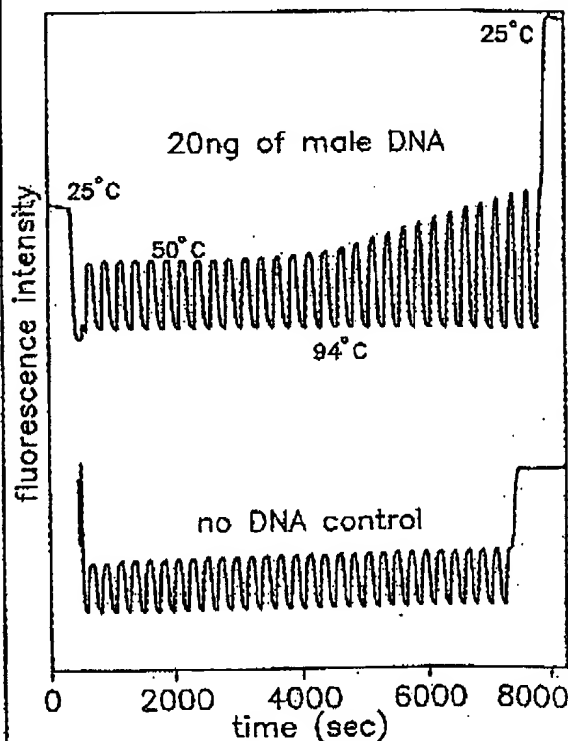


**FIGURE 5** Continuous, real-time monitoring of a PCR. A fiber optic was used to carry excitation light to a PCR in progress and also emitted light back to a fluorometer (see Experimental Protocol). Amplification using human male-DNA specific primers in a PCR starting with 20 ng of human male DNA (top), or in a control PCR without DNA (bottom), were monitored. Thirty cycles of PCR were followed for each. The temperature cycled between 94°C (denaturation) and 50°C (annealing and extension). Note in the male DNA PCR, the cycle (time) dependent increase in fluorescence at the annealing/extension temperature.



DNA—up to microgram amounts—in order to have sufficient numbers of target sequences. This large amount of starting DNA in an amplification significantly increases the background fluorescence over which any additional fluorescence produced by PCR must be detected. An additional complication that occurs with targets in low copy-number is the formation of the "primer-dimer" artifact. This is the result of the extension of one primer using the other primer as a template. Although this occurs infrequently, once it occurs the extension product is a substrate for PCR amplification, and can compete with true PCR targets if those targets are rare. The primer-dimer product is of course dsDNA and thus is a potential source of false signal in this homogeneous assay.

To increase PCR specificity and reduce the effect of primer-dimer amplification, we are investigating a number of approaches, including the use of nested-primer amplifications that take place in a single tube<sup>3</sup>, and the "hot-start", in which nonspecific amplification is reduced by raising the temperature of the reaction before DNA synthesis begins<sup>25</sup>. Preliminary results using these approaches suggest that primer-dimer is effectively reduced and it is possible to detect the increase in EtBr fluorescence in a PCR instigated by a single HIV genome in a background of  $10^5$  cells. With larger numbers of cells, the background fluorescence contributed by genomic DNA becomes problematic. To reduce this background, it may be possible to use sequence-specific DNA-binding dyes that can be made to preferentially bind PCR product over genomic DNA by incorporating the dye-binding DNA sequence into the PCR product through a 5' "add-on" to the oligonucleotide primer<sup>24</sup>.

We have shown that the detection of fluorescence generated by an EtBr-containing PCR is straightforward, both once PCR is completed and continuously during thermocycling. The ease with which automation of specific DNA detection can be accomplished is the most promising aspect of this assay. The fluorescence analysis of completed PCRs is already possible with existing instrumentation in 96-well format<sup>25</sup>. In this format, the fluorescence in each PCR can be quantitated before, after, and even at selected points during thermocycling by moving the rack of PCRs to a 96-microwell plate fluorescence reader<sup>26</sup>.

The instrumentation necessary to continuously monitor multiple PCRs simultaneously is also simple in principle. A direct extension of the apparatus used here is to have multiple fiberoptics transmit the excitation light and fluorescent emissions to and from multiple PCRs. The ability to monitor multiple PCRs continuously may allow quantitation of target DNA copy number. Figure 3 shows that the larger the amount of starting target DNA, the sooner during PCR a fluorescence increase is detected. Preliminary experiments (Higuchi and Dollinger, manuscript in preparation) with continuous monitoring have shown a sensitivity to two-fold differences in initial target DNA concentration.

Conversely, if the number of target molecules is known—as it can be in genetic screening—continuous monitoring may provide a means of detecting false positive and false negative results. With a known number of target molecules, a true positive would exhibit detectable fluorescence by a predictable number of cycles of PCR. Increases in fluorescence detected before or after that cycle would indicate potential artifacts. False negative results due to, for example, inhibition of DNA polymerase, may be detected by including within each PCR an inefficiently amplifying marker. This marker results in a fluorescence increase only after a large number of cycles—many more than are necessary to detect a true

positive. If a sample fails to have a fluorescence increase after this many cycles, inhibition may be suspected. Since, in this assay, conclusions are drawn based on the presence or absence of fluorescence signal alone, such controls may be important. In any event, before any test based on this principle is ready for the clinic, an assessment of its false positive/false negative rates will need to be obtained using a large number of known samples.

In summary, the inclusion in PCR of dyes whose fluorescence is enhanced upon binding dsDNA makes it possible to detect specific DNA amplification from outside the PCR tube. In the future, instruments based upon this principle may facilitate the more widespread use of PCR in applications that demand the high throughput of samples.

#### EXPERIMENTAL PROTOCOL

**Human HLA-DQA gene amplifications containing EtBr.** PCRs were set up in 100  $\mu$ l volumes containing 10 mM Tris-HCl, pH 8.3; 50 mM KCl; 4 mM MgCl<sub>2</sub>; 2.5 units of *Taq* DNA polymerase (Perkin-Elmer Cetus, Norwalk, CT); 20 pmole each of human HLA-DQA gene specific oligonucleotide primers GH26 and GH27<sup>19</sup> and approximately  $10^5$  copies of DQA PCR product diluted from a previous reaction. Ethidium bromide (EtBr; Sigma) was used at the concentrations indicated in Figure 2. Thermocycling proceeded for 20 cycles in a model 480 thermocycler (Perkin-Elmer Cetus, Norwalk, CT) using a "step-cycle" program of 94°C for 1 min, denaturation and 60°C for 30 sec, annealing and 72°C for 30 sec, extension.

**Y-chromosome specific PCR.** PCRs (100  $\mu$ l total reaction volume) containing 0.5  $\mu$ g/ml EtBr were prepared as described for HLA-DQA, except with different primers and target DNAs. These PCRs contained 15 pmole each male DNA-specific primers Y1.1 and Y1.2<sup>20</sup>, and either 60 ng male, 60 ng female, 2 ng male, or no human DNA. Thermocycling was 94°C for 1 min, and 60°C for 1 min using a "step-cycle" program. The number of cycles for a sample were as indicated in Figure 3. Fluorescence measurement is described below.

**Allele-specific, human  $\beta$ -globin gene PCR.** Amplifications of 100  $\mu$ l volume using 0.5  $\mu$ g/ml of EtBr were prepared as described for HLA-DQA above except with different primers and target DNAs. These PCRs contained either primer pair HGP2/HB14A (wild-type globin specific primers) or HGP2/HB14S (sickle-globin specific primers) at 10 pmole each primer per PCR. These primers were developed by Wu et al.<sup>21</sup>. Three different target DNAs were used in separate amplifications—50 ng each of human DNA that was homozygous for the sickle trait (SS), DNA that was heterozygous for the sickle trait (AS), or DNA that was homozygous for the w.t. globin (AA). Thermocycling was for 30 cycles at 94°C for 1 min, and 55°C for 1 min, using a "step-cycle" program. An annealing temperature of 55°C had been shown by Wu et al.<sup>21</sup> to provide allele-specific amplification. Completed PCRs were photographed through a red filter (Wratten 23A) after placing the reaction tubes atop a model TM-36 transilluminator (UV-products San-Gabriel, CA).

**Fluorescence measurement.** Fluorescence measurements were made on PCRs containing EtBr in a Fluorolog-2 fluorometer (SPEX, Edison, NJ). Excitation was at the 500 nm band with about 2 nm bandwidth with a GG 435 nm cut-off filter (Melles Griest, Inc., Irvine, CA) to exclude second-order light. Emitted light was detected at 570 nm with a bandwidth of about 7 nm. An OG 530 nm cut-off filter was used to remove the excitation light.

**Continuous fluorescence monitoring of PCR.** Continuous monitoring of a PCR in progress was accomplished using the spectrofluorometer and settings described above as well as a fiberoptic accessory (SPEX cat. no. 1950) to both send excitation light to, and receive emitted light from, a PCR placed in a well of a model 480 thermocycler (Perkin-Elmer Cetus). The probe end of the fiberoptic cable was attached with "5 minute-epoxy" to the open top of a PCR tube (a 0.5 ml polypropylene centrifuge tube with its cap removed) effectively sealing it. The exposed top of the PCR tube and the end of the fiberoptic cable were shielded from room light and the room lights were kept dimmed during each run. The monitored PCR was an amplification of Y-chromosome-specific repeat sequences as described above, except using an annealing/extension temperature of 50°C. The reaction was covered with mineral oil (2 drops) to prevent evaporation. Thermocycling and fluorescence measurement were started simultaneously. A time-base scan with a 10 second integration time

was used and the emission signal was ratioed to the excitation signal to control for changes in light-source intensity. Data were collected using the dm3000f, version 2.5 (SPEX) data system.

#### Acknowledgments

We thank Bob Jones for help with the spectrofluorometric measurements and Heatherbell Fong for editing this manuscript.

#### References

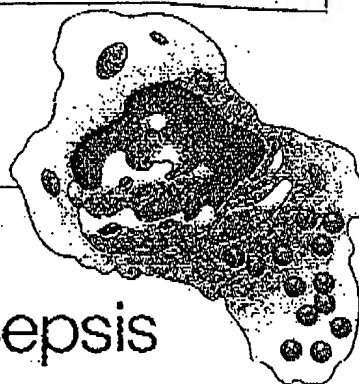
- Mullis, K., Faloona, F., Scharf, S., Saiki, R., Horn, G. and Erlich, H. 1986. Specific enzymatic amplification of DNA *in vitro*: The polymerase chain reaction. *CSHSQB* 51:263-273.
- White, T. J., Arnheim, N. and Erlich, H. A. 1989. The polymerase chain reaction. *Trends Genet.* 5:185-189.
- Erlich, H. A., Gelfand, D. and Smirsky, J. J. 1991. Recent advances in the polymerase chain reaction. *Science* 252:1643-1651.
- Saiki, R. K., Gelfand, D. H., Stoffel, S., Scharf, S. J., Higuchi, R., Horn, G. T., Mullis, K. B. and Erlich, H. A. 1988. Primer-directed enzymatic amplification of DNA with a thermostable DNA polymerase. *Science* 239:487-491.
- Saiki, R. K., Walsh, P. S., Levenson, C. H. and Erlich, H. A. 1989. Genetic analysis of amplified DNA with immobilized sequence-specific oligonucleotide probes. *Proc. Natl. Acad. Sci. USA* 86:6230-6234.
- Kwok, S. Y., Mack, D. H., Mullis, K. B., Fieroz, B. J., Ehrlich, G. D., Blair, D. and Friedman-Kien, A. S. 1987. Identification of human immunodeficiency virus sequences by using *in vitro* enzymatic amplification and oligomer cleavage detection. *J. Virol.* 61:1690-1694.
- Chehab, F. F., Doherty, M., Cai, S. P., Kan, Y. W., Cooper, S. and Rubin, E. M. 1987. Detection of sickle cell anemia and thalassemias. *Nature* 329:203-204.
- Horn, G. T., Richards, B. and Klüger, K. W. 1989. Amplification of a highly polymorphic VNTR segment by the polymerase chain reaction. *Nuc. Acids Res.* 16:2140.
- Katz, E. D. and Dong, M. W. 1990. Rapid analysis and purification of polymerase chain reaction products by high-performance liquid chromatography. *Biotechniques* 8:546-555.
- Heiger, D. N., Cohen, A. S. and Karger, B. L. 1990. Separation of DNA restriction fragments by high performance capillary electrophoresis with low and zero crosslinked polyacrylamide using continuous and pulsed electric fields. *J. Chromatogr.* 516:33-48.
- Kwok, S. Y. and Higuchi, R. G. 1989. Avoiding false positives with PCR. *Nature* 339:237-238.
- Chehab, F. F. and Katz, Y. W. 1989. Detection of specific DNA sequences by fluorescence amplification: a color complementation assay. *Proc. Natl. Acad. Sci. USA* 86:9178-9182.
- Holland, P. M., Abramson, R. D., Watson, R. and Gelfand, D. H. 1991. Detection of specific polymerase chain reaction product by utilizing the 5' to 3' exonuclease activity of *Thermus aquaticus* DNA polymerase. *Proc. Natl. Acad. Sci. USA* 88:7276-7280.
- Markovits, J., Roques, B. P. and Le Feq, J. B. 1979. Ethidium dimer: a new reagent for the fluorimetric determination of nucleic acids. *Anal. Biochem.* 94:259-264.
- Kapuscinski, J. and Sacz, W. 1979. Interactions of 4',6'-diamidino-2-phenylindole with synthetic polynucleotides. *Nuc. Acids Res.* 6:5519-5534.
- Searle, M. S. and Embrey, K. J. 1990. Sequence-specific interaction of Hoechst 33258 with the minor groove of an adenine-tract DNA duplex studied in solution by <sup>1</sup>H NMR spectroscopy. *Nuc. Acids Res.* 18:3752-3762.
- Li, H. H., Gyllenstein, U. B., Cui, X. F., Saiki, R. K., Erlich, H. A. and Arnheim, N. 1988. Amplification and analysis of DNA sequences in single human sperm and diploid cells. *Nature* 336:414-417.
- Abbott, M. A., Fieroz, B. J., Byrne, B. C., Kwok, S. Y., Smirsky, J. J. and Erlich, H. A. 1988. Enzymatic gene amplification: qualitative and quantitative methods for detecting proviral DNA amplified *in vitro*. *J. Infect. Dis.* 158:1158.
- Saiki, R. K., Bugawan, T. L., Horn, G. T., Mullis, K. B. and Erlich, H. A. 1986. Analysis of enzymatically amplified  $\beta$ -globin and HLA-DQA DNA with allele-specific oligonucleotide probes. *Nature* 324:163-166.
- Kogan, S. C., Doherty, M. and Giachieri, J. 1987. An improved method for prenatal diagnosis of genetic diseases by analysis of amplified DNA sequences. *N. Engl. J. Med.* 317:983-990.
- Wu, D. Y., Ugozzoli, L., Fu, B. K. and Wallace, R. B. 1989. Allele-specific enzymatic amplification of  $\beta$ -globin genomic DNA for diagnosis of sickle cell anemia. *Proc. Natl. Acad. Sci. USA* 86:2757-2760.
- Kwok, S., Kellogg, D. E., McKinney, N., Spasic, D., Guda, L., Levenson, C. and Smirsky, J. J. 1990. Effects of primer-template mismatches on the polymerase chain reaction: Human immunodeficiency virus type 1 model studies. *Nuc. Acids Res.* 18:999-1005.
- Chou, Q., Russell, M., Birch, D., Raymond, J. and Bloch, W. 1992. Prevention of pre-PCR mis-priming and primer dimerization improves low-copy-number amplifications. Submitted.
- Higuchi, R. 1989. Using PCR to engineer DNA. p. 61-70. In: *PCR Technology*. H. A. Erlich (Ed.). Stockton Press, New York, N.Y.
- Haff, L., Atwood, J. G., DiCesare, J., Katz, E., Proenza, E., Williams, J. F. and Woudenberg, T. 1991. A high-performance system for automation of the polymerase chain reaction. *Biotechniques* 10:102-109, 106-112.
- Tumosa, N. and Kahen, L. 1989. Fluorescent EIA screening of monoclonal antibodies to cell surface antigens. *J. Immun. Meth.* 116:59-63.

# IBL

IMMUNO BIOLOGICAL LABORATORIES

## SCD-14 ELISA

### Trauma, Shock and Sepsis



The CD-14 molecule is expressed on the surface of monocytes and some macrophages. Membrane-bound CD-14 is a receptor for lipopolysaccharide (LPS) complexed to LPS-Binding-Protein (LBP). The concentration of its soluble form is altered under certain pathological conditions. There is evidence for an important role of sCD-14 with polytrauma, sepsis, burnings and inflammations.

During septic conditions and acute infections it seems to be a prognostic marker and is therefore of value in monitoring these patients.

IBL offers an ELISA for quantitative determination of soluble CD-14 in human serum, -plasma, cell-culture supernatants and other biological fluids.

Assay features: 12x8 determinations (microtiter strips), precoated with a specific monoclonal antibody, 2x1 hour incubation, standard range: 3 - 96 ng/ml, detection limit: 1 ng/ml, CV: intra- and interassay < 8%

For more information call or fax

GESELLSCHAFT FÜR IMMUNCHEMIE UND -BIOLOGIE MBH  
OSTERSTRASSE 86 · D-2000 HAMBURG 20 · GERMANY · TEL. +40/491 00 61-64 · FAX +40/40 11 98

BIO TECHNOLOGY VOL 10 APRIL 1992

417



**GENENTECH, INC.**  
1 DNA Way  
South San Francisco, CA 94080 USA  
Phone: (650) 225-1000

---

FAX: (650) 952-9881

---

**FACSIMILE TRANSMITTAL**

---

**Date:** 19 July 2004

**To:** Anna Barry  
Heller Ehrman

**Re:** Higuchi reference

**Fax No:** 324-6638

**From:** Patty Tobin, Assistant to Elizabeth M. Barnes, Ph.D.  
Genentech, Inc. Legal Department

**Number of Pages including this cover sheet:** 6

## RESEARCH

## SIMULTANEOUS AMPLIFICATION AND DETECTION OF SPECIFIC DNA SEQUENCES

Russell Higuchi\*, Gavin Dollinger<sup>1</sup>, P. Sean Walsh and Robert GriffithRoche Molecular Systems, Inc., 1400 53rd St., Emeryville, CA 94608. <sup>1</sup>Chiron Corporation, 1400 53rd St., Emeryville, CA 94608. \*Corresponding author.

We have enhanced the polymerase chain reaction (PCR) such that specific DNA sequences can be detected without opening the reaction tube. This enhancement requires the addition of ethidium bromide (EtBr) to a PCR. Since the fluorescence of EtBr increases in the presence of double-stranded (ds) DNA an increase in fluorescence in such a PCR indicates a positive amplification, which can be easily monitored externally. In fact, amplification can be continuously monitored in order to follow its progress. The ability to simultaneously amplify specific DNA sequences and detect the product of the amplification both simplifies and improves PCR and may facilitate its automation and more widespread use in the clinic or in other situations requiring high sample throughput.

Although the potential benefits of PCR<sup>1</sup> to clinical diagnostics are well known<sup>2,3</sup>, it is still not widely used in this setting, even though it is four years since thermostable DNA polymerases<sup>4</sup> made PCR practical. Some of the reasons for its slow acceptance are high cost, lack of automation of pre- and post-PCR processing steps, and false positive results from carryover-contamination. The first two points are related in that labor is the largest contributor to cost at the present stage of PCR development. Most current assays require some form of "downstream" processing once thermocycling is done in order to determine whether the target DNA sequence was present and has amplified. These include DNA hybridization<sup>5,6</sup>, gel electrophoresis with or without use of restriction digestion<sup>7,8</sup>, HPLC<sup>9</sup>, or capillary electrophoresis<sup>10</sup>. These methods are labor-intensive, have low throughput, and are difficult to automate. The third point is also closely related to downstream processing. The handling of the PCR product in these downstream processes increases the chances that amplified DNA will spread through the typing lab, resulting in a risk of

"carryover" false positives in subsequent testing<sup>11</sup>.

These downstream processing steps would be eliminated if specific amplification and detection of amplified DNA took place simultaneously within an unopened reaction vessel. Assays in which such different processes take place without the need to separate reaction components have been termed "homogeneous". No truly homogeneous PCR assay has been demonstrated to date, although progress towards this end has been reported. Chehab, et al.<sup>12</sup>, developed a PCR product detection scheme using fluorescent primers that resulted in a fluorescent PCR product. Allele-specific primers, each with different fluorescent tags, were used to indicate the genotype of the DNA. However, the unincorporated primers must still be removed in a downstream process in order to visualize the result. Recently, Holland, et al.<sup>13</sup>, developed an assay in which the endogenous 5' exonuclease assay of *Taq* DNA polymerase was exploited to cleave a labeled oligonucleotide probe. The probe would only cleave if PCR amplification had produced its complementary sequence. In order to detect the cleavage products, however, a subsequent process is again needed.

We have developed a truly homogeneous assay for PCR and PCR product detection based upon the greatly increased fluorescence that ethidium bromide and other DNA binding dyes exhibit when they are bound to ds-DNA<sup>14-16</sup>. As outlined in Figure 1, a prototypic PCR

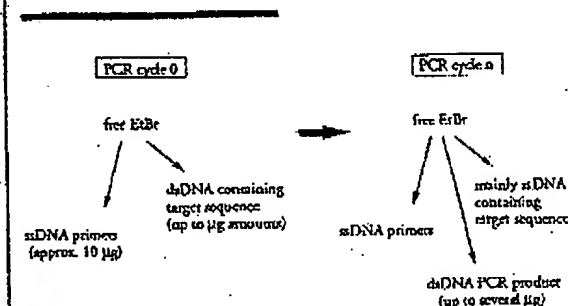


**FIGURE 1** Principle of simultaneous amplification and detection of PCR product. The components of a PCR containing EtBr that are fluorescent are listed—EtBr itself, EtBr bound to either ssDNA or dsDNA. There is a large fluorescence enhancement when EtBr is bound to DNA and binding is greatly enhanced when DNA is double-stranded. After sufficient (n) cycles of PCR, the net increase in dsDNA results in additional EtBr binding, and a net increase in total fluorescence.

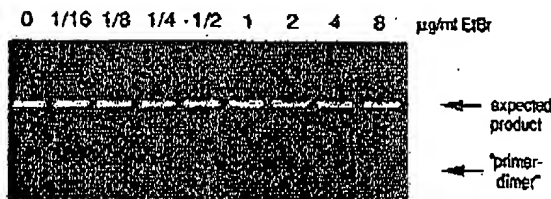


**FIGURE 2** Gel electrophoresis of PCR amplification products of the human nuclear gene, HLA DQA, made in the presence of increasing amounts of EtBr (up to 8 µg/ml). The presence of EtBr has no obvious effect on the yield or specificity of amplification.

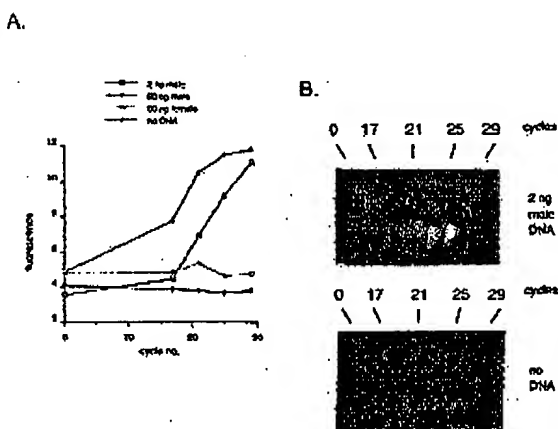


**FIGURE 3** (A) Fluorescence measurements from PCRs that contain 0.5 µg/ml EtBr and that are specific for Y-chromosome repeat sequences. Five replicate PCRs were begun containing each of the DNAs specified. At each indicated cycle, one of the five replicate PCRs for each DNA was removed from thermocycling and its fluorescence measured. Units of fluorescence are arbitrary. (B) UV photography of PCR tubes (0.5 ml Eppendorf-style, polypropylene micro-centrifuge tubes) containing reactions, those starting from 2 ng male DNA and control reactions without any DNA, from (A).

begins with primers that are single-stranded DNA (ss-DNA), dNTPs, and DNA polymerase. An amount of dsDNA containing the target sequence (target DNA) is also typically present. This amount can vary, depending on the application, from single-cell amounts of DNA<sup>17</sup> to micrograms per PCR<sup>18</sup>. If EtBr is present, the reagents that will fluoresce, in order of increasing fluorescence, are free EtBr itself, and EtBr bound to the single-stranded DNA primers and to the double-stranded target DNA (by its intercalation between the stacked bases of the DNA double-helix). After the first denaturation cycle, target DNA will be largely single-stranded. After a PCR is completed, the most significant change is the increase in the amount of dsDNA (the PCR product itself) of up to several micrograms. Formerly free EtBr is bound to the additional dsDNA, resulting in an increase in fluorescence. There is also some decrease in the amount of ssDNA primer, but because the binding of EtBr to ssDNA is much less than to dsDNA, the effect of this change on the total fluorescence of the sample is small. The fluorescence increase can be measured by directing excitation illumination through the walls of the amplification vessel

before and after, or even continuously during, thermocycling.

## RESULTS

**PCR in the presence of EtBr.** In order to assess the effect of EtBr in PCR, amplifications of the human HLA DQA gene<sup>19</sup> were performed with the dye present at concentrations from 0.06 to 8.0 µg/ml (a typical concentration of EtBr used in staining of nucleic acids following gel electrophoresis is 0.5 µg/ml). As shown in Figure 2, gel electrophoresis revealed little or no difference in the yield or quality of the amplification product whether EtBr was absent or present at any of these concentrations, indicating that EtBr does not inhibit PCR.

**Detection of human Y-chromosome specific sequences.** Sequence-specific, fluorescence enhancement of EtBr as a result of PCR was demonstrated in a series of amplifications containing 0.5 µg/ml EtBr and primers specific to repeat DNA sequences found on the human Y-chromosome<sup>20</sup>. These PCRs initially contained either 60 ng male, 60 ng female, 2 ng male human or no DNA. Five replicate PCRs were begun for each DNA. After 0, 17, 21, 24 and 29 cycles of thermocycling, a PCR for each DNA was removed from the thermocycler, and its fluorescence measured in a spectrofluorometer and plotted vs. amplification cycle number (Fig. 3A). The shape of this curve reflects the fact that by the time an increase in fluorescence can be detected, the increase in DNA is becoming linear and not exponential with cycle number. As shown, the fluorescence increased about three-fold over the background fluorescence for the PCRs containing human male DNA, but did not significantly increase for negative control PCRs, which contained either no DNA or human female DNA. The more male DNA present to begin with—60 ng versus 2 ng—the fewer cycles were needed to give a detectable increase in fluorescence. Gel electrophoresis on the products of these amplifications showed that DNA fragments of the expected size were made in the male DNA containing reactions and that little DNA synthesis took place in the control samples.

In addition, the increase in fluorescence was visualized by simply laying the completed, unopened PCRs on a UV transilluminator and photographing them through a red filter. This is shown in figure 3B for the reactions that began with 2 ng male DNA and those with no DNA.

**Detection of specific alleles of the human  $\beta$ -globin gene.** In order to demonstrate that this approach has adequate specificity to allow genetic screening, a detection of the sickle-cell anemia mutation was performed. Figure 4 shows the fluorescence from completed amplifications containing EtBr (0.5 µg/ml) as detected by photography of the reaction tubes on a UV transilluminator. These reactions were performed using primers specific for either the wild-type or sickle-cell mutation of the human  $\beta$ -globin gene<sup>21</sup>. The specificity for each allele is imparted by placing the sickle-mutation site at the terminal 3' nucleotide of one primer. By using an appropriate primer annealing temperature, primer extension—and thus amplification—can take place only if the 3' nucleotide of the primer is complementary to the  $\beta$ -globin allele present<sup>21,22</sup>.

Each pair of amplifications shown in Figure 4 consists of a reaction with either the wild-type allele specific (left tube) or sickle-allele specific (right tube) primers. Three different DNAs were typed: DNA from a homozygous, wild-type  $\beta$ -globin individual (AA); from a heterozygous sickle  $\beta$ -globin individual (AS); and from a homozygous sickle  $\beta$ -globin individual (SS). Each DNA (50 ng genomic DNA to start each PCR) was analyzed in triplicate (3 pairs

monoclonal

ess the  
HLA  
sent at  
oncen-  
lowing  
e 2, gel  
ie yield  
Br was  
ndicat-

fic se-  
nent of  
ries of  
rimers  
human  
either  
DNA.  
fter 0,  
or each  
ts fluo-  
plotted  
of this  
case in  
DNA is  
umber.  
cc-fold  
ontain-  
ncrease  
her no  
DNA  
fewer  
in fluo-  
f these  
the ex-  
taining  
in the

ualized  
n a UV  
h a red  
ns that  
A.  
-globin  
ch has  
etection  
Figure  
ications  
graphy  
These  
for ci-  
human  
nparted  
ual 3'  
primer  
has am-  
c of the  
ent<sup>21,22</sup>  
nsists of  
tic (left  
Three  
zygous,  
ozygous  
zygous  
genomic  
(3 pairs

of reactions each). The DNA type was reflected in the relative fluorescence intensities in each pair of completed amplifications. There was a significant increase in fluorescence only where a  $\beta$ -globin allele DNA matched the primer set. When measured on a spectrofluorometer (data not shown), this fluorescence was about three times that present in a PCR where both  $\beta$ -globin alleles were mismatched to the primer set. Gel electrophoresis (not shown) established that this increase in fluorescence was due to the synthesis of nearly a microgram of a DNA fragment of the expected size for  $\beta$ -globin. There was little synthesis of dsDNA in reactions in which the allele-specific primer was mismatched to both alleles.

**Continuous monitoring of a PCR.** Using a fiber optic device, it is possible to direct excitation illumination from a spectrofluorometer to a PCR undergoing thermocycling and to return its fluorescence to the spectrofluorometer. The fluorescence readout of such an arrangement, directed at an EtBr-containing amplification of Y-chromosome specific sequences from 25 ng of human male DNA, is shown in Figure 5. The readout from a control PCR with no target DNA is also shown. Thirty cycles of PCR were monitored for each.

The fluorescence trace as a function of time clearly shows the effect of the thermocycling. Fluorescence intensity rises and falls inversely with temperature. The fluorescence intensity is minimum at the denaturation temperature (94°C) and maximum at the annealing/extension temperature (50°C). In the negative-control PCR, these fluorescence maxima and minima do not change significantly over the thirty thermocycles, indicating that there is little dsDNA synthesis without the appropriate target DNA, and there is little if any bleaching of EtBr during the continuous illumination of the sample.

In the PCR containing male DNA, the fluorescence maxima at the annealing/extension temperature begin to increase at about 4000 seconds of thermocycling, and continue to increase with time, indicating that dsDNA is being produced at a detectable level. Note that the fluorescence minima at the denaturation temperature do not significantly increase, presumably because at this temperature there is no dsDNA for EtBr to bind. Thus the course of the amplification is followed by tracking the fluorescence increase at the annealing temperature. Analysis of the products of these two amplifications by gel electrophoresis showed a DNA fragment of the expected size for the male DNA containing sample and no detectable DNA synthesis for the control sample.

## DISCUSSION

Downstream processes such as hybridization to a sequence-specific probe can enhance the specificity of DNA detection by PCR. The elimination of these processes means that the specificity of this homogeneous assay depends solely on that of PCR. In the case of sickle-cell disease, we have shown that PCR alone has sufficient DNA sequence specificity to permit genetic screening. Using appropriate amplification conditions, there is little non-specific production of dsDNA in the absence of the appropriate target allele.

The specificity required to detect pathogens can be more or less than that required to do genetic screening, depending on the number of pathogens in the sample and the amount of other DNA that must be taken with the sample. A difficult target is HIV, which requires detection of a viral genome that can be at the level of a few copies per thousands of host cells<sup>6</sup>. Compared with genetic screening, which is performed on cells containing at least one copy of the target sequence, HIV detection requires both more specificity and the input of more total

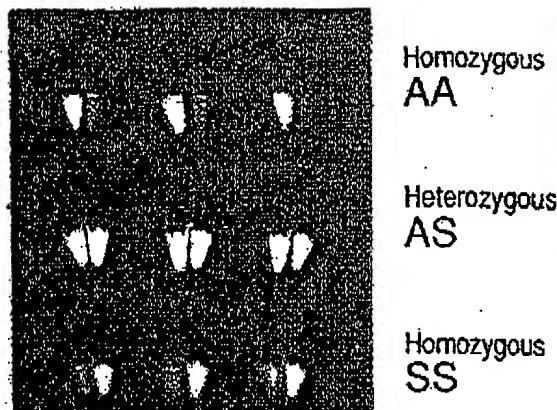


**FIGURE 4** UV photograph of PCR tubes containing amplifications using EtBr that are specific to wild-type (A) or sickle (S) alleles of the human  $\beta$ -globin gene. The left of each pair of tubes contains allele-specific primers to the wild-type alleles, the right tube primers to the sickle allele. The photograph was taken after 30 cycles of PCR, and the input DNAs and the alleles they contain are indicated. Fifty ng of DNA was used to begin PCR. Typing was done in triplicate (3 pairs of PCRs) for each input DNA.

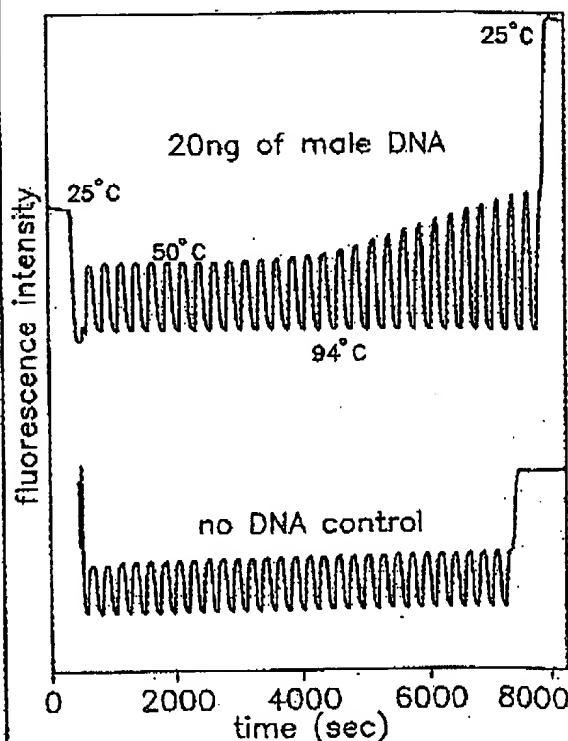


**FIGURE 5** Continuous, real-time monitoring of a PCR. A fiber optic was used to carry excitation light to a PCR in progress and also emitted light back to a fluorometer (see Experimental Protocol). Amplification using human male DNA specific primers in a PCR starting with 20 ng of human male DNA (top), or in a control PCR without DNA (bottom), were monitored. Thirty cycles of PCR were followed for each. The temperature cycled between 94°C (denaturation) and 50°C (annealing and extension). Note in the male DNA PCR, the cycle (time) dependent increase in fluorescence at the annealing/extension temperature.

DNA—up to microgram amounts—in order to have sufficient numbers of target sequences. This large amount of starting DNA in an amplification significantly increases the background fluorescence over which any additional fluorescence produced by PCR must be detected. An additional complication that occurs with targets in low copy-number is the formation of the “primer-dimer” artifact. This is the result of the extension of one primer using the other primer as a template. Although this occurs infrequently, once it occurs the extension product is a substrate for PCR amplification, and can compete with true PCR targets if those targets are rare. The primer-dimer product is of course dsDNA and thus is a potential source of false signal in this homogeneous assay.

To increase PCR specificity and reduce the effect of primer-dimer amplification, we are investigating a number of approaches, including the use of nested-primer amplifications that take place in a single tube<sup>2</sup>, and the “hot-start”, in which nonspecific amplification is reduced by raising the temperature of the reaction before DNA synthesis begins<sup>23</sup>. Preliminary results using these approaches suggest that primer-dimer is effectively reduced and it is possible to detect the increase in EtBr fluorescence in a PCR instigated by a single HIV genome in a background of  $10^5$  cells. With larger numbers of cells, the background fluorescence contributed by genomic DNA becomes problematic. To reduce this background, it may be possible to use sequence-specific DNA-binding dyes that can be made to preferentially bind PCR product over genomic DNA by incorporating the dye-binding DNA sequence into the PCR product through a 5′ “add-on” to the oligonucleotide primer<sup>24</sup>.

We have shown that the detection of fluorescence generated by an EtBr-containing PCR is straightforward, both once PCR is completed and continuously during thermocycling. The ease with which automation of specific DNA detection can be accomplished is the most promising aspect of this assay. The fluorescence analysis of completed PCRs is already possible with existing instrumentation in 96-well format<sup>25</sup>. In this format, the fluorescence in each PCR can be quantitated before, after, and even at selected points during thermocycling by moving the rack of PCRs to a 96-microwell plate fluorescence reader<sup>26</sup>.

The instrumentation necessary to continuously monitor multiple PCRs simultaneously is also simple in principle. A direct extension of the apparatus used here is to have multiple fiberoptics transmit the excitation light and fluorescent emissions to and from multiple PCRs. The ability to monitor multiple PCRs continuously may allow quantitation of target DNA copy number. Figure 3 shows that the larger the amount of starting target DNA, the sooner during PCR a fluorescence increase is detected. Preliminary experiments (Higuchi and Dollinger, manuscript in preparation) with continuous monitoring have shown a sensitivity to two-fold differences in initial target DNA concentration.

Conversely, if the number of target molecules is known—as it can be in genetic screening—continuous monitoring may provide a means of detecting false positive and false negative results. With a known number of target molecules, a true positive would exhibit detectable fluorescence by a predictable number of cycles of PCR. Increases in fluorescence detected before or after that cycle would indicate potential artifacts. False negative results due to, for example, inhibition of DNA polymerase, may be detected by including within each PCR an inefficiently amplifying marker. This marker results in a fluorescence increase only after a large number of cycles—many more than are necessary to detect a true

positive. If a sample fails to have a fluorescence increase after this many cycles, inhibition may be suspected. Since, in this assay, conclusions are drawn based on the presence or absence of fluorescence signal alone, such controls may be important. In any event, before any test based on this principle is ready for the clinic, an assessment of its false positive/false negative rates will need to be obtained using a large number of known samples.

In summary, the inclusion in PCR of dyes whose fluorescence is enhanced upon binding dsDNA makes it possible to detect specific DNA amplification from outside the PCR tube. In the future, instruments based upon this principle may facilitate the more widespread use of PCR in applications that demand the high throughput of samples.

#### EXPERIMENTAL PROTOCOL

**Human HLA-DQ $\alpha$  gene amplifications containing EtBr.** PCRs were set up in 100  $\mu$ l volumes containing 10 mM Tris-HCl, pH 8.3; 50 mM KCl; 4 mM MgCl<sub>2</sub>; 2.5 units of Taq DNA polymerase (Perkin-Elmer Cetus, Norwalk, CT); 20 pmole each of human HLA-DQ $\alpha$  gene specific oligonucleotide primers GH26 and GH27<sup>12</sup> and approximately  $10^5$  copies of DQ $\alpha$  PCR product diluted from a previous reaction. Ethidium bromide (EtBr; Sigma) was used at the concentrations indicated in Figure 2. Thermocycling proceeded for 20 cycles in a model 480 thermocycler (Perkin-Elmer Cetus, Norwalk, CT) using a “step-cycle” program of 94°C for 1 min, denaturation and 60°C for 30 sec, annealing and 72°C for 30 sec, extension.

**Y-chromosome specific PCR.** PCRs (100  $\mu$ l total reaction volume) containing 0.5  $\mu$ g/ml EtBr were prepared as described for HLA-DQ $\alpha$ , except with different primers and target DNAs. These PCRs contained 15 pmole each male DNA-specific primers Y1.1 and Y1.2<sup>20</sup>, and either 60 ng male, 60 ng female, 2 ng male, or no human DNA. Thermocycling was 94°C for 1 min, and 60°C for 1 min using a “step-cycle” program. The number of cycles for a sample were as indicated in Figure 3. Fluorescence measurement is described below.

**Allele-specific, human  $\beta$ -globin gene PCR.** Amplifications of 100  $\mu$ l volume using 0.5  $\mu$ g/ml of EtBr were prepared as described for HLA-DQ $\alpha$  above except with different primers and target DNAs. These PCRs contained either primer pair HGP2/H $\beta$ 14A (wild-type globin specific primers) or HGP2/H $\beta$ 14S (sickle-globin specific primers) at 10 pmole each primer per PCR. These primers were developed by Wu et al.<sup>21</sup>. Three different target DNAs were used in separate amplifications—50 ng each of human DNA that was homozygous for the sickle trait (SS), DNA that was heterozygous for the sickle trait (AS), or DNA that was homozygous for the w.t. globin (AA). Thermocycling was for 30 cycles at 94°C for 1 min, and 55°C for 1 min, using a “step-cycle” program. An annealing temperature of 55°C had been shown by Wu et al.<sup>21</sup> to provide allele-specific amplification. Completed PCRs were photographed through a red filter (Wratten 23A) after placing the reaction tubes atop a model TM-96 transilluminator (UV-products San Gabriel, CA).

**Fluorescence measurement.** Fluorescence measurements were made on PCRs containing EtBr in a Fluorolog-2 fluorometer (SPEX, Edison, NJ). Excitation was at the 500 nm band with about 2 nm bandwidth with a GG 435 nm cut-off filter (Melles Griest, Inc., Irvine, CA) to exclude second-order light. Emitted light was detected at 570 nm with a bandwidth of about 7 nm. An OG 530 nm cut-off filter was used to remove the excitation light.

**Continuous fluorescence monitoring of PCR.** Continuous monitoring of a PCR in progress was accomplished using the spectrofluorometer and settings described above as well as a fiberoptic accessory (SPEX cat. no. 1950) to both send excitation light to, and receive emitted light from, a PCR placed in a well of a model 480 thermocycler (Perkin-Elmer Cetus). The probe end of the fiberoptic cable was attached with “5 minute-epoxy” to the open top of a PCR tube (a 0.5 ml polypropylene centrifuge tube with its cap removed) effectively sealing it. The exposed top of the PCR tube and the end of the fiberoptic cable were shielded from room light and the room lights were kept dimmed during each run. The monitored PCR was an amplification of Y-chromosome-specific repeat sequences as described above, except using an annealing/extension temperature of 50°C. The reaction was covered with mineral oil (2 drops) to prevent evaporation. Thermocycling and fluorescence measurement were started simultaneously. A time-base scan with a 10 second integration time



was used and the emission signal was ratioed to the excitation signal to control for changes in light-source intensity. Data were collected using the dm3000f, version 2.5 (SPEX) data system.

#### Acknowledgments

We thank Bob Jones for help with the spectrofluorometric measurements and Heatherbell Fong for editing this manuscript.

#### References

- Mullis, K., Faloona, F., Scharf, S., Saiki, R., Horn, G. and Erlich, H. 1986. Specific enzymatic amplification of DNA *in vitro*: The polymerase chain reaction. *CSHSQ* 51:263-273.
- White, T. J., Arnheim, N. and Erlich, H. A. 1989. The polymerase chain reaction. *Trends Genet.* 5:185-189.
- Erlich, H. A., Gelfand, D. and Sninsky, J. J. 1991. Recent advances in the polymerase chain reaction. *Science* 252:1643-1651.
- Saiki, R. K., Gelfand, D. H., Stoffel, S., Scharf, S. J., Higuchi, R., Horn, G. T., Mullis, K. B. and Erlich, H. A. 1988. Primer-directed enzymatic amplification of DNA with a thermostable DNA polymerase. *Science* 239:487-491.
- Saiki, R. K., Walsb, P. S., Levenson, C. H. and Erlich, H. A. 1989. Genetic analysis of amplified DNA with immobilized sequence-specific oligonucleotide probes. *Proc. Natl. Acad. Sci. USA* 86:6230-6234.
- Kwok, S. Y., Mack, D. H., Mullis, K. B., Poiesz, E. J., Ehrlich, G. D., Blair, D. and Friedman-Kien, A. S. 1987. Identification of human immunodeficiency virus sequences by using *in vitro* enzymatic amplification and oligomer cleavage detection. *J. Virol.* 61:1690-1694.
- Chehab, F. F., Doherty, M., Cai, S. P., Kan, Y. W., Cooper, S. and Rubin, E. M. 1987. Detection of sickle cell anemia and thalassemia. *Nature* 329:293-294.
- Horn, G. T., Richards, B. and Klinger, K. W. 1989. Amplification of a highly polymorphic VNTR segment by the polymerase chain reaction. *Nuc. Acids Res.* 16:2140.
- Katz, E. D. and Dong, M. W. 1990. Rapid analysis and purification of polymerase chain reaction products by high-performance liquid chromatography. *Biotechniques* 8:546-555.
- Heiger, D. N., Cohen, A. S. and Karger, B. L. 1990. Separation of DNA restriction fragments by high performance capillary electrophoresis with low and zero crosslinked polyacrylamide using continuous and pulsed electric fields. *J. Chromatogr.* 516:33-48.
- Kwok, S. Y. and Higuchi, R. G. 1989. Avoiding false positives with PCR. *Nature* 339:237-238.
- Chehab, F. F. and Kan, Y. W. 1989. Detection of specific DNA sequences by fluorescence amplification: a color complementation assay. *Proc. Natl. Acad. Sci. USA* 86:9178-9182.
- Holland, P. M., Abramson, R. D., Watson, R. and Gelfand, D. H. 1991. Detection of specific polymerase chain reaction product by utilizing the 5' to 3' exonuclease activity of *Thermus aquaticus* DNA polymerase. *Proc. Natl. Acad. Sci. USA* 88:7276-7280.
- Markovits, J., Roques, B. P. and Le Pecq, J. B. 1979. Ethidium dimer: a new reagent for the fluorimetric determination of nucleic acids. *Anal. Biochem.* 94:259-264.
- Kapuscinski, J. and Szer, W. 1979. Interactions of 4',6-diamidino-2-phenylindole with synthetic polynucleotides. *Nuc. Acids Res.* 6:5519-5524.
- Searle, M. S. and Embrey, K. J. 1990. Sequence-specific interaction of Hoechst 33258 with the minor groove of an adenine-tract DNA duplex studied in solution by <sup>1</sup>H NMR spectroscopy. *Nuc. Acids Res.* 18:3752-3762.
- Li, H. H., Gyllenstein, U. B., Cui, X. F., Saiki, R. K., Erlich, H. A. and Arnheim, N. 1988. Amplification and analysis of DNA sequences in single human sperm and diploid cells. *Nature* 336:414-417.
- Abbott, M. A., Poiesz, E. J., Byrne, B. C., Kwok, S. Y., Sninsky, J. J. and Erlich, H. A. 1988. Enzymatic gene amplification: qualitative and quantitative methods for detecting proviral DNA amplified *in vitro*. *J. Infect. Dis.* 158:1158.
- Saiki, R. K., Bugawan, T. L., Horn, G. T., Mullis, K. B. and Erlich, H. A. 1986. Analysis of enzymatically amplified  $\beta$ -globin and HLA-DQA DNA with allele-specific oligonucleotide probes. *Nature* 324:163-166.
- Kogan, S. C., Doherty, M. and Giuschieri, J. 1987. An improved method for prenatal diagnosis of genetic diseases by analysis of amplified DNA sequences. *N. Engl. J. Med.* 317:985-990.
- Wu, D. Y., Ugazoli, L., Pal, B. K. and Wallace, R. B. 1989. Allele-specific enzymatic amplification of  $\beta$ -globin genomic DNA for diagnosis of sickle cell anemia. *Proc. Natl. Acad. Sci. USA* 86:2757-2760.
- Kwok, S., Kellogg, D. E., McKinney, N., Spasic, D., Goda, L., Levenson, C. and Sninsky, J. J. 1990. Effects of primer-template mismatches on the polymerase chain reaction: Human immunodeficiency virus type 1 model studies. *Nuc. Acids Res.* 18:999-1005.
- Chou, Q., Russell, M., Birch, D., Raymond, J. and Bloch, W. 1992. Prevention of pre-PCR mis-priming and primer dimerization improves low-copy-number amplifications. *Submitted.*
- Higuchi, R. 1989. Using PCR to engineer DNA. p. 61-70. In: *PCR Technology*. H. A. Erlich (Ed.). Stockton Press, New York, N.Y.
- Haff, L., Atwood, J. G., DiCesare, J., Katz, E., Proenza, E., Williams, J. F. and Wondenberg, T. 1991. A high-performance system for automation of the polymerase chain reaction. *Biotechniques* 10:102-103, 106-112.
- Tumosa, N. and Kalan, L. 1989. Fluorescent EIA screening of monoclonal antibodies to cell surface antigens. *J. Immun. Med.* 116:59-63.

# IBL

IMMUNO BIOLOGICAL LABORATORIES

## sCD-14 ELISA

### Trauma, Shock and Sepsis

The CD-14 molecule is expressed on the surface of monocytes and some macrophages. Membrane-bound CD-14 is a receptor for lipopolysaccharide (LPS) complexed to LPS-Binding-Protein (LBP). The concentration of its soluble form is altered under certain pathological conditions. There is evidence for an important role of sCD-14 with polytrauma, sepsis, burnings and inflammations.

During septic conditions and acute infections it seems to be a prognostic marker and is therefore of value in monitoring these patients.

IBL offers an ELISA for quantitative determination of soluble CD-14 in human serum, -plasma, cell-culture supernatants and other biological fluids.

Assay features: 12x8 determinations (microtiter strips),  
precoated with a specific monoclonal antibody,  
2x1 hour incubation,  
standard range: 3 - 96 ng/ml  
detection limit: 1 ng/ml  
CV: intra- and interassay < 8%

For more information call or fax

GESELLSCHAFT FÜR IMMUNCHEMIE UND -BIOLOGIE MBH  
OSTERSTRASSE 86 · D-2000 HAMBURG 20 · GERMANY · TEL. +40/491 00 61-64 · FAX +40/40 11 98

BIOTECHNOLOGY VOL 10 APRIL 1992

417

# Oligonucleotides with Fluorescent Dyes at Opposite Ends Provide a Quenched Probe System Useful for Detecting PCR Product and Nucleic Acid Hybridization

Kenneth J. Livak, Susan J.A. Flood, Jeffrey Marmaro, William Giusti, and Karin Deetz

Perkin-Elmer, Applied Biosystems Division, Foster City, California 94404

The 5' nuclease PCR assay detects the accumulation of specific PCR product by hybridization and cleavage of a double-labeled fluorogenic probe during the amplification reaction. The probe is an oligonucleotide with both a reporter fluorescent dye and a quencher dye attached. An increase in reporter fluorescence intensity indicates that the probe has hybridized to the target PCR product and has been cleaved by the 5'→3' nucleolytic activity of *Taq* DNA polymerase. In this study, probes with the quencher dye attached to an internal nucleotide were compared with probes with the quencher dye attached to the 3'-end nucleotide. In all cases, the reporter dye was attached to the 5' end. All intact probes showed quenching of the reporter fluorescence. In general, probes with the quencher dye attached to the 3'-end nucleotide exhibited a larger signal in the 5' nuclease PCR assay than the internally labeled probes. It is proposed that the larger signal is caused by increased likelihood of cleavage by *Taq* DNA polymerase when the probe is hybridized to a template strand during PCR. Probes with the quencher dye attached to the 3'-end nucleotide also exhibited an increase in reporter fluorescence intensity when hybridized to a complementary strand. Thus, oligonucleotides with reporter and quencher dyes attached at opposite ends can be used as homogeneous hybridization probes.

A homogeneous assay for detecting the accumulation of specific PCR product that uses a double-labeled fluorogenic probe was described by Lee et al.<sup>(1)</sup> The assay exploits the 5'→3' nucleolytic activity of *Taq* DNA polymerase<sup>(2,3)</sup> and is diagramed in Figure 1. The fluorogenic probe consists of an oligonucleotide with a reporter fluorescent dye, such as a fluorescein, attached to the 5' end; and a quencher dye, such as a rhodamine, attached internally. When the fluorescein is excited by irradiation, its fluorescent emission will be quenched if the rhodamine is close enough to be excited through the process of fluorescence energy transfer (FET).<sup>(4,5)</sup> During PCR, if the probe is hybridized to a template strand, *Taq* DNA polymerase will cleave the probe because of its inherent 5'→3' nucleolytic activity. If the cleavage occurs between the fluorescein and rhodamine dyes, it causes an increase in fluorescein fluorescence intensity because the fluorescein is no longer quenched. The increase in fluorescein fluorescence intensity indicates that the probe-specific PCR product has been generated. Thus, FET between a reporter dye and a quencher dye is critical to the performance of the probe in the 5' nuclease PCR assay.

Quenching is completely dependent on the physical proximity of the two dyes.<sup>(6)</sup> Because of this, it has been assumed that the quencher dye must be attached near the 5' end. Surprisingly, we have found that attaching a rhodamine dye at the 3' end of a probe still provides adequate quenching for the probe to perform in the 5' nuclease

PCR assay. Furthermore, cleavage of this type of probe is not required to achieve some reduction in quenching. Oligonucleotides with a reporter dye on the 5' end and a quencher dye on the 3' end exhibit a much higher reporter fluorescence when double-stranded as compared with single-stranded. This should make it possible to use this type of double-labeled probe for homogeneous detection of nucleic acid hybridization.

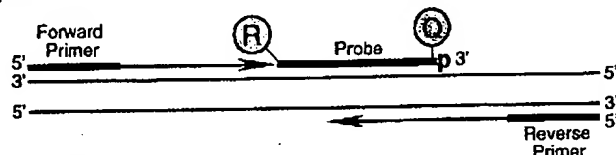
## MATERIALS AND METHODS

### Oligonucleotides

Table 1 shows the nucleotide sequence of the oligonucleotides used in this study. Linker arm nucleotide (LAN) phosphoramidite was obtained from Glen Research. The standard DNA phosphoramidites, 6-carboxyfluorescein (6-FAM) phosphoramidite, 6-carboxy-*tert*-butylmethylrhodamine succinimidyl ester (TAMRA NHS ester), and Phosphalink for attaching a 3'-blocking phosphate, were obtained from Perkin-Elmer, Applied Biosystems Division. Oligonucleotide synthesis was performed using an ABI model 394 DNA synthesizer (Applied Biosystems). Primer and complement oligonucleotides were purified using Oligo Purification Cartridges (Applied Biosystems). Double-labeled probes were synthesized with 6-FAM-labeled phosphoramidite at the 5' end, LAN replacing one of the T's in the sequence, and Phosphalink at the 3' end. Following deprotection and ethanol precipitation, TAMRA NHS ester was coupled to the LAN-containing oligonucleotide in 250

# Research

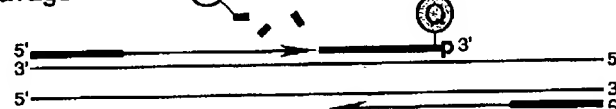
## Polymerization



## Strand displacement



## Cleavage



## Polymerization completed

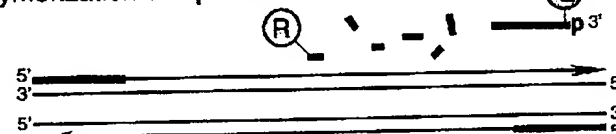


**FIGURE 1** Diagram of 5' nuclease assay. Stepwise representation of the 5' → 3' nucleolytic activity of *Taq* DNA polymerase acting on a fluorogenic probe during one extension phase of PCR.

mm Na-bicarbonate buffer (pH 9.0) at room temperature. Unreacted dye was removed by passage over a PD-10 Sephadex column. Finally, the double-labeled probe was purified by preparative high-performance liquid chromatography (HPLC) using an Aquapore C<sub>8</sub> 220×4.6-mm column with 7-μm particle size. The column was developed with a 24-min linear gradient of 8–20% acetonitrile in 0.1 M TEAA (triethylamine acetate). Probes are named by designating the sequence from Table 1 and the position of the LAN-TAMRA moiety. For example, probe A1-7 has sequence A1 with LAN-TAMRA at nucleotide position 7 from the 5' end.

### PCR Systems

All PCR amplifications were performed in the Perkin-Elmer GeneAmp PCR System 9600 using 50-μl reactions that contained 10 mM Tris-HCl (pH 8.3), 50 mM KCl, 200 μM dATP, 200 μM dCTP, 200 μM dGTP, 400 μM dUTP, 0.5 unit of AmpErase uracil N-glycosylase (Perkin-Elmer), and 1.25 unit of AmpliTaq DNA polymerase (Perkin-Elmer). A 295-bp segment from exon 3 of the human β-actin

gene (nucleotides 2141–2435 in the sequence of Nakajima-Iijima et al.)<sup>(7)</sup> was amplified using primers AFP and ARP (Table 1), which are modified slightly from those of du Breuil et al.<sup>(8)</sup> Actin amplification reactions contained 4 mM MgCl<sub>2</sub>, 20 ng of human genomic DNA, 50 nM A1 or A3 probe, and 300 nM each

primer. The thermal regimen was 50°C (2 min), 95°C (10 min), 40 cycles of 95°C (20 sec), 60°C (1 min), and hold at 72°C. A 515-bp segment was amplified from a plasmid that consists of a segment of λ DNA (nucleotides 32,220–32,747) inserted in the *Sma*I site of vector pUC119. These reactions contained 3.5 mM MgCl<sub>2</sub>, 1 ng of plasmid DNA, 50 nM P2 or P5 probe, 200 nM primer F119, and 200 nM primer R119. The thermal regimen was 50°C (2 min), 95°C (10 min), 25 cycles of 95°C (20 sec), 57°C (1 min), and hold at 72°C.

### Fluorescence Detection

For each amplification reaction, a 40-μl aliquot of a sample was transferred to an individual well of a white, 96-well microtiter plate (Perkin-Elmer). Fluorescence was measured on the Perkin-Elmer TaqMan LS-50B System, which consists of a luminescence spectrometer with plate reader assembly, a 485-nm excitation filter, and a 515-nm emission filter. Excitation was at 488 nm using a 5-nm slit width. Emission was measured at 518 nm for 6-FAM (the reporter or R value) and 582 nm for TAMRA (the quencher or Q value) using a 10-nm slit width. To determine the increase in reporter emission that is caused by cleavage of the probe during PCR, three normalizations are applied to the raw emission data. First, emission intensity of a buffer blank is subtracted for each wavelength. Second, emission intensity of the reporter is

**TABLE 1** Sequences of Oligonucleotides

Name	Type	Sequence
F119	primer	ACCCACAGGAAGTGCACCACTC
R119	primer	ATGTCGCGTTCCGGCTGACGTTCTGC
P2	probe	TCGCATTACTGATCGTGCACCAAGT <sub>p</sub>
P2C	complement	GTACTGGTTGGCAACGATCAGTAATGCGATG
P5	probe	CGGAATTGCTGGTATCTATGACAAGGAT <sub>p</sub>
P5C	complement	TTCATCCTTGTCATAGATACCAGCAATCCG
AFP	primer	TCACCCACACTGTGCCCATCTACGA
ARP	primer	CAGCGGAACCGCTCATTGCCAATGG
A1	probe	ATGCCCTCCCCCATGCCATCCTGCGT <sub>p</sub>
A1C	complement	AGACGCAGGATGGCATGGGGGAGGGCATAC
A3	probe	CGCCCTGGACTTCGAGCAAGAGAT <sub>p</sub>
A3C	complement	CCATCTCTTGCTCGAAGTCCAGGGCGAC

For each oligonucleotide used in this study, the nucleic acid sequence is given, written in the 5' → 3' direction. There are three types of oligonucleotides: PCR primer, fluorogenic probe used in the 5' nuclease assay, and complement used to hybridize to the corresponding probe. For the probes, the underlined base indicates a position where LAN with TAMRA attached was substituted for a T. (p) The presence of a 3' phosphate on each probe.



A1-2 RAQGCCCTCCCCCATGCCATCCTGCGTp  
 A1-7 RATGCCCTCCCCCATGCCATCCTGCGTp  
 A1-14 RATGCCCTCCCCCAQGCCATCCTGCGTp  
 A1-19 RATGCCCTCCCCCATGCCAQCCTGCGTp  
 A1-22 RATGCCCTCCCCCATGCCATCCQCGTp  
 A1-26 RATGCCCTCCCCCATGCCATCCTGCGQp

Probe	518 nm		582 nm		RQ <sup>-</sup>	RQ <sup>+</sup>	$\Delta$ RQ
	no temp.	+ temp.	no temp.	+ temp.			
A1-2	25.5 $\pm$ 2.1	32.7 $\pm$ 1.9	38.2 $\pm$ 3.0	38.2 $\pm$ 2.0	0.67 $\pm$ 0.01	0.86 $\pm$ 0.06	0.19 $\pm$ 0.06
A1-7	53.5 $\pm$ 4.3	395.1 $\pm$ 21.4	108.5 $\pm$ 6.3	110.3 $\pm$ 5.3	0.49 $\pm$ 0.03	3.58 $\pm$ 0.17	3.09 $\pm$ 0.18
A1-14	127.0 $\pm$ 4.9	403.5 $\pm$ 19.1	108.7 $\pm$ 5.3	93.1 $\pm$ 6.3	1.16 $\pm$ 0.02	4.34 $\pm$ 0.15	3.18 $\pm$ 0.15
A1-19	187.5 $\pm$ 17.9	422.7 $\pm$ 7.7	70.3 $\pm$ 7.4	73.0 $\pm$ 2.8	2.67 $\pm$ 0.05	5.80 $\pm$ 0.15	3.13 $\pm$ 0.16
A1-22	224.6 $\pm$ 9.4	482.2 $\pm$ 43.6	100.0 $\pm$ 4.0	96.2 $\pm$ 9.6	2.25 $\pm$ 0.03	5.02 $\pm$ 0.11	2.77 $\pm$ 0.12
A1-26	160.2 $\pm$ 8.9	454.1 $\pm$ 18.4	93.1 $\pm$ 5.4	90.7 $\pm$ 3.2	1.72 $\pm$ 0.02	5.01 $\pm$ 0.08	3.29 $\pm$ 0.08

**FIGURE 2** Results of 5' nuclease assay comparing  $\beta$ -actin probes with TAMRA at different nucleotide positions. As described in Materials and Methods, PCR amplifications containing the indicated probes were performed, and the fluorescence emission was measured at 518 and 582 nm. Reported values are the average  $\pm$  1 S.D. for six reactions run without added template (no temp.) and six reactions run with template (+temp.). The RQ ratio was calculated for each individual reaction and averaged to give the reported RQ<sup>-</sup> and RQ<sup>+</sup> values.

divided by the emission intensity of the quencher to give an RQ ratio for each reaction tube. This normalizes for well-to-well variations in probe concentration and fluorescence measurement. Finally,  $\Delta$ RQ is calculated by subtracting the RQ value of the no-template control (RQ<sup>-</sup>) from the RQ value for the complete reaction including template (RQ<sup>+</sup>).

## RESULTS

A series of probes with increasing distances between the fluorescein reporter and rhodamine quencher were tested to investigate the minimum and maximum spacing that would give an acceptable performance in the 5' nuclease PCR assay. These probes hybridize to a target

sequence in the human  $\beta$ -actin gene. Figure 2 shows the results of an experiment in which these probes were included in PCR that amplified a segment of the  $\beta$ -actin gene containing the target sequence. Performance in the 5' nuclease PCR assay is monitored by the magnitude of  $\Delta$ RQ, which is a measure of the increase in reporter fluorescence caused by PCR amplification of the probe target. Probe A1-2 has a  $\Delta$ RQ value that is close to zero, indicating that the probe was not cleaved appreciably during the amplification reaction. This suggests that with the quencher dye on the second nucleotide from the 5' end, there is insufficient room for *Taq* polymerase to cleave efficiently between the reporter and quencher. The other five probes exhibited comparable  $\Delta$ RQ values that are

clearly different from zero. Thus, all five probes are being cleaved during PCR amplification resulting in a similar increase in reporter fluorescence. It should be noted that complete digestion of a probe produces a much larger increase in reporter fluorescence than that observed in Figure 2 (data not shown). Thus, even in reactions where amplification occurs, the majority of probe molecules remain uncleaved. It is mainly for this reason that the fluorescence intensity of the quencher dye TAMRA changes little with amplification of the target. This is what allows us to use the 582-nm fluorescence reading as a normalization factor.

The magnitude of RQ<sup>-</sup> depends mainly on the quenching efficiency inherent in the specific structure of the probe and the purity of the oligonucleotide. Thus, the larger RQ<sup>-</sup> values indicate that probes A1-14, A1-19, A1-22, and A1-26 probably have reduced quenching as compared with A1-7. Still, the degree of quenching is sufficient to detect a highly significant increase in reporter fluorescence when each of these probes is cleaved during PCR.

To further investigate the ability of TAMRA on the 3' end to quench 6-FAM on the 5' end, three additional pairs of probes were tested in the 5' nuclease PCR assay. For each pair, one probe has TAMRA attached to an internal nucleotide and the other has TAMRA attached to the 3' end nucleotide. The results are shown in Table 2. For all three sets, the probe with the 3' quencher exhibits a  $\Delta$ RQ value that is considerably higher than for the probe with the internal quencher. The RQ<sup>-</sup> values suggest that differences in quenching are not as great as those observed with some of the A1 probes. These results demonstrate that a quencher dye on the 3' end of an oligonucleotide can quench efficiently the

**TABLE 2** Results of 5' Nuclease Assay Comparing Probes with TAMRA Attached to an Internal or 3'-terminal Nucleotide

Probe	518 nm		582 nm		RQ <sup>-</sup>	RQ <sup>+</sup>	$\Delta$ RQ
	no temp.	+ temp.	no temp.	+ temp.			
A3-6	54.6 $\pm$ 3.2	84.8 $\pm$ 3.7	116.2 $\pm$ 6.4	115.6 $\pm$ 2.5	0.47 $\pm$ 0.02	0.73 $\pm$ 0.03	0.26 $\pm$ 0.04
A3-24	72.1 $\pm$ 2.9	236.5 $\pm$ 11.1	84.2 $\pm$ 4.0	90.2 $\pm$ 3.8	0.86 $\pm$ 0.02	2.62 $\pm$ 0.05	1.76 $\pm$ 0.05
P2-7	82.8 $\pm$ 4.4	384.0 $\pm$ 34.1	105.1 $\pm$ 6.4	120.4 $\pm$ 10.2	0.79 $\pm$ 0.02	3.19 $\pm$ 0.16	2.40 $\pm$ 0.16
P2-27	113.4 $\pm$ 6.6	555.4 $\pm$ 14.1	140.7 $\pm$ 8.5	118.7 $\pm$ 4.8	0.81 $\pm$ 0.01	4.68 $\pm$ 0.10	3.88 $\pm$ 0.10
P5-10	77.5 $\pm$ 6.5	244.4 $\pm$ 15.9	86.7 $\pm$ 4.3	95.8 $\pm$ 6.7	0.89 $\pm$ 0.05	2.55 $\pm$ 0.06	1.66 $\pm$ 0.08
P5-28	64.0 $\pm$ 5.2	333.6 $\pm$ 12.1	100.6 $\pm$ 6.1	94.7 $\pm$ 6.3	0.63 $\pm$ 0.02	3.53 $\pm$ 0.12	2.89 $\pm$ 0.13

Reactions containing the indicated probes and calculations were performed as described in Material and Methods and in the legend to Fig. 2.

## Research

fluorescence of a reporter dye on the 5' end. The degree of quenching is sufficient for this type of oligonucleotide to be used as a probe in the 5' nuclease PCR assay.

To test the hypothesis that quenching by a 3' TAMRA depends on the flexibility of the oligonucleotide, fluorescence was measured for probes in the single-stranded and double-stranded states. Table 3 reports the fluorescence observed at 518 and 582 nm. The relative degree of quenching is assessed by calculating the RQ ratio. For probes with TAMRA 6–10 nucleotides from the 5' end, there is little difference in the RQ values when comparing single-stranded with double-stranded oligonucleotides. The results for probes with TAMRA at the 3' end are much different. For these probes, hybridization to a complementary strand causes a dramatic increase in RQ. We propose that this loss of quenching is caused by the rigid structure of double-stranded DNA, which prevents the 5' and 3' ends from being in proximity.

When TAMRA is placed toward the 3' end, there is a marked  $Mg^{2+}$  effect on quenching. Figure 3 shows a plot of observed RQ values for the A1 series of probes as a function of  $Mg^{2+}$  concentration. With TAMRA attached near the 5' end (probe A1-2 or A1-7), the RQ value at 0 mM  $Mg^{2+}$  is only slightly higher than RQ at 10 mM  $Mg^{2+}$ . For probes A1-19, A1-22, and A1-26, the RQ values at 0 mM  $Mg^{2+}$  are very high, indicating a much

reduced quenching efficiency. For each of these probes, there is a marked decrease in RQ at 1 mM  $Mg^{2+}$  followed by a gradual decline as the  $Mg^{2+}$  concentration increases to 10 mM. Probe A1-14 shows an intermediate RQ value at 0 mM  $Mg^{2+}$  with a gradual decline at higher  $Mg^{2+}$  concentrations. In a low-salt environment with no  $Mg^{2+}$  present, a single-stranded oligonucleotide would be expected to adopt an extended conformation because of electrostatic repulsion. The binding of  $Mg^{2+}$  ions acts to shield the negative charge of the phosphate backbone so that the oligonucleotide can adopt conformations where the 3' end is close to the 5' end. Therefore, the observed  $Mg^{2+}$  effects support the notion that quenching of a 5' reporter dye by TAMRA at or near the 3' end depends on the flexibility of the oligonucleotide.

### DISCUSSION

The striking finding of this study is that it seems the rhodamine dye TAMRA, placed at any position in an oligonucleotide, can quench the fluorescent emission of a fluorescein (6-FAM) placed at the 5' end. This implies that a single-stranded, double-labeled oligonucleotide must be able to adopt conformations where the TAMRA is close to the 5' end. It should be noted that the decay of 6-FAM in the excited state requires a certain amount of time. Therefore, what

matters for quenching is not the average distance between 6-FAM and TAMRA but, rather, how close TAMRA can get to 6-FAM during the lifetime of the 6-FAM excited state. As long as the decay time of the excited state is relatively long compared with the molecular motions of the oligonucleotide, quenching can occur. Thus, we propose that TAMRA at the 3' end, or any other position, can quench 6-FAM at the 5' end because TAMRA is in proximity to 6-FAM often enough to be able to accept energy transfer from an excited 6-FAM.

Details of the fluorescence measurements remain puzzling. For example, Table 3 shows that hybridization of probes A1-26, A3-24, and P5-28 to their complementary strands not only causes a large increase in 6-FAM fluorescence at 518 nm but also causes a modest increase in TAMRA fluorescence at 582 nm. If TAMRA is being excited by energy transfer from quenched 6-FAM, then loss of quenching attributable to hybridization should cause a decrease in the fluorescence emission of TAMRA. The fact that the fluorescence emission of TAMRA increases indicates that the situation is more complex. For example, we have anecdotal evidence that the bases of the oligonucleotide, especially G, quench the fluorescence of both 6-FAM and TAMRA to some degree. When double-stranded, base-pairing may reduce the ability of the bases to quench. The primary factor causing the quenching of 6-FAM in an intact probe is the TAMRA dye. Evidence for the importance of TAMRA is that 6-FAM fluorescence remains relatively unchanged when probes labeled only with 6-FAM are used in the 5' nuclease PCR assay (data not shown). Secondary effectors of fluorescence, both before and after cleavage of the probe, need to be explored further.

Regardless of the physical mechanism, the relative independence of position and quenching greatly simplifies the design of probes for the 5' nuclease PCR assay. There are three main factors that determine the performance of a double-labeled fluorescent probe in the 5' nuclease PCR assay. The first factor is the degree of quenching observed in the intact probe. This is characterized by the value of  $RQ^{-}$ , which is the ratio of reporter to quencher fluorescent emissions for a no template control PCR. Influences on the value of  $RQ^{-}$  include the particular reporter and quencher

**TABLE 3** Comparison of Fluorescence Emissions of Single-stranded and Double-stranded Fluorogenic Probes

Probe	518 nm		582 nm		RQ	
	ss	ds	ss	ds	ss	ds
A1-7	27.75	68.53	61.08	138.18	0.45	0.50
A1-26	43.31	509.38	53.50	93.86	0.81	5.43
A3-6	16.75	62.88	39.33	165.57	0.43	0.38
A3-24	30.05	578.64	67.72	140.25	0.45	3.21
P2-7	35.02	70.13	54.63	121.09	0.64	0.58
P2-27	39.89	320.47	65.10	61.13	0.61	5.25
P5-10	27.34	144.85	61.95	165.54	0.44	0.87
P5-28	33.65	462.29	72.39	104.61	0.46	4.43

(ss) Single-stranded. The fluorescence emissions at 518 or 582 nm for solutions containing a final concentration of 50 nM indicated probe, 10 mM Tris-HCl (pH 8.3), 50 mM KCl, and 10 mM  $MgCl_2$ . (ds) Double-stranded. The solutions contained, in addition, 100 nM A1C for probes A1-7 and A1-26, 100 nM A3C for probes A3-6 and A3-24, 100 nM P2C for probes P2-7 and P2-27, or 100 nM P5C for probes P5-10 and P5-28. Before the addition of  $MgCl_2$ , 120  $\mu$ l of each sample was heated at 95°C for 5 min. Following the addition of 80  $\mu$ l of 25 mM  $MgCl_2$ , each sample was allowed to cool to room temperature and the fluorescence emissions were measured. Reported values are the average of three determinations.

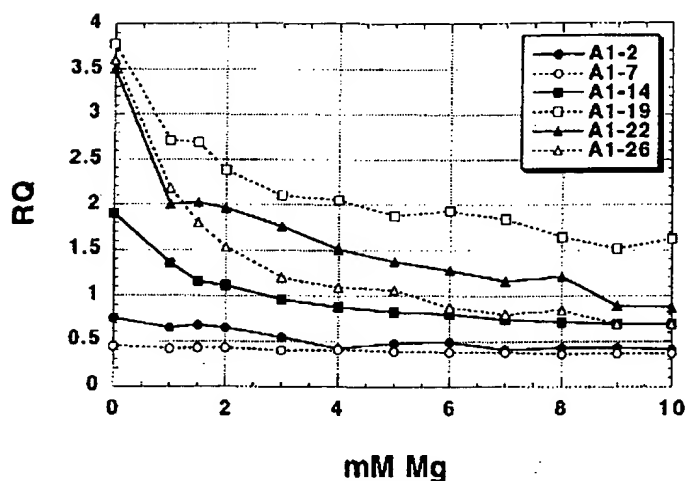


**FIGURE 3** Effect of  $Mg^{2+}$  concentration on RQ ratio for the A1 series of probes. The fluorescence emission intensity at 518 and 582 nm was measured for solutions containing 50 nM probe, 10 mM Tris-HCl (pH 8.3), 50 mM KCl, and varying amounts (0–10 mM) of  $MgCl_2$ . The calculated RQ ratios (518 nm intensity divided by 582 nm intensity) are plotted vs.  $MgCl_2$  concentration (mM Mg). The key (upper right) shows the probes examined.

dyes used, spacing between reporter and quencher dyes, nucleotide sequence context effects, presence of structure or other factors that reduce flexibility of the oligonucleotide, and purity of the probe. The second factor is the efficiency of hybridization, which depends on probe  $T_m$ , presence of secondary structure in probe or template, annealing temperature, and other reaction conditions. The third factor is the efficiency at which *Taq* DNA polymerase cleaves the bound probe between the reporter and quencher dyes. This cleavage is dependent on sequence complementarity between probe and template as shown by the observation that mismatches in the segment between reporter and quencher dyes drastically reduce the cleavage of probe.<sup>(1)</sup>

The rise in  $RQ^-$  values for the A1 series of probes seems to indicate that the degree of quenching is reduced somewhat as the quencher is placed toward the 3' end. The lowest apparent quenching is observed for probe A1-19 (see Fig. 3) rather than for the probe where the TAMRA is at the 3' end (A1-26). This is understandable, as the conformation of the 3' end position would be expected to be less restricted than the conformation of an internal position. In effect, a quencher at the 3' end is freer to adopt conformations close to the 5' reporter dye than is an internally placed quencher. For the other three sets of

probes, the interpretation of  $RQ^-$  values is less clear-cut. The A3 probes show the same trend as A1, with the 3' TAMRA probe having a larger  $RQ^-$  than the internal TAMRA probe. For the P2 pair, both probes have about the same  $RQ^-$  value. For the P5 probes, the  $RQ^-$  for the 3' probe is less than for the internally labeled probe. Another factor that may explain some of the observed variation is that purity affects the  $RQ^-$  value. Although all probes are HPLC purified, a small amount of contamination with unquenched reporter can have a large effect on  $RQ^-$ .

Although there may be a modest effect on degree of quenching, the position of the quencher apparently can have a large effect on the efficiency of probe cleavage. The most drastic effect is observed with probe A1-2, where placement of the TAMRA on the second nucleotide reduces the efficiency of cleavage to almost zero. For the A3, P2, and P5 probes,  $\Delta RQ$  is much greater for the 3' TAMRA probes as compared with the internal TAMRA probes. This is explained most easily by assuming that probes with TAMRA at the 3' end are more likely to be cleaved between reporter and quencher than are probes with TAMRA attached internally. For the A1 probes, the cleavage efficiency of probe A1-7 must already be quite high, as  $\Delta RQ$  does not increase when the quencher is placed closer to the 3' end. This illus-

trates the importance of being able to use probes with a quencher on the 3' end in the 5' nuclease PCR assay. In this assay, an increase in the intensity of reporter fluorescence is observed only when the probe is cleaved between the reporter and quencher dyes. By placing the reporter and quencher dyes on the opposite ends of an oligonucleotide probe, any cleavage that occurs will be detected. When the quencher is attached to an internal nucleotide, sometimes the probe works well (A1-7) and other times not so well (A3-6). The relatively poor performance of probe A3-6 presumably means the probe is being cleaved 3' to the quencher rather than between the reporter and quencher. Therefore, the best chance of having a probe that reliably detects accumulation of PCR product in the 5' nuclease PCR assay is to use a probe with the reporter and quencher dyes on opposite ends.

Placing the quencher dye on the 3' end may also provide a slight benefit in terms of hybridization efficiency. The presence of a quencher attached to an internal nucleotide might be expected to disrupt base-pairing and reduce the  $T_m$  of a probe. In fact, a 2°C–3°C reduction in  $T_m$  has been observed for two probes with internally attached TAMRAs.<sup>(9)</sup> This disruptive effect would be minimized by placing the quencher at the 3' end. Thus, probes with 3' quenchers might exhibit slightly higher hybridization efficiencies than probes with internal quenchers.

The combination of increased cleavage and hybridization efficiencies means that probes with 3' quenchers probably will be more tolerant of mismatches between probe and target as compared with internally labeled probes. This tolerance of mismatches can be advantageous, as when trying to use a single probe to detect PCR-amplified products from samples of different species. Also, it means that cleavage of probe during PCR is less sensitive to alterations in annealing temperature or other reaction conditions. The one application where tolerance of mismatches may be a disadvantage is for allelic discrimination. Lee et al.<sup>(11)</sup> demonstrated that allele-specific probes were cleaved between reporter and quencher only when hybridized to a perfectly complementary target. This allowed them to distinguish the normal human cystic fibrosis allele from the  $\Delta F508$  mutant. Their probes had TAMRA attached to the seventh nucleotide from

## Research

the 5' end and were designed so that any mismatches were between the reporter and quencher. Increasing the distance between reporter and quencher would lessen the disruptive effect of mismatches and allow cleavage of the probe on the incorrect target. Thus, probes with a quencher attached to an internal nucleotide may still be useful for allelic discrimination.

In this study loss of quenching upon hybridization was used to show that quenching by a 3' TAMRA is dependent on the flexibility of a single-stranded oligonucleotide. The increase in reporter fluorescence intensity, though, could also be used to determine whether hybridization has occurred or not. Thus, oligonucleotides with reporter and quencher dyes attached at opposite ends should also be useful as hybridization probes. The ability to detect hybridization in real time means that these probes could be used to measure hybridization kinetics. Also, this type of probe could be used to develop homogeneous hybridization assays for diagnostics or other applications. Bagwell et al.<sup>(10)</sup> describe just this type of homogeneous assay where hybridization of a probe causes an increase in fluorescence caused by a loss of quenching. However, they utilized a complex probe design that requires adding nucleotides to both ends of the probe sequence to form two imperfect hairpins. The results presented here demonstrate that the simple addition of a reporter dye to one end of an oligonucleotide and a quencher dye to the other end generates a fluorogenic probe that can detect hybridization or PCR amplification.

### ACKNOWLEDGMENTS

We acknowledge Lincoln McBride of Perkin-Elmer for his support and encouragement on this project and Mitch Winnik of the University of Toronto for helpful discussions on time-resolved fluorescence.

### REFERENCES

1. Lee, L.G., C.R. Connell, and W. Bloch. 1993. Allelic discrimination by nick-translation PCR with fluorogenic probes. *Nucleic Acids Res.* **21**: 3761-3766.
2. Holland, P.M., R.D. Abramson, R. Watson, and D.H. Gelfand. 1991. Detection of specific polymerase chain reaction prod-

- uct by utilizing the 5' to 3' exonuclease activity of *Thermus aquaticus* DNA polymerase. *Proc. Natl. Acad. Sci.* **88**: 7276-7280.
3. Lyamichev, V., M.A.D. Brow, and J.E. Dahlberg. 1993. Structure-specific endonucleolytic cleavage of nucleic acids by eubacterial DNA polymerases. *Science* **260**: 778-783.
4. Förster, V.Th. 1948. Zwischenmolekulare Energiewanderung und Fluoreszenz. *Ann. Phys. (Leipzig)* **2**: 55-75.
5. Lakowicz, J.R. 1983. Energy transfer. In *Principles of fluorescent spectroscopy*, pp. 303-339. Plenum Press, New York, NY.
6. Stryer, L. and R.P. Haugland. 1967. Energy transfer: A spectroscopic ruler. *Proc. Natl. Acad. Sci.* **58**: 719-726.
7. Nakajima-Iijima, S., H. Hamada, P. Reddy, and T. Kakunaga. 1985. Molecular structure of the human cytoplasmic beta-actin gene: Inter-species homology of sequences in the introns. *Proc. Natl. Acad. Sci.* **82**: 6133-6137.
8. du Breuil, R.M., J.M. Patel, and B.V. Mendelow. 1993. Quantitation of  $\beta$ -actin-specific mRNA transcripts using xeno-competitive PCR. *PCR Methods Applic.* **3**: 57-59.
9. Livak, K.J. (unpubl.).
10. Bagwell, C.B., M.E. Munson, R.L. Christensen, and E.J. Lovett. 1994. A new homogeneous assay system for specific nucleic acid sequences: Poly-dA and poly-A detection. *Nucleic Acids Res.* **22**: 2424-2425.

Received December 20, 1994; accepted in revised form March 6, 1995.

THIS MATERIAL MAY BE PROTECTED  
BY COPYRIGHT LAW (17 U.S. CODE)

## GENOME METHODS

## Real Time Quantitative PCR

Christian A. Heid,<sup>1</sup> Junko Stevens,<sup>2</sup> Kenneth J. Livak,<sup>2</sup> and  
P. Mickey Williams<sup>1,3</sup>

<sup>1</sup>BioAnalytical Technology Department, Genentech, Inc., South San Francisco, California 94080;

<sup>2</sup>Applied BioSystems Division of Perkin Elmer Corp., Foster City, California 94404

We have developed a novel "real time" quantitative PCR method. The method measures PCR product accumulation through a dual-labeled fluorogenic probe (i.e., TaqMan Probe). This method provides very accurate and reproducible quantitation of gene copies. Unlike other quantitative PCR methods, real-time PCR does not require post-PCR sample handling, preventing potential PCR product carry-over contamination and resulting in much faster and higher throughput assays. The real-time PCR method has a very large dynamic range of starting target molecule determination (at least five orders of magnitude). Real-time quantitative PCR is extremely accurate and less labor-intensive than current quantitative PCR methods.

Quantitative nucleic acid sequence analysis has had an important role in many fields of biological research. Measurement of gene expression (RNA) has been used extensively in monitoring biological responses to various stimuli (Tan et al. 1994; Huang et al. 1995a,b; Prud'homme et al. 1995). Quantitative gene analysis (DNA) has been used to determine the genomic quantity of a particular gene, as in the case of the human *HER2* gene, which is amplified in ~30% of breast tumors (Slamon et al. 1987). Gene and genome quantitation (DNA and RNA) also have been used for analysis of human immunodeficiency virus (HIV) burden demonstrating changes in the levels of virus throughout the different phases of the disease (Connor et al. 1993; Platack et al. 1993b; Furtado et al. 1995).

Many methods have been described for the quantitative analysis of nucleic acid sequences (both for RNA and DNA; Southern 1975; Sharp et al. 1980; Thomas 1980). Recently, PCR has proven to be a powerful tool for quantitative nucleic acid analysis. PCR and reverse transcriptase (RT)-PCR have permitted the analysis of minimal starting quantities of nucleic acid (as little as one cell equivalent). This has made possible many experiments that could not have been performed with traditional methods. Although PCR has provided a powerful tool, it is imperative

that it be used properly for quantitation (Rasmussen 1995). Many early reports of quantitative PCR and RT-PCR described quantitation of the PCR product but did not measure the initial target sequence quantity. It is essential to design proper controls for the quantitation of the initial target sequences (Perre 1992; Clementi et al. 1993).

Researchers have developed several methods of quantitative PCR and RT-PCR. One approach measures PCR product quantity in the log phase of the reaction before the plateau (Kellogg et al. 1990; Pang et al. 1990). This method requires that each sample has equal input amounts of nucleic acid and that each sample under analysis amplifies with identical efficiency up to the point of quantitative analysis. A gene sequence (contained in all samples at relatively constant quantities, such as  $\beta$ -actin) can be used for sample amplification efficiency normalization. Using conventional methods of PCR detection and quantitation (gel electrophoresis or plate capture hybridization), it is extremely laborious to assure that all samples are analyzed during the log phase of the reaction (for both the target gene and the normalization gene). Another method, quantitative competitive (QC)-PCR, has been developed and is used widely for PCR quantitation. QC-PCR relies on the inclusion of an internal control competitor in each reaction (Becker-Andre 1991; Platack et al. 1993a,b). The efficiency of each reaction is normalized to the internal competitor. A known amount of internal competitor can be

<sup>3</sup>Corresponding author.

## REAL TIME QUANTITATIVE PCR

## RESULTS

## PCR Product Detection in Real Time

added to each sample. To obtain relative quantitation, the unknown target PCR product is compared with the known competitor PCR product. Success of a quantitative competitive PCR assay relies on developing an internal control that amplifies with the same efficiency as the target molecule. The design of the competitor and the validation of amplification efficiencies require a dedicated effort. However, because QC-PCR does not require that PCR products be analyzed during the log phase of the amplification, it is the easier of the two methods to use.

Several detection systems are used for quantitative PCR and RT-PCR analysis: (1) agarose gels, (2) fluorescent labeling of PCR products and detection with laser-induced fluorescence using capillary electrophoresis (Fusco et al. 1995; Williams et al. 1996) or acrylamide gels, and (3) plate capture and sandwich probe hybridization (Mulder et al. 1994). Although these methods proved successful, each method requires post-PCR manipulations that add time to the analysis and may lead to laboratory contamination. The sample throughput of these methods is limited (with the exception of the plate capture approach), and, therefore, these methods are not well suited for uses demanding high sample throughput (i.e., screening of large numbers of biomolecules or analyzing samples for diagnostics or clinical trials).

Here we report the development of a novel assay for quantitative DNA analysis. The assay is based on the use of the 5' nuclease assay first described by Holland et al. (1991). The method uses the 5' nuclease activity of *Taq* polymerase to cleave a nonextendible hybridization probe during the extension phase of PCR. The approach uses dual-labeled fluorogenic hybridization probes (Lee et al. 1993; Bassler et al. 1995; Livak et al. 1995a,b). One fluorescent dye serves as a reporter (FAM (i.e., 6-carboxyfluorescein)) and its emission spectra is quenched by the second fluorescent dye, TAMRA (i.e., 6-carboxy-tetramethylrhodamine). The nuclease degradation of the hybridization probe releases the quenching of the FAM fluorescent emission, resulting in an increase in peak fluorescent emission at 518 nm. The use of a sequence detector (ABI Prism) allows measurement of fluorescent spectra of all 96 wells of the thermal cycler continuously during the PCR amplification. Therefore, the reactions are monitored in real time. The output data is described and quantitative analysis of input target DNA sequences is discussed below.

The goal was to develop a high-throughput, sensitive, and accurate gene quantitation assay for use in monitoring lipid mediated therapeutic gene delivery. A plasmid encoding human factor VIII gene sequence, p18TM (see Methods), was used as a model therapeutic gene. The assay uses fluorescent Taqman methodology and an instrument capable of measuring fluorescence in real time (ABI Prism 7700 Sequence Detector). The Taqman reaction requires a hybridization probe labeled with two different fluorescent dyes. One dye is a reporter dye (FAM), the other is a quenching dye (TAMRA). When the probe is intact, fluorescent energy transfer occurs and the reporter dye fluorescent emission is absorbed by the quenching dye (TAMRA). During the extension phase of the PCR cycle, the fluorescent hybridization probe is cleaved by the 5'-3' nucleolytic activity of the DNA polymerase. On cleavage of the probe, the reporter dye emission is no longer transferred efficiently to the quenching dye, resulting in an increase of the reporter dye fluorescent emission spectra. PCR primers and probes were designed for the human factor VIII sequence and human  $\beta$ -actin gene (as described in Methods). Optimization reactions were performed to choose the appropriate probe and magnesium concentrations yielding the highest intensity of reporter fluorescent signal without sacrificing specificity. The instrument uses a charge-coupled device (i.e., CCD camera) for measuring the fluorescent emission spectra from 500 to 650 nm. Each PCR tube was monitored sequentially for 25 msec with continuous monitoring throughout the amplification. Each tube was re-examined every 8.5 sec. Computer software was designed to examine the fluorescent intensity of both the reporter dye (FAM) and the quenching dye (TAMRA). The fluorescent intensity of the quenching dye, TAMRA, changes very little over the course of the PCR amplification (data not shown). Therefore, the intensity of TAMRA dye emission serves as an internal standard with which to normalize the reporter dye (FAM) emission variations. The software calculates a value termed  $\Delta Rn$  (or  $\Delta RQ$ ) using the following equation:  $\Delta Rn = (Rn^t) / (Rn^i)$ , where  $Rn^t$  = emission intensity of reporter/emission intensity of quencher at any given time in a reaction tube, and  $Rn^i$  = emission intensity of re-

## HLID ET AL.

porter/emission intensity of quencher measured prior to PCR amplification in that same reaction tube. For the purpose of quantitation, the last three data points ( $\Delta Rn$ s) collected during the extension step for each PCR cycle were analyzed. The nucleolytic degradation of the hybridization probe occurs during the extension phase of PCR, and, therefore, reporter fluorescent emission increases during this time. The three data points were averaged for each PCR cycle and the mean value for each was plotted in an "amplification plot" shown in Figure 1A. The  $\Delta Rn$  mean value is plotted on the y-axis, and time, represented by cycle number, is plotted on the x-axis. During the early cycles of the PCR amplification, the  $\Delta Rn$

value remains at base line. When sufficient hybridization probe has been cleaved by the *Taq* polymerase nuclease activity, the intensity of reporter fluorescent emission increases. Most PCR amplifications reach a plateau phase of reporter fluorescent emission if the reaction is carried out to high cycle numbers. The amplification plot is examined early in the reaction, at a point that represents the log phase of product accumulation. This is done by assigning an arbitrary threshold that is based on the variability of the base-line data. In Figure 1A, the threshold was set at 10 standard deviations above the mean of base line emission calculated from cycles 1 to 15. Once the threshold is chosen, the point at which

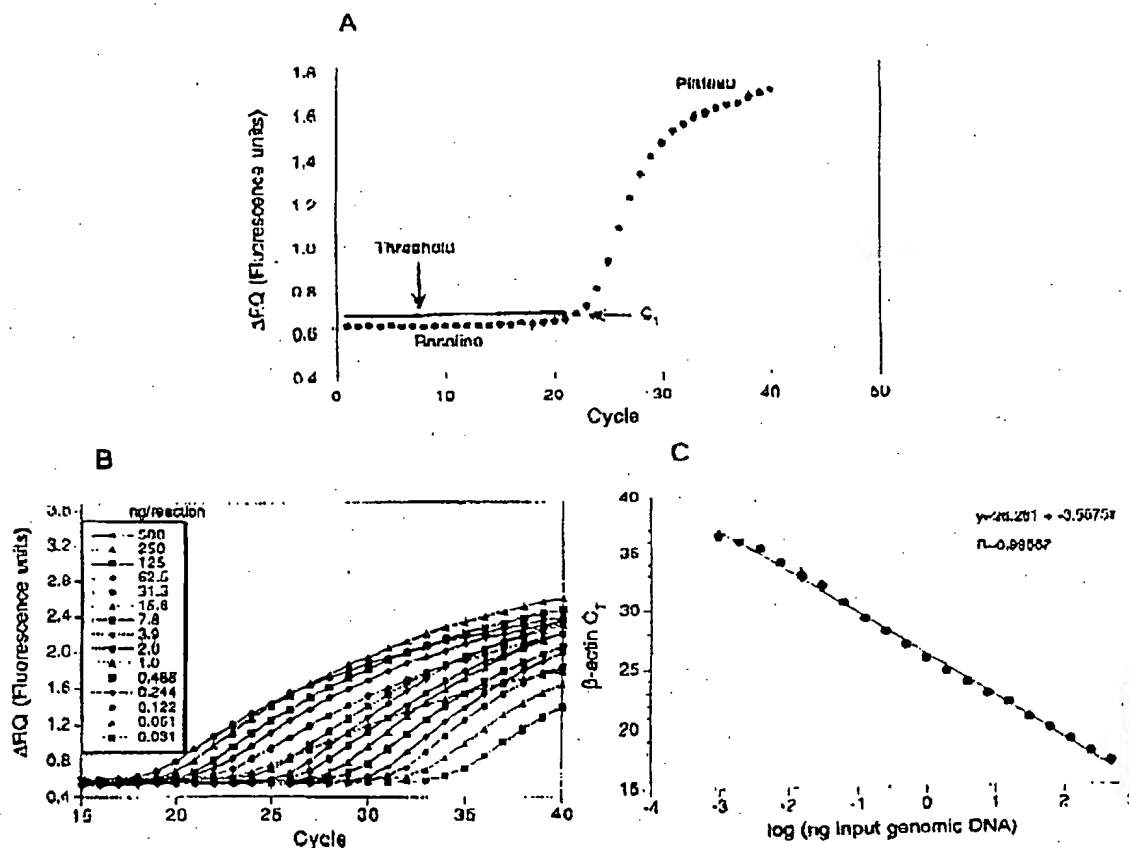


**Figure 1** PCR product detection in real time. (A) The Model 7700 software will construct amplification plots from the extension phase fluorescent emission data collected during the PCR amplification. The standard deviation is determined from the data points collected from the base line of the amplification plot.  $C_t$  values are calculated by determining the point at which the fluorescence exceeds a threshold limit (usually 10 times the standard deviation of the base line). (B) Overlay of amplification plots of serially (1:2) diluted human genomic DNA samples amplified with  $\beta$ -actin primers. (C) Input DNA concentration of the samples plotted versus  $C_t$ . All



## REAL TIME QUANTITATIVE PCR

the amplification plot crosses the threshold is defined as  $C_T$ .  $C_T$  is reported as the cycle number at this point. As will be demonstrated, the  $C_T$  value is predictive of the quantity of input target.

#### $C_T$ Values Provide a Quantitative Measurement of Input Target Sequences

Figure 1B shows amplification plots of 15 different PCR amplifications overlaid. The amplifications were performed on a 1:2 serial dilution of human genomic DNA. The amplified target was human  $\beta$  actin. The amplification plots shift to the right (to higher threshold cycles) as the input target quantity is reduced. This is expected because reactions with fewer starting copies of the target molecule require greater amplification to degrade enough probe to attain the threshold fluorescence. An arbitrary threshold of 10 standard deviations above the base line was used to determine the  $C_T$  values. Figure 1C represents the  $C_T$  values plotted versus the sample dilution value. Each dilution was amplified in triplicate PCR amplifications and plotted as mean values with error bars representing one standard deviation. The  $C_T$  values decrease linearly with increasing target quantity. Thus,  $C_T$  values can be used as a quantitative measurement of the input target number. It should be noted that the amplification plot for the 15.6-ng sample shown in Figure 1B does not reflect the same fluorescent rate of increase exhibited by most of the other samples. The 15.6-ng sample also achieves endpoint plateau at a lower fluorescent value than would be expected based on the input DNA. This phenomenon has been observed occasionally with other samples (data not shown) and may be attributable to late cycle inhibition; this hypothesis is still under investigation. It is important to note that the flattened slope and early plateau do not impact significantly the calculated  $C_T$  value as demonstrated by the fit on the line shown in Figure 1C. All triplicate amplifications resulted in very similar  $C_T$  values—the standard deviation did not exceed 0.5 for any dilution. This experiment contains a >100,000-fold range of input target molecules. Using  $C_T$  values for quantitation permits a much larger assay range than directly using total fluorescent emission intensity for quantitation. The linear range of fluorescent intensity measurement of the ABI Prism 7700 Se-

ments over a very large range of relative starting target quantities.

#### Sample Preparation Validation

Several parameters influence the efficiency of PCR amplification: magnesium and salt concentrations, reaction conditions (i.e., time and temperature), PCR target size and composition, primer sequences, and sample purity. All of the above factors are common to a single PCR assay, except sample to sample purity. In an effort to validate the method of sample preparation for the factor VIII assay, PCR amplification reproducibility and efficiency of 10 replicate sample preparations were examined. After genomic DNA was prepared from the 10 replicate samples, the DNA was quantitated by ultraviolet spectroscopy. Amplifications were performed analyzing  $\beta$ -actin gene content in 100 and 25 ng of total genomic DNA. Each PCR amplification was performed in triplicate. Comparison of  $C_T$  values for each triplicate sample show minimal variation based on standard deviation and coefficient of variance (Table 1). Therefore, each of the triplicate PCR amplifications was highly reproducible, demonstrating that real time PCR using this instrumentation introduces minimal variation into the quantitative PCR analysis. Comparison of the mean  $C_T$  values of the 10 replicate sample preparations also showed minimal variability, indicating that each sample preparation yielded similar results for  $\beta$ -actin gene quantity. The highest  $C_T$  difference between any of the samples was 0.85 and 0.71 for the 100 and 25 ng samples, respectively. Additionally, the amplification of each sample exhibited an equivalent rate of fluorescent emission intensity change per amount of DNA target analyzed as indicated by similar slopes derived from the sample dilutions (Fig. 2). Any sample containing an excess of a PCR inhibitor would exhibit a greater measured  $\beta$ -actin  $C_T$  value for a given quantity of DNA. In addition, the inhibitor would be diluted along with the sample in the dilution analysis (Fig. 2), altering the expected  $C_T$  value change. Each sample amplification yielded a similar result in the analysis, demonstrating that this method of sample preparation is highly reproducible with regard to sample purity.

#### Quantitative Analysis of a Plasmid After

PCR 001 RBR VVJ RC:BT 7007/CN/71



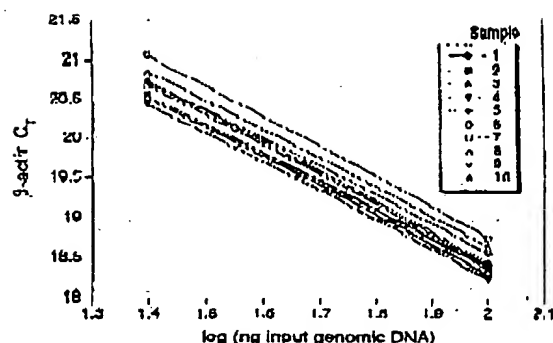
## III ID 1-1 AL

Table 1. Reproducibility of Sample Preparation Method

Sample no.	100 ng				25 ng			
	C <sub>T</sub>	mean	standard deviation	CV	C <sub>T</sub>	mean	standard deviation	CV
1	18.24				20.48			
	18.23				20.55			
	18.33	18.27	0.06	0.32	20.5	20.51	0.03	0.17
2	18.33				20.61			
	18.35				20.59			
	18.44	18.37	0.06	0.32	20.41	20.54	0.11	0.54
3	18.3				20.54			
	18.3				20.6			
	18.42	18.34	0.07	0.36	20.49	20.54	0.06	0.28
4	18.15				20.48			
	18.23				20.44			
	18.32	18.23	0.08	0.46	20.38	20.43	0.05	0.26
5	18.4				20.68			
	18.38				20.87			
	18.46	18.42	0.04	0.23	20.63	20.73	0.13	0.61
6	18.54				21.09			
	18.67				21.04			
	19	18.74	0.24	1.26	21.04	21.06	0.03	0.15
7	18.28				20.67			
	18.36				20.73			
	18.52	18.39	0.12	0.66	20.65	20.68	0.04	0.2
8	18.45				20.98			
	18.7				20.84			
	18.73	18.63	0.16	0.83	20.75	20.86	0.12	0.57
9	18.18				20.46			
	18.34				20.54			
	18.26	18.29	0.1	0.55	20.48	20.51	0.07	0.32
10	18.42				20.79			
	18.57				20.78			
	18.66	18.55	0.12	0.65	20.62	20.73	0.1	0.16
Mean	(1/10)	18.42	0.17	0.90		20.66	0.19	0.94

for containing a partial cDNA for human factor VIII, pF8TM. A series of transfections was set up using a decreasing amount of the plasmid (40, 4, 0.5, and 0.1  $\mu$ g). Twenty-four hours post-transfection, total DNA was purified from each flask of cells.  $\beta$ -Actin gene quantity was chosen as a value for normalization of genomic DNA concentration from each sample. In this experiment,  $\beta$ -actin gene content should remain constant relative to total genomic DNA. Figure 3 shows the result of the  $\beta$ -actin DNA measurement (100 ng total DNA determined by ultraviolet spectroscopy) of each sample. Each sample was analyzed in triplicate and the mean  $\beta$ -actin  $C_T$  values of the triplicates were plotted (error bars represent one standard deviation). The highest difference

between any two sample means was 0.95 C<sub>t</sub>. Ten nanograms of total DNA of each sample were also examined for  $\beta$ -actin. The results again showed that very similar amounts of genomic DNA were present; the maximum mean  $\beta$  actin C<sub>t</sub> value difference was 1.0. As Figure 3 shows, the rate of  $\beta$ -actin C<sub>t</sub> change between the 100 and 10-ng samples was similar (slope values range between 3.56 and -3.45). This verifies again that the method of sample preparation yields samples of identical PCR integrity (i.e., no sample contained an excessive amount of a PCR inhibitor). However, these results indicate that each sample contained slight differences in the actual amount of genomic DNA analyzed. Determination of actual genomic DNA concentration was accomplished



**Figure 2** Sample preparation purity. The replicate samples shown in Table 1 were also amplified in triplicate using 25 ng of each DNA sample. The figure shows the input DNA concentration (100 and 25 ng) vs.  $C_t$ . In the figure, the 100 and 25 ng points for each sample are connected by a line.

by plotting the mean  $\beta$ -actin  $C_t$  value obtained for each 100-ng sample on a  $\beta$ -actin standard curve (shown in Fig. 4C). The actual genomic DNA concentration of each sample,  $a$ , was obtained by extrapolation to the  $x$ -axis.

Figure 1A shows the measured (i.e., non-normalized) quantities of factor VIII plasmid DNA (p8TM) from each of the four transient cell transfections. Each reaction contained 100 ng of total sample DNA (as determined by UV spectroscopy). Each sample was analyzed in triplicate.

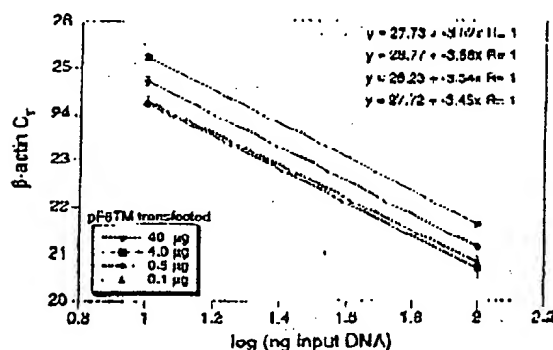


**Figure 3** Analysis of transfected cell DNA quantity and purity. The DNA preparations of the four 293 cell transfections (40, 4, 0.5, and 0.1  $\mu$ g of pF8TM) were analyzed for the  $\beta$ -actin gene. 100 and 10 ng (determined by ultraviolet spectroscopy) of each sample were amplified in triplicate. For each amount of pF8TM that was transfected, the  $\beta$ -actin  $C_T$  values are plotted versus the total input DNA concentration.

### REAL TIME- QUANTITATIVE PCR

PCR amplifications. As shown, pF8TM purified from the 293 cells decreases (mean  $C_i$  values increase) with decreasing amounts of plasmid (transfected). The mean  $C_i$  values obtained for pF8TM in Figure 4A were plotted on a standard curve comprised of serially diluted pF8TM, shown in Figure 4B. The quantity of pF8TM,  $b$ , found in each of the four transfections was determined by extrapolation to the  $x$  axis of the standard curve in Figure 4B. These uncorrected values,  $b$ , for pF8TM were normalized to determine the actual amount of pF8TM found per 100 ng of genomic DNA by using the equation:

$$\frac{b \times 100 \text{ ng}}{a} = \text{actual pFBTM copies per } 100 \text{ ng of genomic DNA}$$

where  $a$  = actual genomic DNA in a sample and  $b$  = pF8TM copies from the standard curve. The normalized quantity of pF8TM per 100 ng of genomic DNA for each of the four transfections is shown in Figure 4J. These results show that the quantity of factor VIII plasmid associated with the 293 cells, 24 hr after transfection, decreases with decreasing plasmid concentration used in the transfection. The quantity of pF8TM associated with 293 cells, after transfection with 40  $\mu$ g of plasmid, was 35 pg per 100 ng genomic DNA. This results in ~520 plasmid copies per cell.

## DISCUSSION

We have described a new method for quantitating gene copy numbers using real-time analysis of PCR amplifications. Real-time PCR is compatible with either of the two PCR (RT-PCR) approaches: (1) quantitative competitive where an internal competitor for each target sequence is used for normalization (data not shown) or (2) quantitative comparative PCR using a normalization gene contained within the sample (i.e.,  $\beta$ -actin) or a "housekeeping" gene for RT-PCR. If equal amounts of nucleic acid are analyzed for each sample and if the amplification efficiency before quantitative analysis is identical for each sample, the internal control (normalization gene or competitor) should give equal signals for all samples.

The real-time PCR method offers several advantages over the other two methods currently employed (see the Introduction). First, the real-time PCR method is performed in a closed-tube system and requires no post-PCR manipulation

HUO ET AL.

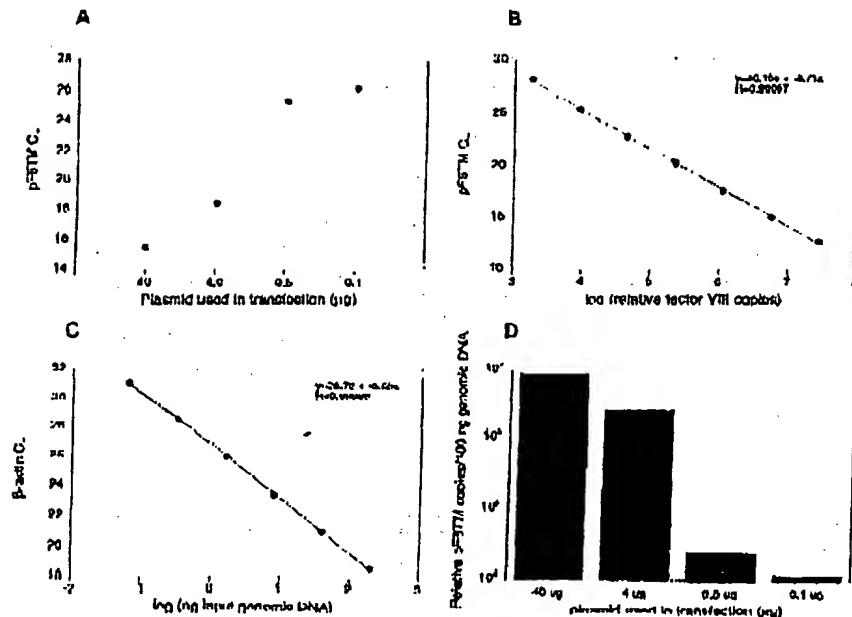


**Figure 4** Quantitative analysis of pF8TM in transfected cells. (A) Amount of plasmid DNA used for the transfection plotted against the mean  $C_t$  value determined for pF8TM remaining 24 hr after transfection. (B,C) Standard curves of pF8TM and  $\beta$ -actin, respectively. pF8TM DNA (B) and genomic DNA (C) were diluted serially 1:5 before amplification with the appropriate primers. The  $\beta$ -actin standard curve was used to normalize the results of A to 100 ng of genomic DNA. (D) The amount of pF8TM present per 100 ng of genomic DNA.

of sample. Therefore, the potential for PCR contamination in the laboratory is reduced because amplified products can be analyzed and disposed of without opening the reaction tubes. Second, this method supports the use of a normalization gene (i.e.,  $\beta$ -actin) for quantitative PCR or house-keeping genes for quantitative RT-PCR controls. Analysis is performed in real time during the log phase of product accumulation. Analysis during log phase permits many different genes (over a wide input target range) to be analyzed simultaneously, without concern of reaching reaction plateau at different cycles. This will make multi-gene analysis assays much easier to develop, because individual internal competitors will not be needed for each gene under analysis. Third, sample throughput will increase dramatically with the new method because there is no post-PCR processing time. Additionally, working in a 96-well format is highly compatible with automation technology.

The real-time PCR method is highly reproducible. Replicate amplifications can be analyzed

for each sample minimizing potential error. The system allows for a very large assay dynamic range (approaching 1,000,000-fold starting target). Using a standard curve for the target of interest, relative copy number values can be determined for any unknown sample. Fluorescent threshold values,  $C_t$ , correlate linearly with relative DNA copy numbers. Real time quantitative RT-PCR methodology (Gibson et al., this issue) has also been developed. Finally, real time quantitative PCR methodology can be used to develop high-throughput screening assays for a variety of applications [quantitative gene expression (RT-PCR), gene copy assays (Her2, HIV, etc.), genotyping (knockout mouse analysis), and immunoprecipitation].

Real-time PCR may also be performed using intercalating dyes (Higuchi et al. 1992) such as ethidium bromide. The fluorogenic probe method offers a major advantage over intercalating dyes—greater specificity (i.e., primer dimers and nonspecific PCR products are not detected).

## METHODS

### Generation of a Plasmid Containing a Partial cDNA for Human Factor VIII

Total RNA was harvested (RNAzol B from Tel Test, Inc., Friendswood, TX) from cells transfected with a factor VIII expression vector, pCIS2.8c251 (Eaton et al. 1986; Gorman et al. 1990). A factor VIII partial cDNA sequence was generated by RT-PCR (Clontech Amp 12, RTM RNA PCR Kit (part N808-0179, PE Applied Biosystems, Foster City, CA)) using the PCR primers F8for and F8rev (primer sequences are shown below). The amplicon was reamplified using modified F8for and F8rev primers (appended with *Hind*III and *Hind*III restriction site sequences at the 5' end) and cloned into pCDM-32 (Promega Corp., Madison, WI). The resulting clone, pF8TM, was used for transient transfection of 293 cells.

### Amplification of Target DNA and Detection of Amplicon Factor VIII Plasmid DNA

(pF8TM) was amplified with the primers F8for 5'-CCGCGTTCGAAGAGCTGACATGTC-3' and F8rev 5'-AAAGCTTCAAGCTGGATGCTGACG-3'. The reaction produced a 422-bp PCR product. The forward primer was designed to recognize a unique sequence found in the 5' untranslated region of the parent pCIS2.8c251 plasmid and therefore does not recognize and amplify the human factor VIII gene. Primers were chosen with the assistance of the computer program Oligo 4.0 (National Biosciences, Inc., Plymouth, MN). The human  $\beta$ -actin gene was amplified with the primers  $\beta$ -actin forward primer 5'-TCACCCACACTGTTGCCATCTACCA-3' and  $\beta$ -actin reverse primer 5'-CAGCGGAACCCGCTCATTTGCCAATGG-3'. The reaction produced a 295-bp PCR product.

Amplification reactions (50  $\mu$ l) contained a DNA sample, 10 $\times$  PCR Buffer II (5  $\mu$ l), 200  $\mu$ M dATP, dCTP, dGTP, and 400  $\mu$ M dTTP, 4 mM MgCl<sub>2</sub>, 1.25 Units AmpliTaq DNA polymerase, 0.5 unit Amperase uracil N-glycosylase (UNG), 50 pmole of each factor VIII primer, and 15 pmole of each  $\beta$ -actin primer. The reactions also contained one of the following detection probes (100 nM each): F8probe 5'-(FAM)AGCTCTTCCACCTGCTTCTTTCTGCTGCCTT(TAMRA)p 3' and  $\beta$ -actin probe 5'-(FAM)ATGCCX(X(TAMRA)CCCCCATGCCATC)p 3' where p indicates phosphorylation and X indicates a linker arm nucleotide. Reaction tubes were MicroAmp Optical Tubes (part number N801 0933, Perkin Elmer) that were frosted (at Perkin Elmer) to prevent light from reflecting. Tube caps were similar to MicroAmp Caps but specially designed to prevent light scattering. All of the PCR consumables were supplied by PE Applied Biosystems (Foster City, CA) except the factor VIII primers, which were synthesized at Genentech, Inc. (South San Francisco, CA). Probes were designed using the Oligo 4.0 software, following guidelines suggested in the Model 7700 Sequence Detector instrument manual. Briefly, probe T<sub>m</sub> should be at least 5°C higher than the annealing temperature used during thermal cycling; primers should not form stable duplexes with the probe.

The thermal cycling conditions included 2 min at 50°C and 10 min at 95°C. Thermal cycling proceeded with

## REAL TIME QUANTITATIVE PCR

reactions were performed in the Model 7700 Sequence Detector (PE Applied Biosystems), which contains a GeneAmp PCR System 9600. Reaction conditions were programmed on a Power Macintosh 7100 (Apple Computer, Santa Clara, CA) linked directly to the Model 7700 Sequence Detector. Analysis of data was also performed on the Macintosh computer. Collection and analysis software was developed at PE Applied Biosystems.

### Transfection of Cells with Factor VIII Construct

Four T175 flasks of 293 cells (ATCC CRL 1573), a human fetal kidney suspension cell line, were grown to 80% confluency and transfected pF8TM. Cells were grown in the following media: 50% HAM'S F12 without GHF, 50% low glucose Dulbecco's modified Eagle medium (DMEM) without glycine with sodium bicarbonate, 10% fetal bovine serum, 2 mM L-glutamine, and 1% penicillin-streptomycin. The media was changed 30 min before the transfection. pF8TM DNA amounts of 40, 4, 0.5, and 0.1  $\mu$ g were added to 1.5 ml of a solution containing 0.125 M CaCl<sub>2</sub> and 1 $\times$  HBPS. The four mixtures were left at room temperature for 10 min and then added dropwise to the cells. The flasks were incubated at 37°C and 5% CO<sub>2</sub> for 24 hr, washed with PBS, and resuspended in PBS. The resuspended cells were divided into aliquots and DNA was extracted immediately using the QIAamp Blood Kit (Qiagen, Chatsworth, CA). DNA was eluted into 200  $\mu$ l of 20 mM Tris-HCl at pH 8.0.

## ACKNOWLEDGMENTS

We thank Genentech's DNA Synthesis Group for primer synthesis and Genentech's Graphics Group for assistance with the figures.

The publication costs of this article were defrayed in part by payment of page charges. This article must therefore be hereby marked "advertisement" in accordance with 18 USC section 1734 solely to indicate this fact.

## REFERENCES

- Bassler, H.A., S.J. Flood, K.J. Livak, J. Marimano, R. Kohn, and C.A. Batt. 1995. Use of a fluorogenic probe in a PCR-based assay for the detection of *Listeria monocytogenes*. *App. Environ. Microbiol.* 61: 3724-3728.
- Becker-Andre, M. 1991. Quantitative evaluation of mRNA levels. *Meth. Mol. Cell. Biol.* 2: 189-201.
- Clement, M., S. Menzo, P. Bagnarelli, A. Manzini, A. Valenza, and P.E. Varaldo. 1993. Quantitative PCR and RT-PCR in virology. [Review]. *PCR Methods Applic.* 2: 191-196.
- Connor, R.J., H. Mohl, Y. Cao, and D.D. Ho. 1993. Increased viral burden and cytopathicity correlate temporally with CD4<sup>+</sup> T-lymphocyte decline and clinical progression in human immunodeficiency virus type 1-infected individuals. *J. Virol.* 67: 1772-1777.
- Eaton, D.L., W.J. Wood, D. Eaton, P.E. Hass, P.

## HFID LI AL

Venar, and C. Gorman. 1986. Construction and characterization of an active factor VIII variant lacking the central one third of the molecule. *Biochemistry* 25: 8343-8347.

Fasco, M.J., C.P. Treanor, S. Spivack, H.L. Pigg, and L.S. Kaminsky. 1995. Quantitative RNA-polymerase chain reaction-DNA analysis by capillary electrophoresis and laser-induced fluorescence. *Anal. Biochem.* 224: 140-147.

Ferre, R. 1992. Quantitative or semi-quantitative PCR: Reality versus myth. *PCR Methods Appl.* 2: 1-9.

Fortado, M.R., L.A. Kingsley, and S.M. Wollinsky. 1995. Changes in the viral mRNA expression pattern correlate with a rapid rate of CD4+ T-cell number decline in human immunodeficiency virus type 1-infected individuals. *J. Virol.* 69: 2092-2100.

Gibson, U.E.M., C.A. Heid, and P.M. Williams. 1996. A novel method for real time quantitative competitive RT-PCR. *Genome Res.* (this issue).

Gorman, C.M., D.R. Gies, and G. McCray. 1990. Transient production of proteins using an adenovirus transformed cell line. *DNA Prot. Engin. Tech.* 2: 3-10.

Higuchi, R., G. Dollinger, P.S. Walsh, and R. Griffith. 1992. Simultaneous amplification and detection of specific DNA sequences. *Biotechnology* 10: 413-417.

Holland, P.M., R.D. Abramson, R. Watson, and D.J. Gelfand. 1991. Detection of specific polymerase chain reaction product by utilizing the 5'-3' exonuclease activity of *Thermus aquaticus* DNA polymerase. *Proc. Natl. Acad. Sci.* 88: 7276-7280.

Huang, S.K., H.Q. Xiao, T.J. Kleine, G. Paciotti, D.G. Marsh, L.M. Lichtenstein, and M.C. Liu. 1995a. IL-13 expression at the sites of allergen challenge in patients with asthma. *J. Immun.* 155: 2688-2694.

Huang, S.K., M. Yi, E. Palmer, and D.G. Marsh. 1995b. A dominant T cell receptor beta-chain in response to a short ragweed allergen. *Ann. N.Y. Acad. Sci.* 754: 6157-6162.

Kellogg, D.E., J.J. Sutrinsky, and S. Kowk. 1990. Quantitation of HIV-1 proviral DNA relative to cellular DNA by the polymerase chain reaction. *Anal. Biochem.* 189: 202-208.

Lee, J.-G., C.R. Connell, and W. Bloch. 1993. Allelic discrimination by nick-translation PCR with fluorogenic probes. *Nucleic Acids Res.* 21: 3761-3766.

Livak, K.J., S.J. Flood, J. Marmaro, W. Giusti, and K. Deetz. 1995a. Oligonucleotides with fluorescent dyes at opposite ends provide a quenched probe system useful for detecting PCR product and nucleic acid hybridization. *PCR Methods Appl.* 4: 357-362.

Livak, K.J., J. Marmaro, and J.A. Todd. 1995b. Towards

fully automated genome-wide polymorphism screening [letter]. *Nature Genet.* 9: 341-342.

Mulder, J., N. McKinney, C. Christopherson, J. Sutrinsky, L. Greenfield, and S. Kwak. 1994. Rapid and simple PCR assay for quantitation of human immunodeficiency virus type 1 RNA in plasma: Application to acute retroviral infection. *J. Clin. Microbiol.* 32: 292-300.

Pang, S., Y. Koyanagi, S. Miles, C. Wiley, H.V. Vinters, and L.S. Chen. 1990. High levels of unintegrated HIV-1 DNA in brain tissue of AIDS dementia patients. *Nature* 343: 85-89.

Platak, M.J., K.C. Luk, B. Williams, and J.D. Lifson. 1995a. Quantitative competitive polymerase chain reaction for accurate quantitation of HIV DNA and RNA species. *AidTechniques* 14: 70-81.

Platak, M.J., M.S. Saag, L.C. Yang, S.J. Clark, J.C. Kappes, K.C. Luk, B.H. Hann, G.M. Shaw, and J.D. Lifson. 1995b. High levels of HIV-1 in plasma during all stages of infection determined by competitive PCR [see Comments]. *Science* 259: 1749-1754.

Prud'homme, G.J., D.H. Kono, and A.N. Theofilopoulos. 1995. Quantitative polymerase chain reaction analysis reveals marked overexpression of interleukin-1 beta, interleukin-1 and interferon-gamma mRNA in the lymph nodes of lupus-prone mice. *Mol. Immunol.* 32: 495-503.

Racymackers, L. 1995. A commentary on the practical applications of competitive PCR. *Genome Res.* 5: 91-94.

Sharp, P.A., A.J. Berk, and S.M. Berget. 1980. Transcription maps of adenovirus. *Methods Enzymol.* 65: 750-768.

Slamon, D.J., G.M. Clark, S.G. Wong, W.J. Levin, A. Ullrich, and W.L. McGuire. 1987. Human breast cancer: Correlation of relapse and survival with amplification of the HER-2/neu oncogene. *Science* 235: 177-182.

Southern, E.M. 1975. Detection of specific sequences among DNA fragments separated by gel electrophoresis. *J. Mol. Biol.* 98: 503-517.

Tan, X., X. Sun, C.F. Gonzalez, and W. Hsueh. 1994. PAF and TNF increase the precursor of Nk-kappa B p50 mRNA in mouse intestine: Quantitative analysis by competitive PCR. *Biochim. Biophys. Acta* 1215: 157-162.

Thomas, P.S. 1980. Hybridization of denatured RNA and small DNA fragments transferred to nitrocellulose. *Proc. Natl. Acad. Sci.* 77: 5201-5205.

Williams, S., C. Schwer, A. Krishnarao, C. Hoid, B. Karger, and P.M. Williams. 1996. Quantitative competitive PCR: Analysis of amplified products of the HIV-1 gag gene by capillary electrophoresis with laser induced fluorescence detection. *Anal. Biochem.* (in press).

Received June 3, 1996; accepted in revised form July 29, 1996.

## WISP genes are members of the connective tissue growth factor family that are up-regulated in Wnt-1-transformed cells and aberrantly expressed in human colon tumors

DIANE PENNICA<sup>\*†</sup>, TODD A. SWANSON<sup>\*</sup>, JAMES W. WELSH<sup>\*</sup>, MARGARET A. ROY<sup>‡</sup>, DAVID A. LAWRENCE<sup>\*</sup>, JAMES LEE<sup>‡</sup>, JENNIFER BRUSH<sup>‡</sup>, LISA A. TANEYHILL<sup>§</sup>, BETHANNE DEUEL<sup>‡</sup>, MICHAEL LEW<sup>¶</sup>, COLIN WATANABE<sup>||</sup>, ROBERT L. COHEN<sup>\*</sup>, MONA F. MELHEM<sup>\*\*</sup>, GENE G. FINLEY<sup>\*\*</sup>, PHIL QUIRKE<sup>††</sup>, AUDREY D. GODDARD<sup>‡</sup>, KENNETH J. HILLAN<sup>¶</sup>, AUSTIN L. GURNEY<sup>‡</sup>, DAVID BOTSTEIN<sup>‡,‡‡</sup>, AND ARNOLD J. LEVINE<sup>§</sup>

Departments of <sup>\*</sup>Molecular Oncology, <sup>‡</sup>Molecular Biology, <sup>§</sup>Scientific Computing, and <sup>¶</sup>Pathology, Genentech Inc., 1 DNA Way, South San Francisco, CA 94080; <sup>\*\*</sup>University of Pittsburgh School of Medicine, Veterans Administration Medical Center, Pittsburgh, PA 15240; <sup>††</sup>University of Leeds, Leeds, LS29JT United Kingdom; <sup>‡‡</sup>Department of Genetics, Stanford University, Palo Alto, CA 94305; and <sup>§</sup>Department of Molecular Biology, Princeton University, Princeton, NJ 08544

Contributed by David Botstein and Arnold J. Levine, October 21, 1998

**ABSTRACT** Wnt family members are critical to many developmental processes, and components of the Wnt signaling pathway have been linked to tumorigenesis in familial and sporadic colon carcinomas. Here we report the identification of two genes, *WISP-1* and *WISP-2*, that are up-regulated in the mouse mammary epithelial cell line C57MG transformed by Wnt-1, but not by Wnt-4. Together with a third related gene, *WISP-3*, these proteins define a subfamily of the connective tissue growth factor family. Two distinct systems demonstrated *WISP* induction to be associated with the expression of Wnt-1. These included (i) C57MG cells infected with a Wnt-1 retroviral vector or expressing Wnt-1 under the control of a tetracycline repressible promoter, and (ii) Wnt-1 transgenic mice. The *WISP-1* gene was localized to human chromosome 8q24.1–8q24.3. *WISP-1* genomic DNA was amplified in colon cancer cell lines and in human colon tumors and its RNA overexpressed (2- to >30-fold) in 84% of the tumors examined compared with patient-matched normal mucosa. *WISP-3* mapped to chromosome 6q22–6q23 and also was overexpressed (4- to >40-fold) in 63% of the colon tumors analyzed. In contrast, *WISP-2* mapped to human chromosome 20q12–20q13 and its DNA was amplified, but RNA expression was reduced (2- to >30-fold) in 79% of the tumors. These results suggest that the *WISP* genes may be downstream of Wnt-1 signaling and that aberrant levels of *WISP* expression in colon cancer may play a role in colon tumorigenesis.

Wnt-1 is a member of an expanding family of cysteine-rich, glycosylated signaling proteins that mediate diverse developmental processes such as the control of cell proliferation, adhesion, cell polarity, and the establishment of cell fates (1, 2). Wnt-1 originally was identified as an oncogene activated by the insertion of mouse mammary tumor virus in virus-induced mammary adenocarcinomas (3, 4). Although Wnt-1 is not expressed in the normal mammary gland, expression of Wnt-1 in transgenic mice causes mammary tumors (5).

In mammalian cells, Wnt family members initiate signaling by binding to the seven-transmembrane spanning Frizzled receptors and recruiting the cytoplasmic protein Dishevelled (Dsh) to the cell membrane (1, 2, 6). Dsh then inhibits the kinase activity of the normally constitutively active glycogen synthase kinase-3 $\beta$  (GSK-3 $\beta$ ) resulting in an increase in  $\beta$ -catenin levels. Stabilized  $\beta$ -catenin interacts with the transcription factor TCF/Lef1, forming a complex that appears in

the nucleus and binds TCF/Lef1 target DNA elements to activate transcription (7, 8). Other experiments suggest that the adenomatous polyposis coli (APC) tumor suppressor gene also plays an important role in Wnt signaling by regulating  $\beta$ -catenin levels (9). APC is phosphorylated by GSK-3 $\beta$ , binds to  $\beta$ -catenin, and facilitates its degradation. Mutations in either APC or  $\beta$ -catenin have been associated with colon carcinomas and melanomas, suggesting these mutations contribute to the development of these types of cancer, implicating the Wnt pathway in tumorigenesis (1).

Although much has been learned about the Wnt signaling pathway over the past several years, only a few of the transcriptionally activated downstream components activated by Wnt have been characterized. Those that have been described cannot account for all of the diverse functions attributed to Wnt signaling. Among the candidate Wnt target genes are those encoding the nodal-related 3 gene, *Xnr3*, a member of the transforming growth factor (TGF)- $\beta$  superfamily, and the homeobox genes, *engrailed*, *gooseoid*, *twin* (*Xtwn*), and *siamois* (2). A recent report also identifies *c-myc* as a target gene of the Wnt signaling pathway (10).

To identify additional downstream genes in the Wnt signaling pathway that are relevant to the transformed cell phenotype, we used a PCR-based cDNA subtraction strategy, suppression subtractive hybridization (SSH) (11), using RNA isolated from C57MG mouse mammary epithelial cells and C57MG cells stably transformed by a Wnt-1 retrovirus. Overexpression of Wnt-1 in this cell line is sufficient to induce a partially transformed phenotype, characterized by elongated and refractile cells that lose contact inhibition and form a multilayered array (12, 13). We reasoned that genes differentially expressed between these two cell lines might contribute to the transformed phenotype.

In this paper, we describe the cloning and characterization of two genes up-regulated in Wnt-1 transformed cells, *WISP-1* and *WISP-2*, and a third related gene, *WISP-3*. The *WISP* genes are members of the CCN family of growth factors, which includes connective tissue growth factor (CTGF), Cyr61, and *nov*, a family not previously linked to Wnt signaling.

### MATERIALS AND METHODS

**SSH.** SSH was performed by using the PCR-Select cDNA Subtraction Kit (CLONTECH). Tester double-stranded

Abbreviations: TGF, transforming growth factor; CTGF, connective tissue growth factor; SSH, suppression subtractive hybridization; VWC, von Willebrand factor type C module.

Data deposition: The sequences reported in this paper have been deposited in the Genbank database (accession nos. AF100777, AF100778, AF100779, AF100780, and AF100781).

<sup>†</sup>To whom reprint requests should be addressed. e-mail: diane@gene.com.

The publication costs of this article were defrayed in part by page charge payment. This article must therefore be hereby marked "advertisement" in accordance with 18 U.S.C. §1734 solely to indicate this fact.

© 1998 by The National Academy of Sciences 0027-8424/98/9514717-6\$2.00/0  
PNAS is available online at www.pnas.org.

cDNA was synthesized from 2  $\mu$ g of poly(A)<sup>+</sup> RNA isolated from the C57MG/Wnt-1 cell line and driver cDNA from 2  $\mu$ g of poly(A)<sup>+</sup> RNA from the parent C57MG cells. The subtracted cDNA library was subcloned into a pGEM-T vector for further analysis.

**cDNA Library Screening.** Clones encoding full-length mouse *WISP-1* were isolated by screening a  $\lambda$ gt10 mouse embryo cDNA library (CLONTECH) with a 70-bp probe from the original partial clone 568 sequence corresponding to amino acids 128–169. Clones encoding full-length human *WISP-1* were isolated by screening  $\lambda$ gt10 lung and fetal kidney cDNA libraries with the same probe at low stringency. Clones encoding full-length mouse and human *WISP-2* were isolated by screening a C57MG/Wnt-1 or human fetal lung cDNA library with a probe corresponding to nucleotides 1463–1512. Full-length cDNAs encoding *WISP-3* were cloned from human bone marrow and fetal kidney libraries.

**Expression of Human *WISP* RNA.** PCR amplification of first-strand cDNA was performed with human Multiple Tissue cDNA panels (CLONTECH) and 300  $\mu$ M of each dNTP at 94°C for 1 sec, 62°C for 30 sec, 72°C for 1 min, for 22–32 cycles. *WISP* and glyceraldehyde-3-phosphate dehydrogenase primer sequences are available on request.

**In Situ Hybridization.** <sup>32</sup>P-labeled sense and antisense riboprobes were transcribed from an 897-bp PCR product corresponding to nucleotides 601–1440 of mouse *WISP-1* or a 294-bp PCR product corresponding to nucleotides 82–375 of mouse *WISP-2*. All tissues were processed as described (40).

**Radiation Hybrid Mapping.** Genomic DNA from each hybrid in the Stanford G3 and Genebridge4 Radiation Hybrid Panels (Research Genetics, Huntsville, AL) and human and hamster control DNAs were PCR-amplified, and the results were submitted to the Stanford or Massachusetts Institute of Technology web servers.

**Cell Lines, Tumors, and Mucosa Specimens.** Tissue specimens were obtained from the Department of Pathology (University of Pittsburgh) for patients undergoing colon resection and from the University of Leeds, United Kingdom. Genomic DNA was isolated (Qiagen) from the pooled blood of 10 normal human donors, surgical specimens, and the following ATCC human cell lines: SW480, COLO 320DM, HT-29, WiDr, and SW403 (colon adenocarcinomas), SW620 (lymph node metastasis, colon adenocarcinoma), HCT 116 (colon carcinoma), SK-CO-1 (colon adenocarcinoma, ascites), and HM7 (a variant of ATCC colon adenocarcinoma cell line LS 174T). DNA concentration was determined by using Hoechst dye 33258 intercalation fluorimetry. Total RNA was prepared by homogenization in 7 M GuSCN followed by centrifugation over CsCl cushions or prepared by using RNeasy.

**Gene Amplification and RNA Expression Analysis.** Relative gene amplification and RNA expression of *WISPs* and *c-myc* in the cell lines, colorectal tumors, and normal mucosa were determined by quantitative PCR. Gene-specific primers and fluorogenic probes (sequences available on request) were designed and used to amplify and quantitate the genes. The relative gene copy number was derived by using the formula  $2^{-\Delta Ct}$  where  $\Delta Ct$  represents the difference in amplification cycles required to detect the *WISP* genes in peripheral blood lymphocyte DNA compared with colon tumor DNA or colon tumor RNA compared with normal mucosal RNA. The  $\Delta$ -method was used for calculation of the SE of the gene copy number or RNA expression level. The *WISP*-specific signal was normalized to that of the glyceraldehyde-3-phosphate dehydrogenase housekeeping gene. All TaqMan assay reagents were obtained from Perkin-Elmer Applied Biosystems.

## RESULTS

**Isolation of *WISP-1* and *WISP-2* by SSH.** To identify Wnt-1-inducible genes, we used the technique of SSH using the

mouse mammary epithelial cell line C57MG and C57MG cells that stably express Wnt-1 (11). Candidate differentially expressed cDNAs (1,384 total) were sequenced. Thirty-nine percent of the sequences matched known genes or homologues, 32% matched expressed sequence tags, and 29% had no match. To confirm that the transcript was differentially expressed, semiquantitative reverse transcription-PCR and Northern analysis were performed by using mRNA from the C57MG and C57MG/Wnt-1 cells.

Two of the cDNAs, *WISP-1* and *WISP-2*, were differentially expressed, being induced in the C57MG/Wnt-1 cell line, but not in the parent C57MG cells or C57MG cells overexpressing Wnt-4 (Fig. 1A and B). Wnt-4, unlike Wnt-1, does not induce the morphological transformation of C57MG cells and has no effect on  $\beta$ -catenin levels (13, 14). Expression of *WISP-1* was up-regulated approximately 3-fold in the C57MG/Wnt-1 cell line and *WISP-2* by approximately 5-fold by both Northern analysis and reverse transcription-PCR.

An independent, but similar, system was used to examine *WISP* expression after Wnt-1 induction. C57MG cells expressing the *Wnt-1* gene under the control of a tetracycline-repressible promoter produce low amounts of Wnt-1 in the repressed state but show a strong induction of *Wnt-1* mRNA and protein within 24 hr after tetracycline removal (8). The levels of Wnt-1 and *WISP* RNA isolated from these cells at various times after tetracycline removal were assessed by quantitative PCR. Strong induction of Wnt-1 mRNA was seen as early as 10 hr after tetracycline removal. Induction of *WISP* mRNA (2- to 6-fold) was seen at 48 and 72 hr (data not shown). These data support our previous observations that show that *WISP* induction is correlated with Wnt-1 expression. Because the induction is slow, occurring after approximately 48 hr, the induction of *WISPs* may be an indirect response to Wnt-1 signaling.

cDNA clones of human *WISP-1* were isolated and the sequence compared with mouse *WISP-1*. The cDNA sequences of mouse and human *WISP-1* were 1,766 and 2,830 bp in length, respectively, and encode proteins of 367 aa, with predicted relative molecular masses of  $\approx 40,000$  ( $M_r$  40 K). Both have hydrophobic N-terminal signal sequences, 38 conserved cysteine residues, and four potential N-linked glycosylation sites and are 84% identical (Fig. 2A).

Full-length cDNA clones of mouse and human *WISP-2* were 1,734 and 1,293 bp in length, respectively, and encode proteins of 251 and 250 aa, respectively, with predicted relative molecular masses of  $\approx 27,000$  ( $M_r$  27 K) (Fig. 2B). Mouse and human *WISP-2* are 73% identical. Human *WISP-2* has no potential N-linked glycosylation sites, and mouse *WISP-2* has one at

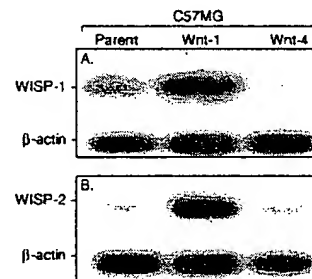


FIG. 1. *WISP-1* and *WISP-2* are induced by Wnt-1, but not Wnt-4, expression in C57MG cells. Northern analysis of *WISP-1* (A) and *WISP-2* (B) expression in C57MG, C57MG/Wnt-1, and C57MG/Wnt-4 cells. Poly(A)<sup>+</sup> RNA (2  $\mu$ g) was subjected to Northern blot analysis and hybridized with a 70-bp mouse *WISP-1*-specific probe (amino acids 278–300) or a 190-bp *WISP-2*-specific probe (nucleotides 1438–1627) in the 3' untranslated region. Blots were rehybridized with human  $\beta$ -actin probe.

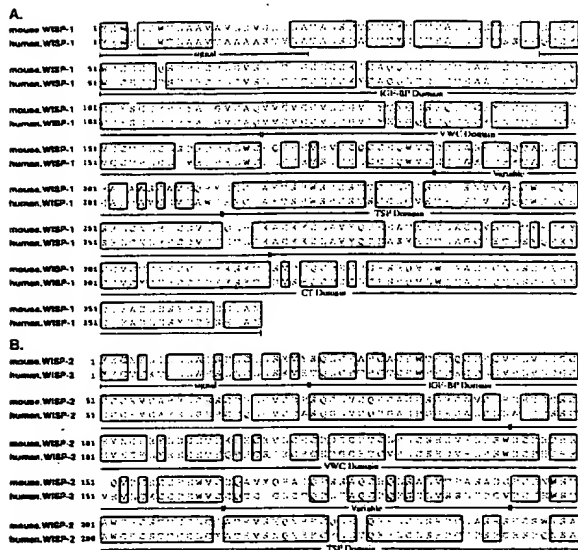


FIG. 2. Encoded amino acid sequence alignment of mouse and human *WISP-1* (A) and mouse and human *WISP-2* (B). The potential signal sequence, insulin-like growth factor-binding protein (IGF-BP), VWC, thrombospondin (TSP), and C-terminal (CT) domains are underlined.

position 197. *WISP-2* has 28 cysteine residues that are conserved among the 38 cysteines found in *WISP-1*.

**Identification of *WISP-3*.** To search for related proteins, we screened expressed sequence tag (EST) databases with the *WISP-1* protein sequence and identified several ESTs as potentially related sequences. We identified a homologous protein that we have called *WISP-3*. A full-length human *WISP-3* cDNA of 1,371 bp was isolated corresponding to those ESTs that encode a 354-aa protein with a predicted molecular mass of 39,293. *WISP-3* has two potential N-linked glycosylation sites and 36 cysteine residues. An alignment of the three human *WISP* proteins shows that *WISP-1* and *WISP-3* are the most similar (42% identity), whereas *WISP-2* has 37% identity with *WISP-1* and 32% identity with *WISP-3* (Fig. 3A).

***WISPs* Are Homologous to the CTGF Family of Proteins.** Human *WISP-1*, *WISP-2*, and *WISP-3* are novel sequences; however, mouse *WISP-1* is the same as the recently identified *Elm1* gene. *Elm1* is expressed in low, but not high, metastatic mouse melanoma cells, and suppresses the *in vivo* growth and metastatic potential of K-1735 mouse melanoma cells (15). Human and mouse *WISP-2* are homologous to the recently described rat gene, *rCop-1* (16). Significant homology (36–44%) was seen to the CCN family of growth factors. This family includes three members, CTGF, Cyr61, and the protooncogene *nov*. CTGF is a chemotactic and mitogenic factor for fibroblasts that is implicated in wound healing and fibrotic disorders and is induced by TGF- $\beta$  (17). Cyr61 is an extracellular matrix signaling molecule that promotes cell adhesion, proliferation, migration, angiogenesis, and tumor growth (18, 19). *nov* (nephroblastoma overexpressed) is an immediate early gene associated with quiescence and found altered in Wilms tumors (20). The proteins of the CCN family share functional, but not sequence, similarity to Wnt-1. All are secreted, cysteine-rich heparin binding glycoproteins that associate with the cell surface and extracellular matrix.

*WISP* proteins exhibit the modular architecture of the CCN family, characterized by four conserved cysteine-rich domains (Fig. 3B) (21). The N-terminal domain, which includes the first 12 cysteine residues, contains a consensus sequence (GCGC-CXXC) conserved in most insulin-like growth factor (IGF)-

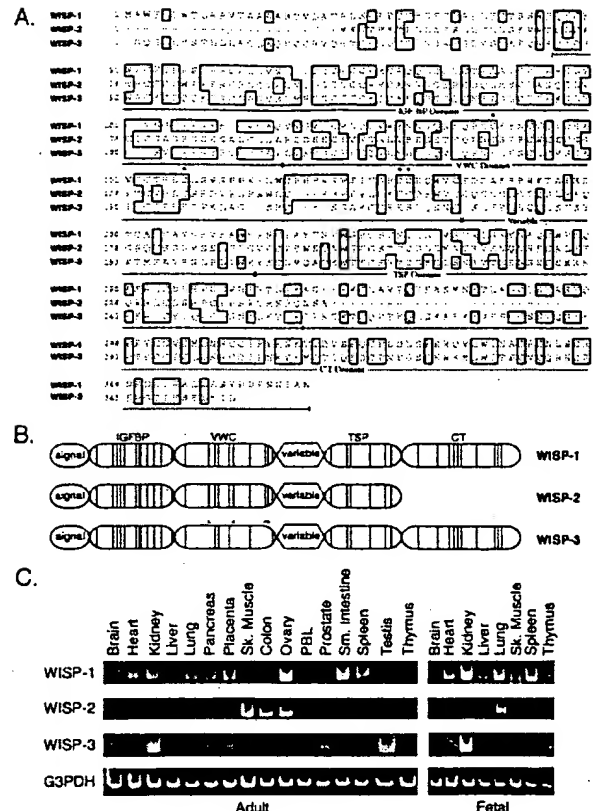


FIG. 3. (A) Encoded amino acid sequence alignment of human *WISPs*. The cysteine residues of *WISP-1* and *WISP-2* that are not present in *WISP-3* are indicated with a dot. (B) Schematic representation of the *WISP* proteins showing the domain structure and cysteine residues (vertical lines). The four cysteine residues in the VWC domain that are absent in *WISP-3* are indicated with a dot. (C) Expression of *WISP* mRNA in human tissues. PCR was performed on human multiple-tissue cDNA panels (CLONTECH) from the indicated adult and fetal tissues.

binding proteins (BP). This sequence is conserved in *WISP-2* and *WISP-3*, whereas *WISP-1* has a glutamine in the third position instead of a glycine. CTGF recently has been shown to specifically bind IGF (22) and a truncated *nov* protein lacking the IGF-BP domain is oncogenic (23). The von Willebrand factor type C module (VWC), also found in certain collagens and mucins, covers the next 10 cysteine residues, and is thought to participate in protein complex formation and oligomerization (24). The VWC domain of *WISP-3* differs from all CCN family members described previously, in that it contains only six of the 10 cysteine residues (Fig. 3A and B). A short variable region follows the VWC domain. The third module, the thrombospondin (TSP) domain is involved in binding to sulfated glycoconjugates and contains six cysteine residues and a conserved WSxCSSxCG motif first identified in thrombospondin (25). The C-terminal (CT) module containing the remaining 10 cysteines is thought to be involved in dimerization and receptor binding (26). The CT domain is present in all CCN family members described to date but is absent in *WISP-2* (Fig. 3A and B). The existence of a putative signal sequence and the absence of a transmembrane domain suggest that *WISPs* are secreted proteins, an observation supported by an analysis of their expression and secretion from mammalian cell and baculovirus cultures (data not shown).

**Expression of *WISP* mRNA in Human Tissues.** Tissue-specific expression of human *WISPs* was characterized by PCR



analysis on adult and fetal multiple tissue cDNA panels. *WISP-1* expression was seen in the adult heart, kidney, lung, pancreas, placenta, ovary, small intestine, and spleen (Fig. 3C). Little or no expression was detected in the brain, liver, skeletal muscle, colon, peripheral blood leukocytes, prostate, testis, or thymus. *WISP-2* had a more restricted tissue expression and was detected in adult skeletal muscle, colon, ovary, and fetal lung. Predominant expression of *WISP-3* was seen in adult kidney and testis and fetal kidney. Lower levels of *WISP-3* expression were detected in placenta, ovary, prostate, and small intestine.

**In Situ Localization of *WISP-1* and *WISP-2*.** Expression of *WISP-1* and *WISP-2* was assessed by *in situ* hybridization in mammary tumors from Wnt-1 transgenic mice. Strong expression of *WISP-1* was observed in stromal fibroblasts lying within the fibrovascular tumor stroma (Fig. 4 A–D). However, low-level *WISP-1* expression also was observed focally within tumor cells (data not shown). No expression was observed in normal breast. Like *WISP-1*, *WISP-2* expression also was seen in the tumor stroma in breast tumors from Wnt-1 transgenic animals (Fig. 4 E–H). However, *WISP-2* expression in the stroma was in spindle-shaped cells adjacent to capillary vessels, whereas

the predominant cell type expressing *WISP-1* was the stromal fibroblasts.

**Chromosome Localization of the *WISP* Genes.** The chromosomal location of the human *WISP* genes was determined by radiation hybrid mapping panels. *WISP-1* is approximately 3.48 cR from the meiotic marker AFM259xc5 [logarithm of odds (lod) score 16.31] on chromosome 8q24.1 to 8q24.3, in the same region as the human locus of the *novH* family member (27) and roughly 4 Mbs distal to *c-myc* (28). Preliminary fine mapping indicates that *WISP-1* is located near D8S1712 STS. *WISP-2* is linked to the marker SHGC-33922 (lod = 1,000) on chromosome 20q12–20q13.1. Human *WISP-3* mapped to chromosome 6q22–6q23 and is linked to the marker AFM211ze5 (lod = 1,000). *WISP-3* is approximately 18 Mbs proximal to CTGF and 23 Mbs proximal to the human cellular oncogene *MYB* (27, 29).

**Amplification and Aberrant Expression of *WISPs* in Human Colon Tumors.** Amplification of protooncogenes is seen in many human tumors and has etiological and prognostic significance. For example, in a variety of tumor types, *c-myc* amplification has been associated with malignant progression and poor prognosis (30). Because *WISP-1* resides in the same general chromosomal location (8q24) as *c-myc*, we asked whether it was a target of gene amplification, and, if so, whether this amplification was independent of the *c-myc* locus. Genomic DNA from human colon cancer cell lines was assessed by quantitative PCR and Southern blot analysis. (Fig. 5 A and B). Both methods detected similar degrees of *WISP-1* amplification. Most cell lines showed significant (2- to 4-fold) amplification, with the HT-29 and WiDr cell lines demonstrating an 8-fold increase. Significantly, the pattern of amplification observed did not correlate with that observed for *c-myc*, indicating that the *c-myc* gene is not part of the amplicon that involves the *WISP-1* locus.

We next examined whether the *WISP* genes were amplified in a panel of 25 primary human colon adenocarcinomas. The relative *WISP* gene copy number in each colon tumor DNA was compared with pooled normal DNA from 10 donors by quantitative PCR (Fig. 6). The copy number of *WISP-1* and *WISP-2* was significantly greater than one, approximately 2-fold for *WISP-1* in about 60% of the tumors and 2- to 4-fold for *WISP-2* in 92% of the tumors ( $P < 0.001$  for each). The copy number for *WISP-3* was indistinguishable from one ( $P = 0.166$ ). In addition, the copy number of *WISP-2* was significantly higher than that of *WISP-1* ( $P < 0.001$ ).

The levels of *WISP* transcripts in RNA isolated from 19 adenocarcinomas and their matched normal mucosa were

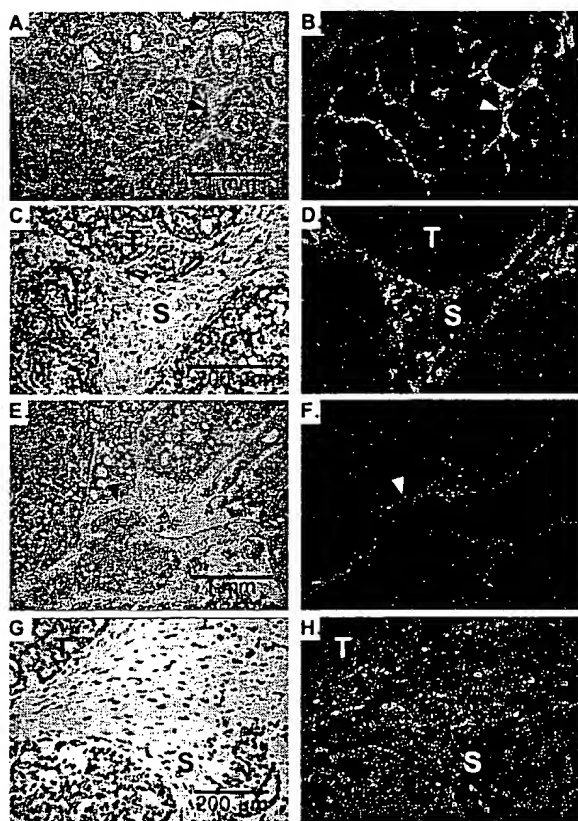


FIG. 4. (A, C, E, and G) Representative hematoxylin/eosin-stained images from breast tumors in Wnt-1 transgenic mice. The corresponding dark-field images showing *WISP-1* expression are shown in B and D. The tumor is a moderately well-differentiated adenocarcinoma showing evidence of adenoid cystic change. At low power (A and B), expression of *WISP-1* is seen in the delicate branching fibrovascular tumor stroma (arrowhead). At higher magnification, expression is seen in the stromal(s) fibroblasts (C and D), and tumor cells are negative. Focal expression of *WISP-1*, however, was observed in tumor cells in some areas. Images of *WISP-2* expression are shown in E–H. At low power (E and F), expression of *WISP-2* is seen in cells lying within the fibrovascular tumor stroma. At higher magnification, these cells appeared to be adjacent to capillary vessels whereas tumor cells are negative (G and H).

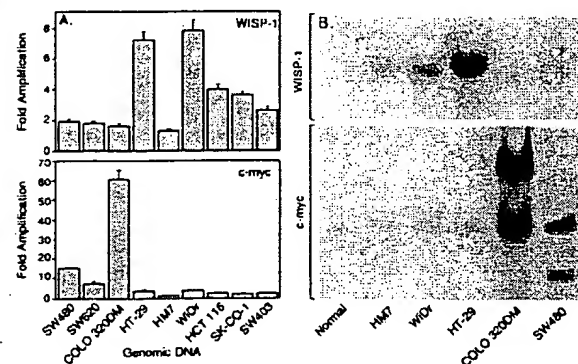


FIG. 5. Amplification of *WISP-1* genomic DNA in colon cancer cell lines. (A) Amplification in cell line DNA was determined by quantitative PCR. (B) Southern blots containing genomic DNA (10  $\mu$ g) digested with *Eco*RI (*WISP-1*) or *Xba*I (*c-myc*) were hybridized with a 100-bp human *WISP-1* probe (amino acids 186–219) or a human *c-myc* probe (located at bp 1901–2000). The *WISP* and *myc* genes are detected in normal human genomic DNA after a longer film exposure.

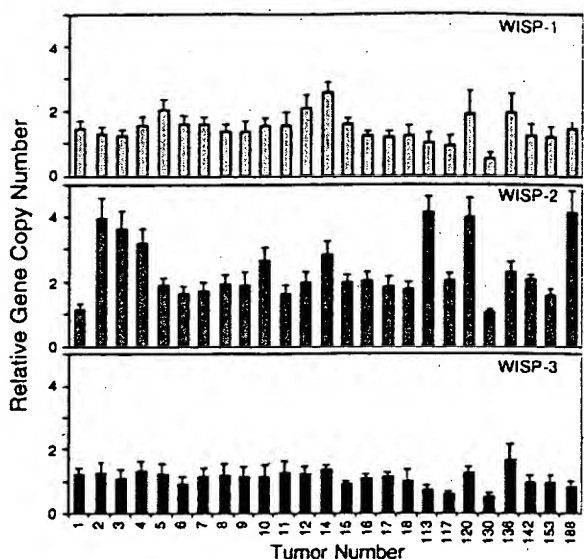


FIG. 6. Genomic amplification of *WISP* genes in human colon tumors. The relative gene copy number of the *WISP* genes in 25 adenocarcinomas was assayed by quantitative PCR, by comparing DNA from primary human tumors with pooled DNA from 10 healthy donors. The data are means  $\pm$  SEM from one experiment done in triplicate. The experiment was repeated at least three times.

assessed by quantitative PCR (Fig. 7). The level of *WISP-1* RNA present in tumor tissue varied but was significantly increased (2- to >25-fold) in 84% (16/19) of the human colon tumors examined compared with normal adjacent mucosa. Four of 19 tumors showed greater than 10-fold overexpression. In contrast, in 79% (15/19) of the tumors examined, *WISP-2* RNA expression was significantly lower in the tumor than the mucosa. Similar to *WISP-1*, *WISP-3* RNA was overexpressed in 63% (12/19) of the colon tumors compared with the normal

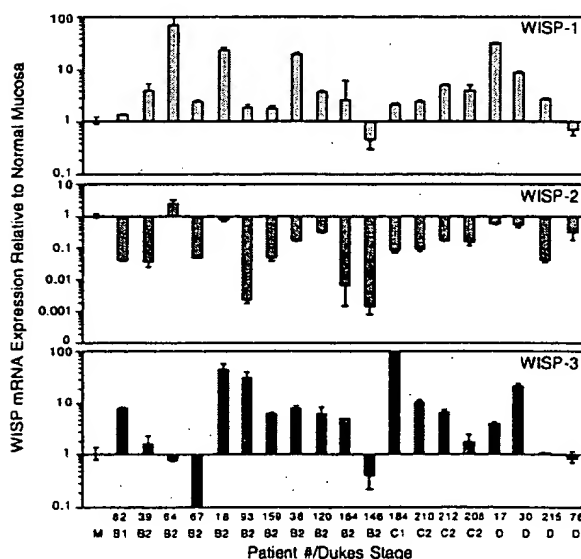


FIG. 7. *WISP* RNA expression in primary human colon tumors relative to expression in normal mucosa from the same patient. Expression of *WISP* mRNA in 19 adenocarcinomas was assayed by quantitative PCR. The Dukes stage of the tumor is listed under the sample number. The data are means  $\pm$  SEM from one experiment done in triplicate. The experiment was repeated at least twice.

mucosa. The amount of overexpression of *WISP-3* ranged from 4- to >40-fold.

## DISCUSSION

One approach to understanding the molecular basis of cancer is to identify differences in gene expression between cancer cells and normal cells. Strategies based on assumptions that steady-state mRNA levels will differ between normal and malignant cells have been used to clone differentially expressed genes (31). We have used a PCR-based selection strategy, SSH, to identify genes selectively expressed in C57MG mouse mammary epithelial cells transformed by Wnt-1.

Three of the genes isolated, *WISP-1*, *WISP-2*, and *WISP-3*, are members of the CCN family of growth factors, which includes CTGF, Cyr61, and *nov*, a family not previously linked to Wnt signaling.

Two independent experimental systems demonstrated that *WISP* induction was associated with the expression of Wnt-1. The first was C57MG cells infected with a Wnt-1 retroviral vector or C57MG cells expressing Wnt-1 under the control of a tetracycline-repressible promoter, and the second was in Wnt-1 transgenic mice, where breast tissue expresses Wnt-1, whereas normal breast tissue does not. No *WISP* RNA expression was detected in mammary tumors induced by polyoma virus middle T antigen (data not shown). These data suggest a link between Wnt-1 and *WISPs* in that in these two situations, *WISP* induction was correlated with Wnt-1 expression.

It is not clear whether the *WISPs* are directly or indirectly induced by the downstream components of the Wnt-1 signaling pathway (i.e.,  $\beta$ -catenin-TCF-1/Lef1). The increased levels of *WISP* RNA were measured in Wnt-1-transformed cells, hours or days after Wnt-1 transformation. Thus, *WISP* expression could result from Wnt-1 signaling directly through  $\beta$ -catenin transcription factor regulation or alternatively through Wnt-1 signaling turning on a transcription factor, which in turn regulates *WISPs*.

The *WISPs* define an additional subfamily of the CCN family of growth factors. One striking difference observed in the protein sequence of *WISP-2* is the absence of a CT domain, which is present in CTGF, Cyr61, *nov*, *WISP-1*, and *WISP-3*. This domain is thought to be involved in receptor binding and dimerization. Growth factors, such as TGF- $\beta$ , platelet-derived growth factor, and nerve growth factor, which contain a cysteine knot motif exist as dimers (32). It is tempting to speculate that *WISP-1* and *WISP-3* may exist as dimers, whereas *WISP-2* exists as a monomer. If the CT domain is also important for receptor binding, *WISP-2* may bind its receptor through a different region of the molecule than the other CCN family members. No specific receptors have been identified for CTGF or *nov*. A recent report has shown that integrin  $\alpha_v\beta_3$  serves as an adhesion receptor for Cyr61 (33).

The strong expression of *WISP-1* and *WISP-2* in cells lying within the fibrovascular tumor stroma in breast tumors from Wnt-1 transgenic animals is consistent with previous observations that transcripts for the related CTGF gene are primarily expressed in the fibrous stroma of mammary tumors (34). Epithelial cells are thought to control the proliferation of connective tissue stroma in mammary tumors by a cascade of growth factor signals similar to that controlling connective tissue formation during wound repair. It has been proposed that mammary tumor cells or inflammatory cells at the tumor interstitial interface secrete TGF- $\beta_1$ , which is the stimulus for stromal proliferation (34). TGF- $\beta_1$  is secreted by a large percentage of malignant breast tumors and may be one of the growth factors that stimulates the production of CTGF and *WISPs* in the stroma.

It was of interest that *WISP-1* and *WISP-2* expression was observed in the stromal cells that surrounded the tumor cells

(epithelial cells) in the Wnt-1 transgenic mouse sections of breast tissue. This finding suggests that paracrine signaling could occur in which the stromal cells could supply WISP-1 and WISP-2 to regulate tumor cell growth on the WISP extracellular matrix. Stromal cell-derived factors in the extracellular matrix have been postulated to play a role in tumor cell migration and proliferation (35). The localization of *WISP-1* and *WISP-2* in the stromal cells of breast tumors supports this paracrine model.

An analysis of *WISP-1* gene amplification and expression in human colon tumors showed a correlation between DNA amplification and overexpression, whereas overexpression of *WISP-3* RNA was seen in the absence of DNA amplification. In contrast, *WISP-2* DNA was amplified in the colon tumors, but its mRNA expression was significantly reduced in the majority of tumors compared with the expression in normal colonic mucosa from the same patient. The gene for human *WISP-2* was localized to chromosome 20q12–20q13, at a region frequently amplified and associated with poor prognosis in node negative breast cancer and many colon cancers, suggesting the existence of one or more oncogenes at this locus (36–38). Because the center of the 20q13 amplicon has not yet been identified, it is possible that the apparent amplification observed for *WISP-2* may be caused by another gene in this amplicon.

A recent manuscript on *rCop-1*, the rat orthologue of *WISP-2*, describes the loss of expression of this gene after cell transformation, suggesting it may be a negative regulator of growth in cell lines (16). Although the mechanism by which *WISP-2* RNA expression is down-regulated during malignant transformation is unknown, the reduced expression of *WISP-2* in colon tumors and cell lines suggests that it may function as a tumor suppressor. These results show that the *WISP* genes are aberrantly expressed in colon cancer and suggest that their altered expression may confer selective growth advantage to the tumor.

Members of the Wnt signaling pathway have been implicated in the pathogenesis of colon cancer, breast cancer, and melanoma, including the tumor suppressor gene adenomatous polyposis coli and  $\beta$ -catenin (39). Mutations in specific regions of either gene can cause the stabilization and accumulation of cytoplasmic  $\beta$ -catenin, which presumably contributes to human carcinogenesis through the activation of target genes such as the *WISPs*. Although the mechanism by which Wnt-1 transforms cells and induces tumorigenesis is unknown, the identification of *WISPs* as genes that may be regulated downstream of Wnt-1 in C57MG cells suggests they could be important mediators of Wnt-1 transformation. The amplification and altered expression patterns of the *WISPs* in human colon tumors may indicate an important role for these genes in tumor development.

We thank the DNA synthesis group for oligonucleotide synthesis, T. Baker for technical assistance, P. Dowd for radiation hybrid mapping, K. Willert and R. Nusse for the tet-repressible C57MG/Wnt-1 cells, V. Dixit for discussions, and D. Wood and A. Bruce for artwork.

- Cadigan, K. M. & Nusse, R. (1997) *Genes Dev.* 11, 3286–3305.
- Dale, T. C. (1998) *Biochem. J.* 329, 209–223.
- Nusse, R. & Varmus, H. E. (1982) *Cell* 31, 99–109.
- van Ooyen, A. & Nusse, R. (1984) *Cell* 39, 233–240.
- Tsukamoto, A. S., Grosschedl, R., Guzman, R. C., Parslow, T. & Varmus, H. E. (1988) *Cell* 55, 619–625.
- Brown, J. D. & Moon, R. T. (1998) *Curr. Opin. Cell Biol.* 10, 182–187.
- Molenaar, M., van de Wetering, M., Oosterwegel, M., Peterson-Maduro, J., Godsave, S., Korinek, V., Roose, J., Destree, O. & Clevers, H. (1996) *Cell* 86, 391–399.
- Korinek, V., Barker, N., Willert, K., Molenaar, M., Roose, J., Wagenaar, G., Markman, M., Lamers, W., Destree, O. & Clevers, H. (1998) *Mol. Cell Biol.* 18, 1248–1256.
- Munemitsu, S., Albert, I., Souza, B., Rubinfeld, B. & Polakis, P. (1995) *Proc. Natl. Acad. Sci. USA* 92, 3046–3050.
- He, T. C., Sparks, A. B., Rago, C., Hermeking, H., Zawel, L., da Costa, L. T., Morin, P. J., Vogelstein, B. & Kinzler, K. W. (1998) *Science* 281, 1509–1512.
- Diatchenko, L., Lau, Y. F., Campbell, A. P., Chenchik, A., Moqadam, F., Huang, B., Lukyanov, S., Lukyanov, K., Gurskaya, N., Sverdlov, E. D. & Siebert, P. D. (1996) *Proc. Natl. Acad. Sci. USA* 93, 6025–6030.
- Brown, A. M., Wildin, R. S., Prendergast, T. J. & Varmus, H. E. (1986) *Cell* 46, 1001–1009.
- Wong, G. T., Gavin, B. J. & McMahon, A. P. (1994) *Mol. Cell Biol.* 14, 6278–6286.
- Shimizu, H., Julius, M. A., Giarre, M., Zheng, Z., Brown, A. M. & Kitajewski, J. (1997) *Cell Growth Differ.* 8, 1349–1358.
- Hashimoto, Y., Shindo-Okada, N., Tani, M., Nagamachi, Y., Takeuchi, K., Shiroishi, T., Toma, H. & Yokota, J. (1998) *J. Exp. Med.* 187, 289–296.
- Zhang, R., Averboukh, L., Zhu, W., Zhang, H., Jo, H., Dempsey, P. J., Coffey, R. J., Pardee, A. B. & Liang, P. (1998) *Mol. Cell Biol.* 18, 6131–6141.
- Grotendorst, G. R. (1997) *Cytokine Growth Factor Rev.* 8, 171–179.
- Kireeva, M. L., Mo, F. E., Yang, G. P. & Lau, L. F. (1996) *Mol. Cell Biol.* 16, 1326–1334.
- Babic, A. M., Kireeva, M. L., Kolesnikova, T. V. & Lau, L. F. (1998) *Proc. Natl. Acad. Sci. USA* 95, 6355–6360.
- Martinerie, C., Huff, V., Joubert, I., Badzioch, M., Saunders, G., Strong, L. & Perbal, B. (1994) *Oncogene* 9, 2729–2732.
- Bork, P. (1993) *FEBS Lett.* 327, 125–130.
- Kim, H. S., Nagalla, S. R., Oh, Y., Wilson, E., Roberts, C. T., Jr. & Rosenfeld, R. G. (1997) *Proc. Natl. Acad. Sci. USA* 94, 12981–12986.
- Joliet, V., Martinerie, C., Dambrine, G., Plassiat, G., Brisac, M., Crochet, J. & Perbal, B. (1992) *Mol. Cell Biol.* 12, 10–21.
- Mancuso, D. J., Tuley, E. A., Westfield, L. A., Worrall, N. K., Shelton-Inloes, B. B., Sorace, J. M., Alevy, Y. G. & Sadler, J. E. (1989) *J. Biol. Chem.* 264, 19514–19527.
- Holt, G. D., Pangburn, M. K. & Ginsburg, V. (1990) *J. Biol. Chem.* 265, 2852–2855.
- Voorberg, J., Fontijn, R., Calafat, J., Janssen, H., van Mourik, J. A. & Pannekoek, H. (1991) *J. Cell Biol.* 113, 195–205.
- Martinerie, C., Viegas-Pequignot, E., Guenard, I., Dutrillaux, B., Nguyen, V. C., Bernheim, A. & Perbal, B. (1992) *Oncogene* 7, 2529–2534.
- Takahashi, E., Hori, T., O'Connell, P., Leppert, M. & White, R. (1991) *Cytogenet. Cell Genet.* 57, 109–111.
- Meese, E., Meltzer, P. S., Witkowski, C. M. & Trent, J. M. (1989) *Genes Chromosomes Cancer* 1, 88–94.
- Garte, S. J. (1993) *Crit. Rev. Oncog.* 4, 435–449.
- Zhang, L., Zhou, W., Velculescu, V. E., Kern, S. E., Hruban, R. H., Hamilton, S. R., Vogelstein, B. & Kinzler, K. W. (1997) *Science* 276, 1268–1272.
- Sun, P. D. & Davies, D. R. (1995) *Annu. Rev. Biophys. Biomol. Struct.* 24, 269–291.
- Kireeva, M. L., Lam, S. C. T. & Lau, L. F. (1998) *J. Biol. Chem.* 273, 3090–3096.
- Frazier, K. S. & Grotendorst, G. R. (1997) *Int. J. Biochem. Cell Biol.* 29, 153–161.
- Wernert, N. (1997) *Virchows Arch.* 430, 433–443.
- Tanner, M. M., Tirkkonen, M., Kallioniemi, A., Collins, C., Stokke, T., Karhu, R., Kowbel, D., Shadravan, F., Hintz, M., Kuo, W. L., *et al.* (1994) *Cancer Res.* 54, 4257–4260.
- Brinkmann, U., Gallo, M., Polymeropoulos, M. H. & Pastan, I. (1996) *Genome Res.* 6, 187–194.
- Bischoff, J. R., Anderson, L., Zhu, Y., Mossie, K., Ng, L., Souza, B., Schryver, B., Flanagan, P., Clairvoyant, F., Ginther, C., *et al.* (1998) *EMBO J.* 17, 3052–3065.
- Morin, P. J., Sparks, A. B., Korinek, V., Barker, N., Clevers, H., Vogelstein, B. & Kinzler, K. W. (1997) *Science* 275, 1787–1790.
- Lu, L. H. & Gillett, N. (1994) *Cell Vision* 1, 169–176.

methods. Peptides AENK or AEQK were dissolved in water, made isotonic with NaCl and diluted into RPMI growth medium. T-cell-proliferation assays were done essentially as described<sup>20,21</sup>. Briefly, after antigen pulsing ( $30 \mu\text{g ml}^{-1}$  TTCF) with tetrapeptides ( $1\text{--}2 \text{ mg ml}^{-1}$ ), PBMCs or EBV-B cells were washed in PBS and fixed for 45 s in 0.05% glutaraldehyde. Glycine was added to a final concentration of 0.1M and the cells were washed five times in RPMI 1640 medium containing 1% FCS before co-culture with T-cell clones in round-bottom 96-well microtitre plates. After 48 h, the cultures were pulsed with  $1 \mu\text{Ci}$  of  $^3\text{H}$ -thymidine and harvested for scintillation counting 16 h later. Predigestion of native TTCF was done by incubating  $200 \mu\text{g}$  TTCF with  $0.25 \mu\text{g}$  pig kidney legumain in  $500 \mu\text{l}$  50 mM citrate buffer, pH 5.5, for 1 h at  $37^\circ\text{C}$ . **Glycopeptide digestions.** The peptides HIDNEEDI, HIDN(N-glucosamine) EEDI and HIDNESDI, which are based on the TTCF sequence, and QQQHFGSNVTDCSGNFCLFR(KKK), which is based on human transferrin, were obtained by custom synthesis. The three C-terminal lysine residues were added to the natural sequence to aid solubility. The transferrin glycopeptide QQQHFGSNVTDCSGNFCLFR was prepared by tryptic (Promega) digestion of 5 mg reduced, carboxy-methylated human transferrin followed by concanavalin A chromatography<sup>21</sup>. Glycopeptides corresponding to residues 622–642 and 421–452 were isolated by reverse-phase HPLC and identified by mass spectrometry and N-terminal sequencing. The lyophilized transferrin-derived peptides were redissolved in 50 mM sodium acetate, pH 5.5, 10 mM dithiothreitol, 20% methanol. Digestions were performed for 3 h at  $30^\circ\text{C}$  with  $5\text{--}50 \text{ mU ml}^{-1}$  pig kidney legumain or B-cell AEP. Products were analysed by HPLC or MALDI-TOF mass spectrometry using a matrix of  $10 \text{ mg ml}^{-1}$   $\alpha$ -cyanocinnamic acid in 50% acetonitrile/0.1% TFA and a PerSeptive Biosystems Elite STR mass spectrometer set to linear or reflector mode. Internal standardization was obtained with a matrix ion of 568.13 mass units.

Received 29 September; accepted 3 November 1998.

- Chen, J. M. *et al.* Cloning, isolation, and characterisation of mammalian legumain, an asparaginyl endopeptidase. *J. Biol. Chem.* **272**, 8090–8098 (1997).
- Kembhavi, A. A., Buttle, D. J., Knight, C. G. & Barrett, A. J. The two cysteine endopeptidases of legume seeds: purification and characterization by use of specific fluorometric assays. *Arch. Biochem. Biophys.* **303**, 208–213 (1993).
- Dalton, J. P., Hala Jambiriska, L. & Bridley, P. J. Asparaginyl endopeptidase activity in adult *Schistosoma mansoni*. *Parasitology* **111**, 575–580 (1995).
- Bennett, K. *et al.* Antigen processing for presentation by class II major histocompatibility complex requires cleavage by cathepsin E. *Eur. J. Immunol.* **22**, 1519–1524 (1992).
- Riese, R. J. *et al.* Essential role for cathepsin S in MHC class II-associated invariant chain processing and peptide loading. *Immunity* **4**, 357–366 (1996).
- Rodríguez, G. M. & Diment, S. Role of cathepsin D in antigen presentation of ovalbumin. *J. Immunol.* **149**, 2894–2898 (1992).
- Hewitt, E. W. *et al.* Natural processing sites for human cathepsin E and cathepsin D in tetanus toxin: implications for T cell epitope generation. *J. Immunol.* **159**, 4693–4699 (1997).
- Watts, C. Capture and processing of exogenous antigens for presentation on MHC molecules. *Annu. Rev. Immunol.* **15**, 821–850 (1997).
- Chapman, H. A. Endosomal proteases and MHC class II function. *Curr. Opin. Immunol.* **10**, 93–102 (1998).
- Fineschi, B. & Miller, J. Endosomal proteases and antigen processing. *Trends Biochem. Sci.* **22**, 377–382 (1997).
- Lu, J. & van Halbeek, H. Complete  $^1\text{H}$  and  $^{13}\text{C}$  resonance assignments of a 21-amino acid glycopeptide prepared from human serum transferrin. *Carbohydr. Res.* **296**, 1–21 (1996).
- Fearon, D. T. & Locksley, R. M. The instructive role of innate immunity in the acquired immune response. *Science* **272**, 50–54 (1996).
- Medzhitov, R. & Janeway, C. A. J. Innate immunity: the virtues of a nonclonal system of recognition. *Cell* **91**, 295–298 (1997).
- Wyatt, R. *et al.* The antigenic structure of the HIV gp120 envelope glycoprotein. *Nature* **393**, 705–711 (1998).
- Botarelli, P. *et al.* N-glycosylation of HIV gp120 may constrain recognition by T lymphocytes. *J. Immunol.* **147**, 3128–3132 (1991).
- Davidson, H. W., West, M. A. & Watts, C. Endocytosis, intracellular trafficking, and processing of membrane IgG and monovalent antigen/membrane IgG complexes in B lymphocytes. *J. Immunol.* **144**, 4101–4109 (1990).
- Barrett, A. J. & Kirschke, H. Cathepsin B, cathepsin H and cathepsin L. *Methods Enzymol.* **80**, 535–559 (1981).
- Makoff, A. J., Ballantine, S. P., Smallwood, A. E. & Fairweather, N. F. Expression of tetanus toxin fragment C in *E. coli*: its purification and potential use as a vaccine. *Biotechnology* **7**, 1043–1046 (1989).
- Lane, D. P. & Harlow, E. *Antibodies: A Laboratory Manual* (Cold Spring Harbor Laboratory Press, 1988).
- Lanzavecchia, A. Antigen-specific interaction between T and B cells. *Nature* **314**, 537–539 (1985).
- Pond, L. & Watts, C. Characterization of transport of newly assembled, T cell-stimulatory MHC class II-peptide complexes from MHC class II compartments to the cell surface. *J. Immunol.* **159**, 543–553 (1997).

**Acknowledgements.** We thank M. Ferguson for helpful discussions and advice; E. Smythe and L. Grayson for advice and technical assistance; B. Spruce, A. Knight and the BTS (Ninewells Hospital) for help with blood monocyte preparation; and our colleagues for many helpful comments on the manuscript. This work was supported by the Wellcome Trust and by an EMBO Long-term fellowship to B. M.

Correspondence and requests for materials should be addressed to C.W. (e-mail: c.watts@dundee.ac.uk).

## Genomic amplification of a decoy receptor for Fas ligand in lung and colon cancer

Robert M. Pitti<sup>†</sup>, Scot A. Marsters<sup>†</sup>, David A. Lawrence<sup>†</sup>, Margaret Roy<sup>\*</sup>, Frank C. Kischkel<sup>\*</sup>, Patrick Dowd<sup>\*</sup>, Arthur Huang<sup>\*</sup>, Christopher J. Donahue<sup>\*</sup>, Steven W. Sherwood<sup>\*</sup>, Daryl T. Baldwin<sup>\*</sup>, Paul J. Godowski<sup>\*</sup>, William I. Wood<sup>\*</sup>, Austin L. Gurney<sup>\*</sup>, Kenneth J. Hillan<sup>\*</sup>, Robert L. Cohen<sup>\*</sup>, Audrey D. Goddard<sup>\*</sup>, David Botstein<sup>‡</sup> & Avi Ashkenazi<sup>\*</sup>

<sup>\*</sup> Departments of Molecular Oncology, Molecular Biology, and Immunology, Genentech Inc., 1 DNA Way, South San Francisco, California 94080, USA

<sup>‡</sup> Department of Genetics, Stanford University, Stanford, California 94305, USA

<sup>†</sup> These authors contributed equally to this work

Fas ligand (FasL) is produced by activated T cells and natural killer cells and it induces apoptosis (programmed cell death) in target cells through the death receptor Fas/Apo1/CD95 (ref. 1). One important role of FasL and Fas is to mediate immune-cytotoxic killing of cells that are potentially harmful to the organism, such as virus-infected or tumour cells<sup>1</sup>. Here we report the discovery of a soluble decoy receptor, termed decoy receptor 3 (DcR3), that binds to FasL and inhibits FasL-induced apoptosis. The DcR3 gene was amplified in about half of 35 primary lung and colon tumours studied, and DcR3 messenger RNA was expressed in malignant tissue. Thus, certain tumours may escape FasL-dependent immune-cytotoxic attack by expressing a decoy receptor that blocks FasL.

By searching expressed sequence tag (EST) databases, we identified a set of related ESTs that showed homology to the tumour necrosis factor (TNF) receptor (TNFR) gene superfamily<sup>2</sup>. Using the overlapping sequence, we isolated a previously unknown full-length complementary DNA from human fetal lung. We named the protein encoded by this cDNA decoy receptor 3 (DcR3). The cDNA encodes a 300-amino-acid polypeptide that resembles members of the TNFR family (Fig. 1a): the amino terminus contains a leader sequence, which is followed by four tandem cysteine-rich domains (CRDs). Like one other TNFR homologue, osteoprotegerin (OPG)<sup>3</sup>, DcR3 lacks an apparent transmembrane sequence, which indicates that it may be a secreted, rather than a membrane-associated, molecule. We expressed a recombinant, histidine-tagged form of DcR3 in mammalian cells; DcR3 was secreted into the cell culture medium, and migrated on polyacrylamide gels as a protein of relative molecular mass 35,000 (data not shown). DcR3 shares sequence identity in particular with OPG (31%) and TNFR2 (29%), and has relatively less homology with Fas (17%). All of the cysteines in the four CRDs of DcR3 and OPG are conserved; however, the carboxy-terminal portion of DcR3 is 101 residues shorter.

We analysed expression of DcR3 mRNA in human tissues by northern blotting (Fig. 1b). We detected a predominant 1.2-kilobase transcript in fetal lung, brain, and liver, and in adult spleen, colon and lung. In addition, we observed relatively high DcR3 mRNA expression in the human colon carcinoma cell line SW480.

To investigate potential ligand interactions of DcR3, we generated a recombinant, Fc-tagged DcR3 protein. We tested binding of DcR3–Fc to human 293 cells transfected with individual TNF-family ligands, which are expressed as type 2 transmembrane proteins (these transmembrane proteins have their N termini in the cytosol). DcR3–Fc showed a significant increase in binding to cells transfected with FasL<sup>4</sup> (Fig. 2a), but not to cells transfected with TNF<sup>5</sup>, Apo2L/TRAIL<sup>6,7</sup>, Apo3L/TWEAK<sup>8,9</sup>, or OPGL/TRANCE/

RANKL<sup>10-12</sup> (data not shown). DcR3-Fc immunoprecipitated shed FasL from FasL-transfected 293 cells (Fig. 2b) and purified soluble FasL (Fig. 2c), as did the Fc-tagged ectodomain of Fas but not TNFR1. Gel-filtration chromatography showed that DcR3-Fc and soluble FasL formed a stable complex (Fig. 2d). Equilibrium analysis indicated that DcR3-Fc and Fas-Fc bound to soluble FasL with a comparable affinity ( $K_d = 0.8 \pm 0.2$  and  $1.1 \pm 0.1$  nM, respectively; Fig. 2e), and that DcR3-Fc could block nearly all of the binding of soluble FasL to Fas-Fc (Fig. 2e, inset). Thus, DcR3 competes with Fas for binding to FasL.

To determine whether binding of DcR3 inhibits FasL activity, we tested the effect of DcR3-Fc on apoptosis induction by soluble FasL in Jurkat T leukaemia cells, which express Fas (Fig. 3a). DcR3-Fc and Fas-Fc blocked soluble-FasL-induced apoptosis in a similar dose-dependent manner, with half-maximal inhibition at  $\sim 0.1 \mu\text{g ml}^{-1}$ . Time-course analysis showed that the inhibition did not merely delay cell death, but rather persisted for at least 24 hours (Fig. 3b). We also tested the effect of DcR3-Fc on activation-induced cell death (AICD) of mature T lymphocytes, a FasL-dependent process<sup>1</sup>. Consistent with previous results<sup>13</sup>, activation of interleukin-2-stimulated CD4-positive T cells with anti-CD3 antibody increased the level of apoptosis twofold, and Fas-Fc blocked this effect substantially (Fig. 3c); DcR3-Fc blocked the

induction of apoptosis to a similar extent. Thus, DcR3 binding blocks apoptosis induction by FasL.

FasL-induced apoptosis is important in elimination of virus-infected cells and cancer cells by natural killer cells and cytotoxic T lymphocytes; an alternative mechanism involves perforin and granzymes<sup>1,14-16</sup>. Peripheral blood natural killer cells triggered marked cell death in Jurkat T leukaemia cells (Fig. 3d); DcR3-Fc and Fas-Fc each reduced killing of target cells from  $\sim 65\%$  to  $\sim 30\%$ , with half-maximal inhibition at  $\sim 1 \mu\text{g ml}^{-1}$ ; the residual killing was probably mediated by the perforin/granzyme pathway. Thus, DcR3 binding blocks FasL-dependent natural killer cell activity. Higher DcR3-Fc and Fas-Fc concentrations were required to block soluble FasL activity, which is consistent with the greater potency of membrane-associated FasL compared with soluble FasL<sup>17</sup>.

Given the role of immune-cytotoxic cells in elimination of tumour cells and the fact that DcR3 can act as an inhibitor of FasL, we proposed that DcR3 expression might contribute to the ability of some tumours to escape immune-cytotoxic attack. As genomic amplification frequently contributes to tumorigenesis, we investigated whether the DcR3 gene is amplified in cancer. We analysed DcR3 gene-copy number by quantitative polymerase chain

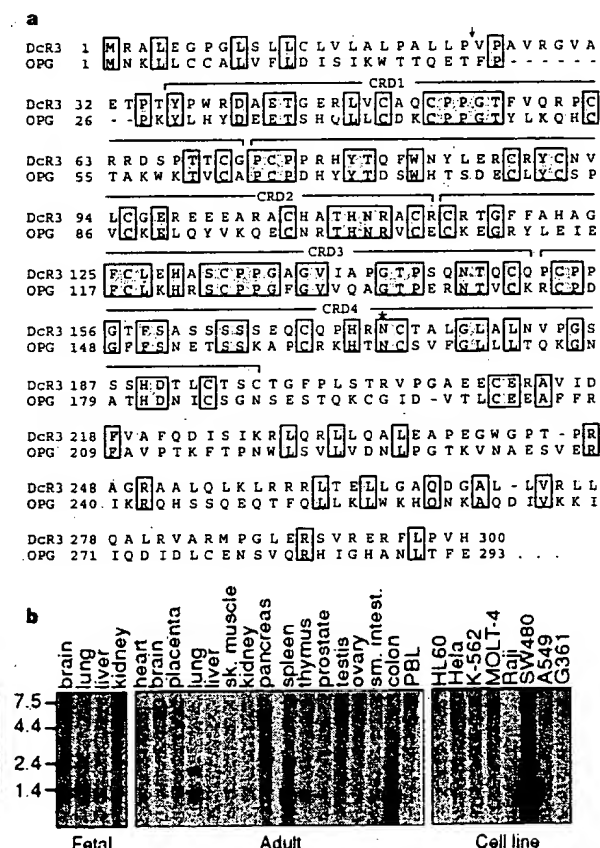


**Figure 1** Primary structure and expression of human DcR3. **a**, Alignment of the amino-acid sequences of DcR3 and of osteoprotegerin (OPG); the C-terminal 101 residues of OPG are not shown. The putative signal cleavage site (arrow), the cysteine-rich domains (CRD 1-4), and the N-linked glycosylation site (asterisk) are shown. **b**, Expression of DcR3 mRNA. Northern hybridization analysis was done using the DcR3 cDNA as a probe and blots of poly(A)<sup>+</sup> RNA (Clontech) from human fetal and adult tissues or cancer cell lines. PBL, peripheral blood lymphocyte.

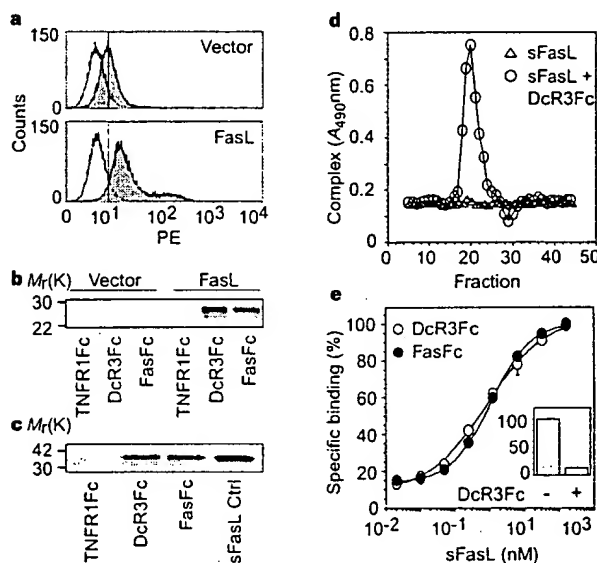


**Figure 2** Interaction of DcR3 with FasL. **a**, 293 cells were transfected with pRK5 vector (top) or with pRK5 encoding full-length FasL (bottom), incubated with DcR3-Fc (solid line, shaded area), TNFR1-Fc (dotted line) or buffer control (dashed line) (the dashed and dotted lines overlap), and analysed for binding by FACS. Statistical analysis showed a significant difference ( $P < 0.001$ ) between the binding of DcR3-Fc to cells transfected with FasL or pRK5. PE, phycoerythrin-labelled cells. **b**, 293 cells were transfected as in **a** and metabolically labelled, and cell supernatants were immunoprecipitated with Fc-tagged TNFR1, DcR3 or Fas. **c**, Purified soluble FasL (sFasL) was immunoprecipitated with TNFR1-Fc, DcR3-Fc or Fas-Fc and visualized by immunoblot with anti-FasL antibody. sFasL was loaded directly for comparison in the right-hand lane. **d**, Flag-tagged sFasL was incubated with DcR3-Fc or with buffer and resolved by gel filtration; column fractions were analysed in an assay that detects complexes containing DcR3-Fc and sFasL-Flag. **e**, Equilibrium binding of DcR3-Fc or Fas-Fc to sFasL-Flag. Inset, competition of DcR3-Fc with Fas-Fc for binding to sFasL-Flag.

reaction (PCR)<sup>18</sup> in genomic DNA from 35 primary lung and colon tumours, relative to pooled genomic DNA from peripheral blood leukocytes (PBLs) of 10 healthy donors. Eight of 18 lung tumours and 9 of 17 colon tumours showed DcR3 gene amplification, ranging from 2- to 18-fold (Fig. 4a, b). To confirm this result, we analysed the colon tumour DNAs with three more, independent sets of DcR3-based PCR primers and probes; we observed nearly the same amplification (data not shown).

We then analysed DcR3 mRNA expression in primary tumour tissue sections by *in situ* hybridization. We detected DcR3 expression in 6 out of 15 lung tumours, 2 out of 2 colon tumours, 2 out of 5 breast tumours, and 1 out of 1 gastric tumour (data not shown). A section through a squamous-cell carcinoma of the lung is shown in Fig. 4c. DcR3 mRNA was localized to infiltrating malignant epithelium, but was essentially absent from adjacent stroma, indicating tumour-specific expression. Although the individual tumour specimens that we analysed for mRNA expression and gene amplification were different, the *in situ* hybridization results are consistent with the finding that the DcR3 gene is amplified frequently in tumours. SW480 colon carcinoma cells, which showed abundant DcR3 mRNA expression (Fig. 1b), also had marked DcR3 gene amplification, as shown by quantitative PCR (fourfold) and by Southern blot hybridization (fivefold) (data not shown).

If DcR3 amplification in cancer is functionally relevant, then DcR3 should be amplified more than neighbouring genomic regions that are not important for tumour survival. To test this,

we mapped the human DcR3 gene by radiation-hybrid analysis; DcR3 showed linkage to marker AFM218xe7 (T160), which maps to chromosome position 20q13. Next, we isolated from a bacterial artificial chromosome (BAC) library a human genomic clone that carries DcR3, and sequenced the ends of the clone's insert. We then determined, from the nine colon tumours that showed twofold or greater amplification of DcR3, the copy number of the DcR3-flanking sequences (reverse and forward) from the BAC, and of seven genomic markers that span chromosome 20 (Fig. 4d). The DcR3-linked reverse marker showed an average amplification of roughly threefold, slightly less than the approximately fourfold amplification of DcR3; the other markers showed little or no amplification. These data indicate that DcR3 may be at the 'epicentre' of a distal chromosome 20 region that is amplified in colon cancer, consistent with the possibility that DcR3 amplification promotes tumour survival.

Our results show that DcR3 binds specifically to FasL and inhibits FasL activity. We did not detect DcR3 binding to several other TNF-ligand-family members; however, this does not rule out the possibility that DcR3 interacts with other ligands, as do some other TNFR family members, including OPG<sup>2,19</sup>.

FasL is important in regulating the immune response; however, little is known about how FasL function is controlled. One mechanism involves the molecule cFLIP, which modulates apoptosis signalling downstream of Fas<sup>20</sup>. A second mechanism involves proteolytic shedding of FasL from the cell surface<sup>17</sup>. DcR3 competes with Fas for

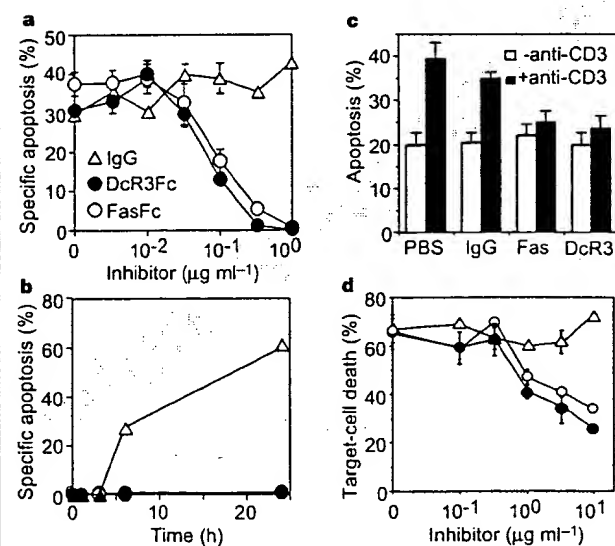


**Figure 3** Inhibition of FasL activity by DcR3. **a**, Human Jurkat T leukaemia cells were incubated with Flag-tagged soluble FasL (sFasL; 5 ng ml<sup>-1</sup>) oligomerized with anti-Flag antibody (0.1 μg ml<sup>-1</sup>) in the presence of the proposed inhibitors DcR3-Fc, Fas-Fc or human IgG1 and assayed for apoptosis (mean ± s.e.m. of triplicates). **b**, Jurkat cells were incubated with sFasL-Flag plus anti-Flag antibody as in **a**, in presence of 1 μg ml<sup>-1</sup> DcR3-Fc (filled circles), Fas-Fc (open circles) or human IgG1 (triangles), and apoptosis was determined at the indicated time points. **c**, Peripheral blood T cells were stimulated with PHA and interleukin-2, followed by control (white bars) or anti-CD3 antibody (filled bars), together with phosphate-buffered saline (PBS), human IgG1, Fas-Fc, or DcR3-Fc (10 μg ml<sup>-1</sup>). After 16 h, apoptosis of CD4<sup>+</sup> cells was determined (mean ± s.e.m. of results from five donors). **d**, Peripheral blood natural killer cells were incubated with <sup>51</sup>Cr-labelled Jurkat cells in the presence of DcR3-Fc (filled circles), Fas-Fc (open circles) or human IgG1 (triangles), and target-cell death was determined by release of <sup>51</sup>Cr (mean ± s.d. for two donors, each in triplicate).

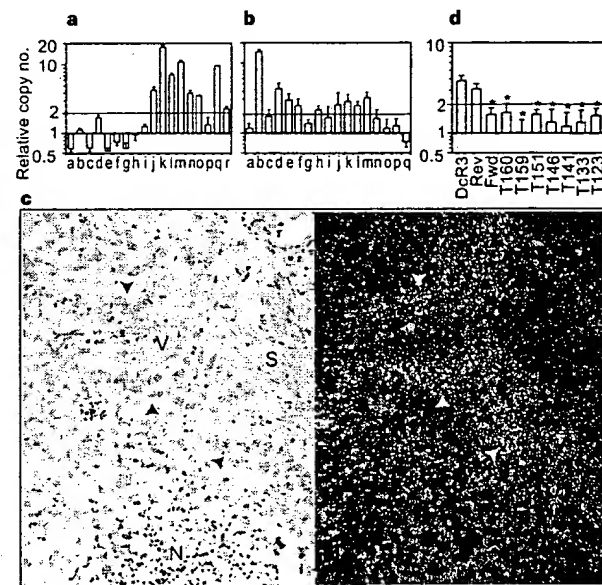


**Figure 4** Genomic amplification of DcR3 in tumours. **a**, Lung cancers, comprising eight adenocarcinomas (c, d, f, g, h, j, k, r), seven squamous-cell carcinomas (a, e, m, n, o, p, q), one non-small-cell carcinoma (b), one small-cell carcinoma (i), and one bronchial adenocarcinoma (l). The data are means ± s.d. of 2 experiments done in duplicate. **b**, Colon tumours, comprising 17 adenocarcinomas. Data are means ± s.e.m. of five experiments done in duplicate. **c**, *In situ* hybridization analysis of DcR3 mRNA expression in a squamous-cell carcinoma of the lung. A representative bright-field image (left) and the corresponding dark-field image (right) show DcR3 mRNA over infiltrating malignant epithelium (arrowheads). Adjacent non-malignant stroma (S), blood vessel (V) and necrotic tumour tissue (N) are also shown. **d**, Average amplification of DcR3 compared with amplification of neighbouring genomic regions (reverse and forward, Rev and Fwd), the DcR3-linked marker T160, and other chromosome-20 markers, in the nine colon tumours showing DcR3 amplification of twofold or more (b). Data are from two experiments done in duplicate. Asterisk indicates  $P < 0.01$  for a Student's *t*-test comparing each marker with DcR3.



FasL binding; hence, it may represent a third mechanism of extracellular regulation of FasL activity. A decoy receptor that modulates the function of the cytokine interleukin-1 has been described<sup>21</sup>. In addition, two decoy receptors that belong to the TNFR family, DcR1 and DcR2, regulate the FasL-related apoptosis-inducing molecule Apo2L<sup>22</sup>. Unlike DcR1 and DcR2, which are membrane-associated proteins, DcR3 is directly secreted into the extracellular space. One other secreted TNFR-family member is OPG<sup>3</sup>, which shares greater sequence homology with DcR3 (31%) than do DcR1 (17%) or DcR2 (19%); OPG functions as a third decoy for Apo2L<sup>19</sup>. Thus, DcR3 and OPG define a new subset of TNFR-family members that function as secreted decoys to modulate ligands that induce apoptosis. Pox viruses produce soluble TNFR homologues that neutralize specific TNF-family ligands, thereby modulating the antiviral immune response<sup>2</sup>. Our results indicate that a similar mechanism, namely, production of a soluble decoy receptor for FasL, may contribute to immune evasion by certain tumours. □

## Methods

**Isolation of DcR3 cDNA.** Several overlapping ESTs in GenBank (accession numbers AA025672, AA025673 and W67560) and in Lifeseq™ (Incyte Pharmaceuticals; accession numbers 1339238, 1533571, 1533650, 1542861, 1789372 and 2207027) showed similarity to members of the TNFR family. We screened human cDNA libraries by PCR with primers based on the region of EST consensus; fetal lung was positive for a product of the expected size. By hybridization to a PCR-generated probe based on the ESTs, one positive clone (DNA30942) was identified. When searching for potential alternatively spliced forms of DcR3 that might encode a transmembrane protein, we isolated 50 more clones; the coding regions of these clones were identical in size to that of the initial clone (data not shown).

**Fc-fusion proteins (immunoadhesins).** The entire DcR3 sequence, or the ectodomain of Fas or TNFR1, was fused to the hinge and Fc region of human IgG1, expressed in insect SF9 cells or in human 293 cells, and purified as described<sup>23</sup>.

**Fluorescence-activated cell sorting (FACS) analysis.** We transfected 293 cells using calcium phosphate or Effectene (Qiagen) with pRK5 vector or pRK5 encoding full-length human FasL (2 µg), together with pRK5 encoding CrmA (2 µg) to prevent cell death. After 16 h, the cells were incubated with biotinylated DcR3-Fc or TNFR1-Fc and then with phycoerythrin-conjugated streptavidin (GibcoBRL), and were assayed by FACS. The data were analysed by Kolmogorov-Smirnov statistical analysis. There was some detectable staining of vector-transfected cells by DcR3-Fc; as these cells express little FasL (data not shown), it is possible that DcR3 recognized some other factor that is expressed constitutively on 293 cells.

**Immunoprecipitation.** Human 293 cells were transfected as above, and metabolically labelled with [<sup>35</sup>S]cysteine and [<sup>35</sup>S]methionine (0.5 mCi; Amersham). After 16 h of culture in the presence of z-VAD-fmk (10 µM), the medium was immunoprecipitated with DcR3-Fc, Fas-Fc or TNFR1-Fc (5 µg), followed by protein A-Sepharose (Repligen). The precipitates were resolved by SDS-PAGE and visualized on a phosphorimager (Fuji BAS2000). Alternatively, purified, Flag-tagged soluble FasL (1 µg) (Alexis) was incubated with each Fc-fusion protein (1 µg), precipitated with protein A-Sepharose, resolved by SDS-PAGE and visualized by immunoblotting with rabbit anti-FasL antibody (Oncogene Research).

**Analysis of complex formation.** Flag-tagged soluble FasL (25 µg) was incubated with buffer or with DcR3-Fc (40 µg) for 1.5 h at 24°C. The reaction was loaded onto a Superdex 200 HR 10/30 column (Pharmacia) and developed with PBS; 0.6-ml fractions were collected. The presence of DcR3-Fc-FasL complex in each fraction was analysed by placing 100 µl aliquots into microtitre wells pre-coated with anti-human IgG (Boehringer) to capture DcR3-Fc, followed by detection with biotinylated anti-Flag antibody Bio M2 (Kodak) and streptavidin-horseradish peroxidase (Amersham). Calibration of the column indicated an apparent relative molecular mass of the complex of 420K (data not shown), which is consistent with a stoichiometry of two DcR3-Fc homodimers to two soluble FasL homotrimers.

**Equilibrium binding analysis.** Microtitre wells were coated with anti-human

IgG, blocked with 2% BSA in PBS. DcR3-Fc or Fas-Fc was added, followed by serially diluted Flag-tagged soluble FasL. Bound ligand was detected with anti-Flag antibody as above. In the competition assay, Fas-Fc was immobilized as above, and the wells were blocked with excess IgG1 before addition of Flag-tagged soluble FasL plus DcR3-Fc.

**T-cell AICD.** CD3<sup>+</sup> lymphocytes were isolated from peripheral blood of individual donors using anti-CD3 magnetic beads (Miltenyi Biotech), stimulated with phytohaemagglutinin (PHA; 2 µg ml<sup>-1</sup>) for 24 h, and cultured in the presence of interleukin-2 (100 U ml<sup>-1</sup>) for 5 days. The cells were plated in wells coated with anti-CD3 antibody (Pharmingen) and analysed for apoptosis 16 h later by FACS analysis of annexin-V-binding of CD4<sup>+</sup> cells<sup>24</sup>.

**Natural killer cell activity.** Natural killer cells were isolated from peripheral blood of individual donors using anti-CD56 magnetic beads (Miltenyi Biotech), and incubated for 16 h with <sup>51</sup>Cr-loaded Jurkat cells at an effector-to-target ratio of 1:1 in the presence of DcR3-Fc, Fas-Fc or human IgG1. Target-cell death was determined by release of <sup>51</sup>Cr in effector-target cocultures relative to release of <sup>51</sup>Cr by detergent lysis of equal numbers of Jurkat cells.

**Gene-amplification analysis.** Surgical specimens were provided by J. Kern (lung tumours) and P. Quirke (colon tumours). Genomic DNA was extracted (Qiagen) and the concentration was determined using Hoechst dye 33258 intercalation fluorimetry. Amplification was determined by quantitative PCR<sup>18</sup> using a TaqMan instrument (ABI). The method was validated by comparison of PCR and Southern hybridization data for the Myc and HER-2 oncogenes (data not shown). Gene-specific primers and fluorogenic probes were designed on the basis of the sequence of DcR3 or of nearby regions identified on a BAC carrying the human DcR3 gene; alternatively, primers and probes were based on Stanford Human Genome Center marker AFM218x7 (T160), which is linked to DcR3 (likelihood score = 5.4), SHGC-36268 (T159), the nearest available marker which maps to ~500 kilobases from T160, and five extra markers that span chromosome 20. The DcR3-specific primer sequences were 5'-CTTCTTCGCGCAGCTG-3' and 5'-ATCACGCCGGCACCAG-3' and the fluorogenic probe sequence was 5'-(FAM-ACACGATGCGGTGCTCAAGCAG AAp-(TAMARA), where FAM is 5'-fluorescein phosphoramidite. Relative gene-copy numbers were derived using the formula 2<sup>(ΔCT)</sup>, where ΔCT is the difference in amplification cycles required to detect DcR3 in peripheral blood lymphocyte DNA compared to test DNA.

Received 24 September; accepted 6 November 1998.

1. Nagata, S. Apoptosis by death factor. *Cell* 88, 355-365 (1997).
2. Smith, C. A., Farrah, T. & Goodwin, R. G. The TNF receptor superfamily of cellular and viral proteins: activation, costimulation, and death. *Cell* 76, 959-962 (1994).
3. Simonet, W. S. et al. Osteoprotegerin: a novel secreted protein involved in the regulation of bone density. *Cell* 89, 309-319 (1997).
4. Suda, T., Takahashi, T., Golstein, P. & Nagata, S. Molecular cloning and expression of Fas ligand, a novel member of the TNF family. *Cell* 75, 1169-1178 (1993).
5. Pennica, D. et al. Human tumour necrosis factor: precursor structure, expression and homology to lymphotoxin. *Nature* 312, 724-729 (1984).
6. Pitti, R. M. et al. Induction of apoptosis by Apo-2 ligand, a new member of the tumor necrosis factor receptor family. *J. Biol. Chem.* 271, 12687-12690 (1996).
7. Wiley, S. R. et al. Identification and characterization of a new member of the TNF family that induces apoptosis. *Immunity* 3, 673-682 (1995).
8. Marsters, S. A. et al. Identification of a ligand for the death-domain-containing receptor Apo3. *Curr. Biol.* 8, 525-528 (1998).
9. Chicheportiche, Y. et al. TWEAK, a new secreted ligand in the TNF family that weakly induces apoptosis. *J. Biol. Chem.* 272, 32401-32410 (1997).
10. Wong, B. R. et al. TRANCE is a novel ligand of the TNFR family that activates c-Jun-N-terminal kinase in T cells. *J. Biol. Chem.* 272, 25190-25194 (1997).
11. Anderson, D. M. et al. A homolog of the TNF receptor and its ligand enhance T-cell growth and dendritic cell function. *Nature* 390, 175-179 (1997).
12. Lacey, D. L. et al. Osteoprotegerin ligand is a cytokine that regulates osteoclast differentiation and activation. *Cell* 93, 165-176 (1998).
13. Dhein, J., Walczak, H., Baumler, C., Debatin, K. M. & Krammer, P. H. Autocrine T-cell suicide mediated by Apo1/Fas/CD95. *Nature* 373, 438-441 (1995).
14. Arase, H., Arase, N. & Saito, T. Fas-mediated cytotoxicity by freshly isolated natural killer cells. *J. Exp. Med.* 181, 1235-1238 (1995).
15. Medvedev, A. E. et al. Regulation of Fas and Fas ligand expression in NK cells by cytokines and the involvement of Fas ligand in NK/LAK cell-mediated cytotoxicity. *Cytokine* 9, 394-404 (1997).
16. Moretta, A. Mechanisms in cell-mediated cytotoxicity. *Cell* 90, 13-18 (1997).
17. Tanaka, M., Itai, T., Adachi, M. & Nagata, S. Downregulation of Fas ligand by shedding. *Nature Med.* 4, 31-36 (1998).
18. Gelmini, S. et al. Quantitative PCR-based homogeneous assay with fluorogenic probes to measure c-erbB-2 oncogene amplification. *Clin. Chem.* 43, 752-758 (1997).
19. Emery, J. G. et al. Osteoprotegerin is a receptor for the cytotoxic ligand TRAIL. *J. Biol. Chem.* 273, 14363-14367 (1998).
20. Wallach, D. Placing death under control. *Nature* 388, 123-125 (1997).
21. Collier, F. et al. Interleukin-1 type II receptor: a decoy target for IL-1 that is regulated by IL-4. *Science* 261, 472-475 (1993).

22. Ashkenazi, A. & Dixit, V. M. Death receptors: signaling and modulation. *Science* 281, 1305–1308 (1998).
23. Ashkenazi, A. & Chomow, S. M. Immunoadhesins as research tools and therapeutic agents. *Curr. Opin. Immunol.* 9, 195–200 (1997).
24. Marsters, S. et al. Activation of apoptosis by Apo-2 ligand is independent of FADD but blocked by CrmA. *Curr. Biol.* 6, 750–752 (1996).

Acknowledgements. We thank C. Clark, D. Pennica and V. Dixit for comments, and J. Kern and P. Quirke for tumour specimens.

Correspondence and requests for materials should be addressed to A.A. (e-mail: aa@gene.com). The GenBank accession number for the DcR3 cDNA sequence is AF104419.

## Crystal structure of the ATP-binding subunit of an ABC transporter

Li-Wei Hung\*, Iris Xiaoyan Wang†, Kishiko Nikaido†, Pei-Qi Liu†, Giovanna Ferro-Luzzi Ames† & Sung-Hou Kim\*‡

\* E. O. Lawrence Berkeley National Laboratory, † Department of Molecular and Cell Biology, and ‡ Department of Chemistry, University of California at Berkeley, Berkeley, California 94720, USA

ABC transporters (also known as traffic ATPases) form a large family of proteins responsible for the translocation of a variety of compounds across membranes of both prokaryotes and eukaryotes<sup>1</sup>. The recently completed *Escherichia coli* genome sequence revealed that the largest family of paralogous *E. coli* proteins is composed of ABC transporters<sup>2</sup>. Many eukaryotic proteins of medical significance belong to this family, such as the cystic fibrosis transmembrane conductance regulator (CFTR), the P-glycoprotein (or multidrug-resistance protein) and the heterodimeric transporter associated with antigen processing (Tap1–Tap2). Here we report the crystal structure at 1.5 Å resolution of HisP, the ATP-binding subunit of the histidine permease, which is an ABC transporter from *Salmonella typhimurium*. We correlate the details of this structure with the biochemical, genetic and biophysical properties of the wild-type and several mutant HisP proteins. The structure provides a basis for understanding properties of ABC transporters and of defective CFTR proteins.

ABC transporters contain four structural domains: two nucleotide-binding domains (NBDs), which are highly conserved throughout the family, and two transmembrane domains<sup>1</sup>. In prokaryotes these domains are often separate subunits which are assembled into a membrane-bound complex; in eukaryotes the domains are generally fused into a single polypeptide chain. The periplasmic histidine permease of *S. typhimurium* and *E. coli*<sup>3–6</sup> is a well-characterized ABC transporter that is a good model for this superfamily. It consists of a membrane-bound complex, HisQMP<sub>2</sub>, which comprises integral membrane subunits, HisQ and HisM, and two copies of HisP, the ATP-binding subunit. HisP, which has properties intermediate between those of integral and peripheral membrane proteins<sup>9</sup>, is accessible from both sides of the membrane, presumably by its interaction with HisQ and HisM<sup>6</sup>. The two HisP subunits form a dimer, as shown by their cooperativity in ATP hydrolysis<sup>5</sup>, the requirement for both subunits to be present for activity<sup>8</sup>, and the formation of a HisP dimer upon chemical cross-linking. Soluble HisP also forms a dimer<sup>3</sup>. HisP has been purified and characterized in an active soluble form<sup>3</sup> which can be reconstituted into a fully active membrane-bound complex<sup>8</sup>.

The overall shape of the crystal structure of the HisP monomer is that of an 'L' with two thick arms (arm I and arm II); the ATP-binding pocket is near the end of arm I (Fig. 1). A six-stranded  $\beta$ -sheet ( $\beta 3$  and  $\beta 8$ – $\beta 12$ ) spans both arms of the L, with a domain of a  $\alpha$ -plus  $\beta$ -type structure ( $\beta 1$ ,  $\beta 2$ ,  $\beta 4$ – $\beta 7$ ,  $\alpha 1$  and  $\alpha 2$ ) on one side (within arm I) and a domain of mostly  $\alpha$ -helices ( $\alpha 3$ – $\alpha 9$ ) on the

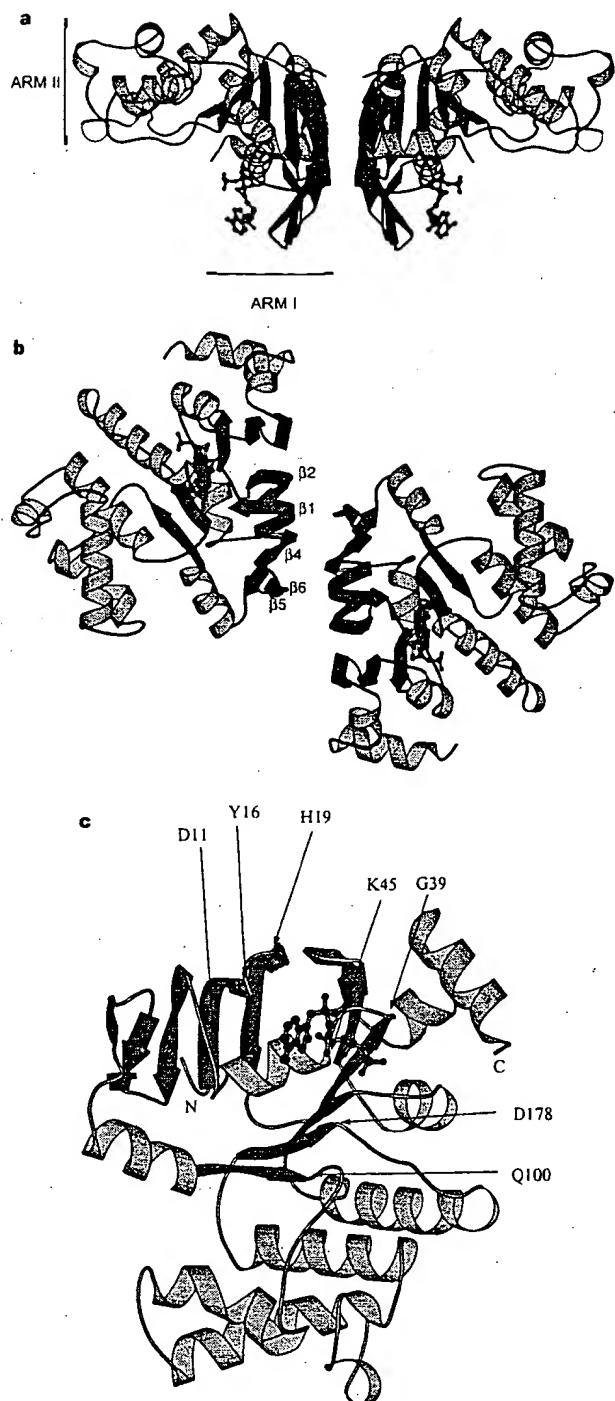


**Figure 1** Crystal structure of HisP. **a**, View of the dimer along an axis perpendicular to its two-fold axis. The top and bottom of the dimer are suggested to face towards the periplasmic and cytoplasmic sides, respectively (see text). The thickness of arm II is about 25 Å, comparable to that of membrane.  $\alpha$ -Helices are shown in orange and  $\beta$ -sheets in green. **b**, View along the two-fold axis of the HisP dimer, showing the relative displacement of the monomers not apparent in **a**. The  $\beta$ -strands at the dimer interface are labelled. **c**, View of one monomer from the bottom of arm I, as shown in **a**, towards arm II, showing the ATP-binding pocket. **a–c**, The protein and the bound ATP are in 'ribbon' and 'ball-and-stick' representations, respectively. Key residues discussed in the text are indicated in **c**. These figures were prepared with MOLSCRIPT<sup>28</sup>. N, amino terminus; C, C terminus.



## NOVEL APPROACH TO QUANTITATIVE POLYMERASE CHAIN REACTION USING REAL-TIME DETECTION: APPLICATION TO THE DETECTION OF GENE AMPLIFICATION IN BREAST CANCER

Ivan BIÈCHE<sup>1,2</sup>, Martine OLIVI<sup>1</sup>, Marie-Hélène CHAMPÈME<sup>2</sup>, Dominique VIDAUD<sup>1</sup>, Rosette LIDEREAU<sup>2</sup> and Michel VIDAUD<sup>1\*</sup>

<sup>1</sup>Laboratoire de Génétique Moléculaire, Faculté des Sciences Pharmaceutiques et Biologiques de Paris, Paris, France

<sup>2</sup>Laboratoire d'Oncogénétique, Centre René Huguenin, St-Cloud, France

Gene amplification is a common event in the progression of human cancers, and amplified oncogenes have been shown to have diagnostic, prognostic and therapeutic relevance. A kinetic quantitative polymerase-chain-reaction (PCR) method, based on fluorescent TaqMan methodology and a new instrument (ABI Prism 7700 Sequence Detection System) capable of measuring fluorescence in real-time, was used to quantify gene amplification in tumor DNA. Reactions are characterized by the point during cycling when PCR amplification is still in the exponential phase, rather than the amount of PCR product accumulated after a fixed number of cycles. None of the reaction components is limited during the exponential phase, meaning that values are highly reproducible in reactions starting with the same copy number. This greatly improves the precision of DNA quantification. Moreover, real-time PCR does not require post-PCR sample handling, thereby preventing potential PCR-product carry-over contamination; it possesses a wide dynamic range of quantification and results in much faster and higher sample throughput. The real-time PCR method, was used to develop and validate a simple and rapid assay for the detection and quantification of the 3 most frequently amplified genes (*myc*, *ccnd1* and *erbB2*) in breast tumors. Extra copies of *myc*, *ccnd1* and *erbB2* were observed in 10, 23 and 15%, respectively, of 108 breast-tumor DNA; the largest observed numbers of gene copies were 4.6, 18.6 and 15.1, respectively. These results correlated well with those of Southern blotting. The use of this new semi-automated technique will make molecular analysis of human cancers simpler and more reliable, and should find broad applications in clinical and research settings. *Int. J. Cancer* 78:661–666, 1998.

© 1998 Wiley-Liss, Inc.

Gene amplification plays an important role in the pathogenesis of various solid tumors, including breast cancer, probably because over-expression of the amplified target genes confers a selective advantage. The first technique used to detect genomic amplification was cytogenetic analysis. Amplification of several chromosome regions, visualized either as extrachromosomal double minutes (dmins) or as integrated homogeneously staining regions (HSRs), are among the main visible cytogenetic abnormalities in breast tumors. Other techniques such as comparative genomic hybridization (CGH) (Kallioniemi *et al.*, 1994) have also been used in broad searches for regions of increased DNA copy numbers in tumor cells, and have revealed some 20 amplified chromosome regions in breast tumors. Positional cloning efforts are underway to identify the critical gene(s) in each amplified region. To date, genes known to be amplified frequently in breast cancers include *myc* (8q24), *ccnd1* (11q13), and *erbB2* (17q12-q21) (for review, see Bièche and Lidereau, 1995).

Amplification of the *myc*, *ccnd1*, and *erbB2* proto-oncogenes should have clinical relevance in breast cancer, since independent studies have shown that these alterations can be used to identify sub-populations with a worse prognosis (Berns *et al.*, 1992; Schuurin *et al.*, 1992; Slamon *et al.*, 1987). Muss *et al.* (1994) suggested that these gene alterations may also be useful for the prediction and assessment of the efficacy of adjuvant chemotherapy and hormone therapy.

However, published results diverge both in terms of the frequency of these alterations and their clinical value. For instance, over 500 studies in 10 years have failed to resolve the controversy

surrounding the link suggested by Slamon *et al.* (1987) between *erbB2* amplification and disease progression. These discrepancies are partly due to the clinical, histological and ethnic heterogeneity of breast cancer, but technical considerations are also probably involved.

Specific genes (DNA) were initially quantified in tumor cells by means of blotting procedures such as Southern and slot blotting. These batch techniques require large amounts of DNA (5–10 µg/reaction) to yield reliable quantitative results. Furthermore, meticulous care is required at all stages of the procedures to generate blots of sufficient quality for reliable dosage analysis. Recently, PCR has proven to be a powerful tool for quantitative DNA analysis, especially with minimal starting quantities of tumor samples (small, early-stage tumors and formalin-fixed, paraffin-embedded tissues).

Quantitative PCR can be performed by evaluating the amount of product either after a given number of cycles (end-point quantitative PCR) or after a varying number of cycles during the exponential phase (kinetic quantitative PCR). In the first case, an internal standard distinct from the target molecule is required to ascertain PCR efficiency. The method is relatively easy but implies generating, quantifying and storing an internal standard for each gene studied. Nevertheless, it is the most frequently applied method to date.

One of the major advantages of the kinetic method is its rapidity in quantifying a new gene, since no internal standard is required (an external standard curve is sufficient). Moreover, the kinetic method has a wide dynamic range (at least 5 orders of magnitude), giving an accurate value for samples differing in their copy number. Unfortunately, the method is cumbersome and has therefore been rarely used. It involves aliquot sampling of each assay mix at regular intervals and quantifying, for each aliquot, the amplification product. Interest in the kinetic method has been stimulated by a novel approach using fluorescent TaqMan methodology and a new instrument (ABI Prism 7700 Sequence Detection System) capable of measuring fluorescence in real time (Gibson *et al.*, 1996; Heid *et al.*, 1996). The TaqMan reaction is based on the 5' nuclease assay first described by Holland *et al.* (1991). The latter uses the 5' nuclease activity of Taq polymerase to cleave a specific fluorogenic oligonucleotide probe during the extension phase of PCR. The approach uses dual-labeled fluorogenic hybridization probes (Lee *et al.*, 1993). One fluorescent dye, co-valently linked to the 5' end of the oligonucleotide, serves as a reporter [FAM (*i.e.*, 6-carboxy-fluorescein)] and its emission spectrum is quenched by a second fluorescent dye, TAMRA (*i.e.*, 6-carboxy-tetramethyl-rhodamine) attached to the 3' end. During the extension phase of the PCR

Grant sponsors: Association Pour la Recherche sur le Cancer and Ministère de l'Enseignement Supérieur et de la Recherche.

\*Correspondence to: Laboratoire de Génétique Moléculaire, Faculté des Sciences Pharmaceutiques et Biologiques de Paris, 4 Avenue de l'Observatoire, F-75006 Paris, France. Fax: (33)1-4407-1754. E-mail: mvidauid@teaser.fr

Received 2 May 1998; Revised 30 June 1998

cycle, the fluorescent hybridization probe is hydrolyzed by the 5'-3' nucleolytic activity of DNA polymerase. Nuclease degradation of the probe releases the quenching of FAM fluorescence emission, resulting in an increase in peak fluorescence emission. The fluorescence signal is normalized by dividing the emission intensity of the reporter dye (FAM) by the emission intensity of a reference dye (i.e., ROX, 6-carboxy-X-rhodamine) included in TaqMan buffer, to obtain a ratio defined as the  $R_n$  (normalized reporter) for a given reaction tube. The use of a sequence detector enables the fluorescence spectra of all 96 wells of the thermal cycler to be measured continuously during PCR amplification.

The real-time PCR method offers several advantages over other current quantitative PCR methods (Celi *et al.*, 1994): (i) the probe-based homogeneous assay provides a real-time method for detecting only specific amplification products, since specific hybridization of both the primers and the probe is necessary to generate a signal; (ii) the  $C_t$  (threshold cycle) value used for quantification is measured when PCR amplification is still in the log phase of PCR product accumulation. This is the main reason why  $C_t$  is a more reliable measure of the starting copy number than are end-point measurements, in which a slight difference in a limiting component can have a drastic effect on the amount of product; (iii) use of  $C_t$  values gives a wider dynamic range (at least 5 orders of magnitude), reducing the need for serial dilution; (iv) The real-time PCR method is run in a closed-tube system and requires no post-PCR sample handling, thus avoiding potential contamination; (v) the system is highly automated, since the instrument continuously measures fluorescence in all 96 wells of the thermal cycler during PCR amplification and the corresponding software processes, and analyzes the fluorescence data; (vi) the assay is rapid, as results are available just one minute after thermal cycling is complete; (vii) the sample throughput of the method is high, since 96 reactions can be analyzed in 2 hr.

Here, we applied this semi-automated procedure to determine the copy numbers of the 3 most frequently amplified genes in breast tumors (*myc*, *ccnd1* and *erbB2*), as well as 2 genes (*alb* and *app*) located in a chromosome region in which no genetic changes have been observed in breast tumors. The results for 108 breast tumors were compared with previous Southern-blot data for the same samples.

#### MATERIAL AND METHODS

##### Tumor and blood samples

Samples were obtained from 108 primary breast tumors removed surgically from patients at the Centre René Huguénin; none of the patients had undergone radiotherapy or chemotherapy. Immediately after surgery, the tumor samples were placed in liquid nitrogen until extraction of high-molecular-weight DNA. Patients were included in this study if the tumor sample used for DNA preparation contained more than 60% of tumor cells (histological analysis). A blood sample was also taken from 18 of the same patients.

DNA was extracted from tumor tissue and blood leukocytes according to standard methods.

##### Real-time PCR

**Theoretical basis.** Reactions are characterized by the point during cycling when amplification of the PCR product is first detected, rather than by the amount of PCR product accumulated after a fixed number of cycles. The higher the starting copy number of the genomic DNA target, the earlier a significant increase in fluorescence is observed. The parameter  $C_t$  (threshold cycle) is defined as the fractional cycle number at which the fluorescence generated by cleavage of the probe passes a fixed threshold above baseline. The target gene copy number in unknown samples is quantified by measuring  $C_t$  and by using a standard curve to determine the starting copy number. The precise amount of genomic DNA (based on optical density) and its quality (i.e., lack

of extensive degradation) are both difficult to assess. We therefore also quantified a control gene (*alb*) mapping to chromosome region 4q11-q13, in which no genetic alterations have been found in breast-tumor DNA by means of CGH (Kallioniemi *et al.*, 1994).

Thus, the ratio of the copy number of the target gene to the copy number of the *alb* gene normalizes the amount and quality of genomic DNA. The ratio defining the level of amplification is termed "N", and is determined as follows:

$$N = \frac{\text{copy number of target gene (app, myc, ccnd1, erbB2)}}{\text{copy number of reference gene (alb)}}$$

**Primers, probes, reference human genomic DNA and PCR consumables.** Primers and probes were chosen with the assistance of the computer programs Oligo 4.0 (National Biosciences, Plymouth, MN), EuGene (Daniben Systems, Cincinnati, OH) and Primer Express (Perkin-Elmer Applied Biosystems, Foster City, CA).

Primers were purchased from DNAgency (Malvern, PA) and probes from Perkin-Elmer Applied Biosystems.

Nucleotide sequences for the oligonucleotide hybridization probes and primers are available on request.

The TaqMan PCR Core reagent kit, MicroAmp optical tubes, and MicroAmp caps were from Perkin-Elmer Applied Biosystems.

**Standard-curve construction.** The kinetic method requires a standard curve. The latter was constructed with serial dilutions of specific PCR products, according to Piatak *et al.* (1993). In practice, each specific PCR product was obtained by amplifying 20 ng of a standard human genomic DNA (Boehringer, Mannheim, Germany) with the same primer pairs as those used later for real-time quantitative PCR. The 5 PCR products were purified using MicroSpin S-400 HR columns (Pharmacia, Uppsala, Sweden) electrophoresed through an acrylamide gel and stained with ethidium bromide to check their quality. The PCR products were then quantified spectrophotometrically and pooled, and serially diluted 10-fold in mouse genomic DNA (Clontech, Palo Alto, CA) at a constant concentration of 2 ng/ $\mu$ l. The standard curve used for real-time quantitative PCR was based on serial dilutions of the pool of PCR products ranging from  $10^{-7}$  ( $10^5$  copies of each gene) to  $10^{-10}$  ( $10^2$  copies). This series of diluted PCR products was aliquoted and stored at  $-80^\circ\text{C}$  until use.

The standard curve was validated by analyzing 2 known quantities of calibrator human genomic DNA (20 ng and 50 ng).

**PCR amplification.** Amplification mixes (50  $\mu$ l) contained the sample DNA (around 20 ng, around 6600 copies of disomic genes),  $10\times$  TaqMan buffer (5  $\mu$ l), 200  $\mu$ M dATP, dCTP, dGTP, and 400  $\mu$ M dUTP, 5 mM  $\text{MgCl}_2$ , 1.25 units of AmpliTaq Gold, 0.5 units of AmpErase uracil N-glycosylase (UNG), 200 nM each primer and 100 nM probe. The thermal cycling conditions comprised 2 min at  $50^\circ\text{C}$  and 10 min at  $95^\circ\text{C}$ . Thermal cycling consisted of 40 cycles at  $95^\circ\text{C}$  for 15 s and  $65^\circ\text{C}$  for 1 min. Each assay included: a standard curve (from  $10^5$  to  $10^2$  copies) in duplicate, a no-template control, 20 ng and 50 ng of calibrator human genomic DNA (Boehringer) in triplicate, and about 20 ng of unknown genomic DNA in triplicate (26 samples can thus be analyzed on a 96-well microplate). All samples with a coefficient of variation (CV) higher than 10% were retested.

All reactions were performed in the ABI Prism 7700 Sequence Detection System (Perkin-Elmer Applied Biosystems), which detects the signal from the fluorogenic probe during PCR.

**Equipment for real-time detection.** The 7700 system has a built-in thermal cycler and a laser directed via fiber optical cables to each of the 96 sample wells. A charge-coupled-device (CDD) camera collects the emission from each sample and the data are analyzed automatically. The software accompanying the 7700 system calculates  $C_t$  and determines the starting copy number in the samples.

**Determination of gene amplification.** Gene amplification was calculated as described above. Only samples with an N value higher than 2 were considered to be amplified.

### RESULTS

To validate the method, real-time PCR was performed on genomic DNA extracted from 108 primary breast tumors, and 18 normal leukocyte DNA samples from some of the same patients. The target genes were the *myc*, *ccnd1*, and *erbB2* proto-oncogenes, and the  $\beta$ -amyloid precursor protein gene (*app*), which maps to a chromosome region (21q21.2) in which no genetic alterations have been found in breast tumors (Kallioniemi *et al.*, 1994). The reference disomic gene was the albumin gene (*alb*, chromosome 4q11-q13).

### Validation of the standard curve and dynamic range of real-time PCR

The standard curve was constructed from PCR products serially diluted in genomic mouse DNA at a constant concentration of 2 ng/ $\mu$ l. It should be noted that the 5 primer pairs chosen to analyze the 5 target genes do not amplify genomic mouse DNA (data not shown). Figure 1 shows the real-time PCR standard curve for the *alb* gene. The dynamic range was wide (at least 4 orders of magnitude), with samples containing as few as  $10^2$  copies or as many as  $10^5$  copies.

### Copy-number ratio of the 2 reference genes (*app* and *alb*)

The *app* to *alb* copy-number ratio was determined in 18 normal leukocyte DNA samples and all 108 primary breast-tumor DNA

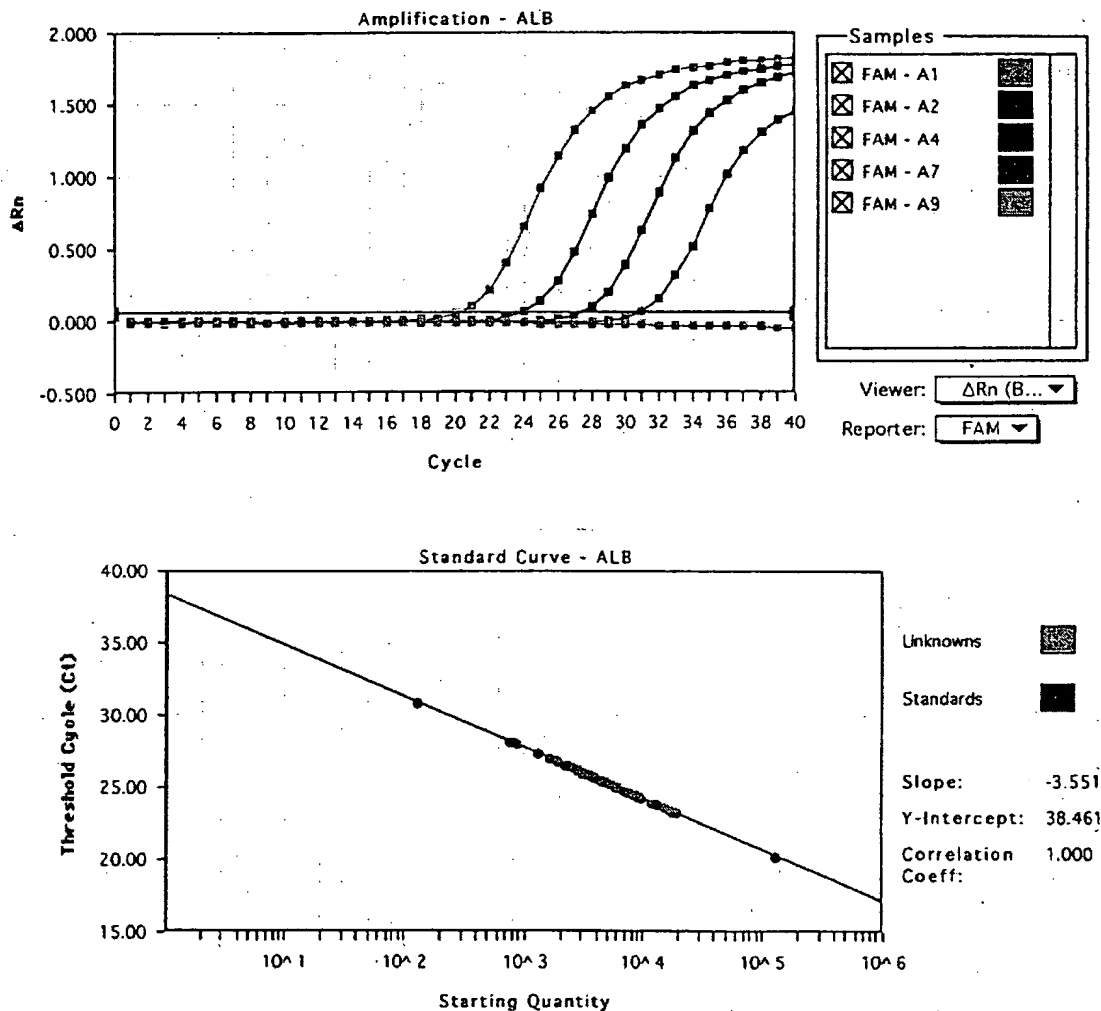


**FIGURE 1** – Albumin (*alb*) gene dosage by real-time PCR. Top: Amplification plots for reactions with starting *alb* gene copy number ranging from  $10^5$  (A9),  $10^4$  (A7),  $10^3$  (A4) to  $10^2$  (A2) and a no-template control (A1). Cycle number is plotted vs. change in normalized reporter signal ( $\Delta Rn$ ). For each reaction tube, the fluorescence signal of the reporter dye (FAM) is divided by the fluorescence signal of the passive reference dye (ROX), to obtain a ratio defined as the normalized reporter signal (Rn).  $\Delta Rn$  represents the normalized reporter signal (Rn) minus the baseline signal established in the first 15 PCR cycles.  $\Delta Rn$  increases during PCR as *alb* PCR product copy number increases until the reaction reaches a plateau.  $C_t$  (threshold cycle) represents the fractional cycle number at which a significant increase in Rn above a baseline signal (horizontal black line) can first be detected. Two replicate plots were performed for each standard sample, but the data for only one are shown here. Bottom: Standard curve plotting log starting copy number vs.  $C_t$  (threshold cycle). The black dots represent the data for standard samples plotted in duplicate and the red dots the data for unknown genomic DNA samples plotted in triplicate. The standard curve shows 4 orders of linear dynamic range.

samples. We selected these 2 genes because they are located in 2 chromosome regions (*app*, 21q21.2; *alb*, 4q11-q13) in which no obvious genetic changes (including gains or losses) have been observed in breast cancers (Kallioniemi *et al.*, 1994). The ratio for the 18 normal leukocyte DNA samples fell between 0.7 and 1.3 (mean  $1.02 \pm 0.21$ ), and was similar for the 108 primary breast-tumor DNA samples (0.6 to 1.6, mean  $1.06 \pm 0.25$ ), confirming that *alb* and *app* are appropriate reference disomic genes for breast-tumor DNA. The low range of the ratios also confirmed that the nucleotide sequences chosen for the primers and probes were not polymorphic, as mismatches of their primers or probes with the subject's DNA would have resulted in differential amplification.

#### *myc*, *ccnd1* and *erbB2* gene dose in normal leukocyte DNA

To determine the cut-off point for gene amplification in breast-cancer tissue, 18 normal leukocyte DNA samples were tested for the gene dose (N), calculated as described in "Material and Methods". The N value of these samples ranged from 0.5 to 1.3 (mean  $0.84 \pm 0.22$ ) for *myc*, 0.7 to 1.6 (mean  $1.06 \pm 0.23$ ) for *ccnd1* and 0.6 to 1.3 (mean  $0.91 \pm 0.19$ ) for *erbB2*. Since N values for *myc*, *ccnd1* and *erbB2* in normal leukocyte DNA consistently fell between 0.5 and 1.6, values of 2 or more were considered to represent gene amplification in tumor DNA.

#### *myc*, *ccnd1* and *erbB2* gene dose in breast-tumor DNA

*myc*, *ccnd1* and *erbB2* gene copy numbers in the 108 primary breast tumors are reported in Table I. Extra copies of *ccnd1* were more frequent (23%, 25/108) than extra copies of *erbB2* (15%, 16/108) and *myc* (10%, 11/108), and ranged from 2 to 18.6 for *ccnd1*, 2 to 15.1 for *erbB2*, and only 2 to 4.6 for the *myc* gene. Figure 2 and Table II represent tumors in which the *ccnd1* gene was amplified 16-fold (T145), 6-fold (T133) and non-amplified (T118). The 3 genes were never found to be co-amplified in the same tumor. *erbB2* and *ccnd1* were co-amplified in only 3 cases, *myc* and *ccnd1* in 2 cases and *myc* and *erbB2* in 1 case. This favors the hypothesis that gene amplifications are independent events in breast cancer. Interestingly, 5 tumors showed a decrease of at least 50% in the *erbB2* copy number ( $N < 0.5$ ), suggesting that they bore deletions of the 17q21 region (the site of *erbB2*). No such decrease in copy number was observed with the other 2 proto-oncogenes.

#### Comparison of gene dose determined by real-time quantitative PCR and Southern-blot analysis

Southern-blot analysis of *myc*, *ccnd1* and *erbB2* amplifications had previously been done on the same 108 primary breast tumors. A perfect correlation between the results of real-time PCR and Southern blot was obtained for tumors with high copy numbers ( $N \geq 5$ ). However, there were cases (1 *myc*, 6 *ccnd1* and 4 *erbB2*) in which real-time PCR showed gene amplification whereas Southern-blot did not, but these were mainly cases with low extra copy numbers (N from 2 to 2.9).

### DISCUSSION

The clinical applications of gene amplification assays are currently limited, but would certainly increase if a simple, standardized and rapid method were perfected. Gene amplification status has been studied mainly by means of Southern blotting, but this method is not sensitive enough to detect low-level gene amplification nor accurate enough to quantify the full range of amplification values. Southern blotting is also time-consuming, uses radioactive

reagents and requires relatively large amounts of high-quality genomic DNA, which means it cannot be used routinely in many laboratories. An amplification step is therefore required to determine the copy number of a given target gene from minimal quantities of tumor DNA (small early-stage tumors, cytopuncture specimens or formalin-fixed, paraffin-embedded tissues).

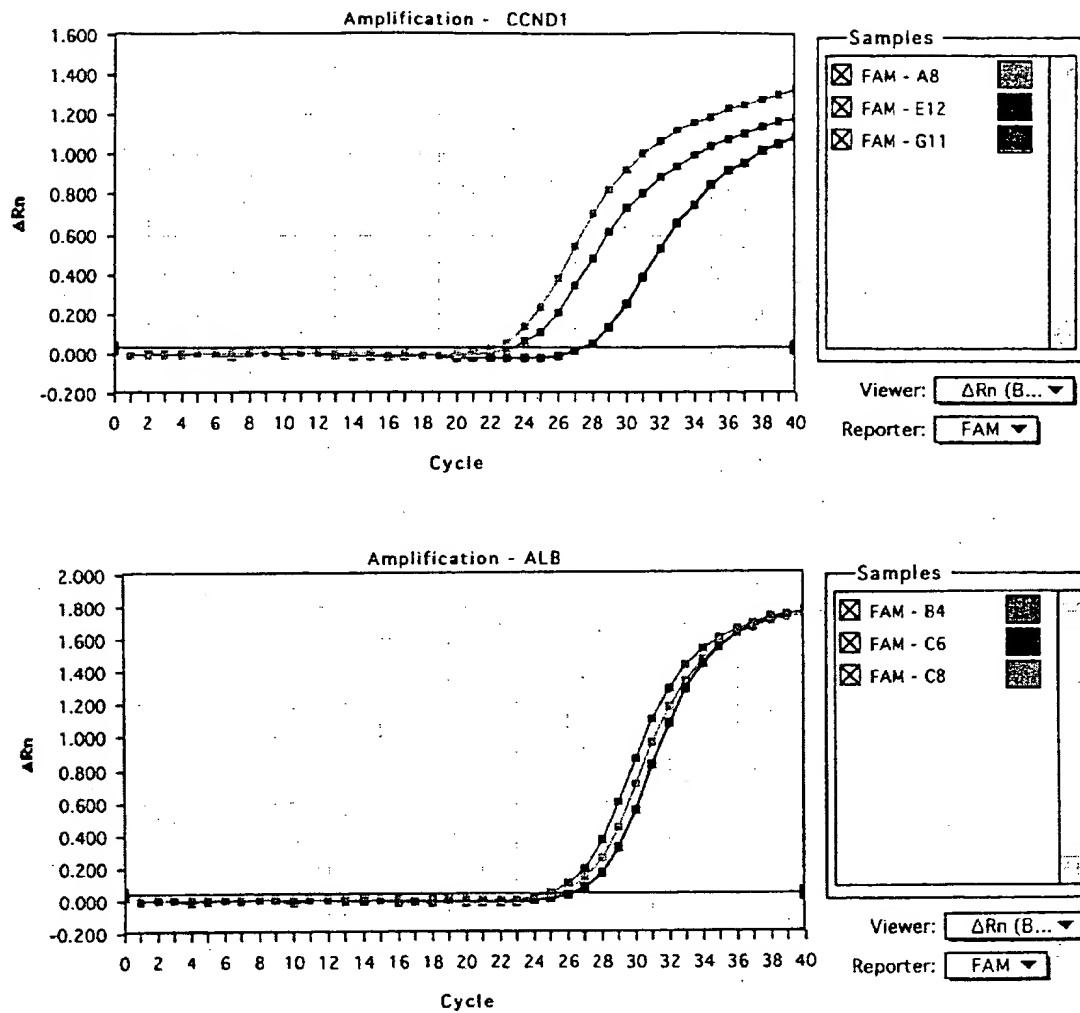
In this study, we validated a PCR method developed for the quantification of gene over-representation in tumors. The method, based on real-time analysis of PCR amplification, has several advantages over other PCR-based quantitative assays such as competitive quantitative PCR (Celi *et al.*, 1994). First, the real-time PCR method is performed in a closed-tube system, avoiding the risk of contamination by amplified products. Re-amplification of carryover PCR products in subsequent experiments can also be prevented by using the enzyme uracil N-glycosylase (UNG) (Longo *et al.*, 1990). The second advantage is the simplicity and rapidity of sample analysis, since no post-PCR manipulations are required. Our results show that the automated method is reliable. We found it possible to determine, in triplicate, the number of copies of a target gene in more than 100 tumors per day. Third, the system has a linear dynamic range of at least 4 orders of magnitude, meaning that samples do not have to contain equal starting amounts of DNA. This technique should therefore be suitable for analyzing formalin-fixed, paraffin-embedded tissues. Fourth, and above all, real-time PCR makes DNA quantification much more precise and reproducible, since it is based on  $C_t$  values rather than end-point measurement of the amount of accumulated PCR product. Indeed, the ABI Prism 7700 Sequence Detection System enables  $C_t$  to be calculated when PCR amplification is still in the exponential phase and when none of the reaction components is rate-limiting. The within-run CV of the  $C_t$  value for calibrator human DNA (5 replicates) was always below 5%, and the between-assay precision in 5 different runs was always below 10% (data not shown). In addition, the use of a standard curve is not absolutely necessary, since the copy number can be determined simply by comparing the  $C_t$  ratio of the target gene with that of reference genes. The results obtained by the 2 methods (with and without a standard curve) are similar in our experiments (data not shown). Moreover, unlike competitive quantitative PCR, real-time PCR does not require an internal control (the design and storage of internal controls and the validation of their amplification efficiency is laborious).

The only potential disadvantage of real-time PCR, like all other PCR-based methods and solid-matrix blotting techniques (Southern blots and dot blots) is that it cannot avoid dilution artifacts inherent in the extraction of DNA from tumor cells contained in heterogeneous tissue specimens. Only FISH and immunohistochemistry can measure alterations on a cell-by-cell basis (Pauletti *et al.*, 1996; Slamon *et al.*, 1989). However, FISH requires expensive equipment and trained personnel and is also time-consuming. Moreover, FISH does not assess gene expression and therefore cannot detect cases in which the gene product is over-expressed in the absence of gene amplification, which will be possible in the future by real-time quantitative RT-PCR. Immunohistochemistry is subject to considerable variations in the hands of different teams, owing to alterations of target proteins during the procedure, the different primary antibodies and fixation methods used and the criteria used to define positive staining.

The results of this study are in agreement with those reported in the literature. (i) Chromosome regions 4q11-q13 and 21q21.2 (which bear *alb* and *app*, respectively) showed no genetic alterations in the breast-cancer samples studied here, in keeping with the results of CGH (Kallioniemi *et al.*, 1994). (ii) We found that amplifications of these 3 oncogenes were independent events, as reported by other teams (Berns *et al.*, 1992; Borg *et al.*, 1992). (iii) The frequency and degree of *myc* amplification in our breast tumor DNA series were lower than those of *ccnd1* and *erbB2* amplification, confirming the findings of Borg *et al.* (1992) and Courjal *et al.* (1997). (iv) The maxima of *ccnd1* and *erbB2* over-representation were 18-fold and 15-fold, also in keeping with earlier results (about

TABLE I - DISTRIBUTION OF AMPLIFICATION LEVEL (N) FOR *myc*, *ccnd1* AND *erbB2* GENES IN 108 HUMAN BREAST TUMORS

Gene	Amplification level (N)			
	<0.5	0.5-1.9	2-4.9	$\geq 5$
<i>myc</i>	0	97 (89.8%)	11 (10.2%)	0
<i>ccnd1</i>	0	83 (76.9%)	17 (15.7%)	8 (7.4%)
<i>erbB2</i>	5 (4.6%)	87 (80.6%)	8 (7.4%)	8 (7.4%)



Tumor	CCND1		ALB	
	$C_t$	Copy number	$C_t$	Copy number
T118	27.3	4605	26.5	4365
T133	23.2	61659	25.2	10092
T145	22.1	125892	25.6	7762

FIGURE 2 - *ccnd1* and *alb* gene dosage by real-time PCR in 3 breast tumor samples: T118 (E12, C6, black squares), T133 (G11, B4, red squares) and T145 (A8, C8, blue squares). Given the  $C_t$  of each sample, the initial copy number is inferred from the standard curve obtained during the same experiment. Triplicate plots were performed for each tumor sample, but the data for only one are shown here. The results are shown in Table II.

30-fold maximum) (Berns *et al.*, 1992; Borg *et al.*, 1992; Courjal *et al.*, 1997). (v) The *erbB2* copy numbers obtained with real-time PCR were in good agreement with data obtained with other quantitative PCR-based assays in terms of the frequency and degree of amplification (An *et al.*, 1995; Deng *et al.*, 1996; Valeron

*et al.*, 1996). Our results also correlate well with those recently published by Gelmini *et al.* (1997), who used the TaqMan system to measure *erbB2* amplification in a small series of breast tumors ( $n = 25$ ), but with an instrument (LS-50B luminescence spectrometer, Perkin-Elmer Applied Biosystems) which only allows end-

TABLE II - EXAMPLES OF *ccnd1* GENE DOSAGE RESULTS FROM 3 BREAST TUMORS<sup>1</sup>

Tumor	<i>ccnd1</i>			<i>alb</i>			<i>Nccnd1/alb</i>
	Copy number	Mean	SD	Copy number	Mean	SD	
T118	4525	4603	77	4223	4325	89	1.06
	4605			4365			
	4678			4387			
T133	59821	61100	1111	9787	10137	375	6.03
	61659			10092			
	61821			10533			
T145	128563	125392	3448	7321	7672	316	16.34
	125892			7762			
	121722			7933			

<sup>1</sup>For each sample, 3 replicate experiments were performed and the mean and the standard deviation (SD) was determined. The level of *ccnd1* gene amplification (*Nccnd1/alb*) is determined by dividing the average *ccnd1* copy number value by the average *alb* copy number value.

point measurement of fluorescence intensity. Here we report *myc* and *ccnd1* gene dosage in breast cancer by means of quantitative PCR. (vi) We found a high degree of concordance between real-time quantitative PCR and Southern blot analysis in terms of gene amplification, especially for samples with high copy numbers ( $\geq 5$ -fold). The slightly higher frequency of gene amplification (especially *ccnd1* and *erbB2*) observed by means of real-time quantitative PCR as compared with Southern-blot analysis may be explained by the higher sensitivity of the former method. However, we cannot rule out the possibility that some tumors with a few extra

gene copies observed in real-time PCR had additional copies of an arm or a whole chromosome (trisomy, tetrasomy or polysomy) rather than true gene amplification. These 2 types of genetic alteration (polysomy and gene amplification) could be easily distinguished in the future by using an additional probe located on the same chromosome arm, but some distance from the target gene. It is noteworthy that high gene copy numbers have the greatest prognostic significance in breast carcinoma (Borg *et al.*, 1992; Slamon *et al.*, 1987).

Finally, this technique can be applied to the detection of gene deletion as well as gene amplification. Indeed, we found a decreased copy number of *erbB2* (but not of the other 2 proto-oncogenes) in several tumors; *erbB2* is located in a chromosome region (17q21) reported to contain both deletions and amplifications in breast cancer (Bièche and Lidereau, 1995).

In conclusion, gene amplification in various cancers can be used as a marker of pre-neoplasia, also for early diagnosis of cancer, staging, prognostication and choice of treatment. Southern blotting is not sufficiently sensitive, and FISH is lengthy and complex. Real-time quantitative PCR overcomes both these limitations, and is a sensitive and accurate method of analyzing large numbers of samples in a short time. It should find a place in routine clinical gene dosage.

#### ACKNOWLEDGEMENTS

RL is a research director at the Institut National de la Santé et de la Recherche Médicale (INSERM). We thank the staff of the Centre René Huguenin for assistance in specimen collection and patient care.

#### REFERENCES

- AN, H.X., NIEDERACHER, D., BECKMANN, M.W., GÖHRING, U.J., SCHARL, A., PICARD, F., VAN ROEYEN, C., SCHNÜRCH, H.G. and BENDER, H.G., *erbB2* gene amplification detected by fluorescent differential polymerase chain reaction in paraffin-embedded breast carcinoma tissues. *Int. J. Cancer (Pred. Oncol.)*, **64**, 291-297 (1995).
- BERNS, E.M.J.J., KLIJN, J.G.M., VAN PUTTEN, W.L.J., VAN STAVEREN, I.L., PORTINGEN, H. and FOEKENS, J.A., *c-myc* amplification is a better prognostic factor than *HER2/neu* amplification in primary breast cancer. *Cancer Res.*, **52**, 1107-1113 (1992).
- BIÈCHE, I. and LIDEREAU, R., Genetic alterations in breast cancer. *Genes Chrom. Cancer*, **14**, 227-251 (1995).
- BORG, A., BALDETORP, B., FERNO, M., OLSSON, H. and SIGURDSSON, H., *c-myc* amplification is an independent prognostic factor in post-menopausal breast cancer. *Int. J. Cancer*, **51**, 687-691 (1992).
- CELI, F.S., COHEN, M.M., ANTONARAKIS, S.E., WERTHEIMER, E., ROTH, J. and SHULDINER, A.R., Determination of gene dosage by a quantitative adaptation of the polymerase chain reaction (qd-PCR): rapid detection of deletions and duplications of gene sequences. *Genomics*, **21**, 304-310 (1994).
- COURJAL, F., CUNY, M., SIMONY-LAFONTAINE, J., LOUASSON, G., SPEISER, P., ZEILLINGER, R., RODRIGUEZ, C. and THEILLET, C., Mapping of DNA amplifications at 15 chromosomal localizations in 1875 breast tumors: definition of phenotypic groups. *Cancer Res.*, **57**, 4360-4367 (1997).
- DENG, G., YU, M., CHEN, L.C., MOORE, D., KURISU, W., KALLIONIEMI, A., WALDMAN, F.M., COLLINS, C. and SMITH, H.S., Amplifications of oncogene *erbB-2* and chromosome 20q in breast cancer determined by differentially competitive polymerase chain reaction. *Breast Cancer Res. Treat.*, **40**, 271-281 (1996).
- GELMINI, S., ORLANDO, C., SESTINI, R., VONA, G., PINZANI, P., RUOCCO, L. and PAZZAGLI, M., Quantitative polymerase chain reaction-based homogeneous assay with fluorogenic probes to measure *c-erbB-2* oncogene amplification. *Clin. Chem.*, **43**, 752-758 (1997).
- GIBSON, U.E.M., HEID, C.A. and WILLIAMS, P.M., A novel method for real-time quantitative RT-PCR. *Genome Res.*, **6**, 995-1001 (1996).
- HEID, C.A., STEVENS, J., LIVAK, K.J. and WILLIAMS, P.M., Real-time quantitative PCR. *Genome Res.*, **6**, 986-994 (1996).
- HOLLAND, P.M., ABRAMSON, R.D., WATSON, R. and GELFAND, D.H., Detection of specific polymerase chain reaction product by utilizing the 5' to 3' exonuclease activity of *Thermus aquaticus* DNA polymerase. *Proc. nat. Acad. Sci. (Wash.)*, **88**, 7276-7280 (1991).
- KALLIONIEMI, A., KALLIONIEMI, O.P., PIPER, J., TANNER, M., STOKKES, T., CHEN, L., SMITH, H.S., PINKEL, D., GRAY, J.W. and WALDMAN, F.M., Detection and mapping of amplified DNA sequences in breast cancer by comparative genomic hybridization. *Proc. nat. Acad. Sci. (Wash.)*, **91**, 2156-2160 (1994).
- LEE, L.G., CONNELL, C.R. and BIOCH, W., Allelic discrimination by nick-translation PCR with fluorogenic probe. *Nucleic Acids Res.*, **21**, 3761-3766 (1993).
- LONGO, N., BERNINGER, N.S. and HARTLEY, J.L., Use of uracil DNA glycosylase to control carry-over contamination in polymerase chain reactions. *Gene*, **93**, 125-128 (1990).
- MUSS, H.B., THOR, A.D., BERRY, D.A., KUTE, T., LIU, E.T., KOERNER, F., CIRRICIONE, C.T., BUDMAN, D.R., WOOD, W.C., BARCOS, M. and HENDERSON, I.C., *c-erbB-2* expression and response to adjuvant therapy in women with node-positive early breast cancer. *New Engl. J. Med.*, **330**, 1260-1266 (1994).
- PAULETTI, G., GODOLPHIN, W., PRESS, M.F. and SALMON, D.J., Detection and quantification of *HER-2/neu* gene amplification in human breast cancer archival material using fluorescence *in situ* hybridization. *Oncogene*, **13**, 63-72 (1996).
- PIATAK, M., LUK, K.C., WILLIAMS, B. and LIFSON, J.D., Quantitative competitive polymerase chain reaction for accurate quantitation of HIV DNA and RNA species. *Biotechniques*, **14**, 70-80 (1993).
- SCHUURING, E., VERHOEVEN, E., VAN TINTEREN, H., PETERSE, J.L., NUNNIK, B., THUNNISSEN, F.B.J.M., DEVILLE, P., CORNELISSE, C.J., VAN DE VUIVER, M.J., MOOI, W.J. and MICHALIDES, R.J.A.M., Amplification of genes within the chromosome 11q13 region is indicative of poor prognosis in patients with operable breast cancer. *Cancer Res.*, **52**, 5229-5234 (1992).
- SLAMON, D.J., CLARK, G.M., WONG, S.G., LEVIN, W.S., ULLRICH, A. and MCGUIRE, W.L., Human breast cancer: correlation of relapse and survival with amplification of the *HER-2/neu* oncogene. *Science*, **235**, 177-182 (1987).
- SLAMON, D.J., GODOLPHIN, W., JONES, L.A., HOLT, J.A., WONG, S.G., KEITH, D.E., LEVIN, W.J., STUART, S.G., UDOLFE, J., ULLRICH, A. and PRESS, M.F., Studies of the *HER-2/neu* proto-oncogene in human breast and ovarian cancer. *Science*, **244**, 707-712 (1989).
- VALERON, P.F., CHIRINO, R., FERNANDEZ, L., TORRES, S., NAVARRO, D., AGUIAR, J., CABRERA, J.J., DIAZ-CHICO, B.N. and DIAZ-CHICO, J.C., Validation of a differential PCR and an ELISA procedure in studying *HER-2/neu* status in breast cancer. *Int. J. Cancer*, **65**, 129-133 (1996).

**This Page is Inserted by IFW Indexing and Scanning  
Operations and is not part of the Official Record**

**BEST AVAILABLE IMAGES**

Defective images within this document are accurate representations of the original documents submitted by the applicant.

Defects in the images include but are not limited to the items checked:

- ☐ **BLACK BORDERS**
- ☐ **IMAGE CUT OFF AT TOP, BOTTOM OR SIDES**
- ☐ **FADED TEXT OR DRAWING**
- ☐ **BLURRED OR ILLEGIBLE TEXT OR DRAWING**
- ☐ **SKEWED/SLANTED IMAGES**
- ☐ **COLOR OR BLACK AND WHITE PHOTOGRAPHS**
- ☐ **GRAY SCALE DOCUMENTS**
- ☐ **LINES OR MARKS ON ORIGINAL DOCUMENT**
- ☐ **REFERENCE(S) OR EXHIBIT(S) SUBMITTED ARE POOR QUALITY**
- ☐ **OTHER:** \_\_\_\_\_

**IMAGES ARE BEST AVAILABLE COPY.**

**As rescanning these documents will not correct the image problems checked, please do not report these problems to the IFW Image Problem Mailbox.**